

REACTION ANALYSIS OF TEMPLATED POLYMER SYSTEMS

Except where reference is made to the work of others, the work described in this dissertation is my own or was done in collaboration with my advisory committee. This dissertation does include proprietary or classified information.

Asa Dee Vaughan

Certificate of Approval:

Ram B. Gupta
Professor
Chemical Engineering

Mark E. Byrne, Chair
Assistant Professor
Chemical Engineering

Barton C. Prorok
Associate Professor
Materials Engineering

Steve R. Duke
Associate Professor
Chemical Engineering

George T. Flowers
Interim Dean
Graduate School

REACTION ANALYSIS OF TEMPLATED POLYMER SYSTEMS

Asa Dee Vaughan

A Dissertation

Submitted to

the Graduate Faculty of

Auburn University

in Partial Fulfillment of the

Requirements for the

Degree of

Doctor of Philosophy

Auburn, Alabama

August 9, 2008

REACTION ANALYSIS OF TEMPLATED POLYMER SYSTEMS

Asa Dee Vaughan

Permission is granted to Auburn University to make copies of this dissertation at its discretion, upon request of individuals or institutions and at their expense. The author reserves all publication rights.

Signature of Author

Date of Graduation

DISSERTATION ABSTRACT
REACTION ANALYSIS OF TEMPLATED POLYMER SYSTEMS

Asa Dee Vaughan

Doctor of Philosophy, August 9, 2008
(B.S., Auburn University, 2003)

290 Typed Pages

Directed by Mark E. Byrne

Templated polymer systems have unique “trained” binding characteristics that make them of high interest within chromatography, sensors, diagnostic devices, and drug delivery carriers. In this work, a typical highly crosslinked recognitive polymer from the literature was synthesized (poly(methacrylic acid-co-ethylene glycol dimethacrylate) (poly(MAA-co-EGDMA)) imprinted network). Reaction analysis of this system revealed low double bond conversions ($(35.0 \pm 2.3) \%$) which indicate the feed composition with a short bi-functional crosslinker are not representative of the final polymer network. Parameters such as monomer-template ratio, crosslinking percentage, crosslinking monomer length, reaction temperature, initiator wt%, solvent wt%, and reaction mechanism were varied to determine effects upon the polymerization and template

binding parameters. “Living/controlled” polymerization techniques used to synthesize poly(MAA-co-EGDMA) imprinted networks achieved a 63% increase in template binding capacity over imprinting via standard free-radical polymerization methodologies and demonstrated a 85% increase in template affinity at equivalent double bond conversions over imprinting via standard free-radical polymerization.

Weakly crosslinked poly(MAA-co-EGDMA) and poly(diethylaminoethyl-methacrylate-co-2-hydroxyethyl-methacrylate-co-polyethylene-glycol200dimethacrylate) (poly(DEAEM-co-HEMA-co-PEG200DMA) imprinted gels synthesized via “living/controlled” polymerization techniques demonstrate a significant increase in template binding capacity (90% and 89%) over imprinting via conventional free radical polymerization, respectively. Poly(DEAEM-co-HEMA-co-PEG200DMA) gels show a significant decrease in mesh size with the use of “living/controlled” polymerization techniques from 30.3 ± 1.7 to $19.7 \pm 2.1 \text{ \AA}$. Template dynamic release studies for poly(DEAEM-co-HEMA-co-PEG200DMA) imprinted gels synthesized via “living/controlled” polymerization techniques demonstrate a two fold extended release and a more constant (zero-order) release. Kinetic analysis reveals “living/controlled” reaction mechanisms increase the chemically controlled propagation mechanism during the polymerization thus decreasing the growing chain frustrations within the network potentially providing an optimum environment for the formation of “tailored” macromolecular memory binding sites. The use of “living/controlled” polymerization techniques within templated mediated polymers presented in this dissertation have the potential to significantly enhance the binding parameters and the tailorability of templated polymer networks for sensors, diagnostic devices, and drug delivery carriers.

ACKNOWLEDGEMENTS

First of all, thank you to my Savior and Lord, Jesus Christ, for giving me the strength and endurance to complete this work, and thank you Jesus for all the friends and colleagues that you have placed in my life that have helped me complete this dissertation. Thank you to Mom and Dad for your love, support and decision to home school many years ago. Thank you, Dad, for telling me not to quit and telling me to stick it out. Dr. Byrne, thank you for your high standards which helped me achieve more than I ever would on my own. I want to extend my thanks to my committee, Dr. Duke, Dr. Gupta, Dr. Prorok, and my outside reader, Dr. Auad, for their active participation in my transition from graduate student to Ph.D. Thank you to the entire faculty and staff of the Auburn University Department of Chemical Engineering for their friendship, support, and advice over the course of my undergraduate and graduate tenure at Auburn University. Thank you to Wendel and Matt, the glass masters, from the AU Glass Shop. Dr. Placek, thank you for your assistance with visual basic programming. Thank you to Dr. Roberts and Dr. Chambers for listening ears and the subsequent advice. Dr. Maples, thank you for your friendship, advice, and assistance. Jordan Roberts, thank you for your friendship and advice. Parker S. Sizemore and Jeney Zhang thank you for your assistance in obtaining experimental data, and the opportunity to work with you. Thank you to the entire Byrne Group (past and present) for your friendship and advice; it has

been an honor to know each of you. Thank you, Ryanne Noss, Maryam Ali, Siddarth Venkatesh, Matthew Eggert, Debbie Bacik, and Zenda Davis for your friendship. Thank you to all that I have and have not mentioned that have helped me succeed. Funding for this dissertation has been sponsored in part by the National Science Foundation (NSF-CBET-0730903, grant G00003191), the U.S. Department of Education (GAANN grant P200A060184), the U.S. Department of Agriculture, the Auburn University Detection and Food Safety Center (AUDFS), and the Auburn University Competitive Research Grant. War Damn Eagle! Gratefully, Dr. Dee

Style manual or journal used: Journal of the American Chemical Society

Computer software used: Microsoft Word, Microsoft Excel, and Endnote

TABLE OF CONTENTS

	Page
LIST OF TABLES	xv
LIST OF FIGURES	xvi
1.0 INTRODUCTION	1
2.0 TEMPLATED POLYMER SYSTEMS.....	4
2.1 Overview of Templated Polymer Systems	5
2.1.1 Introduction to Artificial Recognition via Imprinting	7
2.1.2 Template Binding Site Formation.....	9
2.1.3 Current Trends in Recognitive Technology.....	11
2.2 Parameters that Alter Network Control of Copolymer and Recognitive Systems	12
2.2.1 Temperature Effects.....	13
2.2.2 Solvent Effects.....	16
2.2.3 Monomer-Template Composition Effects	19
2.2.4 Crosslinking Monomer Composition Effects	21
2.2.5 Binding Site Modification.....	22
2.2.6 Initiation Mechanisms.....	23
2.2.6.1 Kinetic Steps within a Polymerization Reaction	24

	Page
2.2.6.1.1 Initiation.....	24
2.2.6.1.2 Propagation	25
2.2.6.1.3 Termination.....	25
2.2.6.2 Thermal Free Radical Polymerization	26
2.2.6.3 UV Photo-polymerization.....	26
2.4 List of References	27
3.0 REACTION ANALYSIS OF A TYPICAL MOLECULARLY IMPRINTED SYSTEM	55
3.1 Scientific Rationale.....	56
3.2 Synthesis of a Typical Recognitive Polymer	57
3.2.1 Materials	57
3.2.2 Methods: Polymer Synthesis.....	58
3.2.3 Methods: Evaluation of Template Binding Parameters.....	61
3.2.4 Methods: Binding Affinity and Capacity from Freundlich Analysis....	64
3.3 Results and Discussion	65
3.3.1 Double Bond Conversion via Reaction Analysis.....	66
3.3.2 Assessment of Binding Parameters.....	72
3.4 Conclusions.....	76
3.5 List of References	77
4.0 “LIVING/CONTROLLED” POLYMERIZATION TO PRODUCE RECOGNITIVE NETWORKS	94
4.1 Introduction to “Living/Controlled” Polymerization.....	95

	Page
4.2 Hypothesis.....	99
4.3 Recognitive Polymer Synthesis via “Living/Controlled” Polymerization	
Techniques	99
4.3.1 Materials	100
4.3.2 Methods: Synthesis for “Living/Controlled” Poly(MAA-co-EGDMA)	
Networks	100
4.4 Results and Discussion	102
4.4.1 Template Loading Capacity Enhancement	102
4.4.2 Template Binding Affinity Enhancement.....	105
4.4.3 Selectivity	109
4.5 Conclusions.....	113
4.6 List of References	114
5.0 ENHANCED TEMPLATE LOADING AND CONTROLLED RELEASE VIA	
“LIVING/CONTROLLED” POLYMERIZATION REACTIONS: FOCUSING	
ON POTENTIAL DRUG DELIVERY CARRIERS.....	132
5.1 Introduction to Controlled Drug Delivery	133
5.2 Hypothesis.....	135
5.3 Materials and Methods.....	135
5.3.1 Materials	136
5.3.2 Methods: Synthesis of Poly(MAA-co-EGDMA) Recognitive Gels...	137
5.3.3 Methods: Synthesis of Poly(DEAEM-co-HEMA-co-PEG200DMA)	
Recognitive Gels	138

	Page
5.3.4 Methods: Binding Studies for Poly(MAA-co-EGDMA) Gels	139
5.3.5 Methods: Binding Studies for Poly(DEAEM-co-HEMA-co- PEG200DMA) Gels	139
5.3.6 Methods: Template Diffusion Analysis of Poly(MAA-co-EGDMA) Gels	140
5.3.7 Methods: One-Dimensional Transport Analysis from Poly(DEAEM-co-HEMA-co-PEG200DMA) Gels	141
5.3.8 Methods: Determination of Polymer Gel Specific Volume/Swelling Studies.....	143
5.3.9 Methods: Calculation of Mesh Size.....	144
5.3.10 Methods: Dynamic Template Release Profiles.....	147
5.3.11 Analysis of Kinetic Parameters.....	147
5.4 Results and Discussion	149
5.5 Conclusions.....	172
5.6 List of References	173
6.0 CONCLUSIONS.....	187
APPENDICES	
Appendix A:.....	190
A.1 Nitrogen Purge Times	190
A.2 Poly(MAA-co-EGDMA) Recognitive Networks Binding Isotherm Fit Analysis	192

	Page
A.3 Raw Data from Static Experiment for Calculations of Mesh Size for Poly(MAA-co-EGDMA) and Poly(DEAEM-co-HEMA-co-PEG200DMA) Recognitive Gels	196
A.4 Data used for the Calculation of Diffusion Coefficients	201
A.5 Linearization of Selected Data for Freundlich Isotherm Analysis.....	204
Appendix B:	207
B.1 Method of Micro-Soxhlet Extraction for Poly(MAA-co-EGDMA) Recognitive Polymer Disks.....	207
B.2 Results of Micro-Soxhlet Extraction for Poly(MAA-co-EGDMA) Recognitive Polymer Disks.....	208
B.3 Calculation of EA9A Bound, Removed, and Initially for EA9A Imprinted Poly(MAA-co-EGDMA) Polymer Networks	211
B.4 Discussion of Results.....	214
B.5 References.....	215
Appendix C:	217
C.1 Program Setup.....	217
C.2 Program Code for “SAE”.....	218
Appendix D:.....	244
D.1 Program Setup and Use.....	244
D.2 Program Code for “KINO”	245
Appendix E:	268

	Page
E.1 Error Analysis	268

LIST OF TABLES

Table	Page
2.1 Selection of Imprinted Systems Published in 2007.....	14
3.1 Quantitive Binding Parameters of Poly (MAA-co-EGDMA) Networks	74
4.1 Calculated Binding Parameters for Poly(MAA-co-EGDMA) Recognitive Networks using Freundlich Isotherm Analysis: Increase in Template Loading ..	104
4.2 Calculated Binding Parameters for Poly(MAA-co-EGDMA) Recognitive Networks using Freundlich Isotherm Analysis: Increase in Template Binding Affinity	108
4.3 Calculated Binding Parameters for Poly(MAA-co-EGDMA) Recognitive Networks using Freundlich Isotherm Analysis	110
4.4 Calculated Selectivity Numbers based upon Affinities and Capacity for Poly(MAA-co-EGDMA) Recognitive Networks.....	112
5.1 Poly(MAA-co-EGDMA) Recognitive Gel Binding Characteristics.....	152
5.2 Poly(DEAEM-co-HEMA-co-PEG(200)DMA) Recognitive Gel Binding Characteristics	155
5.3 Characteristics that Influence Template Diffusion in Imprinted Gels	165

Table	Page
B.1 Amounts of EA9A Contained in the Synthesis, Loading, and Wash Effluent for Poly(MAA-co-EGDMA) Recognitive Networks	216

LIST OF FIGURES

Figure	Page
2.1 General Schematic of a Crosslinked Polymer Network	50
2.2 Recognitive Polymer Synthesis	51
2.3 General Schematic of Mesh Size	52
2.4 Porosity and Mesh Size.....	53
2.5 General Schematic of Interconnecting within Polymer Networks	54
3.1 Procedure for Imprinted Polymer Synthesis to Binding Analysis	81
3.2 Differential Photo Calorimeter Cell Schematic	82
3.2 Heat Flow from Differential Photo Calorimeter.....	83
3.4 Reaction Signature Quality Control for Poly(MAA-co-EGDMA) Network Synthesis	84
3.5 Dynamic Double Bond Conversion of a Poly(MAA-co-EGDMA) Imprinted Network: A Typical Recognitive Polymer	85
3.6 Pendant Double Bond Schematic.....	86
3.7 Poly(MAA-co-EGDMA) Recognitive Polymer Rate of Polymerization at Various Temperatures	87
3.8 Temperature Influence on Fractional Double Bond Conversion.....	88
3.9 Photoinitiator Wt% Effect upon Double Bond Conversion.....	89

Figure	Page
3.10 Fractional Double Bond Conversion of Poly(MAA-co-EGDMA) Recognitive Networks.....	90
3.11 Equilibrium Binding Isotherm for Poly(MAA-co-EGDMA) Recognitive Polymers	91
3.12 Template and Analogue Molecular Structure	92
3.13 Selectivity Study for Poly(MAA-co-EGDMA) Recognitive Polymers.....	93
4.1 Schematic of the “Living/Controlled” Polymerization upon Linear Chains	121
4.2 Schematic of the Distribution of Linear Polymer Chains	122
4.3 Polymerization Time for “Living/Controlled” versus Standard Free-radical Polymerization of Poly(MAA-co-EGDMA) Imprinted Networks	123
4.4 Dynamic Double Bond Conversion of a Poly(MAA-co-EGDMA) Network via “Living/controlled” Polymerization.....	124
4.5 Reversible Termination.....	125
4.6 Equilibrium Binding Isotherm for a Poly(MAA-co-EGDMA) Recognitive Polymer Synthesized via “Living/controlled” Polymerization Techniques	126
4.7 Controlled/Living Polymerization and the Effect on Imprinted Network Structure.....	127
4.8 Equilibrium Binding Isotherm for Poly(MAA-co-EGDMA) Recognitive Polymer Synthesized via “Living/controlled” Polymerization Techniques: Matching Double Bond Conversions.....	128

Figure	Page
4.9 Binding Isotherm Comparison of All EA9A Imprinted Poly(MAA-co-EGDMA) Networks Conventional Free-Radical versus “Living/controlled” Polymerization Techniques	129
4.10 Selectivity Comparison for Poly(MAA-co-EGDMA) Recognitive Networks for Ethyladenine (EA9A).....	130
4.11 Poly(MAA-co-EGDMA) Networks Binding Isotherms for EA9A and EADOP: Selectivity Analysis	131
5.1 Poly(MAA-co-EGDMA) Dark Reaction Kinetic Analysis	178
5.2 Poly(MAA-co-EGDMA) Recognitive Gel Binding Isotherms	179
5.3 Poly(DEAEM-co-HEMA-co-PEG200DMA) Recognitive Gel Binding Isotherms.....	180
5.4 Equilibrium Swelling Studies for Poly(DEAEM-co-HEMA-co-PEG200DMA) Recognitive Gels	181
5.5 Dynamic Release Studies for Poly(DEAEM-co-HEMA-co-PEG200DMA) Recognitive Gels	182
5.6 Fractional Release for Poly(DEAEM-co-HEMA-co-PEG200DMA) Recognitive Gels	183
5.7 Propagation Constant from Poly(MAA-co-EGDMA) Kinetic Analysis	184
5.8 Termination Constant from Poly(MAA-co-EGDMA) Kinetic Analysis.....	185
5.9 Ratio of k_t/k_p from Poly(MAA-co-EGDMA) Kinetic Analysis	186
A.1 Purge Time Experiments for Poly(MAA-co-EGDMA) Recognitive Gels.....	191
A.2 Scatchard Plot of Poly(MAA-co-EGDMA) Recognitive Polymers	193

Figure	Page
A.3 Langmuir Isotherm Linear Regression of Poly(MAA-co-EGDMA) Recognitive Polymers	194
A.4 Freundlich Isotherm Linear Regression of Poly(MAA-co-EGDMA) Recognitive Polymers(LOG-LOG).....	195
A.5 Raw Stress versus Strain Data for Three Poly(MAA-co-EGDMA) Recognitive Gels.....	197
A.6 Raw Stress versus Strain Data for Three Poly(MAA-co-EGDMA) Recognitive Gels via “Living/controlled” Polymerization.....	198
A.7 Raw Stress versus Strain Data for Three Poly(DEAEM-co-HEMA-co-PEG200DMA) Recognitive Gels	199
A.8 Raw Stress versus Strain Data for Poly(DEAEM-co-HEMA-co-PEG200DMA)Recognitive Gels via “Living/controlled” Polymerization.....	200
A.9 Fractional Release for the Calculation of Diffusion Coefficients for EA9A Imprinted Poly(MAA-co-EGDMA) Gels.....	202
A.10 One Dimensional Transport Data for Diclofenac Sodium Imprinted Poly(DEAEM-co-HEMA-co-PEG200DMA) Gels	203
A.11 Freundlich Isotherm Linear Regression of Poly(MAA-co-EGDMA) Recognitive Polymers via “Living” Polymerization (35% Double Bond Conversion) (LOG-LOG)	205
A.12 Freundlich Isotherm Linear Regression of Poly(MAA-co-EGDMA) Recognitive Polymers for Selectivity Analysis (LOG-LOG).....	206

Figure	Page
B.1 Wash Analysis for Highly Crosslinked Poly(MAA-co-EGDMA) Recognitive Networks.....	209
B.2 Schematic of Diffusion Through a Crosslinked Polymer Network	210

1.0 INTRODUCTION

Templated polymer networks are unique materials that have a wide variety of potential applications within the fields of chromatography, sensors, diagnostic devices, and advanced drug delivery. The major attraction of these materials is their “trained” macromolecular recognition for a particular template molecule. It is in this regard that the term molecular imprinting is used to describe these materials. Molecular imprinting is the process of using a molecule with specific functionality which is defined as the template molecule, as a template through non-covalent bonding with the forming copolymer network to form molecular specific binding pockets during the polymerization. In addition, these recognitive materials display robust recognition within a wide variety of environments. The large number of articles focusing on the subject of non-covalent molecular imprinting describes the fundamental building block of the recognition site. Recognition is due to multiple non-covalent interactions between the functional monomers and the template molecule.

The field of molecular imprinting has a significant amount of published research articles; however, intense study of these articles highlights a significant deficiency within the current literature. Previous work primarily deals with how the imprinted system was synthesized, how the binding parameters are calculated, how the imprinted system is relevant, and how the system would be applied to current technology. A few research

articles deal with methods to enhance binding characteristics by removing non-specific binding sites within the imprinted polymer in a post polymerization process; however, none of the articles enhance or optimize binding characteristics during the actual polymerization reaction. Fundamental research with specific emphasis upon the enhancement and optimization of templated polymer networks has not been studied within the field of molecular imprinting.

This dissertation presents reaction analysis and methods to positively influence the binding parameters and characteristics of imprinted polymer networks. In addition, the introduction of “living/controlled” polymerization techniques allows a greater degree of control over the formation of the imprinted network. The main object of this work is to study and develop methods to enhance and optimize the imprinted polymer binding parameters.

An overview of the field of macromolecular recognition along with parameters that affect the recognitive polymer properties is presented in Chapter 2. In Chapter 3, the synthesis of a typical molecularly imprinted polymer is presented in conjunction with the technique of reaction analysis. “Living/controlled” polymerization is described and applied to templated polymer systems within Chapter 4. Potential applications within the field of drug delivery implementing “living/controlled” polymerization techniques to enhance loading are presented in Chapter 5 along with structural analysis and kinetic analysis.

A proper understanding of the imprinting polymerization reaction and its affect on the properties of imprinted materials can be used to create or modify techniques to fine

tune imprinted networks for specific applications within sensors, diagnostic materials, and drug delivery carriers.

2.0 TEMPLATED POLYMER SYSTEMS

This chapter presents current and historical literature trends of imprinted polymer systems. Template binding parameters such as affinity, capacity, and selectivity are extremely important to the field. However, very few research papers optimize or enhance the binding parameters of imprinted networks. The formation of imprinted polymers is affected by environmental and compositional parameters, such as temperature, solvent, monomer-template ratio, crosslinking monomer (type and concentration), macromolecular structure, and initiation mechanisms. It is important to note that these parameters have a direct effect upon the length of growing polymer chains (i.e., kinetic chain length), the structural architecture of the macromolecule or network, and the formation of the template binding site. Examination of feed compositions, reaction mechanisms, and macromolecular structure will yield important correlations between these parameters and the resulting binding characteristics of imprinted systems. However, analysis of the literature reveals that no investigators are currently studying or developing pre-polymerization techniques to enhance or optimize the binding parameters of templated polymer systems. Templated polymer networks promise to be robust artificial receptors for the use in point-of-care diagnostic devices, chromatography, sensors, and controlled drug delivery.

2.1 Overview of Templated Polymer Systems

Templated polymer systems, also known as imprinted polymers or recognitive polymers, are materials with the unique ability to recognize molecules and biomolecules with “trained” macromolecular recognition, given the molecule contains certain functional interactions¹⁻¹⁸. The advantage of these artificial recognition materials, developed by molecular self assembly, is their ability to be patterned for a wide variety of molecules. Other desirable characteristics of these materials is the ability to retain their binding characteristics of affinity, selectivity, and loading capacity for a specific template molecule within a variety of solvents and operate within a large range of pH and temperature environments^{19,20}. The field has primarily focused upon the development of imprinted polymers for the recognition non-biological molecules, with increased interest in biological molecules and therapeutics in the last decade. Over 80% of the field uses a poly(methacrylic acid-co-ethylene glycol dimethacrylate) (poly(MAA-co-EGDMA)) network to provide the framework for macromolecular recognition⁴.

The poly(MAA-co-EGDMA) network is a crosslinked network which consists of linear monomer chains attached to one another by covalent links formed by the incorporation of a crosslinking monomer. A crosslink by definition is a chemical linkage between the linear chains of polymer²¹. In this case, the crosslinking monomer is a monomer that has two carbon-carbon double bonds that can react and link two growing linear polymer chains together. Figure 2.1 is a schematic of a crosslinked polymer network that is made up of linear polymer chains connected by crosslinking monomers.

The resulting macromolecular structure formed by the crosslinking polymer reaction forms the backbone for the site specific template binding pockets.

Crosslinked polymer networks do not dissolve and are not soluble in solvent. The crosslinks between linear chains form an interlinked macromolecule that can swell in the solvent, depending on how well the solvent interacts or solvates the polymer chains. The gel point or gelation point during a polymerization reaction is the point at which the polymer becomes no longer soluble in solvent.

There are three reviews that give great insight into the field of imprinted polymers ^{7, 19, 20}. Macromolecular memory within these polymer structures are formed through non-covalent complexation between a template or “guest” molecule and the functional monomers during the polymerization reaction. The concept of macromolecular recognition manifests itself from two major synergistic effects, (i) shape specific cavities that match the template molecule, which provide stabilization of the chemistry in a crosslinked matrix, and (ii) chemical groups oriented to form multiple complexation points with the template. During the polymerization reaction, the functional monomer within the non-covalent complex with the template molecule covalently bond with the forming polymer matrix via a carbon-carbon double bond. The polymer network forms around and interconnects with these complexes to give a support structure locking the template monomer complex within the polymer network. After the original template is removed or washed out of the polymer, a rigid crosslinked network retains the three-dimensional size specific cavity of chemical functionality which is target molecule specific ^{19, 22}. Hypothetically, variations in the structural architecture of the polymer

network will influence the three-dimensional cavity of functionality. By optimizing the polymer network structure, the binding parameters may also be optimized.

2.1.1 Introduction to Artificial Recognition via Imprinting

Artificial recognition is the use of a synthetic material to create artificial receptors that exploit non-covalent mechanisms to achieve a specific interaction with chemical functionality on a target molecule^{2-4, 6, 23-29}. Artificial recognition has been around for a little over six decades with imprinting upon silica gel³⁰ and over three decades considering imprinting upon polymer substrates^{19, 31-37}. Intrinsic to the binding event is the complex orientation of individual elements along with functional groups to form non-covalent bonds that promote molecular recognition. Naturally occurring biological systems have extremely efficient and tight binding parameters with small dissociation constants. One of the strongest biological examples of ligand-receptor binding is the dissociation constant of biotin-streptavidin which is equal to 10^{-15} mol/l^{4, 38}. This dissociation constant is unattainable with current artificial recognition techniques; however, artificial molecularly imprinted polymers have come close to the biological range of protein-carbohydrate dissociation constants ranging from (10^{-3} to 10^{-6} M) with theophylline ($(2.31 \pm 0.012) \times 10^{-7}$)³⁹ and morphine ($(1.2 \pm 0.2) \times 10^{-6}$)⁴⁰.

The structural stability of the surrounding three-dimensional network is essential to retain the orientation of the non-covalent interactions within the receptor site. Proteins which act as biological receptors have very specific primary structures of amino acids with a secondary structure of α helices and β sheets that form a precise binding site

orientation. The precise orientation of the protein structure has a committed three-dimensional spatial arrangement that typically aligns the receptor amino acid chemistry. An interlocking polymeric structure forms the backbone for the “trained” macromolecular memory of templated polymer networks. Both biological and artificial receptors depend upon the support network surrounding the binding site for correct orientation of the non-covalent interactions to retain their binding effectiveness.

The choice of artificial receptor versus a biological receptor is an interesting one. While natural receptors have stronger and more specific binding, artificial receptors have a lower production cost with a less restrictive and longer shelf life. In addition, artificial materials have the benefit of having more robust operation within a wide range of temperature and pH environments. For example, Xizhi and coworkers have shown poly(MAA-co-EGDMA) imprinted polymers retain their affinity for the target molecule, reserpine, in various pHs from (2.0-4.0)⁴¹. Li-Qin and coworkers show retention of binding parameters for sinomenine at various temperatures between 20°C and 60°C⁴². In these harsh environments, most proteins would lose their structure and denature.

Until recently, there have been no commercial products available employing imprinted polymer systems. Recently a company named IMIP, which is a subsidiary of Sigma-Aldrich, produces a few products^{43, 44} that are available and employ imprinted polymer networks; however, the binding parameters of these materials have not been effectively optimized. The key factor that will enhance the overall applicability of imprinted materials is the tailorability of the binding characteristics to suit specific sensing, drug delivery, or extraction needs.

2.1.2 Template Binding Site Formation

The basic method of forming binding sites, which are intrinsic to the imprinted polymer, is shown in Figure 2.2. The binding site is dependent on non-covalent bonds between the functional monomer and the template molecule. The functional monomer or monomers used are dependent on the functionality on the template molecule. Due to non-covalent interactions, self assembly of the template-functional monomer complex takes place within the pre-polymerization mixture.

Functional interactions forming non-covalent bonds are essential to the formation of effective binding sites. The functionality of the template molecule forms non-covalent bonds with functional monomer via ionic bonding, hydrogen bonding, hydrophobic interactions, and Van der Waals forces. Multiple functional monomers have been used to form multiple non-covalent interactions with the template to provide better binding sites of increased template affinity and selectivity ⁶.

The pre-polymerization mixture contains functional monomer(s), crosslinking monomer, initiator, and template molecule. Within this solution the functional groups interact and form non-covalent bonds to reduce the Gibbs free energy of the solution and form a complex known as the template molecule-functional monomer complex, this complex forms the basis for the artificial recognition binding site. Depending upon the material properties of the final recognitive polymer, a porogen may be used to increase the transport of the template through the macromolecular structure. Solvent can also be used to limit monomer-monomer interaction. It is important that the solvent must not

interfere with the non-covalent bonding between the target molecule and the functional monomers.

During the polymerization process, the polymer network forms around the template molecule-functional monomer complex forming a macromolecular structure. The macromolecular structure formed by the polymerization reaction is the backbone for the binding sites. On the length scale of the template, the crosslinked polymer network holds the binding site in a three dimensional special arrangement of functionality that conforms uniquely to the template molecule.

In order for an imprinted polymer network to recognize the target molecule, the original target molecule must be removed. A washing process removes the target molecule exposing the “trained” recognition sites. Once the target molecule is removed, the resulting polymer network has specific binding parameters for the target molecule.

Affinity, capacity or loading, and selectivity of the network for the template are the binding parameters that are “trained” during the synthesis of the templated polymer networks. Binding affinity can be best described thermodynamically with Gibbs free energy models based upon ligand-receptor interactions.

$$\Delta G_{\text{bind}} = \Delta G_{\text{t+r}} + \Delta G_{\text{r}} + \Delta G_{\text{h}} + \sum \Delta G_{\text{p}} \quad 2.1$$

Where the Gibbs free energy of binding ΔG_{bind} , which is equivalent to the addition of the sum of translational and rotational free energies $\Delta G_{\text{t+r}}$, the energy change resulting in restriction of rotors on complexion ΔG_{r} , the free energy change due to the hydrophobic effect ΔG_{h} , and the intrinsic free energies of binding for each set of interacting groups summed over all polar interactions with this term encompassing residual vibrational modes $\sum \Delta G_{\text{p}}$ ⁴⁵. The equation presented is based upon the conformation strain of each

component is introduced upon complex formation, and the complex conforms well to the binding molecule. The free energy of binding is then related to binding affinity K_a , a function of temperature T , and the binding constant k_B ⁴⁶.

$$\Delta G_{\text{bind}} = -k_B T \ln(K_a) \quad 2.2$$

The affinity is represented by the association constant which is a measure of the extent of a reversible association between two molecular species at equilibrium or the dissociation constant which is the reciprocal of the association constant. Loading or capacity is the quantity of target molecule the polymer network can retain and absorb. Selectivity is a measure of how well the imprinted network can differentiate between the target molecule and other molecules having similar shape and functionality.

2.1.3 Current Trends in Recognitive Technology

Templated polymer networks have very few products that have been developed and marketed. However, recent literature suggest these materials will provide excellent platforms for point of care testing, selective sensor coatings, and drug delivery carriers^{3, 4, 19, 47, 48}. Current literature analysis shows development for sensor coatings on microcantilever arrays, catalysis, and separations^{13, 49, 50}. Recognitive materials for sensors have been developed for glucose⁵, ephedrine⁵¹, proteins and macromolecules^{23, 52, 53}, tryptophan⁵⁴, hydroxyzine⁵⁵, fructosyl valine⁵⁶, digoxin⁵⁷, and DNA⁵⁸. Within the field of drug delivery, recognitive polymers have been developed for delivery of copper salicylate⁵⁹, ketotifen fumarate^{1, 6, 60}, dexamethasone⁶¹, norfloxacin⁶², and timolol⁶³.

Table 2.1 gives a selection of template molecules and their intended purposes that have been published in the year 2007.

Imprinted systems have great application potential for sensor, extraction, separation, and drug delivery materials. The wide variety of molecules and biomolecules that can be imprinted within a polymer network is apparent. However, as previously stated none of these articles focus on the relationship between the binding characteristics of the imprinted polymer and the polymerization reaction, feed composition, kinetic parameters, and macromolecular structure. Knowledge of how binding parameters are influenced by pre-polymerization conditions and reaction parameters will lead to procedure for optimization. Optimizing template binding affinity, loading capacity, and selectivity are essential to develop methods to effectively tailor the material for a specific application.

2.2 Parameters that Alter Network Structure of Copolymer and Recognitive Systems

Differences in environmental and compositional parameters can change the polymer structure and alter binding parameters. Network control using variations in environmental conditions such as temperature and compositional parameters such as solvent, monomer-template composition, and crosslinking monomer composition (type and concentration) can hypothetically be used to manipulate binding parameters. In addition initiation mechanisms (UV versus thermal polymerizations) and binding site modification can be used to manipulate binding parameters. It is important to note that

research on how environmental and compositional parameters can be used to optimize and enhance the imprinted polymer binding parameters has not been done within current literature. These parameters are described in this section along with any trends associated with binding characteristics. It is also important to note computer simulation programs have been developed to model the formation of imprinted polymer networks to determine imprinting quality and binding characteristics. These simulations are based upon functional interactions with the template and functional monomer along with thermodynamic constraints within the pre-polymerization complex^{5,64}.

2.2.1 Temperature Effects

For polymerization reactions, temperature has shown an Arrhenius relationship with conversion. For acrylate and dimethacrylate copolymer networks increasing the temperature increases both the polymerization rate and the double bond conversion. The polymerization temperature can be varied, but the structural characteristics of the polymer product are better described by the final double bond conversion. For example, a polymer polymerized at 70°C with a double bond conversion of 50% has the same glass-transition temperature, T_g as the same polymer polymerized at 40°C with a double bond conversion of 50%⁶⁵⁻⁶⁷. Glass transition temperature is the temperature where a smaller second order transition occurs at which amorphous portions of a polymer soften and become rubbery⁶⁸. Higher temperatures correspond to higher double bond conversion and are a direct result of increased vibrational energy which translates to more flexibility within the growing network resulting in fewer steric hinderances.

Table 2.1 Selection of Imprinted Systems Published in 2007

Template	Purpose	Ref	Template	Purpose	Ref
Sudan I	Sensor	69	Tobacco Mosaic virus	Sensor	70
Propranolol	Renewable Functional Monomer/Sensor	71	Lysozyme	Refolding Lysozyme	72
Peptide	Analysis/Sensor	73	Desmetryn	Sensor	74
β – Lactoglobulin	Sensor	75	Way-1006935	Comparitive Study	76
2,4,6 Trinitrotoluene	Sensor	77, 78	Triazine/ Herbicide	Extraction	79
Protein	Sensor/Interaction	53, 80	Proprietary Drug	Extraction	81
Uranyl Ion	Extraction	82	Boc-L- Tryptophan	Separation	83
Phosphonate	Sensor	84	Penicillin G	Assay/Sensor	13, 85
Propazine	Extraction	86	Ribonuclease	Sensor	87, 88
Diazepam	Extraction	89	Bilirubin	Separation	90
Domoic Acid	Extraction	91	2,4-D	Sensor/Assay	92
Fluoroquinolones	Extraction/ Separation	93, 94	Nafcillin	Sensor	95
o-Xylene	Separation	96	D- Phenylalanine	Separation	97
Chloramphenicol	Sensor	98, 99	Copper Ions	Separation	100
Terbuthylazine	Sensor	101	Multiblock Copolymers	Sensor	102
Lytotropic Liquid Crystalline	Tissue Engineering	103	Ketotifen Fumarate	Drug Delivery	1, 6
Dexamethasone	Drug Delivery	61	Fluorescein Sodium/ Chloromphenicol	Drug Delivery	104
Thorium(IV)	Extraction	105	Tetracycline	Extraction	106
Uric Acid	Extraction	107	Triterpene Acid	Extraction	108
Norfloxacin	Extraction	109	Ciproflaxacin	Extraction	110
B-blockers	Extraction	111	Dimethoate	Sensor	112
Uranyl Ions	Separation	113	17 β -estadiol	Sensor	114
Diacetyl Morphine	Extraction	115	4,6-dinitro-o-cresol	Sensor	116
Phenolic Estrogen	Extraction	117	Lipomono-saccharide	Extraction	118
Hydroquinone	Sensor	119	L-lysine	Separation	120

The kinetic chain length of a polymer is defined as the number of monomer units that make up one dynamically growing polymer chain. The average kinetic chain length is the average number of monomer molecules for each chain initiated. Polydispersity is a measure of how diverse the kinetic chain length is over the entire population of chains. It is a measure of the distribution of lengths of the polymer chains. Polydispersity index is the ratio of the average molecular weight of the polymer over the number-average molecular weight (defined as the total weight of all the molecules in the polymer sample divided by the total number of moles present)^{21, 121, 122}. Increasing the double bond conversion decreases the kinetic chain length thus affecting the structural properties of crosslinked polymer systems^{65, 121, 122}.

Within imprinted polymer networks, temperature has a similar effect upon the copolymer double bond conversion²². However, in recognitive polymer networks, binding characteristics are inversely proportional to temperature increased since they are based upon non-covalent interactions in the pre-polymerization solution. Non-covalent bonds that can form non-covalent bonds are ionic bonding, hydrogen bonding, Van der Waals forces, dipole-dipole bonds, and hydrophobic interactions. However, hydrogen bonding characterizes the majority of non-covalent interactions used to create macromolecular memory. Hydrogen bonding strengths are much stronger at lower temperatures and decrease in strength as temperature is increased¹²³. Imprinted polymers synthesized at lower temperatures of polymerization reduce the kinetic energy of the molecules within the system thus increasing hydrogen bonding forces between the template molecule and the functional monomers. This results in higher template affinities along with higher capacities^{15, 124-129}. It has been shown for initiation

temperatures of 40°C imprinted polymers have a higher capacity than that of those initiated at 60°C ⁸.

Methacrylic polymerization reactions are exothermic, and the heat given off by the reaction is proportional to the number of double bonds reacting within the polymerization. The heat rise within the polymerization solution is proportional to the molar amount of reacting double bonds within the polymerization solution. The temperature rises as the reaction proceeds, and most researchers do not provide a constant temperature of reaction by removing the heat from the reaction. Lack of temperature control will result in reaction temperatures during polymerization reaction to be much higher than initiation temperatures. For an example, polymerization reactions conducted within a differential photo-calorimeter, which has a high degree of temperature control within the polymerization cell, have only a 1-2°C temperature rise throughout the polymerization with an 8-10 mg sample size.

2.2.2 Solvent Effects

Solvent has been used in the synthesis of crosslinked polymer systems to change the swelling characteristics of the polymer network and to increase the porosity within highly crosslinked imprinted networks (this is necessary for the diffusion of template through the network structure). Porosity is defined as the void fraction within the macromolecular structure. An increase in the porosity of the network will increase the relative surface area and allow mass transport through the macromolecule.

Crosslinked polymers when in contact with a suitable solvent will exhibit swelling behavior by absorbing a large quantity of a solvent within the network. Swelling behavior within crosslinked polymer networks is very similar to linear polymer chains being solvated by a solvent to form a polymer solution. Swelling behavior is dictated by the change in Gibbs free energy change ΔG (2.3), which is a combination of Gibbs free energy of mixing G_m , and Gibbs elastic free energy G_{el} . ΔG_m is further defined in 2.4.

$$\Delta G = \Delta G_m + \Delta G_{el} \quad 2.3$$

$$\Delta G_m = \Delta H_m - T\Delta S_m \quad 2.4$$

is shown in 2.4. Where ΔH_m is the enthalpy of mixing (heat of mixing), T is the temperature, and ΔS_m is the entropy of mixing. The elastic free energy is calculated by equation 2.5, where T is temperature and ΔS_{el} is the entropy change associated with the

$$\Delta G_{el} = -T\Delta S_{el} \quad 2.5$$

change in configuration of the network.

The Flory solvent interaction parameter χ_1 , is a unitless quantity to represent the enthalpy of mixing. The free energy of mixing equation using the Flory solvent interaction parameter is shown in equation 2.6. Where k is a combination of the universal gas constant R , multiplied by the temperature T , N_1 and N_2 are the number of molecules for species 1 and species 2, respectively and v_1 and v_2 are the volume fraction

$$\Delta G_m = kT(N_1 \ln v_1 + N_2 \ln v_2 + \chi_1 N_1 v_2) \quad 2.6$$

of polymer 1 and polymer 2, respectively. Swelling behavior would be augmented by ($\chi_1 < 0$) and diminished by ($\chi_1 > 0$)^{21, 68, 121}.

The mesh size of a crosslinked polymer network is defined as the average distance between the linear polymer chains, and it is representative of the space available within the polymer network for diffusion¹³⁰ (Figure 2.3). The average mesh size of a crosslinked polymer structure can be altered by the amount feed crosslinker (i.e. moles of crosslinking monomer over the moles of all monomers) and by the length and branching of crosslinking monomer. In addition, a change in solvent or pH of the solvent would alter the Flory interaction parameter thus alter the swelling behavior which will directly affect the mesh size. High numbers of junction points or crosslinks within a polymer network are the reason that highly crosslinked polymer networks do not exemplify swelling behavior. Increasing the crosslinking monomer length has shown to increase the mesh size^{121, 122}. It is important to note that porosity and mesh size are on very different scales and the differences are shown in Figure 2.4.

By changing the swelling characteristics or the porosity of the network, the diffusion characteristics of the template molecule through the polymer will change¹³¹. Recent literature demonstrates that an increase in solvent concentration in the pre-polymerization formulation results in a polymer network with increased mesh size which would increase the diffusional transport of template through the macromolecular structure¹³²⁻¹³⁴. Explanation for the change in transport properties is that the solvent does not become actively incorporated into the growing polymer chains and the growing polymer chains have to form around the solvent within the system. Increasing the average mesh size of the macromolecular structure allows for increased diffusional transport through the polymer matrix.

In the synthesis of imprinted polymer networks, solvent is used as a porogen which creates pores within the macromolecular structure which will allow for faster diffusion of the template molecule through the polymer architecture¹³⁵. However, one cannot neglect that the type of solvent can affect the template affinity, capacity, and selectivity of a given system^{26, 136}. Solvents have the capability to hydrogen bond, represented by the Kamlet and Taft solvatochromic parameter (β), which can enhance or disrupt the interaction between functional monomer and template molecule¹³⁷⁻¹⁴⁰. While different solvents can be used, in order to maximize the binding characteristics, the solvent hydrogen bonding capability must be known in order to select the correct solvent to enhance the stability and formation of the functional monomer-template molecule complex. The microenvironment surrounding the complex must increase the thermodynamic stability of the complex.

2.2.3 Monomer-Template Composition Effects

The monomer-template (M/T) ratio is defined as the moles of functional monomer divided by the moles of template molecule. The M/T ratio represents the population of functional groups for every template molecule. Linear polymerizations can be affected by addition of template, which was shown for linear poly(methacrylic acid) polymerization to increase the rate of polymerization. The reason the template complex lowers critical chain length and increases the polymerization reaction rate^{6, 141, 142} is that the monomer attaches non-covalently with the template and reacts. The faster reaction

rate with the addition of template indicates an organization of double bonds on the template.

It has been shown that higher M/T ratios have produced higher populations of template-functional monomer complexes resulting in higher binding affinities^{125, 143-145}. Template binding affinity and capacity are dependant on template binding pockets formed by the non-covalent forces between the template and the functional monomers. By optimizing the M/T ratio within the pre-polymerization solution a maximum number of effective template binding pockets would be formed during the polymerization. The imprinting effect is based upon template molecule – functional monomer interactions that cause the complexation of the artificial binding site^{143, 146-148}. Template and functional monomer must be matched so as to provide optimal binding sites¹⁴⁹.

In loosely crosslinked systems, a decrease in the rate of polymerization has been shown with increasing template concentration¹⁴³ for a multiple monomer system employing acrylamide, acrylic acid, N-vinyl-2-pyrrolidinone and 2-hydroxyethylmethacrylate. For highly crosslinked networks employing methacrylic acid as the functional monomer no change in the rate of reaction was seen with a change in M/T ratio²². Highly crosslinked networks versus loosely crosslinked networks have different amounts of crosslinking monomer. Crosslinking monomers contribute two double bonds to the reaction compared to the one double bond contributed by the functional monomers. Higher amounts of double bond reacting due to high amounts of crosslinking monomer within the polymerization would overshadow any effect upon the reaction contributed by the change in M/T ratio while loosely crosslinked network polymerizations would be more sensitive to changes in the template concentration.

2.2.4 Crosslinking Monomer Composition Effects

The crosslinking monomer is the monomer that provides two or more linking points between linear polymer chains. In order to produce a network, crosslinking monomers must have more than one double-bond. Double bond functionality indicates how many directions the polymer can branch out from the crosslinking junction point⁶⁸. Of course, crosslinking monomers can possess higher orders of functionality and be bifunctional, trifunctional, etc. Crosslinking is not the only junction that can occur within linear polymer chains. Branching within a polymer chain can occur in which the polymer chain grows in two or more directions. Primary and secondary cycles can occur within polymer chains in which a polymer chain bends back around and reacts with itself creating a cycle (Figure 2.5) and are not conducive to an ideal polymer network.

The crosslinking density of a polymer network is equal to number of chemical crosslinks between linear polymer chains in the polymer network. Increasing the feed crosslinking percent, which is moles of crosslinking monomer over moles of all monomers, increases the crosslinking density^{5, 150, 151}.

The degree of flexibility of the polymer network chains is heavily influenced by the amount of crosslinking and type of crosslinking molecule within the polymer network. Highly crosslinked imprinted polymer networks with short bifunctional crosslinking monomers have little to no flexibility within the network and have higher affinities, binding capacities, and selectivity compared to less crosslinked polymers^{22, 137}. Imprinted polymers of low crosslinking percentage demonstrate lower affinities, capacities, and selectivity which are a direct result of the flexibility in the polymer

network. It is important to note that the degree of crosslinking is also important to the swelling behavior and the expansion of the polymer network. Highly crosslinked materials do not exemplify swelling behavior because of the high crosslinking density.

The crosslinking monomer amount and length can have an effect upon double bond conversion and the diffusion characteristics of the template molecule through the macromolecular structure ^{5, 22}. For example, Noss and co-workers explored binding characteristics and diffusion characterization of testosterone imprinted polymers with various feed crosslinking percents and crosslinking monomer lengths. The results showed that higher feed crosslinking percentages within imprinted networks yielded higher affinities, capacities, and selectivity. Results also showed high feed crosslinking percentages have lower diffusion coefficients ¹⁵². For non-imprinted networks, diffusion of drugs have been well studied and have shown that increasing the crosslinking monomer length in highly crosslinked polymer systems increases the diffusion coefficients of the drug through the polymer matrix ⁵.

2.2.5 Binding Site Modification

Molecularly imprinted binding sites are typically classified as having populations of low affinity and high affinity recognition sites. Non-specific binding takes place when random orientations of the functional monomer bind the template molecule. Control networks or co-polymer networks formed without template molecule are an example of non-specific binding because the orientations of the functional monomer are random and not guided by the templating or imprinted process.

In recent work, Shimizu and coworkers¹³⁷ describe post-polymerization binding site modification of imprinted networks. In this work, they hypothesized that the binding limitations of imprinted polymer networks are due to the heterogeneous nature of the binding sites. In order to correct the heterogeneous nature of the binding sites, the researchers devised a method using diazomethane in diethyl ether or phenyldiazomethane in toluene to remove the non-selective sites by esterification. The high affinity sites were protected by the bound template molecule, ethyl adenine-9-acetate. The results of this experiment show that the removal of the non-selective sites resulted in a higher population of selective or high affinity sites. The work demonstrates the ability to modify binding characteristics by manipulation of the existing binding sites. They shifted the heterogeneity of non-specific and specific binding sites to more specific high affinity sites thus yielding an enhanced overall template affinity¹³⁷. Once again, it is important to note that this enhancement of the templated polymer network is done post-polymerization.

2.2.6 Initiation Mechanisms

Two types of free-radical initiation methods have been used to create imprinted polymer networks, thermal and UV initiation. In both thermal and UV initiated polymerizations, an increase in initiator concentration can theoretically lead to a decrease in the kinetic chain length. Kinetic chain length is inversely proportional to the rate of polymerization. Increase in initiator increases the rate of polymerization thus decreasing the kinetic chain length¹²¹. Thus, attempts to increase polymerization rate by increasing

radical concentration produces smaller sized polymer chains¹²². The amount of initiator has an effect upon the double bond conversion and the macromolecular structure. Both double bond conversion and macromolecular structure are expected to significantly influence the binding parameters of imprinted polymer networks.

2.2.6.1 Kinetic Steps within a Polymerization Reaction

A polymer is a high-molecular weight molecule that is comprised of repeating units in a linear, branched, or crosslinked architecture that is formed during a polymerization reaction. There are several different types of reactions used to create polymers; however, in this work all polymerization reactions were free-radical initiated and had the following steps: initiation, propagation, and termination. It is important to note that “living/controlled” polymerizations introduced in Chapter 4 are initiated by free radicals. However, “living/controlled” polymerizations have a reversible termination step additional to the termination step presented in this section. The polymerization reaction can be broken down into three steps which are described in the next three subsections.

2.2.6.1.1 Initiation Step

The initiation step within the polymerization reaction is a two part process in which the initiator, I , breaks up into radicals, $R\bullet$, and the radical attaches itself to a monomer, M , to form a monomer radical, $M\bullet$. One such initiator, which was used in the

experimental work presented in this dissertation, is azo-bisisobutyronitrile (AIBN). When irradiated with UV light, AIBN breaks into two 2-cyanoprop-2-yl radicals and two nitrogen molecules. The radical produced by the breaking of AIBN reacts with the carbon-carbon double bond within the monomer to form a monomer radical.



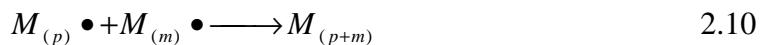
2.2.6.1.2 Propagation Step

The propagation step in the polymerization is the growth step of the polymer chain. This step can be where a monomer radical, $M_{(p)} \bullet$, attaches to a monomer and forms a larger monomer radical, $M_{(p+1)} \bullet$, where p and m equals the number of repeating monomer units. This process continues until the termination step occurs.



2.2.6.1.3 Termination Step

The termination step of the polymerization reaction begins when two monomer radicals come together to form a dead polymer chain. All of the double bonds have reacted within this “dead” chain to form inter-linking between monomer units. Monomer radicals, $M_{(p)} \bullet$ and $M_{(m)} \bullet$ come together to form the dead polymer chain, $M_{(p+m)} \bullet$.



2.2.6.2 Thermal Free Radical Polymerizations

Thermal initiated free-radical polymerizations are based upon heat energy breaking the initiation molecule into radicals from which point the polymerization reaction starts. The microstructure of UV and thermal initiated crosslinked polymer structures have been shown to be similar ¹⁵³. Thermal polymerizations at higher temperatures will have a faster rate of reaction, but double bond conversion is a better indicator of final polymer structure ⁶⁵⁻⁶⁷. Thermal initiation takes place in most cases above a temperature of 40°C. Hydrogen bond strength decreases with an increase in temperature and results in weaker non-covalent bonding within the template molecule – functional monomer complex thus giving lower affinity binding sites and lower population density of binding sites within the final recognitive polymer structure ^{15, 125-127}.

2.2.6.3 UV Photo-polymerization

Photoinitiated free radical polymerization employs a photoinitiator that will break up into radicals upon irradiation with ultra violet light. In photo-polymerization reactions the amount and concentration of incident light plays an important role in the rate of radicals forming within the polymerizing mixture thus affecting the polymerization rate. The next paragraph closely follows the framework presented by Odian ¹²².

The rate of photochemical initiation (R_i) is given by the following equation,

$$R_i = 2\phi I_a \quad 2.11$$

where I_a is the intensity of absorbed light in moles (Einsteins), and φ is the quantum yield for initiation. The factor of two indicates that two radicals are produced when initiator decays with irradiation or heat. To further describe the polymerization rate (R_p) when using UV-initiation methods, the following equation applies,

$$R_p = k_p [M] \left(\frac{\varphi I_a}{k_t} \right)^{\frac{1}{2}} \quad 2.12$$

where k_p is the propagation constant, $[M]$ is the monomer concentration and k_t is the termination constant. Absorbed light I_a can be quantified easier by the following equation,

$$I_a = I_o \varepsilon [M] [A] b \quad 2.13$$

where I_o is the incident light intensity, ε is extinction coefficient of initiator, $[A]$ is the concentration of initiator, and b is the thickness of the irradiated sample.

An increase in intensity will yield an increase in the rate of reaction and double bond conversion^{154, 155}. Advantages of photo-polymerization for recognitive polymer systems is the ability to have lower temperatures which increase non-covalent bonds strengths thus increasing the stability of the template molecule –functional monomer complex. This results in more effective binding sites^{15, 125-127}.

2.5 List of References

1. Ali, M.; Horikawa, S.; Venkatesh, S.; Saha, J.; Hong, J. W.; Byrne, M. E., Zero-order Therapeutic Release from Imprinted Hydrogel Contact Lenses within in vitro Physiological Ocular Tear Flow. *Journal of Controlled Release* **2007**, 124, (3), 154-162.

2. Byrne, M. E.; Oral, E. J.; Hilt, Z.; Peppas, N. A., Networks for Recognition of Biomolecules: Molecular Imprinting and Micropatterning Poly(ethylene glycol)-Containing Films. *Polymers for Advanced Technologies* **2002**, 13, (10-12), 798-816.
3. Byrne, M. E.; Park, K.; Peppas, N. A., Molecular Imprinting within Hydrogels. *Advanced Drug Delivery Reviews* **2002**, 54, (1), 149-161.
4. Hilt, J. Z.; Byrne, M. E., Configurational Biomimesis in Drug delivery: Molecular Imprinting of Biologically Significant Molecules. *Advanced Drug Delivery Reviews* **2004**, 56, (11), 1599-1620.
5. Hilt, J. Z.; Byrne, M. E.; Peppas, N. A., Microfabrication of Intelligent Biomimetic Networks for Recognition of D-Glucose. *Chem. Mater.* **2006**, 18, (25), 5869-5875.
6. Venkatesh, S.; Sizemore, S. P.; Byrne, M. E., Biomimetic Hydrogels for Enhanced Loading and Extended Release of Ocular Therapeutics. *Biomaterials* **2007**, 28, (4), 717-724.
7. Sellergren, B., Noncovalent Molecular Imprinting: Antibody-like Molecular Recognition in Polymeric Network Materials. *TrAC Trends in Analytical Chemistry* **1997**, 16, (6), 310-320.
8. Sellergren, B., Enantioselectivity and Binding Capacity of Polymers Prepared under Conditions Favoring the Formation of Template Complexes. *Die Makromolekulare Chemie* **1989**, 190, 2703-2711.
9. Shea, K. J.; Spivak, D. A.; Sellergren, B., Polymer Complements to Nucleotide Bases. Selective Binding of Adenine Derivatives to Imprinted Polymers. *J. Am. Chem. Soc.* **1993**, 115, (8), 3368-3369.

10. Sulitzky, C.; Ruckert, B.; Hall, A. J.; Lanza, F.; Unger, K.; Sellergren, B., Grafting of Molecularly Imprinted Polymer Films on Silica Supports Containing Surface-Bound Free Radical Initiators. *Macromolecules* **2002**, 35, (1), 79-91.
11. Tamayo, F. G.; Titirici, M. M.; Martin-Esteban, A.; Sellergren, B., Synthesis and Evaluation of New Propazine-imprinted Polymer Formats for Use as Stationary Phases in Liquid Chromatography. *Analytica Chimica Acta* **2005**, 542, (1), 38-46.
12. Titirici, M. M.; Sellergren, B., Thin Molecularly Imprinted Polymer Films via Reversible Addition-Fragmentation Chain Transfer Polymerization. *Chemistry of Materials* **2006**, 18, (7), 1773-1779.
13. Urraca, J. L.; Moreno-Bondi, M. C.; Hall, A. J.; Sellergren, B., Direct Extraction of Penicillin G and Derivatives from Aqueous Samples Using a Stoichiometrically Imprinted Polymer. *Analytical Chemistry* **2007**, 79, (2), 695-701.
14. Mathew-Krotz, J.; Shea, K. J., Imprinted Polymer Membranes for the Selective Transport of Targeted Neutral Molecules. *J. Am. Chem. Soc.* **1996**, 118, (34), 8154-8155.
15. Spivak, D.; Gilmore, M. A.; Shea, K. J., Evaluation of Binding and Origins of Specificity of 9-Ethyladenine Imprinted Polymers. *J. Am. Chem. Soc.* **1997**, 119, (19), 4388-4393.
16. Spivak, D.; Shea, K. J., Molecular Imprinting of Carboxylic Acids Employing Novel Functional Macroporous Polymers. *J. Org. Chem.* **1999**, 64, (13), 4627-4634.
17. Spivak, D. A.; Shea, K. J., Investigation into the Scope and Limitations of Molecular Imprinting with DNA Molecules. *Analytica Chimica Acta* **2001**, 435, (1), 65-74.

18. Spivak, D. A.; Shea, K. J., Binding of Nucleotide Bases by Imprinted Polymers. *Macromolecules* **1998**, 31, (7), 2160-2165.
19. Wulff, G., Molecular Imprinting in Cross-Linked Materials with the Aid of Molecular Templates - A Way towards Artificial Antibodies. *Angewandte Chemie International Edition in English* **1995**, 34, (17), 1812-1832.
20. Hedin-Dahlstrom, J.; Rosengren-Holmberg, J. P.; Legrand, S.; Wikman, S.; Nicholls, I. A., A Class II Aldolase Mimic *J. Org. Chem.* **2006**, 71, (13), 4845-4853.
21. Allcock, H. R.; Lampe, F. W., *Contemporary Polymer Chemistry*. 2 ed.; Prentice Hall: Englewood Cliffs, 1990.
22. Vaughan, A. D.; Sizemore, S. P.; Byrne, M. E., Enhancing Molecularly Imprinted Polymer Binding Properties via Controlled/living Radical Polymerization and Reaction Analysis. *Polymer* **2007**, 48, (1), 74-81.
23. Bergmann, N. M.; Peppas, N. A., Molecularly Imprinted Polymers with Specific Recognition for Macromolecules and Proteins. *Progress in Polymer Science* **2008**, 33, (3), 271-288.
24. Chen, R.; Wang, C.; Huang, Y.; Le, H., An Efficient Biomimetic Process for Fabrication of Artificial Nacre with Ordered-nanostructure. *Materials Science and Engineering: C* **2008**, 28, (2), 218-222.
25. Gelinsky, M.; Welzel, P. B.; Simon, P.; Bernhardt, A.; Konig, U., Porous Three-dimensional Scaffolds Made of Mineralised Collagen: Preparation and Properties of a Biomimetic Nanocomposite Material for Tissue Engineering of Bone. *Chemical Engineering Journal* **2008**, 137, (1), 84-96.

26. Gorbatchuk, V. V.; Mironov, N. A.; Solomonov, B. N.; Habicher, W. D., Biomimetic Cooperative Interactions of Dried Cross-Linked Poly(N-6-aminohexylacrylamide) with Binary Mixtures of Solvent Vapors. *Biomacromolecules* **2004**, 5, (4), 1615-1623.
27. Huang, C. P.; Chen, X. M.; Chen, Z. Q., Biomimetic Construction of Poly(3-hydroxybutyrate-co-3-hydroxyvalerate)/apatite Composite Materials by an Alternate Incubation Process. *Materials Letters* **2008**, 62, (10-11), 1499-1502.
28. Ma, P. X., Biomimetic Materials for Tissue Engineering. *Advanced Drug Delivery Reviews* **2008**, 60, (2), 184-198.
29. Mahony, J. O.; Nolan, K.; Smyth, M. R.; Mizaikoff, B., Molecularly Imprinted Polymers--Potential and Challenges in Analytical Chemistry. *Analytica Chimica Acta* **2005**, 534, (1), 31-39.
30. Holthoff, E. L.; Bright, F. V., Molecularly Imprinted Xerogels as Platforms for Sensing. *Accounts of Chemical Research* **2007**, 40, (9), 756-767.
31. Wulff, G.; Poll, H.-G., Enzyme-analogue Built Polymers, 23. Influence of the Structure of the Binding Sites on the Selectivity for Racemic Resolution. *Die Makromolekulare Chemie* **1987**, 188, (4), 741-748.
32. Wulff, G.; Vietmeier, J.; Poll, H.-G., Enzyme-analogue Built Polymers, 22. Influence of the Nature of the Crosslinking Agent on the Performance of Imprinted Polymers in Racemic Resolution. *Die Makromolekulare Chemie* **1987**, 188, (4), 731-740.
33. Pande, V. S.; Grosberg, A. Y.; Tanaka, T., Phase Diagram of Heteropolymers with an Imprinted Conformation. *Macromolecules* **1995**, 28, (7), 2218-2227.

34. Glad, M.; Norrlow, O.; Sellergren, B.; Siegbahn, N.; Mosbach, K., Use of Silane Monomers for Molecular Imprinting and Enzyme Entrapment in Polysiloxane-coated Porous Silica. *Journal of Chromatography A* **1985**, 347, 11-23.
35. Norrlow, O.; Glad, M.; Mosbach, K., Acrylic Polymer Preparations Containing Recognition Sites Obtained by Imprinting with Substrates. *Journal of Chromatography A* **1984**, 299, 29-41.
36. O'Shannessy, D. J.; Ekberg, B.; Andersson, L. I.; Mosbach, K., Recent Advances in the Preparation and Use of Molecularly Imprinted Polymers for Enantiomeric Resolution of Amino Acid Derivatives. *Journal of Chromatography A* **1989**, 470, (2), 391-399.
37. Sellergren, B.; Lepistoe, M.; Mosbach, K., Highly Enantioselective and Substrate-selective Polymers Obtained by Molecular Imprinting utilizing Noncovalent Interactions. NMR and Chromatographic Studies on the Nature of Recognition. *Journal of the American Chemical Society* **1988**, 110, (17), 5853-5860.
38. Weber, P. C.; Ohlendorf, D. H.; Wendoloski, J. J.; Salemme, F. R., Structural Origins of High-affinity Biotin Binding to Streptavidin. *Science* **1989**, 243, 85-88.
39. Svenson, J.; Nicholls, I. A., On the Thermal and Chemical Stability of Molecularly Imprinted Polymers. *Analytica Chimica Acta* **2001**, 435, (1), 19-24.
40. Anderson, L. I.; Muller, R.; Vlatakis, G.; Mosbach, K., Mimics of the Binding Sites of Opioid Receptors Obtained by Molecular Imprinting of Enkephalin and Morphine. *Proceedings of the National Academies of Sciences* **1995**, 92, (11), 4788-4792.

41. Shi, X.; Wu, A.; Qu, G.; Li, R.; Zhang, D., Development and Characterisation of Molecularly Imprinted Polymers based on Methacrylic Acid for Selective Recognition of Drugs. *Biomaterials* **2007**, 28, (25), 3741-3749.
42. Lin, L.-Q.; Li, Y.-C.; Fu, Q.; He, L.-C.; Zhang, J.; Zhang, Q.-Q., Preparation of Molecularly Imprinted Polymer for Sinomenine and Study on its Molecular Recognition Mechanism. *Polymer* **2006**, 47, (11), 3792-3798.
43. Fast And Cost-effective Molecularly Imprinted Polymer Technique Has Applications In Testing Of Tobacco-specific Nitrosamines In Urine. <http://www.medicalnewstoday.com/articles/71882.php> (03-15-08),
44. MIP Technologies and Supelco Launch a New Selective SPE Product for the Extraction of Amphetamine and Related Drugs. http://www.miptechnologies.com/pdf/080110_Amphetamines.pdf (03-15-08),
45. Nicholls, I. A., An Approach Toward the Semiquantitation of Molecular Recognition Phenomena in Non-Covalent Molecularly Imprinted Polymer Systems: Consequences for Molecularly Imprinted Polymer Design. *Advances in Molecular and Cell Biology* **1996**, 15B, 671-679.
46. Cera, E. D., *Thermodynamic Theory of Site-Specific Binding Processes in Biological Macromolecules*. Cambridge University Press: New York, 1995.
47. Lavignac, N.; Allender, C. J.; Brain, K. R., Current Status of Molecularly Imprinted Polymers as Alternatives to Antibodies in Sorbent Assays. *Analytica Chimica Acta* **2004**, 510, (2), 139-145.
48. Alvarez-Lorenzo, C.; Concheiro, A., Molecularly Imprinted Polymers for Drug Delivery. *Journal of Chromatography B* **2004**, 804, (1), 231-245.

49. Kempe, H.; Kempe, M., Development and Evaluation of Spherical Molecularly Imprinted Polymer Beads. *Analytical Chemistry* **2006**, 78, (11), 3659-3666.
50. Chronakis, I. S.; Jakob, A.; Hagstrom, B.; Ye, L., Encapsulation and Selective Recognition of Molecularly Imprinted Theophylline and Estradiol Nanoparticles within Electrospun Polymer Nanofibers. *Langmuir* **2006**, 22, (21), 8960-8965.
51. Mazzotta, E.; Picca, R. A.; Malitesta, C.; Piletsky, S. A.; Piletska, E. V., Development of a Sensor Prepared by Entrapment of MIP Particles in Electrosynthesised Polymer Films for Electrochemical Detection of Ephedrine. *Biosensors and Bioelectronics* **2008**, 23, (7), 1152-1156.
52. Li, F.; Li, J.; Zhang, S., Molecularly Imprinted Polymer Grafted on Polysaccharide Microsphere Surface by the Sol-gel Process for Protein Recognition. *Talanta* **2008**, 74, (5), 1247-1255.
53. Bossi, A.; Bonini, F.; Turner, A. P. F.; Piletsky, S. A., Molecularly Imprinted Polymers for the Recognition of Proteins: The State of the Art. *Biosensors and Bioelectronics* **2007**, 22, (6), 1131-1137.
54. Qin, L.; He, X.-W.; Li, W.-Y.; Zhang, Y.-K., Molecularly Imprinted Polymer Prepared with Bonded [Beta]-cyclodextrin and Acrylamide on Functionalized Silica Gel for Selective Recognition of Tryptophan in Aqueous Media. *Journal of Chromatography A* **2008**, 1187, (2), 94-102.
55. Javanbakht, M.; Fard, S. E.; Mohammadi, A.; Abdouss, M.; Ganjali, M. R.; Norouzi, P.; Safaraliev, L., Molecularly Imprinted Polymer Based Potentiometric Sensor for the Determination of Hydroxyzine in Tablets and Biological Fluids. *Analytica Chimica Acta* **2008**, 612, (1), 65-74.

56. Rajkumar, R.; Katterle, M.; Warsinke, A.; Mohwald, H.; Scheller, F. W., Thermometric MIP Sensor for Fructosyl Valine. *Biosensors and Bioelectronics* **2008**, *23*, (7), 1195-1199.
57. Gonzalez, G. P.; Hernando, P. F.; Alegria, J. S. D., Determination of Digoxin in Serum Samples using a Flow-through Fluorosensor based on a Molecularly Imprinted Polymer. *Biosensors and Bioelectronics* **2008**, *23*, (11), 1754-1758.
58. Diltemiz, S. E.; Say, R.; Buyuktiryaki, S.; Hur, D.; Denizli, A.; Ersoz, A., Quantum Dot Nanocrystals having Guanosine Imprinted Nanoshell for DNA Recognition. *Talanta* **2008**, *74*, (4), 890-896.
59. Sumi, V. S.; Kala, R.; Praveen, R. S.; Prasada Rao, T., Imprinted Polymers as Drug Delivery Vehicles for Metal-based Anti-inflammatory Drug. *International Journal of Pharmaceutics* **2008**, *349*, (1-2), 30-37.
60. Venkatesh, S.; Saha, J.; Pass, S.; Byrne, M. E., Transport and Structural Analysis of Molecular Imprinted Hydrogels for Controlled Drug Delivery. *European Journal of Pharmaceutics and Biopharmaceutics* **2008**, doi: 10.1016/j.ejpb.2008.01.036.
61. Kim, J.; Chauhan, A., Dexamethasone Transport and Ocular Delivery from Poly(hydroxyethyl methacrylate) Gels. *International Journal of Pharmaceutics* **2008**, *353*, (2), 205-222.
62. Alvarez-Lorenzo, C.; Yanez, F.; Barreiro-Iglesias, R.; Concheiro, A., Imprinted Soft Contact Lenses as Norfloxacin Delivery Systems. *Journal of Controlled Release* **2006**, *113*, (3), 236-244.

63. Hiratani, H.; Fujiwara, A.; Tamiya, Y.; Mizutani, Y.; Alvarez-Lorenzo, C., Ocular Release of Timolol from Molecularly Imprinted Soft Contact Lenses. *Biomaterials* **2005**, 26, (11), 1293-1298.
64. Henthorn, D. B.; Peppas, N. A., Molecular Simulations of Recognitive Behavior of Molecularly Imprinted Intelligent Polymeric Networks. *Ind. Eng. Chem. Res.* **2007**, 46, (19), 6084-6091.
65. Lovell, L. G.; Lu, H.; Elliott, J. E.; Stansbury, J. W.; Bowman, C. N., The Effect of Cure Rate on the Mechanical Properties of Dental Resins. *Dental Materials* **2001**, 17, (6), 504-511.
66. Lecamp, L.; Youssef, B.; Bunel, C.; Lebaudy, P., Photoinitiated polymerization of a dimethacrylate oligomer: 1. Influence of Photoinitiator Concentration, Temperature and Light intensity. *Polymer* **1997**, 38, (25), 6089-6096.
67. Cook, W. D.; Simon, G. P.; Burchill, P. J.; Lau, M.; Fitch, T. J., Curing Kinetics and Thermal Properties of Vinyl Ester Resins. *Journal of Applied Polymer Science* **1997**, 64, (4), 769-781.
68. Sperling, L. H., *Introduction to Physical Polymer Science*. 4th ed.; John Wiley & Sons, Inc: Hoboken, 2005.
69. Wang, S.; Xu, Z.; Fang, G.; Duan, Z.; Zhang, Y.; Chen, S., Synthesis and Characterization of a Molecularly Imprinted Silica Gel Sorbent for the On-Line Determination of Trace Sudan I in Chilli Powder through High-Performance Liquid Chromatography. *J. Agric. Food Chem.* **2007**, 55, (10), 3869-3876.

70. Bolisay, L. D.; Culver, J. N.; Kofinas, P., Optimization of Virus Imprinting Methods To Improve Selectivity and Reduce Nonspecific Binding. *Biomacromolecules* **2007**, 8, (12), 3893-3899.
71. Philip, J. Y. N.; Buchweishaija, J.; Mkyula, L. L.; Ye, L., Preparation of Molecularly Imprinted Polymers Using Anacardic Acid Monomers Derived from Cashew Nut Shell Liquid. *J. Agric. Food Chem.* **2007**, 55, (22), 8870-8876.
72. Haruki, M.; Konnai, Y.; Shimada, A.; Takeuchi, H., Molecularly Imprinted Polymer-Assisted Refolding of Lysozyme. *Biotechnol. Prog.* **2007**, 23, (5), 1254-1257.
73. Song, S.; Shirasaka, K.; Katayama, M.; Nagaoka, S.; Yoshihara, S.; Osawa, T.; Sumaoka, J.; Asanuma, H.; Komiyama, M., Recognition of Solution Structures of Peptides by Molecularly Imprinted Cyclodextrin Polymers. *Macromolecules* **2007**, 40, (10), 3530-3532.
74. Delaney, T. L.; Zimin, D.; Rahm, M.; Weiss, D.; Wolfbeis, O. S.; Mirsky, V. M., Capacitive Detection in Ultrathin Chemosensors Prepared by Molecularly Imprinted Grafting Photopolymerization. *Anal. Chem.* **2007**, 79, (8), 3220-3225.
75. Turner, N. W.; Liu, X.; Piletsky, S. A.; Hlady, V.; Britt, D. W., Recognition of Conformational Changes in α -Lactoglobulin by Molecularly Imprinted Thin Films *Biomacromolecules* **2007**, 8, (9), 2781-2787.
76. O'Connor, N. A.; Paisner, D. A.; Huryn, D.; Shea, K. J., Screening of 5-HT_{1A} Receptor Antagonists using Molecularly Imprinted Polymers. *J. Am. Chem. Soc.* **2007**, 129, (6), 1680-1689.

77. Gao, D.; Zhang, Z.; Wu, M.; Xie, C.; Guan, G.; Wang, D., A Surface Functional Monomer-Directing Strategy for Highly Dense Imprinting of TNT at Surface of Silica Nanoparticles. *J. Am. Chem. Soc.* **2007**, 129, (25), 7859-7866.
78. Li, J.; Kendig, C. E.; Nesterov, E. E., Chemosensory Performance of Molecularly Imprinted Fluorescent Conjugated Polymer Materials. *J. Am. Chem. Soc.* **2007**, 129, (51), 15911-15918.
79. Matsui, J.; Goji, S.; Murashima, T.; Miyoshi, D.; Komai, S.; Shigeyasu, A.; Kushida, T.; Miyazawa, T.; Yamada, T.; Tamaki, K.; Sugimoto, N., Molecular Imprinting under Molecular Crowding Conditions: An Aid to the Synthesis of a High-Capacity Polymeric Sorbent for Triazine Herbicides. *Anal. Chem.* **2007**, 79, (4), 1749-1757.
80. Kimhi, O.; Bianco-Peled, H., Study of the Interactions between Protein-Imprinted Hydrogels and Their Templates. *Langmuir* **2007**, 23, (11), 6329-6335.
81. Koesdjojo, M. T.; Rasmussen, H. T.; Fermier, A. M.; Patel, P.; Remcho, V. T., The Development of a Semiautomated Procedure for the Synthesis and Screening of a Large Group of Molecularly Imprinted Polymers. *J. Comb. Chem.* **2007**, 9, (6), 929-934.
82. Shamsipur, M.; Fasihi, J.; Ashtari, K., Grafting of Ion-Imprinted Polymers on the Surface of Silica Gel Particles through Covalently Surface-Bound Initiators: A Selective Sorbent for Uranyl Ion. *Anal. Chem.* **2007**, 79, (18), 7116-7123.
83. Wei, X.; Husson, S. M., Surface-Grafted, Molecularly Imprinted Polymers Grown from Silica Gel for Chromatographic Separations. *Ind. Eng. Chem. Res.* **2007**, 46, (7), 2117-2124.

84. Southard, G. E.; VanHouten, K. A.; Murray, G. M., Soluble and Processable Phosphonate Sensing Star Molecularly Imprinted Polymers. *Macromolecules* **2007**, *40*, (5), 1395-1400.
85. Urraca, J. L.; Moreno-Bondi, M. C.; Orellana, G.; Sellergren, B.; Hall, A. J., Molecularly Imprinted Polymers as Antibody Mimics in Automated On-Line Fluorescent Competitive Assays. *Anal. Chem.* **2007**, *79*, (13), 4915-4923.
86. Turiel, E.; Tadeo, J. L.; Martin-Esteban, A., Molecularly Imprinted Polymeric Fibers for Solid-Phase Microextraction. *Anal. Chem.* **2007**, *79*, (8), 3099-3104.
87. Tan, C. J.; Tong, Y. W., The Effect of Protein Structural Conformation on Nanoparticle Molecular Imprinting of Ribonuclease A Using Miniemulsion Polymerization. *Langmuir* **2007**, *23*, (5), 2722-2730.
88. Tan, C. J.; Tong, Y. W., Preparation of Superparamagnetic Ribonuclease A Surface-Imprinted Submicrometer Particles for Protein Recognition in Aqueous Media. *Anal. Chem.* **2007**, *79*, (1), 299-306.
89. Ariffin, M. M.; Miller, E. I.; Cormack, P. A. G.; Anderson, R. A., Molecularly Imprinted Solid-Phase Extraction of Diazepam and Its Metabolites from Hair Samples. *Anal. Chem.* **2007**, *79*, (1), 256-262.
90. Baydemir, G.; Andac, M.; Bereli, N.; Say, R.; Denizli, A., Selective Removal of Bilirubin from Human Plasma with Bilirubin-Imprinted Particles. *Ind. Eng. Chem. Res.* **2007**, *46*, (9), 2843-2852.
91. Nemoto, K.; Kubo, T.; Nomachi, M.; Sano, T.; Matsumoto, T.; Hosoya, K.; Hattori, T.; Kaya, K., Simple and Effective 3D Recognition of Domoic Acid Using a Molecularly Imprinted Polymer. *J. Am. Chem. Soc.* **2007**, *129*, (44), 13626-13632.

92. Lu, C. H.; Zhou, W. H.; Han, B.; Yang, H. H.; Chen, X.; Wang, X. R., Surface-Imprinted Core-Shell Nanoparticles for Sorbent Assays. *Anal. Chem.* **2007**, 79, (14), 5457-5461.
93. Yan, H.; Qiao, F.; Row, K. H., Molecularly Imprinted-Matrix Solid-Phase Dispersion for Selective Extraction of Five Fluoroquinolones in Eggs and Tissue. *Anal. Chem.* **2007**, 79, (21), 8242-8248.
94. Turiel, E.; Martin-Esteban, A.; Tadeo, J. L., Molecular Imprinting-based Separation Methods for Selective Analysis of Fluoroquinolones in Soils. *Journal of Chromatography A* **2007**, 1172, (2), 97-104.
95. Guardia, L.; Badia, R.; Diaz-Garcia, M. E., Molecularly Imprinted Sol-Gels for Nafcillin Determination in Milk-Based Products. *J. Agric. Food Chem.* **2007**, 55, (3), 566-570.
96. Espinosa-Garcia, B. M.; Arguelles-Monal, W. M.; Hernandez, J.; Felix-Valenzuela, L.; Acosta, N.; Goycoolea, F. M., Molecularly Imprinted Chitosan-Genipin Hydrogels with Recognition Capacity toward o-Xylene. *Biomacromolecules* **2007**, 8, (11), 3355-3364.
97. Gabashvili, A.; Medina, D. D.; Gedanken, A.; Mastai, Y., Templating Mesoporous Silica with Chiral Block Copolymers and Its Application for Enantioselective Separation. *J. Phys. Chem. B* **2007**, 111, (38), 11105-11110.
98. Mohamed, R.; Richoz-Payot, J.; Gremaud, E.; Mottier, P.; Yilmaz, E.; Tabet, J. C.; Guy, P. A., Advantages of Molecularly Imprinted Polymers LC-ESI-MS/MS for the Selective Extraction and Quantification of Chloramphenicol in Milk-Based Matrixes. Comparison with a Classical Sample Preparation. *Anal. Chem.* **2007**, 79, (24), 9557-9565.

99. Boyd, B.; Bjork, H.; Billing, J.; Shimelis, O.; Axelsson, S.; Leonora, M.; Yilmaz, E., Development of an Improved Method for Trace Analysis of Chloramphenicol using Molecularly Imprinted Polymers. *Journal of Chromatography A* **2007**, 1174, (1-2), 63-71.
100. Bi, X.; Lau, R. J.; Yang, K. L., Preparation of Ion-Imprinted Silica Gels Functionalized with Glycine, Diglycine, and Triglycine and Their Adsorption Properties for Copper Ions. *Langmuir* **2007**, 23, (15), 8079-8086.
101. Papadopoulos, N.; Gikas, E.; Zalidis, G.; Tsarbopoulos, A., Simultaneous Determination of Terbutylazine and Its Major Hydroxy and Dealkylated Metabolites in Wetland Water Samples Using Solid-Phase Extraction and High-Performance Liquid Chromatography with Diode-Array Detection. *J. Agric. Food Chem.* **2007**, 55, (18), 7270-7277.
102. Chen, H.; Peng, C.; Ye, Z.; Liu, H.; Hu, Y.; Jiang, J., Recognition of Multiblock Copolymers on Nanopatterned Surfaces: Insight from Molecular Simulations. *Langmuir* **2007**, 23, (5), 2430-2436.
103. Clapper, J. D.; Iverson, S. L.; Guymon, C. A., Nanostructured Biodegradable Polymer Networks Using Lyotropic Liquid Crystalline Templates. *Biomacromolecules* **2007**, 8, (7), 2104-2111.
104. Pijls, R. T.; Cruysberg, L. P. J.; Nuijts, R. M. M. A.; Dias, A. A.; Koole, L. H., Capacity and Tolerance of a New Device for Ocular Drug Delivery. *International Journal of Pharmaceutics* **2007**, 341, (1-2), 152-161.
105. He, Q.; Chang, X.; Wu, Q.; Huang, X.; Hu, Z.; Zhai, Y., Synthesis and Applications of Surface-grafted Th(IV)-imprinted Polymers for Selective Solid-phase Extraction of Thorium(IV). *Analytica Chimica Acta* **2007**, 605, (2), 192-197.

106. Jing, T.; Gao, X. D.; Wang, P.; Wang, Y.; Lin, Y. F.; zong, X. C.; Zhou, Y. K.; Mei, S. R., Preparation of High Selective Molecularly Imprinted Polymers for Tetracycline by Precipitation Polymerization. *Chinese Chemical Letters* **2007**, 18, (12), 1535-1538.
107. Prasad, B. B.; Sharma, P. S.; Lakshmi, D., Molecularly Imprinted Polymer-based Solid-phase Extraction Combined with Molecularly Imprinted Polymer-based Sensor for Detection of Uric Acid. *Journal of Chromatography A* **2007**, 1173, (1-2), 18-26.
108. Claude, B.; Morin, P.; Lafosse, M.; Belmont, A.-S.; Haupt, K., Selective Solid-phase Extraction of a Triterpene Acid from a Plant Extract by Molecularly Imprinted Polymer. *Talanta* **2008**, 75, (2), 344-350.
109. Xu, Z.; Kuang, D.; Liu, L.; Deng, Q., Selective Adsorption of Norfloxacin in Aqueous Media by an Imprinted Polymer based on Hydrophobic and Electrostatic Interactions. *Journal of Pharmaceutical and Biomedical Analysis* **2007**, 45, (1), 54-61.
110. Yan, H.; Row, K. H.; Yang, G., Water-Compatible Molecularly Imprinted Polymers for Selective Extraction of Ciprofloxacin from Human Urine. *Talanta* **2008**, 75, (1), 227-232.
111. Gros, M.; Pizzolato, T.-M.; Petrovic, M.; de Alda, M. J. L.; Barcelo, D., Trace Level Determination of [Beta]-blockers in Waste Waters by Highly Selective Molecularly Imprinted Polymers Extraction followed by liquid Chromatography-Quadrupole-Linear Ion Trap Mass Spectrometry. *Journal of Chromatography A* **2008**, 1189, (2), 374-384.

112. Lv, Y.; Lin, Z.; Feng, W.; Zhou, X.; Tan, T., Selective Recognition and Large Enrichment of Dimethoate from Tea Leaves by Molecularly Imprinted Polymers. *Biochemical Engineering Journal* **2007**, 36, (3), 221-229.
113. Sadeghi, S.; Mofrad, A. A., Synthesis of a New Ion Imprinted Polymer Material for Separation and Preconcentration of Traces of Uranyl Ions. *Reactive and Functional Polymers* **2007**, 67, (10), 966-976.
114. Wei, S.; Mizaikoff, B., Binding Site Characteristics of 17[beta]-estradiol Imprinted Polymers. *Biosensors and Bioelectronics* **2007**, 23, (2), 201-209.
115. Djozan, D.; Baheri, T., Preparation and Evaluation of Solid-phase Microextraction Fibers Based on Monolithic Molecularly Imprinted Polymers for Selective Extraction of Diacetylmorphine and Analogous Compounds. *Journal of Chromatography A* **2007**, 1166, (1-2), 16-23.
116. Gomez-Caballero, A.; Unceta, N.; Aranzazu Goicolea, M.; Barrio, R. J., Evaluation of the Selective Detection of 4,6-dinitro-o-cresol by a Molecularly Imprinted Polymer Based Microsensor Electrosynthesized in a Semiorganic Media. *Sensors and Actuators B: Chemical* **2008**, 130, (2), 713-722.
117. Lin, Y.; Shi, Y.; Jiang, M.; Jin, Y.; Peng, Y.; Lu, B.; Dai, K., Removal of Phenolic Estrogen Pollutants From Different Sources of Water using Molecularly Imprinted Polymeric Microspheres. *Environmental Pollution* **2008**, 153, (2), 483-491.
118. Maury, D.; Couderc, F.; Garrigues, J. C.; Poinot, V., Synthesis and Evaluation of New Lipomonosaccharide-imprinted Polymers as MISPE Supports. *Talanta* **2007**, 73, (2), 340-345.

119. Kan, X.; Zhao, Q.; Zhang, Z.; Wang, Z.; Zhu, J.-J., Molecularly Imprinted Polymers Microsphere prepared by Precipitation Polymerization for Hydroquinone Recognition. *Talanta* **2008**, 75, (1), 22-26.
120. Panahi, R.; Vasheghani-Farahani, E.; Shojaosadati, S. A., Separation of l-lysine from Dilute Aqueous Solution using Molecular Imprinting Technique. *Biochemical Engineering Journal* **2007**, 35, (3), 352-356.
121. Flory, P. J., *Principles of Polymer Chemistry*. 1st ed.; Cornell University Press: Ithica, 1953; p 663.
122. Odian, G., *Principles of Polymerization*. 2cd edition ed.; John Wiley & Sons: New York, 1981.
123. Bruice, P. Y., *Organic Chemistry*. 4th ed.; Pearson/Prentice Hall: Upper Saddle River, 2004.
124. Khutoryanskiy, V. V.; Dubolazov, A. V.; Nurkeeva, Z. S.; Mun, G. A., pH Effects in the Complex Formation and Blending of Poly(acrylic acid) with Poly(ethylene oxide). *Langmuir* **2004**, 20, (9), 3785-3790.
125. Rampey, A. M.; Umpleby, R. J.; Rushton, G. T.; Iseman, J. C.; Shah, R. N.; Shimizu, K. D., Characterization of the Imprint Effect and the Influence of Imprinting Conditions on Affinity, Capacity, and Heterogeneity in Molecularly Imprinted Polymers Using the Freundlich Isotherm-Affinity Distribution Analysis. *Anal. Chem.* **2004**, 76, (4), 1123-1133.
126. Piletsky, S. A.; Mijangos, I.; Guerreiro, A.; Piletska, E. V.; Chianella, I.; Karim, K.; Turner, A. P. F., Polymer Cookery: Influence of Polymerization Time and Different

Initiation Conditions on Performance of Molecularly Imprinted Polymers. *Macromolecules* **2005**, 38, (4), 1410-1414.

127. Piletsky, S. A.; Piletska, E. V.; Karim, K.; Freebairn, K. W.; Legge, C. H.; Turner, A. P. F., Polymer Cookery: Influence of Polymerization Conditions on the Performance of Molecularly Imprinted Polymers. *Macromolecules* **2002**, 35, (19), 7499-7504.

128. Ishiduki, K.; Esumi, K., The Effect of pH on Adsorption of Poly(acrylic acid) and Poly(vinylpyrrolidone) on Alumina from Their Binary Mixtures. *Langmuir* **1997**, 13, (6), 1587-1591.

129. Dowding, P. J.; Atkin, R.; Vincent, B.; Bouillot, P., Oil Core/Polymer Shell Microcapsules by Internal Phase Separation from Emulsion Droplets. II: Controlling the Release Profile of Active Molecules. *Langmuir* **2005**, 21, (12), 5278-5284.

130. Brazel, C. S.; Peppas, N. A., Synthesis and Characterization of Thermo- and Chemomechanically Responsive Poly(N-isopropylacrylamide-co-methacrylic acid) Hydrogels. *Macromolecules* **1995**, 28, (24), 8016-8020.

131. Small, H., Chemical Modification of Crosslinked Polymers. New Approach to Synthesis of Ion Exchange and Chelating Resins. *Ind. Eng. Chem. Prod. Res. Dev.* **1967**, 6, (3), 147-150.

132. Watkins, A. W.; Anseth, K. S., Investigation of Molecular Transport and Distributions in Poly(ethylene glycol) Hydrogels with Confocal Laser Scanning Microscopy. *Macromolecules* **2005**, 38, (4), 1326-1334.

133. Saha, B.; Streat, M., Adsorption of Trace Heavy Metals: Application of Surface Complexation Theory to a Macroporous Polymer and a Weakly Acidic Ion-Exchange Resin. *Ind. Eng. Chem. Res.* **2005**, 44, (23), 8671-8681.

134. Figuly, G. D.; Royce, S. D.; Khasat, N. P.; Schock, L. E.; Wu, S. D.; Davidson, F.; Campbell, G. C.; Keating, M. Y.; Chen, H. W.; Shimshick, E. J.; Fischer, R. T.; Grimminger, L. C.; Thomas, B. E.; Smith, L. H.; Gillies, P. J., Preparation and Characterization of Novel Poly(alkylamine)-Based Hydrogels Designed for Use as Bile Acid Sequestrants. *Macromolecules* **1997**, 30, (20), 6174-6184.
135. Spizzirri, U. G.; Peppas, N. A., Structural Analysis and Diffusional Behavior of Molecularly Imprinted Polymer Networks for Cholesterol Recognition. *Chem. Mater.* **2005**, 17, (26), 6719-6727.
136. Piletsky, S. A.; Andersson, H. S.; Nicholls, I. A., Combined Hydrophobic and Electrostatic Interaction-Based Recognition in Molecularly Imprinted Polymers. *Macromolecules* **1999**, 32, (3), 633-636.
137. Umpleby II, R. J.; Rushton, G. T.; Shah, R. N.; Rampey, A. M.; Bradshaw, J. C.; Berch, J. K.; Shimizu, K. D., Recognition Directed Site-Selective Chemical Modification of Molecularly Imprinted Polymers. *Macromolecules* **2001**, 34, (24), 8446-8452.
138. Piletsky, S. A.; Guerreiro, A.; Piletska, E. V.; Chianella, I.; Karim, K.; Turner, A. P. F., Polymer Cookery. 2. Influence of Polymerization Pressure and Polymer Swelling on the Performance of Molecularly Imprinted Polymers. *Macromolecules* **2004**, 37, (13), 5018-5022.
139. Mitchell-Koch, J. T.; Borovik, A. S., Immobilization of a Europium Salen Complex within Porous Organic Hosts: Modulation of Luminescence Properties in Different Chemical Environments. *Chem. Mater.* **2003**, 15, (18), 3490-3495.
140. Hapiot, P.; Moiroux, J.; Saveant, J. M., Electrochemistry of NADH/NAD⁺ analogs. A Detailed Mechanistic Kinetic and Thermodynamic Analysis of the 10-

methylacridan/10-methylacridinium Couple in Acetonitrile. *J. Am. Chem. Soc.* **1990**, 112, (4), 1337-1343.

141. Van de Grampel, H. T.; Tan, Y. Y.; Challa, G., Template Polymerization of N-vinylimidazole along Poly(methacrylic acid) in Water. 2. Kinetics of the Template Polymerization. *Macromolecules* **1991**, 24, (13), 3767-3772.

142. Van de Grampel, H. T.; Tan, Y. Y.; Challa, G., Template Polymerization of N-vinylimidazole along Poly(methacrylic acid) in Water. 4. Complex Formation between Poly(N-vinylimidazole) and Poly(methacrylic acid). *Macromolecules* **1992**, 25, (3), 1041-1048.

143. Kim, H.; Spivak, D. A., New Insight into Modeling Non-Covalently Imprinted Polymers. *J. Am. Chem. Soc.* **2003**, 125, (37), 11269-11275.

144. Piletsky, S. A.; Piletskaya, E. V.; Sergeyeva, T. A.; Panasyuk, T. L.; El'skaya, A. V., Molecularly Imprinted Self-assembled Films with Specificity to Cholesterol. *Sensors and Actuators B: Chemical* **1999**, 60, (2-3), 216-220.

145. Sergeyeva, T. A.; Piletsky, S. A.; Brovko, A. A.; Slinchenko, E. A.; Sergeeva, L. M.; El'skaya, A. V., Selective Recognition of Atrazine by Molecularly Imprinted Polymer Membranes. Development of Conductometric Sensor for Herbicides Detection. *Analytica Chimica Acta* **1999**, 392, (2-3), 105-111.

146. Matsui, J.; Miyoshi, Y.; Doblhoff-Dier, O.; Takeuchi, T., A Molecularly Imprinted Synthetic Polymer Receptor Selective for Atrazine. *Anal. Chem.* **1995**, 67, (23), 4404-4408.

147. Haupt, K., Molecularly Imprinted Polymers: The Next Generation. *Analytical Chemistry A-pages* **2003**, 75, (17), 376A-383A.

148. Sibrian-Vazquez, M.; Spivak, D. A., Molecular Imprinting Made Easy. *J. Am. Chem. Soc.* **2004**, 126, (25), 7827-7833.
149. Yoshida, M.; Uezu, K.; Goto, M.; Furusaki, S., Required Properties for Functional Monomers To Produce a Metal Template Effect by a Surface Molecular Imprinting Technique. *Macromolecules* **1999**, 32, (4), 1237-1243.
150. Lovestead, T. M.; Berchtold, K. A.; Bowman, C. N., An Investigation of Chain Length Dependent Termination and Reaction Diffusion Controlled Termination during the Free Radical Photopolymerization of Multivinyl Monomers. *Macromolecules* **2005**, 38, (15), 6374-6381.
151. Lovestead, T. M.; Bowman, C. N., A Modeling Investigation of Chain Length Dependent Termination during Multivinyl Free Radical Chain Photopolymerizations: Accounting for the Gel. *Macromolecules* **2005**, 38, (11), 4913-4918.
152. Noss, K. R.; Vaughan, A. D.; Byrne, M. E., Tailored Binding and Transport Parameters of Molecularly Imprinted Films via Macromolecular Structure: The Rational Design of Recognitive Polymers. *Journal of Applied Polymer Science* **2008**, 107, (6), 3435-3441.
153. Schmuhl, N.; Davis, E.; Cheung, H. M., Morphology of Thermally Polymerized Microporous Polymer Materials Prepared from Methyl Methacrylate and 2-Hydroxyethyl Methacrylate Microemulsions. *Langmuir* **1998**, 14, (4), 757-761.
154. Bowman, C. N.; Peppas, N. A., Coupling of Kinetics and Volume Relaxation During Polymerizations of Multiacrylates and Multimethacrylates. *Macromolecules* **1991**, 24, (8), 1914-1920.

155. Anseth, K. S.; Kline, L. M.; Walker, T. A.; Anderson, K. J.; Bowman, C. N.,
Reaction Kinetics and Volume Relaxation during Polymerizations of Multiethylene
Glycol Dimethacrylates. *Macromolecules* **1995**, 28, (7), 2491-2499.

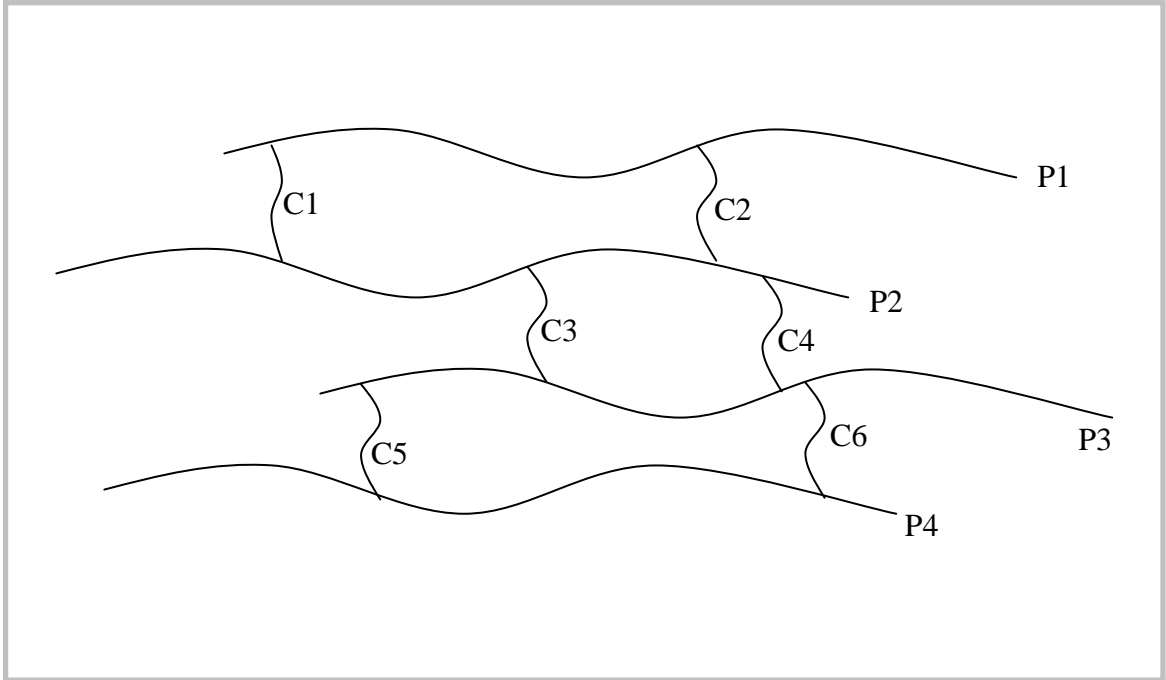


Figure 2.1. General Schematic of a Crosslinked Polymer Network. P1, P2, P3, and P4 represent four linear polymer chains within the network. C1, C2, C3, C4, C5, and C6 are the crosslinking monomer joining the four polymer chains together to form one large crosslinked macromolecule.

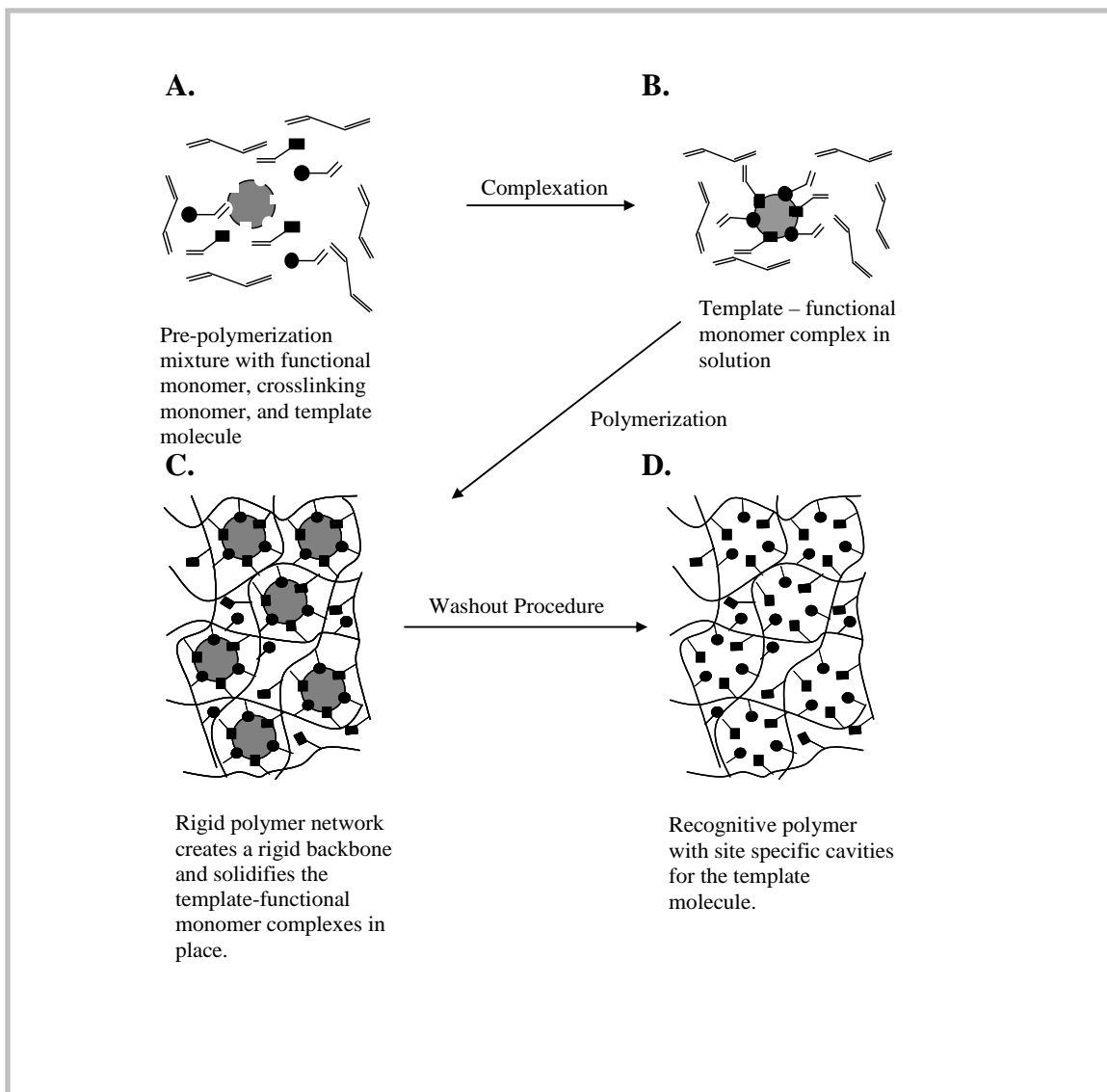


Figure 2.2. Recognitive Polymer Synthesis. **A.** Solution mixture of template, functional monomer(s) (squares and circles), crosslinking monomer, solvent, and initiator(s). **B.** The pre-polymerization complex is formed via covalent or non-covalent chemistry. **C.** The formation of the network (template mediated molecular imprinting process). **D.** Wash step where original template is removed.

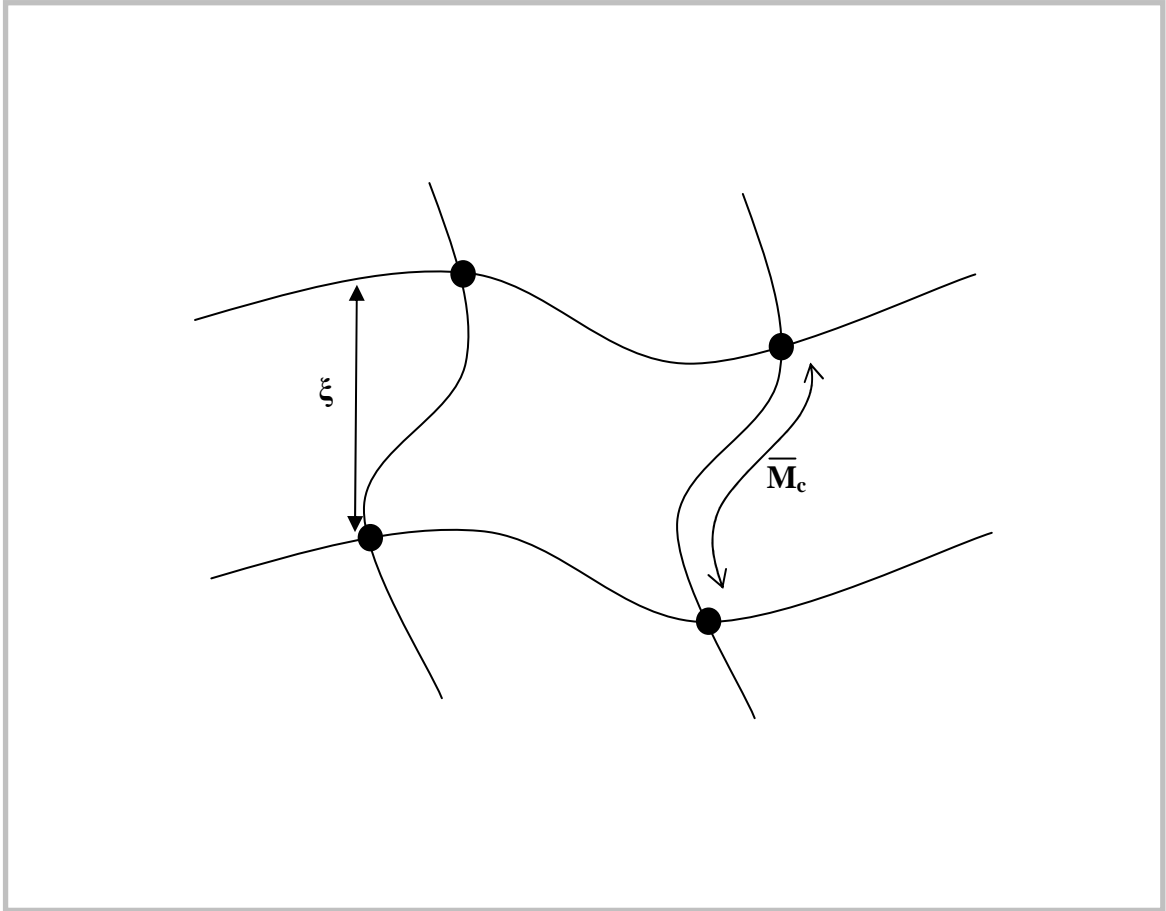


Figure 2.3. General Schematic of Mesh Size. The average mesh size (ξ) of the polymer represents the space available within the macromolecule for transport. The average molecular weight between crosslinks, \overline{M}_c , is represented by the molecular weight of the linear polymer between the linkage points.

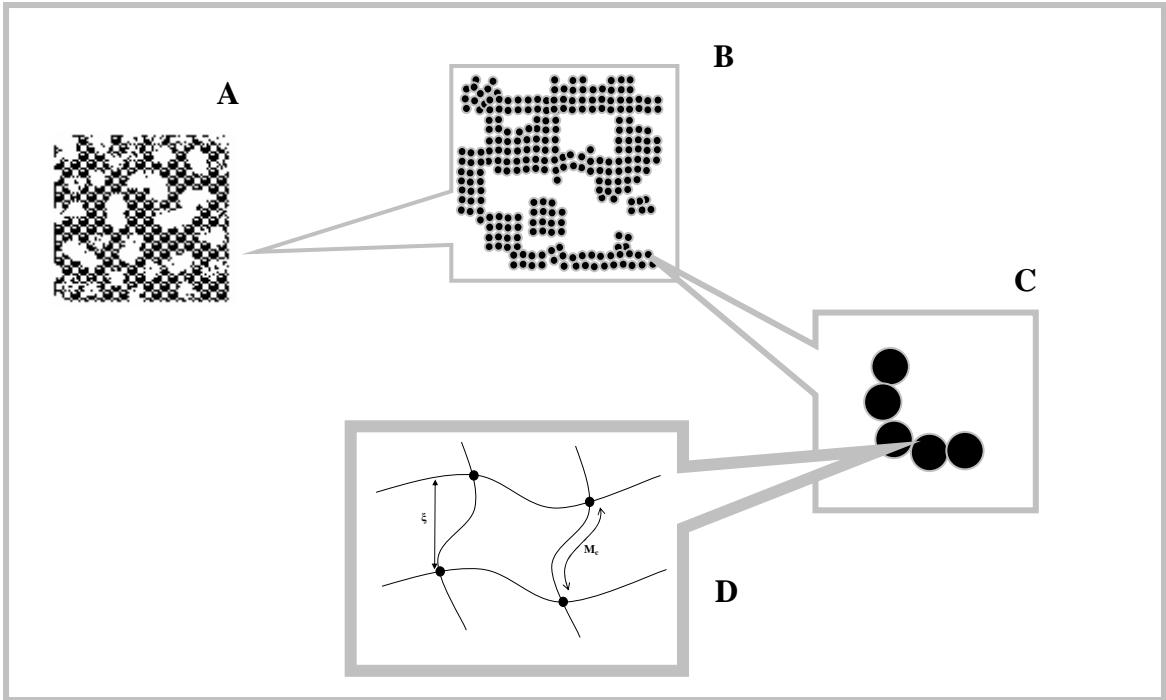


Figure 2.4. Porosity and Mesh Size. A polymer network having porosity has large holes in the macromolecular structure similar to a sponge (A). A blow up of portion of the polymer network gives better resolution of the pores that make up the porosity of the network (B). The black circles represent the polymer network (C). Mesh size ξ , and the molecular weight between crosslinks \overline{M}_c , can only be seen at the molecular level (D).

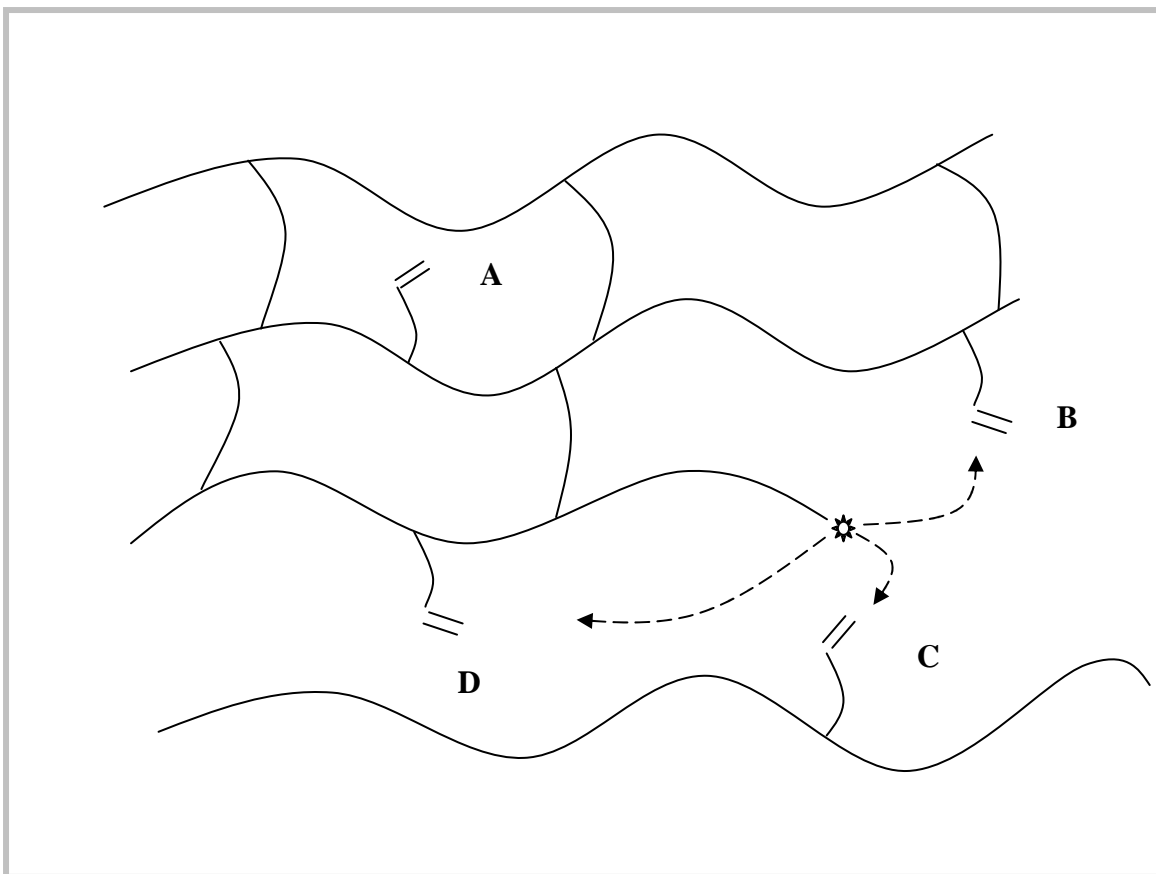


Figure 2.5. General Schematic of Interconnecting Linear Chains within Polymer Networks. In this figure **A** represents a pendant double bond, **B** represents a secondary cycle, **C** represents a crosslink, and **D** represents a primary cycle.

3.0 REACTION ANALYSIS OF A TYPICAL MOLECULARLY IMPRINTED SYSTEM

Fractional double bond conversion and associated template binding parameters of molecularly imprinted polymers will be explored in this chapter in relation to initiator concentration, crosslinking monomer length, monomer-template composition, temperature, and solvent concentration. A representative example from the current literature was chosen as a typical molecularly imprinted system. The specific network synthesized and analyzed was a poly(methacrylic acid-co-ethylene glycol dimethacrylate) (poly(MAA-co-EGDMA) network. It is important to note that poly(MAA-co-EGDMA) copolymer networks account for 80% of the imprinted polymer networks to date. Therefore, this work has significant merit despite the study of one copolymer system. Reaction analysis was conducted via differential scanning calorimetry which yielded fractional double bond conversion and temperature control of the polymerization. Template binding parameters of affinity, capacity, and selectivity were calculated via Freundlich binding isotherm analysis. The results presented in this Chapter and Chapter 4 have been published as a research article ¹, which is a significant, novel contribution to the imprinting field.

3.1 Scientific Rationale

In this work, we studied, synthesized, and characterized an imprinted system from literature with well documented binding parameters that has been studied by multiple investigators. We chose an ethyl-adenine-9-acetate (EA9A) imprinted poly(MAA-co-EGDMA) network²⁻⁶. The objective was to analyze the polymer reaction and ascertain potential template binding parameter optimization strategies. To begin we, synthesized the imprinted polymer via matching all conditions stated within the published work. During the polymerization, reaction analysis was used to determine the double bond conversion of the imprinted polymer. The binding characteristics were determined and compared to documented literature values in order to ensure the same network was accurately reproduced.

Also highlighted in this chapter is our use of reaction analysis to determine how double bond conversion is affected by the initiator concentration, solvent concentration, monomer-template ratio, and crosslinking monomer type. In addition, the temperature of the polymerization reaction was varied in order to see the changes in final double bond conversion. Our hypothesis was that through observation of the polymerization via reaction analysis valuable information for optimization or enhancement techniques will be determined. Enhancement techniques used to synthesize imprinted polymers will yield materials with tailorable binding characteristics.

3.2 Synthesis of a Typical Recognitive Polymer

Described in this section are the materials and methods used in the synthesis of a EA9A templated poly(MAA-co-EGDMA) recognitive network with an 80% feed crosslinker composition (moles of crosslinking monomer divided by moles of all monomers) and a monomer to template (M/T) ratio of 11.79. Variations to the original poly(MAA-co-EGDMA) network are included in this section. A schematic of the basic synthesis and analysis procedure is presented in Figure 3.1.

3.2.1 Materials

The functional monomer, methacrylic acid (MAA), and crosslinking monomer, ethylene glycol dimethacrylate (EGDMA), were shipped with inhibitor from Aldrich (Milwaukee, WI). The inhibitor was removed via inhibitor removal packing sieves or vacuum distillation prior to polymerization. The initiator, azo-bis(isobutyronitrile) (AIBN), template molecule, ethyl adenine-9-acetate (EA9A)), and analog molecule for selectivity, ethyl 2-amino-1,6-dihydro-6-oxo-4-pyrimidineacetate (EADOP), were used as received. Monomers, inhibitor removal packing sieves, initiator, template, and template analogue were purchased from Aldrich (Milwaukee, WI). Acetonitrile and methanol (HPLC grade) were used as received from Fisher Scientific (Pittsburgh, PA). The polymerization solvent was acetonitrile, and the polymer wash solvent used to remove template and unreacted monomer was acetonitrile/methanol at a 4:1 volume ratio.

3.2.2 Methods: Polymer Synthesis

A typical polymerization solution forming a poly(MAA-co-EGDMA) imprinted network, which matched the literature formulation in reference ⁴, was made with 2.61 mL EGDMA(13.83 mmol), 0.16 mL MAA(1.87 mmol), 3.96 mL acetonitrile(70.430 mmol), 26.3 mg of AIBN, and 35.4 mg of EA9A. During the course of the experiments, it was determined that the addition sequence of chemicals was very important. Monomers were added and mixed, and then template, solvent, and initiator were added to the solution. Failure to do this in sequence resulted in template not dissolving completely in the pre-polymerization solution. Solutions were placed in a sonicator after each solid was added for several minutes until the solid was dissolved in solution. After all components had been mixed, the poly(MAA-co-EGDMA) pre-polymerization solution was made. The solution was then ready for polymerization. The polymerization was carried out via UV-free radical polymerization in a Q-100 differential photo calorimeter (DPC) from TA Instruments (New Castle, Delaware). A poly(MAA-co-EGDMA) control polymer solution was made exactly in the same manner as the imprinted polymer solution except no template was added. Another poly(MAA-co-EGDMA) cognitive polymer exemplifying a higher degree of double bond conversion was produced by increasing the amount of initiator to 157.6 mg. All experimental materials and conditions such as the temperature of polymerization ($0^{\circ}\text{C} \pm 1^{\circ}\text{C}$ throughout exothermic reaction), template, functional monomer, crosslinking monomer, solvent wt%, initiator concentration, purge gas, and the UV light source (mercury arc source and intensity) were matched with the literature reference ⁴.

All polymerization reactions were carried out in the DPC. The DPC measures the heat flow from the sample relative to a reference pan. The heat evolved was measured as a function of time, and the theoretical reaction enthalpy of the monomer solution was used to calculate the rate of polymerization, R_p , in units of fractional double bond conversion per second. Figure 3.2 shows a schematic of the DPC. Integration of the rate of polymerization curve versus time yielded the experimental heat of reaction. The experimental heat of reaction and the theoretical heat of reaction are used to determine the final double bond conversion. The calculations were analyzed by a visual basic program within Microsoft Excel, a copy of the code is attached within Appendix C.

The assumptions in the copolymerization of multiple monomers (i.e., two types in this case, functional and crosslinking monomer) were that each monomer had equal reactivity and the theoretical reaction enthalpy derived for a co-monomer mixture was calculated by the summation of component mole fraction multiplied by the monomer heat of reaction. The theoretical enthalpy of methacrylate double bonds was equal to 13.1 kcal mole^{-17, 8}. Due to the overwhelming fraction of ethylene glycol dimethacrylate (EGDMA) in the system (i.e., 88% crosslinking or 13.83 mmoles of EGDMA and 1.87 mmoles of MAA), the majority of the heat of reaction was due to EGDMA double bonds reacting. EGDMA has two moles of double bond per mole of monomer which gives the number of double bonds that are associated with EGDMA to be approximately 94% of all double bonds in solution. Therefore, this system can be considered EGDMA in acetonitrile with a dilute amount of MAA.

In a typical experiment involving poly(MAA-co-EGDMA) networks, a recognitive polymer disk was produced by placing 12.5 μ L of pre-polymerization

solution within an aluminum hermetic pan, and placing it in the cell of the DPC. The solution was allowed to purge with nitrogen for 5 minutes at a 40 mL/min purge rate and a temperature of 20°C. To prevent possible evaporation of the solvent, a small quartz plate was placed on top of the pan after the 5 minute purge time. Also, since oxygen is a free radical scavenger, separate oxygen inhibition experiments were conducted to assure adequate nitrogen purge times (Appendix A, Figure A.1). Nitrogen continued to flow for the duration of the experiment at a purge rate of 40 mL/min. The solution was then cooled to the polymerization temperature of 0°C and was held at 0°C for 15 minutes. The shutter on the UV light source (Novacure 2100, Exfo, Canada, with a 100 Watt mercury arc light bulb) was opened and the solution was irradiated by 52.5 mW/cm² UV light (checked with internal radiometer) for 17 minutes at which time the polymerization reaction was ensured to be over (i.e., the typical polymerization time was on the order of a few minutes). The temperature of the sample was held between 0°C to 1°C throughout the reaction, and the end point of each reaction was determined when the heat flow changed less than 1%. Figure 3.3 shows a typical heat flow versus time curve from the DPC. All polymerization reactions to produce the poly(MAA-co-EGDMA) networks described in this chapter were all created in this manner. It is important to note that in the research article the original poly(MAA-co-EGDMA) imprinted network was taken from, the monomer solutions were purged with nitrogen and irradiated with UV light for much longer polymerization times (i.e., approximately 24 hours). The extended cure time is due to the polymer mold yielding a significant amount of monomer solution along the axis of the light source. With a low transmittance of UV light through a bulk polymer solution⁹, this would lead to significantly longer cure times.

During the course of making the polymer samples, a drop in the heat flow data was observed in some of the samples. The drop in the data was due to the polymer sample lifting off the bottom of the pan during the course of the reaction causing air to be in between the sample and the bottom of the aluminum pan. To correct this problem the sample volume size was limited to 12 μL within the aluminum pans.

3.2.3 Methods: Evaluation of Template Binding Parameters

The polymer disks were removed from the DPC pans and washed by Soxhlet extraction with a solution of acetonitrile/methanol in a 4:1 ratio. Extraction was performed for 2 ½ weeks and confirmed by analysis of the template in the wash. The washing procedure was run until EA9A was no longer detected in the wash solution via absorbance measurements using a Synergy UV-Vis spectrophotometer (BioTek Instruments, Winooski, Vermont). The disks were then taken out of the Soxhlet extraction device and allowed to dry in a fume hood at ambient temperature for a 24 hour period. The drying in ambient temperature reduced sudden stress cracking by rapid evaporation of solvent. The samples were then placed in a vacuum oven at 30°C and 25 inches of mercury vacuum.

The average disk weight for each of the samples was 3.69 ± 0.29 mg. The disk diameter was 4mm with width of 0.5 mm on the outside of the disk with concavity of less than 0.1 mm in the center of the disk. All samples had a reaction signature that was within one standard deviation from the mean to maintain a high degree of quality control

for the reaction analysis and resultant polymer networks. Figure 3.4 shows 5 samples within the standard deviation on a heat flow versus time curve.

Dynamic binding analysis was determined by placing disks in 200 μL of various concentrations of EA9A in acetonitrile (0.01 to 2.0 mM solutions). After equilibrium was reached, a 100 μL aliquot of the solution was taken and absorbance measured at 265 nm using a Biotek UV-Vis spectrophotometer. Binding parameters were calculated using various isotherms (e.g., Scatchard, Langmuir, Freundlich).

The equations for Scatchard, Langmuir, and Freundlich isotherms are shown in equations 3.1, 3.2, and 3.3, respectively. The linear form of the Scatchard equation is shown in 3.1

$$\frac{Q}{C_e} = -K_a Q + Q_{\max} \quad 3.1$$

where Q is the bound amount of template, C_e is the equilibrium concentration of template in the solution, the template equilibrium binding affinity is represented by K_a , and Q_{\max} is the maximum capacity. The affinity and the maximum template loading capacity are calculated via linear regression of the data.

The Langmuir isotherm is represented by the following equation 3.2

$$Q = \frac{K_a Q_{\max} C_e}{1 + K_a C_e} \quad 3.2$$

where Q is the bound amount of template, C_e is the equilibrium concentration of the template in solution, the template binding affinity is K_a , and Q_{\max} is the maximum template loading capacity. Linear regression of the Langmuir equation is used to find the affinity and capacity. The Langmuir isotherm assumes that there is uniform one-layer

adsorption of the template molecule, equilibrium conditions, and that the surface is homogeneous.

The Freundlich isotherm is an empirical equation that can have multiplicity of sites on a surface and can be applied to heterogeneous surfaces^{10, 11}. The Freundlich isotherm is shown in equation, 3.3

$$Q = k_f C_e^n \quad 3.3$$

where Q represents the bound amount of template, C_e represents the equilibrium concentration of template solution, and k_f represents the Freundlich equilibrium template binding affinity constant. The Freundlich affinity constant and the exponent (n) are found from a linear regression of this equation. A detailed analysis of the calculation of the average affinity and average number of sites from the Freundlich isotherm can be viewed in section 3.2.4. The isotherm that gave the best fit to the data was used to determine the binding parameters. In most polymers described in this work, the Freundlich isotherm gave the best fit. The use of the Freundlich isotherm to characterize molecularly imprinted polymers has been validated by Shimizu and coworkers¹⁰, Spivak and coworkers¹², and Sellergren and coworkers¹³. Once the equilibrium concentration of the solution was determined, a mass balance yielded the bound concentration.

Selectivity studies for the recognitive polymers were conducted in similar fashion to the rebinding studies. Disks were placed in a 2mM solution of EADOP in acetonitrile and allowed to reach equilibrium. Once equilibrium was reached, a 100 μ L aliquot of solution was sampled and the absorbance measured at a wavelength of 282 nm. The equilibrium concentration was calculated, and a mass balance was used to determine the bound concentration. In addition, further analysis was performed to measure the

selectivity number which is equal to the average affinity of EA9A divided by the average affinity of EADOP. Affinity of the poly(MAA-co-EGDMA) recognitive polymers for EADOP was also measured via the Freundlich isotherm since it yielded the best fit to the data.

3.2.4 Methods: Binding Affinity and Capacity from Freundlich Analysis

Freundlich analysis takes the values from the linear regression of the Freundlich isotherm and calculates the average affinity and capacity for the recognitive polymers. This analysis was used on all recognitive systems studied within this dissertation. The method of analysis was taken from Rampey and coworkers in their analysis of molecularly imprinted polymers². Equation 3.4 is the Freundlich Isotherm where Q is

$$Q = k_f C_e^n \quad 3.4$$

the amount bound by the recognitive polymer, the equilibrium concentration is C_e , the freundlich affinity is k_f , and the exponent value is n .

The following equations and their explanations are the basis for the results presented within this dissertation. Equation 3.5 and 3.4 give the maximum affinity (K_{max}) and minimum affinity (K_{min}). K_{max} and K_{min} represent the limits at which the affinity spectrum can be from and are determined from the maximum ($C_{e\ max}$) and minimum equilibrium concentrations ($C_{e\ min}$).

$$K_{min} = \frac{1}{C_{e\ max}} \quad 3.5$$

$$K_{\max} = \frac{1}{C_{e \min}} \quad 3.6$$

The number of sites ($N_{K_1-K_2}$) was taken between K_1 and K_2 . K_1 and K_2 are affinity values between K_{\min} and K_{\max} . Equation 3.7 is the equation used for the number of sites.

$$N_{K_1-K_2} = k_f (1 - n^2)(K_1^{-n} - K_2^{-n}) \quad 3.7$$

The average affinity ($\bar{K}_{K_1-K_2}$) is calculated by equation 3.8.

$$\bar{K}_{K_1-K_2} = \left(\frac{n}{n-1} \right) \left(\frac{K_1^{1-n} - K_2^{1-n}}{K_1^{-n} - K_2^{-n}} \right) \quad 3.8$$

It is important to note that for all the poly(MAA-co-EGDMA) recognitive polymers the values for K_1 and K_2 were all equivalent which allowed for a comparison between systems.

3.3 Results and Discussion

This section highlights reaction analysis and binding parameters assessment for a typical poly(MAA-co-EGDMA) imprinted network described in recent literature. Initiator concentration, solvent concentration, crosslinking monomer length, and temperature were varied to determine their respective affect on the double bond conversion and template binding parameters. A poly(MAA-co-EGDMA) imprinted network with enhanced double bond conversion was also synthesized with the purpose of comparing the resulting binding parameters with the imprinted polymer synthesized from literature.

3.3.1 Double Bond Conversion via Reaction Analysis

The poly(MAA-co-EGDMA) literature network was calculated to have a monomer to template ratio of 11.79 (moles of functional monomer divided by the moles of template), and the degree of feed crosslinking in the system was calculated to be 88 mole% (mole crosslinking monomer/mole all monomers). The polymer was analyzed and the number of total number of double bonds reacted via DPC revealed a low level of fractional double bond conversion ($35.0 \pm 2.3\%$). The low double bond conversion for this poly(MAA-co-EGDMA) has never been shown before in the literature. The result is significant because most researchers in the literature classify their recognitive polymers by the feed composition. A low double bond conversion for short bi-functional monomers indicates that the feed composition does not accurately describe the final polymer network. Figure 3.5 shows the double bond conversion versus time. The reason for the low double bond conversion within this polymer network is described via a discussion of pendant double bonds. It is important to note an analysis of the wash indicated little unreacted crosslinker coming from the polymers, thus pendant bonds are a good assumption. Pendant double bonds are double bonds that are sterically hindered by the growing polymer network, due to limited mobility they cannot react with surrounding radicals. A schematic of pendant double bonds within a forming polymer network is shown in Figure 3.6.

In order to verify this hypothesis, a study on the effect of crosslinking monomer length upon the double bond conversion for this imprinted system was undertaken. An equivalent experiment was conducted using a slightly longer bifunctional crosslinking

monomer (poly(ethylene glycol) dimethacrylate, PEG200DMA, where the average number of ethylene glycol groups is 4.5 as opposed to 1 with EGDMA. The longer crosslinking monomer will have increased flexibility along the polymer chain to react. The same reaction conditions were used in both experiments with the EGDMA and PEG200DMA crosslinked monomers. The double bond conversion calculated for the poly(MAA-co-PEG200DMA) crosslinked polymer was $53.0 \pm 2.0\%$ at a polymerization temperature of 0°C . The increase in conversion indicated that there were lower amounts of pendant double bonds, which can be attributed to the increased diffusional mobility of the longer crosslinking monomer to react.

A longer crosslinking monomer increases the flexibility of the growing polymer network chains and reduces the steric hinderances that lead to unreacted pendant double bonds. Literature analysis reveals double bond conversions for similar systems using PEG200DMA equal to 68-69% with a polymerization temperature of 25°C ¹⁴⁻¹⁷. Therefore, for the molecular imprinting field these results highlight that a significant amount of EGDMA crosslinking monomer in the formulation results in a severely constrained network formation. Specifically, there is a decrease in the diffusional ability of pendant double bonds in the growing polymeric network to react or limited diffusion of radicals on the growing network which lowers conversion. More importantly, it also highlights that the final polymer composition does not represent the initial formulation when using significant amounts of short, bifunctional crosslinking monomer (i.e., when intra-molecular distances between crosslinking monomer double bonds are short). This is significant to the field of molecular imprinting since most groups use high amounts of EGDMA as crosslinking monomer to produce imprinted networks and report feed

crosslinker compositions in relation to binding properties (affinity, capacity, and selectivity). Therefore, reaction analysis provides a basis for the accurate comparison of molecularly imprinted systems; furthermore, while double bond conversion has been studied in highly crosslinked networks¹⁸ this is the first study to confirm low double bond conversion within highly crosslinked molecularly imprinted polymer systems and the associated effect on the binding properties.

Contrary to our results, ¹³C NMR studies of poly(MAA-co-EGDMA) imprinted polymers with 83% feed crosslinker produced at a constant temperature of 25°C estimated 83% final double bond conversion¹⁹. Within the molecular imprinting literature, to the best of our knowledge, this has been the only study of a highly crosslinked imprinted poly(MAA-co-EGDMA) network to analyze the double bond conversion. It gives an uncharacteristically high double bond conversion for dilute MAA in EGDMA (91% of the double bonds are attributed to EGDMA). Double bond conversions of pure EGDMA (non-imprinted) have been reported to be 69% at 60°C²⁰. Since the temperatures of reaction are different, additional experimental analysis was warranted to compare conversions and ascertain the effect of temperature on the rate of reaction and conversion for this system.

By using the DPC, temperature could be kept constant within $\pm 1^\circ\text{C}$ during the course of the polymerization reaction. Temperature of reaction was set a 0 °C, 25 °C, and 50 °C which resulted in $35.0 \pm 2.3\%$, $51.0 \pm 1.2\%$, and $54.0 \pm 1.9\%$ final double bond conversion for our imprinted system, respectively. The rate of polymerization versus time for temperatures of -25°C, 0°C, 25°C, and 50°C is shown in Figure 3.7. Double bond conversions of poly(MAA-co-EGDMA) networks versus polymerization

temperature is shown in Figure 3.8. For pure EGDMA, we experimentally found the double bond conversion at 0°C to be $36.1 \pm 2.5\%$, very close in value to our imprinted system. Even if none of the MAA reacts in our system, which is highly unlikely, the double bond conversion at 0 °C is calculated at $(39.3 \pm 2.3) \%$. Therefore, this confirms that the majority of the heat of reaction is due to EGDMA double bonds reacting. However, MAA is incorporated into the system as reflected in template binding analysis.

Studies which use extraction methods and subsequent measurement of unreacted monomers will overestimate conversion by not counting crosslinking monomers that do not diffuse from the structure due to partial reaction that result in dangling, unreacted pendant double bonds.

Since termination events are more frequent at higher temperatures with a small increase in the propagation constant, the result is shorter kinetic chain lengths. The temperature increase during the reaction increased the rate of reaction and overall conversion, but typically led to decreased affinity since hydrogen bonding and the formation of binding sites decreased with increasing temperature. This is in agreement with studies involving changes in polymerization temperature and associated binding parameters⁶. Therefore, for non-covalent imprinting within free radical hetero/homopolymerization reactions of multifunctional monomers, the strength of template-monomer interactions is an important variable as are the network properties that influence the stability of the binding site (e.g., crosslinking density and homogeneity).

The effect of photoinitiator and solvent concentration on the fractional double bond conversion is presented in Figure 3.9 and Figure 3.10, respectively. An increase in the photoinitiator concentration from 0.4 wt.% (the value of the poly(MAA-co-EGDMA)

imprinted polymer literature network) to 4.6 wt. % increased the double bond conversion from $35 \pm 2.3\%$ to $48 \pm 2.1\%$ (Figure 3.9). This can be attributed to an increase in the concentration of free radicals which provides an increased rate of chain initiating species and an increased rate of reaction (i.e., the rate scales to the square root of initiator concentration) that ultimately increases the conversion. After 2.4 wt% initiator, the fractional double bond conversion remained constant.

The rate equation applied to the square root of the initiator can be derived from the rate expression. The following derivation closely matches the derivation of Odian²¹. The rate of polymerization can be described with equation 3.9, with $[M]$ being the

$$-\frac{d[M]}{dt} = R_i + R_p \quad 3.9$$

monomer concentration and R_i and R_p being the rate of initiation and propagation, respectively. The rate of initiation is typically much lower than the rate of propagation and can be neglected. The result means that the rate of polymerization is closely approximated to the rate of propagation. Also, the rate constants for the propagation steps are equivalent. The rate expression for the polymerization reaction can be expressed as equation 3.10, where $[M\bullet]$ is the radical concentration and k_p is the

$$R_p = k_p [M\bullet][M] \quad 3.10$$

propagation constant. Because the radical concentration in polymerization reactions are hard to characterize, the radical concentration is typically removed from the equation. Using a steady-state assumption, the radical concentration during the polymerization is considered zero during the polymerization reaction. The steady state assumption also states that the initiation (R_i) and termination (R_t) rates are equivalent, 3.11.

$$R_t = R_i = 2k_t[M\bullet]^2 \quad 3.11$$

The termination rate constant is represented by k_t . Solving this equation for the radical concentration and substituting in equation 3.10 results in equation 3.12.

$$R_p = k_p[M] \left(\frac{R_i}{2k_t} \right)^{\frac{1}{2}} \quad 3.12$$

At this point, the initiation rate can be defined when the initiator is used as equation 3.13.

$$R_i = 2f k_d[I] \quad 3.13$$

In equation 3.13 the initiator efficiency is represented by f , the initiator concentration is given as $[I]$, and the rate constant of initiation is k_d . Combining equation 3.13 with equation 3.12 yields the equation in which the rate of polymerization is scaled to the square root of the initiator.

$$R_p = k_p[M] \left(\frac{2f k_d[I]}{2k_t} \right)^{\frac{1}{2}} \cong [I]^{\frac{1}{2}} \quad 3.14$$

Increasing the solvent wt% had an opposite affect and decreased the double bond conversion (Figure 3.10). This is due to a decreased concentration of initiator and a decreased concentration of monomers. The effect of solvent is important for recognitive polymer systems since increased amounts of solvent have been shown to increase matrix porosity which is beneficial for diffusional transport ²²; however, increasing the solvent wt% without a corresponding increase in photoinitiator concentration may negatively impact the double bond conversion and overall stability or fidelity of the binding sites (e.g. after 60 wt. % solvent the double bond conversion decreased substantially). Since the solvent does not get incorporated into the growing polymer chains, the polymeric

network must form around the solvent and this produces an accessible porous structure for adequate template diffusional transport.

3.3.2 Assessment of Binding Parameters

Equilibrium binding isotherms were conducted on the poly(MAA-co-EGDMA) recognitive polymer synthesized from literature, the poly(MAA-co-EGDMA) recognitive network with 48% double bond conversion, and the associated poly(MAA-co-EGDMA) control network (i.e., no target molecule present in the formulation). Figure 3.11 shows the binding isotherms for the two recognitive polymers and the control polymer. In this particular set of experiments, we hypothesized that due to the increased double bond conversion a change in the binding characteristics would be observed.

The poly(MAA-co-EGDMA) recognitive network literature network showed statistically good agreement with reported data in the literature (template affinity constant of $3.23 \pm 0.21 \text{ mM}^{-1}$)² with a capacity of $(776 \pm 54) \text{ } \mu\text{mole/gram}$. The Freundlich isotherm was used as the basis for analysis of average binding affinity along with number of binding sites, since the Freundlich isotherm gave the best fit to the data, based upon R^2 values (i.e. square of the correlation coefficient). The binding parameter evaluations for the Langmuir, Scatchard, and additional information regarding the Freundlich isotherms along with the linear regression fitting of the data with R^2 values are presented in Appendix A, section A.2. The poly(MAA-co-EGDMA) recognitive polymer with 48% double bond conversion gave a modest increase in the number of binding sites; however, statistically the binding capacity was within the standard deviation of the synthesized

poly(MAA-co-EGDMA) recognitive polymer literature network. In Table 3.1, poly(MAA-co-EGDMA) with 48% double bond conversion had a modest higher mean binding capacity of (860 ± 60) $\mu\text{mole/gram}$ at a slightly reduced affinity of (2.63 ± 0.17) mM^{-1} . It is important to note that average affinity values take into account site sub-populations of varying affinity. While the concentration of initiator should not be overlooked in optimization, the increased conversion did not lead to an improved average binding affinity or capacity in this case. An increase in initiator concentration can theoretically lead to a decrease in the kinetic chain length which, and we hypothesize with an increase in conversion, may result in increased binding site stabilization and increased structural homogeneity. The kinetic chain length represents the average number of monomers reacting with an active center from initiation to termination, and it is inversely proportional to the radical concentration and the rate of polymerization²³. Thus, attempts to increase polymerization rate by increasing radical concentration produces smaller sized polymer chains²¹.

Selectivity studies were performed using a molecule with similar chemical functionality of EA9A (Figure 3.12-A), ethyl 2-amino-1,6-dihydro-6-oxo-4-pyrimidineacetate (EADOP) (Figure 3.12-B). Binding capacity of EA9A and EADOP values for poly(MAA-co-EGDMA) recognitive network with 48% double bond conversion are shown in Figure 3.13; additionally, selectivity numbers (bound template/bound other molecule) at 2mM concentration were 2.4 ± 1.0 for the recognitive polymer with 48% double bond conversion. In this particular analysis, the poly(MAA-co-EGDMA) network synthesized using literature data did not show selectivity for the

**Table 3.1. Quantitive Binding Parameters of Poly (MAA-co-EGDMA) Networks
using Freundlich Isotherm Analysis.**

Polymer	Affinity (K)	Units	Capacity	Units
Poly(MAA-co-EGDMA) recognitive polymer literature match	3.12 ± 0.21	mM^{-1}	776 ± 54	$\mu\text{mole/gram}$
Poly(MAA-co-EGDMA) recognitive polymer with 48% double bond conversion	2.63 ± 0.17	mM^{-1}	860 ± 60	$\mu\text{mole/gram}$

target molecule, EA9A. Also the original article does not report selectivity data. Therefore, increasing the double bond conversion of a poly(MAA-co-EGDMA) recognitive network did not conclusively lead to statistically significant, improved binding affinity or capacity, but increased the selectivity. This is hypothesized to be due to a decrease in the kinetic chain length with increased binding site stabilization and increased structural homogeneity due to an increase in the initiator concentration. Therefore, even optimization of conventional photo-initiator can lead to small improvements in binding parameters. It is also important to note that the average affinity of these recognitive polymers take into account high affinity sites and low affinity sites. The increase in selectivity in this study could indicate a better quality high affinity site population; however, since the higher affinity site population is typically very low compared to the population of lower affinity sites, it is very difficult to quantify these differences.

In addition to this study, a more thorough analysis of selectivity was performed on the poly(MAA-co-EGDMA) recognitive polymer from the literature and the poly(MAA-co-EGDMA) recognitive polymer with 48% double bond conversion. This study was performed exactly in the same manner as the original binding study except the molecule EA9A was exchanged with EADOP, and the selectivity number was calculated with affinities instead of capacities. Results were also analyzed via the Freundlich isotherm which gave the best fit. The selectivity number was calculated dividing the affinity of the template divided by the affinity of the analogue. The selectivity numbers were 1.63 ± 0.11 and 1.81 ± 0.12 for poly(MAA-co-EGDMA) recognitive polymer literature network and the poly(MAA-co-EGDMA) recognitive polymer with 48% double bond conversion,

respectively. Selectivities calculated by using the affinities are a much better representation of selectivity of the imprinted polymers when compared to selectivity calculated with capacities. Selectivity number results show an increase in selectivity for the imprinted polymer with the increased conversion. In addition to these studies a detailed washing analysis presented on the quantities of template EA9A theoretically in the polymer network, bound by the polymer network (assessed by binding isotherms), and the amount washed out using Soxhlet extraction. These studies are presented and discussed in Appendix B.

3.4 Conclusion

The results presented in this chapter prove that reaction analysis of molecularly imprinted polymerization reactions has the potential to yield a greater understanding of the imprinting mechanism and associated binding parameters as related to the structural architecture of the polymeric network. Pendant double bonds contribute to low double bond conversions of poly(MAA-co-EGDMA) imprinted networks (35 ± 2.3 %). Low double bond conversions are significant because most researchers within the literature use feed compositions to represent the final polymer product. In addition, 80% of the imprinting field uses a poly(MAA-co-EGDMA) copolymer network as the backbone for their imprinted polymers. Increases in temperature and crosslinking monomer length increase the double bond conversion by increasing the flexibility of the network thus decreasing pendant double bonds. Solvent wt% increases above 60% show significant decreases in double bond conversion. Increases in initiator wt% can increase the double

bond conversion up to 48% double bond conversions for EA9A templated poly(MAA-co-EGDMA) networks polymerized at 0°C. Increases in double bond conversion slightly increased the template binding capacity of the poly(MAA-co-EGDMA) imprinted network with similar binding capacities and retention of selectivity.

In Chapter 4, additional work with “living/controlled” polymerization techniques to create recognitive polymers is done in order to add structural control to the polymerization reaction. “Living/controlled” polymerizations show significant control over linear polymer kinetic chain length. Control of the kinetic chain length within an imprinted copolymer network could contribute to a more homogenous material which would give more structural control over the macromolecular architecture. The reason for the added structural control is the necessity for these materials to be engineered for specific applications. By additional control upon the network structure, the tailorability of these networks increases; therefore, tailorability will inevitably lead to improved binding characteristics via a rationally optimized macromolecular structure.

3.5 List of References

1. Vaughan, A. D.; Sizemore, S. P.; Byrne, M. E., Enhancing Molecularly Imprinted Polymer Binding Properties via Controlled/living Radical Polymerization and Reaction Analysis. *Polymer* **2007**, 48, (1), 74-81.
2. Rampey, A. M.; Umpleby, R. J.; Rushton, G. T.; Iseman, J. C.; Shah, R. N.; Shimizu, K. D., Characterization of the Imprint Effect and the Influence of Imprinting Conditions on Affinity, Capacity, and Heterogeneity in Molecularly Imprinted Polymers

Using the Freundlich Isotherm-Affinity Distribution Analysis. *Anal. Chem.* **2004**, 76, (4), 1123-1133.

3. Umpleby II, R. J.; Bode, M.; Shimizu, K. D., Measurement of the Continuous Distribution of Binding Sites in Molecularly Imprinted Polymers *Analyst* **2000**, 125, (7), 1261-1265.

4. Umpleby II, R. J.; Rushton, G. T.; Shah, R. N.; Rampey, A. M.; Bradshaw, J. C.; Berch, J. K.; Shimizu, K. D., Recognition Directed Site-Selective Chemical Modification of Molecularly Imprinted Polymers. *Macromolecules* **2001**, 34, (24), 8446-8452.

5. Shea, K. J.; Spivak, D. A.; Sellergren, B., Polymer Complements to Nucleotide Bases. Selective Binding of Adenine Derivatives to Imprinted Polymers. *J. Am. Chem. Soc.* **1993**, 115, (8), 3368-3369.

6. Spivak, D.; Gilmore, M. A.; Shea, K. J., Evaluation of Binding and Origins of Specificity of 9-Ethyladenine Imprinted Polymers. *J. Am. Chem. Soc.* **1997**, 119, (19), 4388-4393.

7. Anseth, K. S.; Wang, C. M.; Bowman, C. N., Reaction Behaviour and Kinetic Constants for Photopolymerizations of Multi(meth)acrylate Monomers. *Polymer* **1994**, 35, (15), 3243-3250.

8. Ward, J. H.; Shahar, A.; Peppas, N. A., Kinetics of 'Living' Radical Polymerizations of Multifunctional Monomers. *Polymer* **2002**, 43, (6), 1745-1752.

9. Bowman, C. N.; Peppas, N. A., Coupling of Kinetics and Volume Relaxation During Polymerizations of Multiacrylates and Multimethacrylates. *Macromolecules* **1991**, 24, (8), 1914-1920.

10. Umpleby, R. J.; Baxter, S. C.; Bode, M.; Berch, J. K.; Shah, R. N.; Shimizu, K. D., Application of the Freundlich Adsorption Isotherm in the Characterization of Molecularly Imprinted Polymers. *Analytica Chimica Acta* **2001**, 435, (1), 35-42.
11. Umpleby, R. J.; Baxter, S. C.; Rampey, A. M.; Rushton, G. T.; Chen, Y.; Shimizu, K. D., Characterization of the Heterogeneous Binding Site Affinity Distributions in Molecularly Imprinted Polymers. *Journal of Chromatography B* **2004**, 804, (1), 141-149.
12. Kim, H.; Spivak, D. A., New Insight into Modeling Non-Covalently Imprinted Polymers. *J. Am. Chem. Soc.* **2003**, 125, (37), 11269-11275.
13. Szabelski, P.; Kaczmarek, K.; Cavazzini, A.; Chen, Y. B.; Sellergren, B.; Guiochon, G., Energetic Heterogeneity of the Surface of a Molecularly Imprinted Polymer Studied by High-performance Liquid Chromatography. *Journal of Chromatography A* **2002**, 964, (1-2), 99-111.
14. Bowman, C. N.; Peppas, N. A., Coupling of Kinetics and Volume Relaxation during Polymerizations of Multiacrylates and Multimethacrylates. *Macromolecules* **1991**, 24, (8), 1914-1920.
15. Scott, R. A.; Peppas, N. A., Kinetics of Copolymerization of PEG-Containing Multiacrylates with Acrylic Acid. *Macromolecules* **1999**, 32, (19), 6149-6158.
16. Elliott, J. E.; Bowman, C. N., Kinetics of Primary Cyclization Reactions in Cross-Linked Polymers: An Analytical and Numerical Approach to Heterogeneity in Network Formation. *Macromolecules* **1999**, 32, (25), 8621-8628.

17. Anseth, K. S.; Kline, L. M.; Walker, T. A.; Anderson, K. J.; Bowman, C. N., Reaction Kinetics and Volume Relaxation during Polymerizations of Multiethylene Glycol Dimethacrylates. *Macromolecules* **1995**, 28, (7), 2491-2499.
18. Lu, H.; Lovell, L. G.; Bowman, C. N., Exploiting the Heterogeneity of Cross-Linked Photopolymers To Create High-Tg Polymers from Polymerizations Performed at Ambient Conditions. *Macromolecules* **2001**, 34, (23), 8021-8025.
19. Sibrian-Vazquez, M.; Spivak, D. A., Characterization of Molecularly Imprinted Polymers Employing Crosslinkers with Nonsymmetric Polymerizable Groups. *Journal of Polymer Science Part A: Polymer Chemistry* **2004**, 42, (15), 3668-3675.
20. Sun, X.; Chiu, Y. Y.; Lee, L. J., Microgel Formation in the Free Radical Cross-Linking Copolymerization of Methyl Methacrylate (MMA) and Ethylene Glycol Dimethacrylate (EGDMA). *Ind. Eng. Chem. Res.* **1997**, 36, (4), 1343-1351.
21. Odian, G., *Principles of Polymerization*. 2nd edition ed.; John Wiley & Sons: New York, 1981.
22. Spizzirri, U. G.; Peppas, N. A., Structural Analysis and Diffusional Behavior of Molecularly Imprinted Polymer Networks for Cholesterol Recognition. *Chem. Mater.* **2005**, 17, (26), 6719-6727.
23. Flory, P. J., *Principles of Polymer Chemistry*. 1st ed.; Cornell University Press: Ithaca, 1953; p 663.

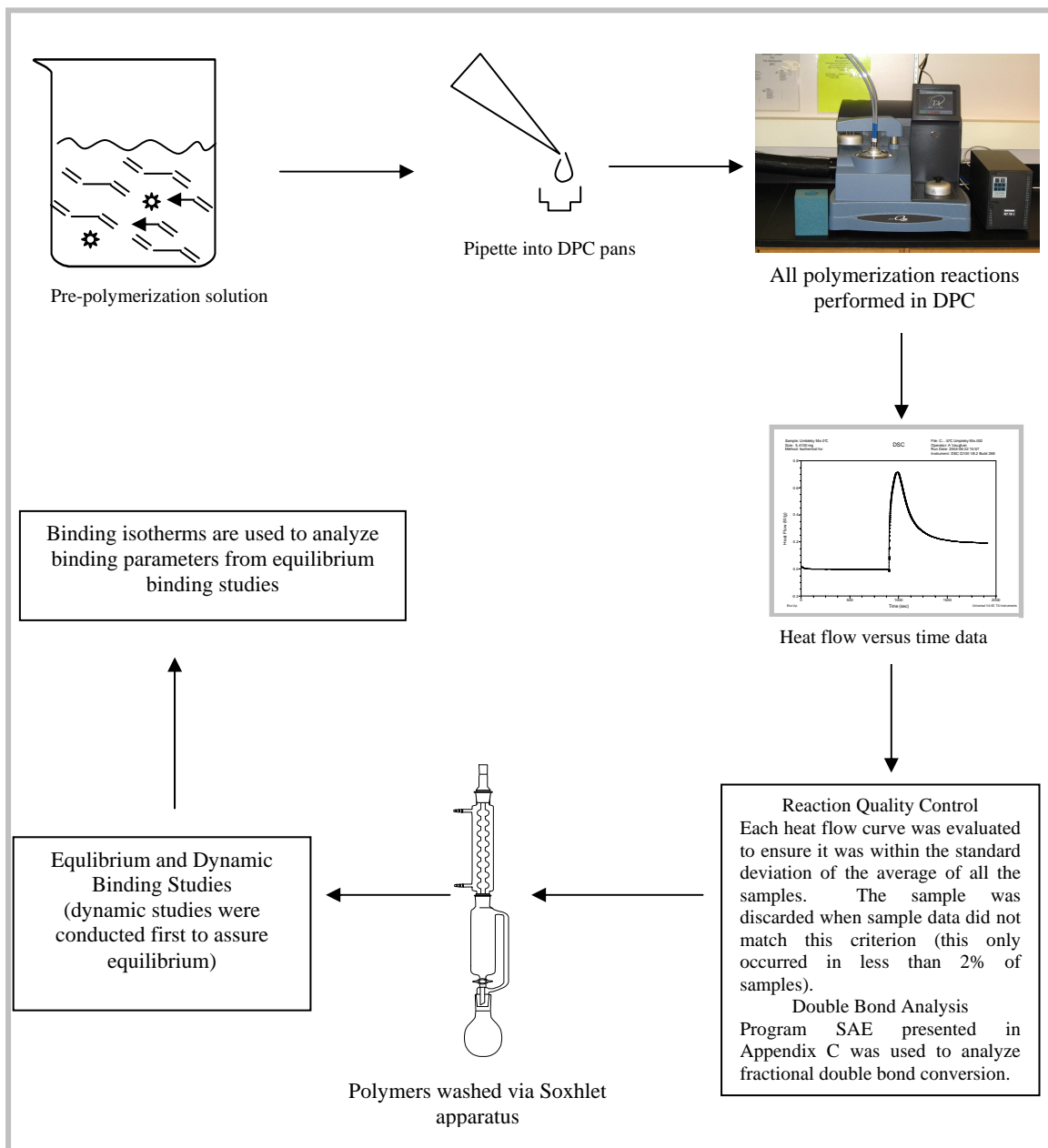


Figure 3.1 Procedure for Imprinted Polymer Synthesis to Binding Analysis. The highly crosslinked imprinted polymers presented in this work are synthesized outlined in this basic procedure schematic from pre-polymerization mixture to analysis of binding parameters.

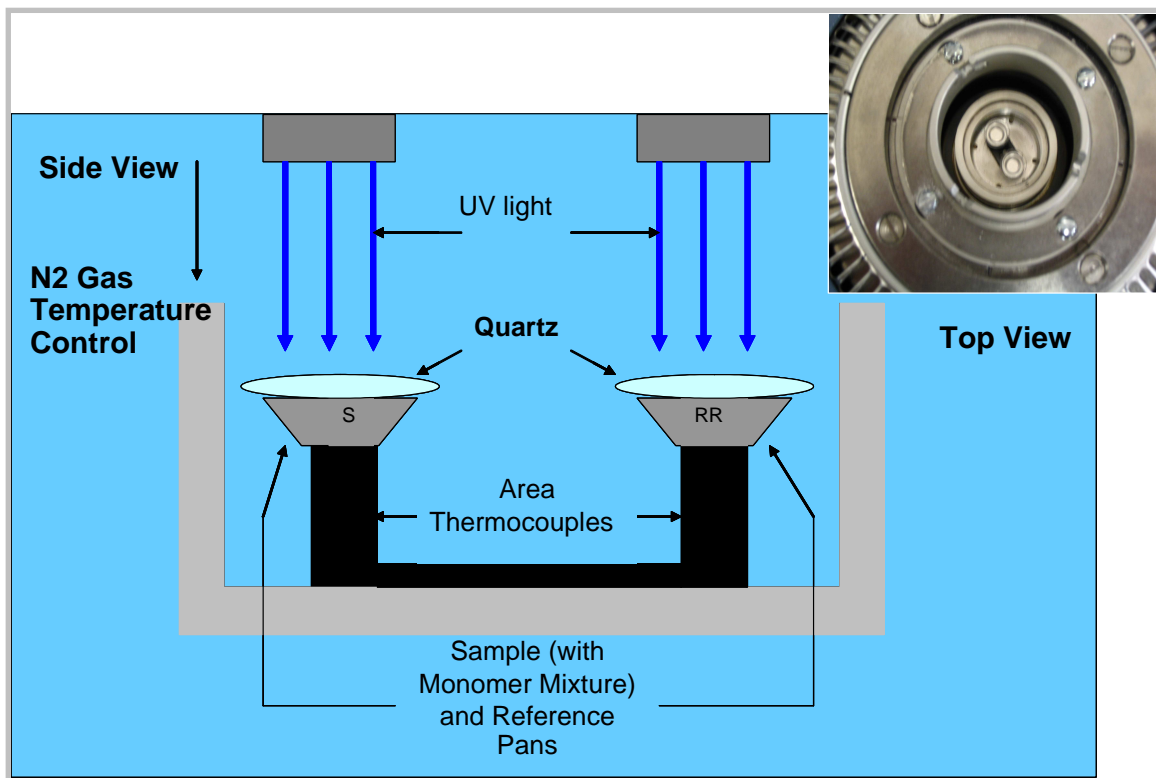


Figure 3.2 Differential Photo Calorimeter Cell Schematic. The polymer sample was placed in the sample pan (**S**) and allowed to purge with nitrogen for 5 minutes. Then a quartz cover-slip was placed over the sample to reduce solvent evaporation. Heat flow was measured between the sample and reference pan (**RR**) during the polymerization reaction. Top right is an actual photo of the top of the cell with the sample and reference pan in the cell.

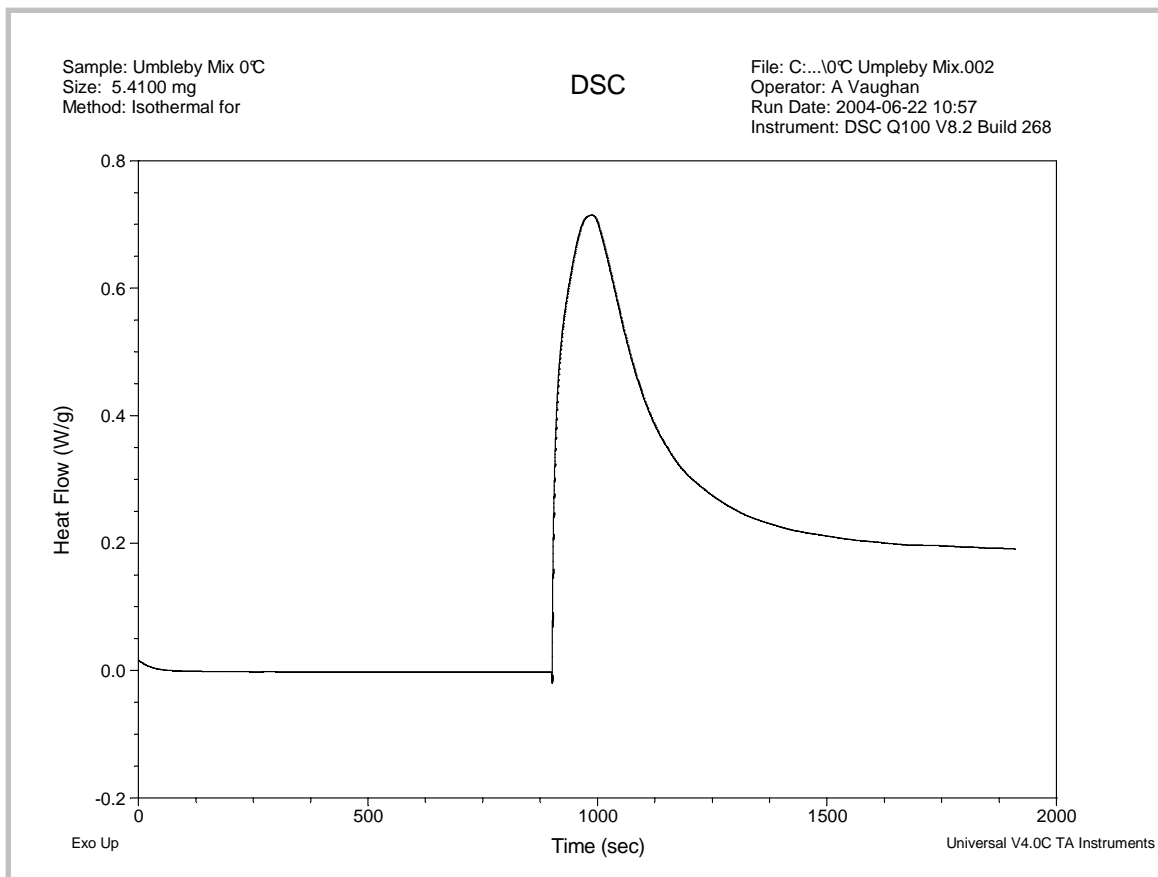


Figure 3.3 Heat Flow from Differential Photo Calorimeter. Heat flow is measured versus time for the polymerization reaction. The data is analyzed to find the experimental heat of reaction. The experimental heat of reaction divided by the theoretical heat of reaction will give the double bond conversion.

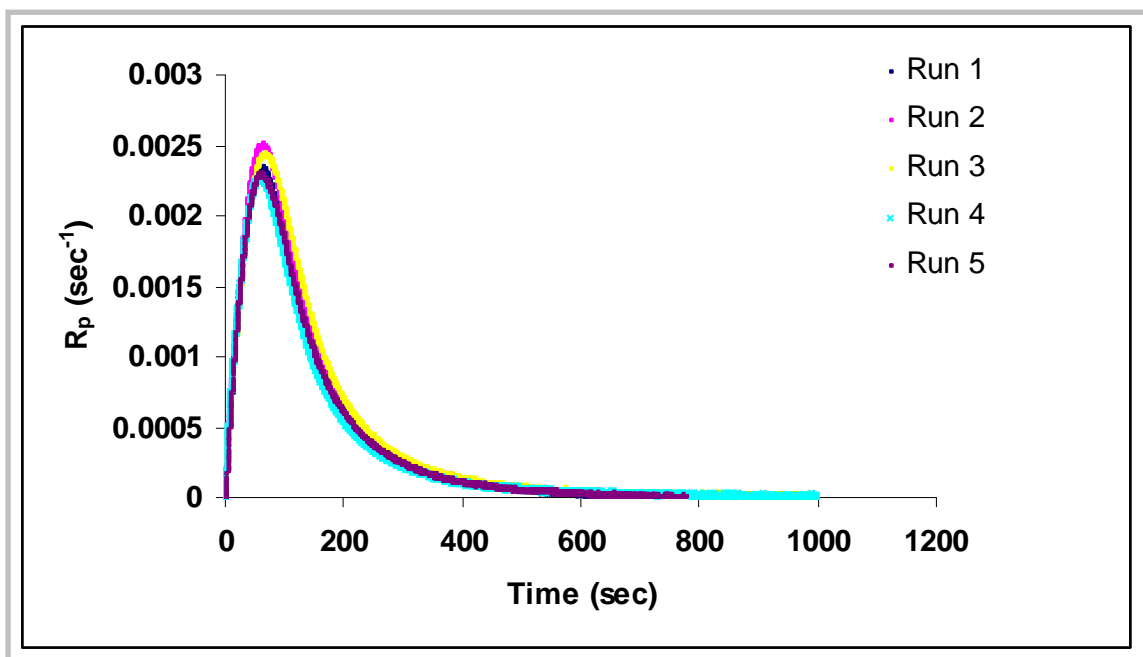


Figure 3.4 Reaction Signature Quality Control for Poly(MAA-co-EGDMA) Network Synthesis. Reaction rate versus time (reaction signature) was compared for each network produced. If the reaction signature was one standard deviation or more from the mean, the polymer was discarded. Using the DPC, the reaction signature was well controlled and network values deviated less than 5%.

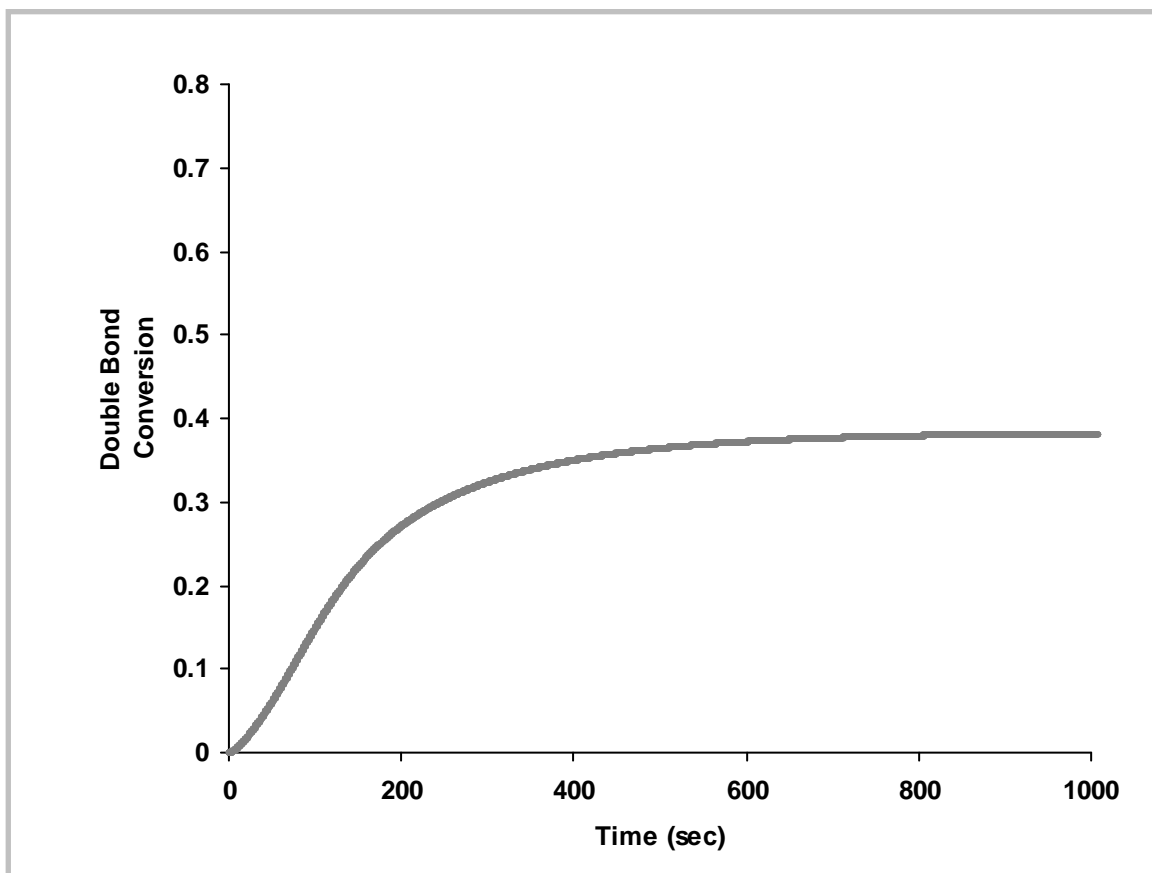


Figure 3.5 Dynamic Double Bond Conversion of a Poly(MAA-co-EGDMA) Imprinted Network: A Typical Recognitive Polymer. Double bond conversion verses time for a typical recognitive polymer with 88% feed crosslinker and monomer-template ratio of 11.79. The final double bond conversion reached is 35%, drastically different incorporation of junction points compared to the feed percent of crosslinking monomer.

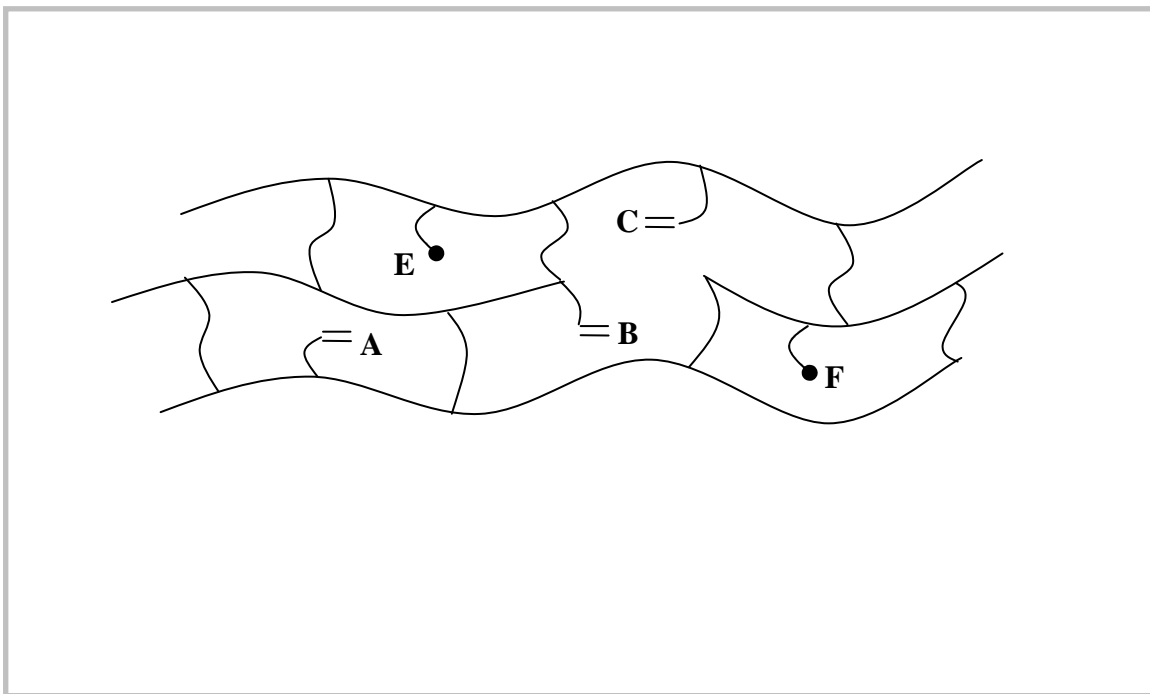


Figure 3.6 Pendant Double Bond Schematic. Pendant double bonds (**A**, **B**, and **C**) are double bonds that are sterically hindered by the surrounding polymer network such that they cannot bend around and react with surrounding radicals (**E** and **F**).

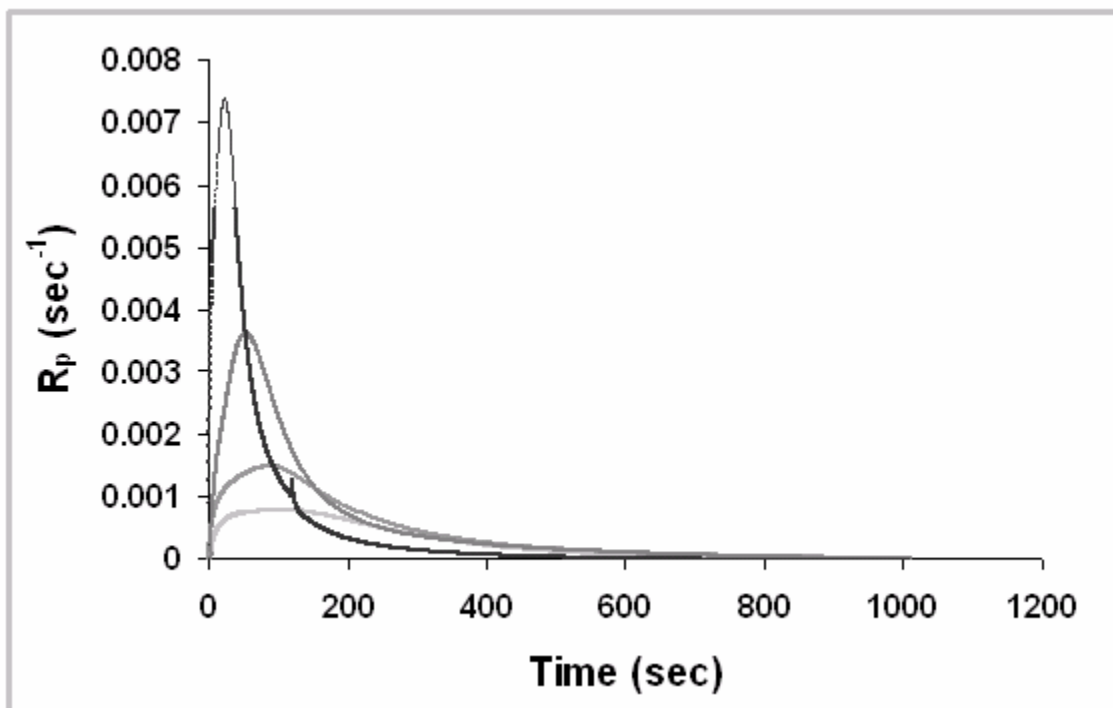


Figure 3.7 Poly(MAA-co-EGDMA) Recognitive Polymer Rate of Polymerization at Various Temperatures. The rate of reaction was measured at -25°C (---), 0°C (—), 25°C (—), and 50°C (—). The rate of reaction increased as the temperature increased.

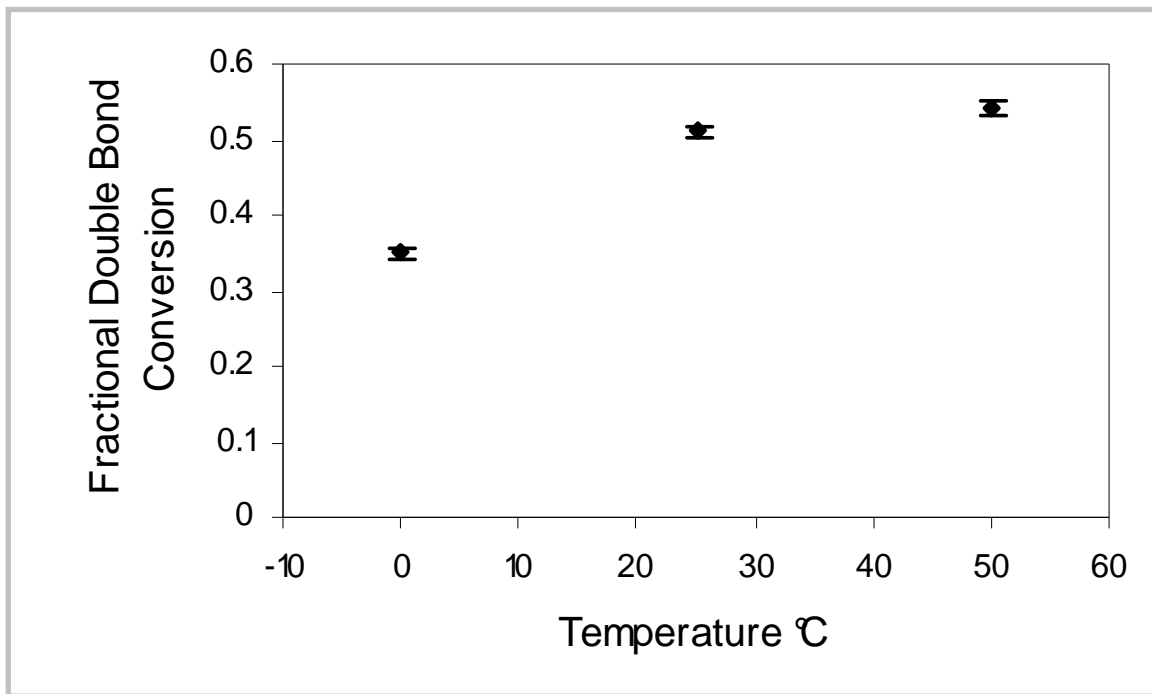


Figure 3.8 Temperature Influence on Fractional Double Bond Conversion.

Fractional double bond conversion versus temperature for a poly (MAA-co-EGDMA) recognitive polymer network shows an increase in double bond conversion with an increase in polymerization temperature.

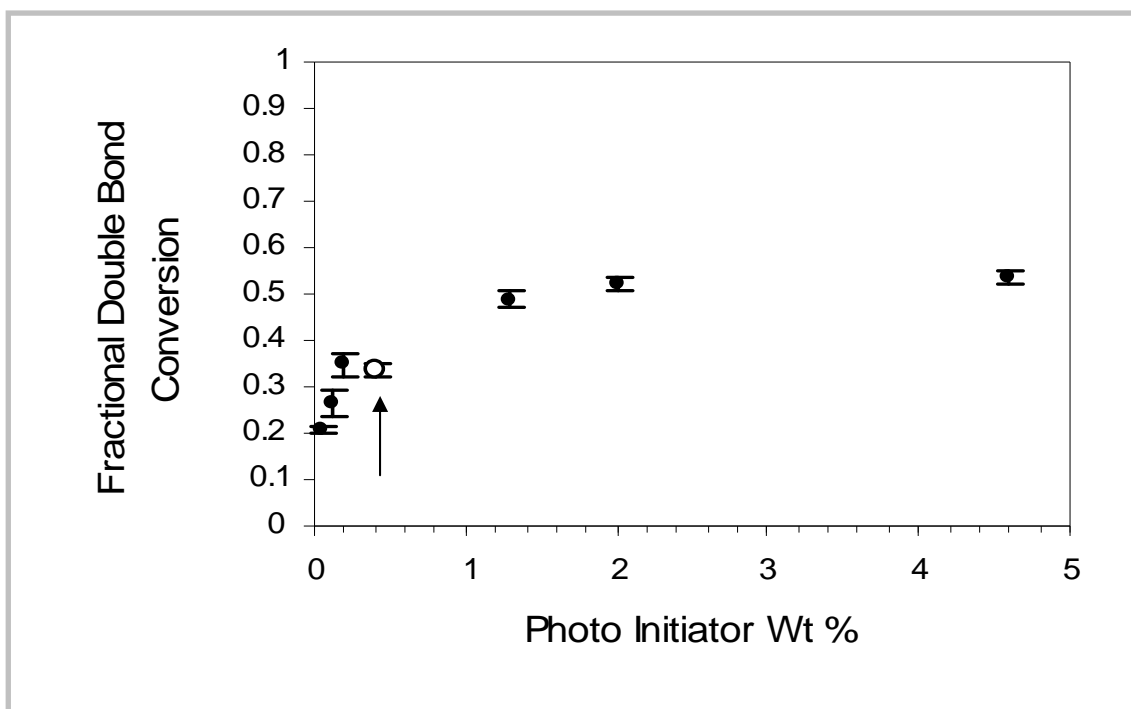


Figure 3.9 Photoinitiator Wt% Effect upon Double Bond Conversion. Parameters such as feed crosslinking percent (88%), solvent wt% (50%), and monomer template ratio (11.79) are held constant. Error bars represent standard deviation ($n = 3$). Arrow indicates the weight percent of initiator of the original poly(MAA-co-EGDMA) recognitive polymer literature network.

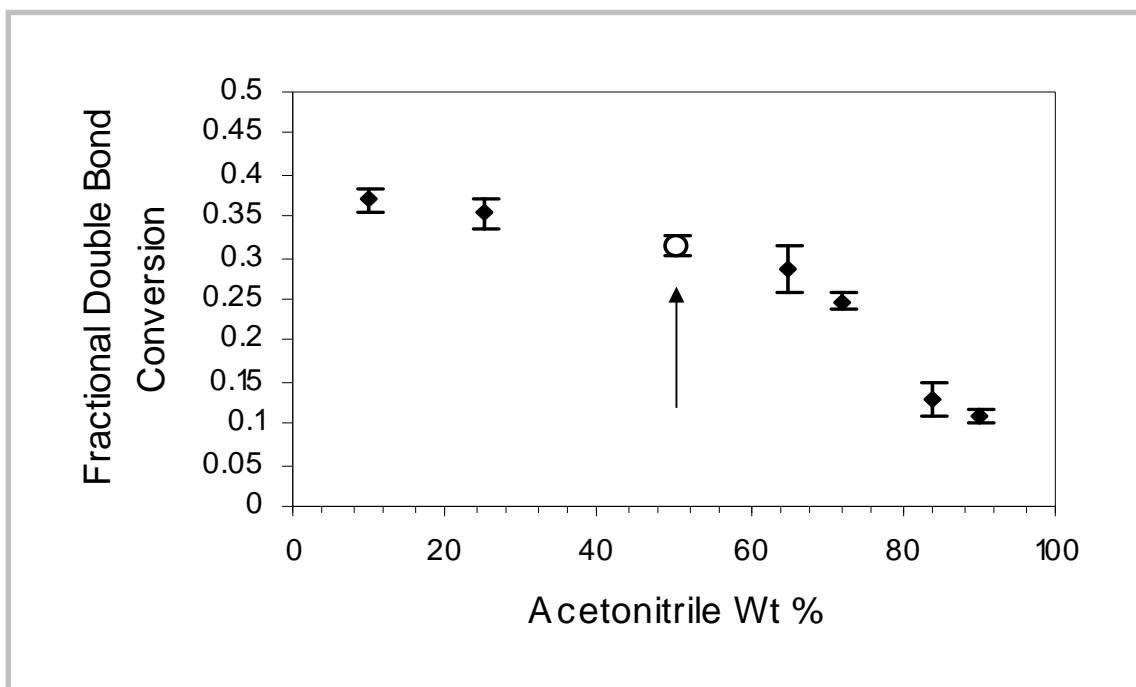


Figure 3.10 Fractional Double Bond Conversion of Poly(MAA-co-EGDMA) Recognitive Networks: Solvent wt% Effect Upon Double Bond Conversion. Note: Parameters such as feed crosslinking percent (88%), wt%(0.4 wt%) initiator, and monomer template ratio (11.79) are held constant. Error bars represent standard deviation ($n = 3$). Arrow indicates poly(MAA-co-EGDMA) recognitive polymer from literature.

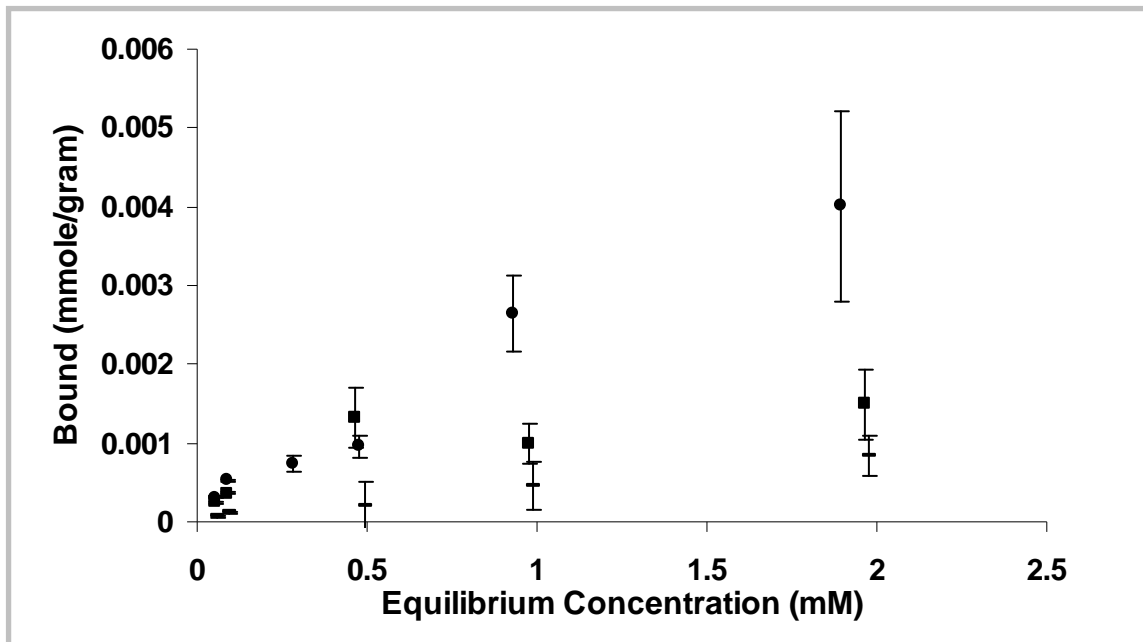


Figure 3.11 Equilibrium Binding Isotherm for Poly(MAA-co-EGDMA) Recognitive Polymers. Poly(MAA-co-EGDMA) recognitive polymer literature match has a 0.4 wt % initiator with a 35% final double bond conversion(■). Poly(MAA-co-EGDMA) recognitive polymer with 2.4 wt % initiator which demonstrated an increased double bond conversion of 48% (●). A modest increase in the capacity of the poly(MAA-co-EGDMA) recognitive polymer is seen. The control (—) has only non-specific binding. Note: Error bars represent the standard error (n = 4).

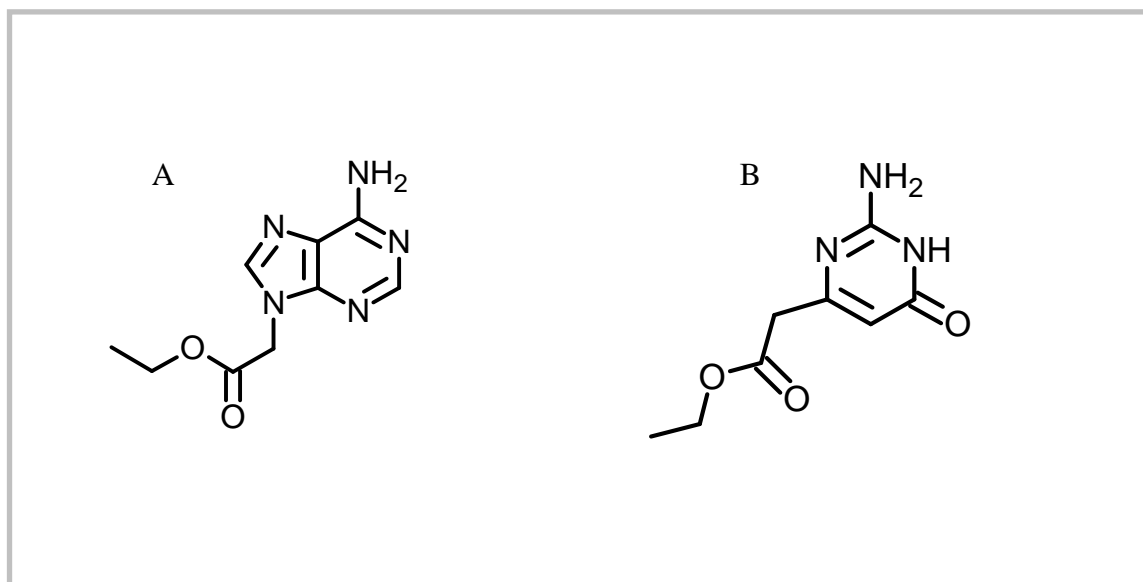


Figure 3.12 Template and Analogue Molecular Structure. Template Molecule , ethyl-adenine-9-acetate (EA9A) (A). Selectivity molecule, ethyl-2-amino-1,6-dihydro-6-oxo-4-pyrimidineacetate (EADOP) (B).

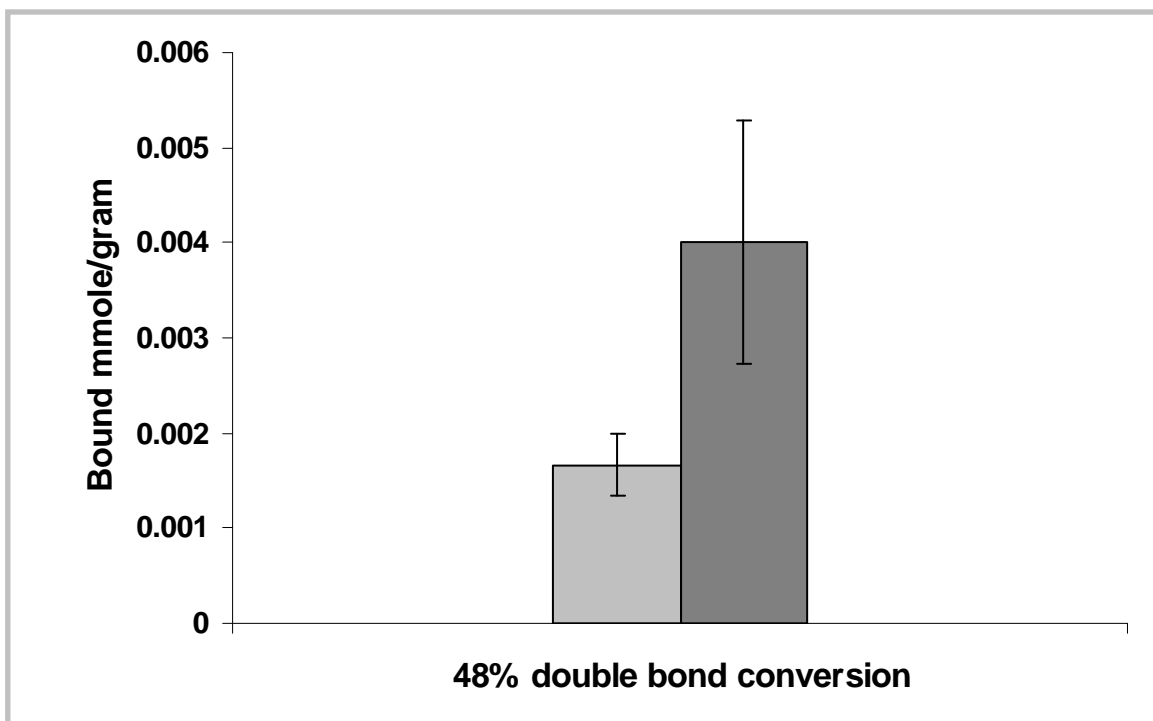


Figure 3.13 Selectivity Study for Poly(MAA-co-EGDMA) Recognitive Polymers.

Poly(MAA-co-EGDMA) recognitive polymer with 48% double bond conversion was selective toward the template, EA9A, (■) at a concentration of 2.0 mM. The EADOP (■) bound by the imprinted polymer presented here is less than half of the EA9A bound by the imprinted network. In this particular study the poly(MAA-co-EGDMA) recognitive polymer literature network, with a double bond conversion of 35%, was not selective.

Note: n = 3 and error bars represent the standard error.

4.0 “LIVING/CONTROLLED” POLYMERIZATION TO PRODUCE RECOGNITIVE NETWORKS

In this chapter, we explore the use of “living/controlled” polymerization to further optimize the template binding parameters of imprinted polymers. “Living/controlled” polymerizations show significant control over linear polymer kinetic chain length. Control of the kinetic chain length within an imprinted copolymer network could contribute to a more homogenous material which would give more structural control over the macromolecular architecture. The reason for the added structural control is the necessity for these materials to be engineered for specific applications. By additional control upon the network structure, the tailorability of these networks increases; therefore, tailorability will inevitably lead to improved binding characteristics via a rationally optimized macromolecular structure. The reaction analysis was used to characterize the imprinted polymers prepared “living/controlled” polymerization reaction techniques, and the binding parameters such as affinity, capacity, and selectivity of different networks were compared. It is important to note that “controlled” polymerization techniques have never been applied to the synthesis of imprinted polymer networks.

4.1 Introduction to “Living/Controlled” Polymerization

Iniferters, which are initiator-chain transfer molecules pioneered by Otzu^{1,2}, have been used to create linear polymer chains with low polydispersities³⁻⁵. Polydispersity or polydispersity index (PDI) is the ratio of the average molecular weight of the chains divided by the number-average molecular weight (Figure 4.1 and Figure 4.2). “Living/controlled” polymerization reactions have been used to create linear polymers of uniform chain length⁶⁻⁹, specific block copolymers¹⁰⁻¹⁵, and grafted polymers on silicon surfaces¹⁶⁻²¹. Shorter kinetic chain lengths have been shown with “living/controlled” homopolymerization of methacrylic anhydride²².

Since its initial discovery, “living” polymerizations have developed greatly into a wide variety of methodologies. Examples of “living/controlled” techniques include, the use of ring opening metathesis polymerization (ROMP)²³, organometallic molecules^{6,24}, atom transfer radical polymerization^{6,25} (ATRP), reverse ATRP^{8,26}, anionic or cationic polymerization, living Ziegler-Natta polymerization, telluride-mediated polymerization (TERP), and iodide transfer polymerization²³.

Polymerization using a “living” polymerization technique, similar to conventional free-radical polymerizations, has initiation, propagation, and termination events as previously presented in Chapter 2, section 2.2.6. During the initiation step in a conventional free-radical polymerization, the initiator is irradiated with UV light and breaks into highly reactive carbon radicals. The carbon radicals actively initiate the polymerization reaction. However, iniferters within “living” polymerization reactions decay upon UV irradiation into more stable dithiocarbamyl (DTC) radicals which do not

actively initiate the polymerization. Therefore, DTC radicals do not actively participate within the propagation step. Conversely, the termination step within “living” polymerization is significantly different from conventional free-radical termination events. Within “living” polymerization, the DTC radical reacts with the propagating chain forming a macro-iniferter. The macro-iniferter can decay back into a DTC radical and a propagating chain during the polymerization. Thus “living/controlled” polymerization adds a reversible termination step to the polymerization reaction^{27, 28}. It is important to note that while there are many different type mechanisms, virtually all the methodologies have the reversible termination step.

“Living/controlled” polymerization approaches have had a significant impact upon the field of linear homo-polymerization²⁹. Qin and coworkers have used living/controlled polymerization techniques to obtain linear poly(methyl methacrylate) (poly(MMA)) with a low polydispersity index (PDI=1.30)⁸. In addition, they show that the polydispersity remains relatively constant while the molecular weight of the growing poly(MMA) increase from 60,100 to 182,000 g/mole and the double bond conversion increases from 27% to 78%²⁶. Matyjaszewski and coworkers have demonstrated that similar results are obtained with “living/controlled” mechanism in the formation of polyacrylonitrile, and results show a polymer chain molecular weight increase during a 23 hour time period with a low polydispersity (PDI=1.05)⁶.

Similarly, “living/controlled” mechanisms have led to the formation of specific block copolymers with well-controlled polydispersities. Block copolymer chains are linear hetero-polymer chains with blocks of specific repeating monomer segments. Research in the field of “living/controlled” polymerization has involved the building of

specific block copolymers with highly controlled monomer segments within the polymer chain in order to create chains of low polydispersity with specific functionality^{12, 15, 30}. For example, a hydroxystyrene-*b*-isobutylene-*b*-hydroxystyrene unique triblock copolymer has been developed exploiting “living/controlled” polymerization for the release of paclitaxel from heart stent coatings³¹. Malinowska and coworkers used a novel bifunctional initiator in the presence of a CuCl catalyst to develop specific block copolymers of methyl methacrylate and tert butyl acrylate with low polydispersities (PDI=1.13-1.56)⁶. In biomedical research, block copolymer chains have been used to produce hydrogels with increased hydrophilicity and subsequent swelling¹⁰, and self-assembled polymersomes of various size and morphologies, degradable networks for use as scaffolds for tissue regrowth¹⁴.

Living/controlled polymerization techniques have also been used to graft polymer chains and networks onto silicon, glass, or polymer substrates in effect covalently binding polymer chains to the surface of the substrate^{16, 20}. Nakayama and coworkers have used “living” polymerization to create specific poly *N,N*-dimethylacrylamide-poly *N*-[3-(dimethylamino)propyl]acrylamide block hetero-polymers grafted on a polystyrene substrate. Additionally, Nakayama and coworkers using similar “living” polymerization techniques have grafted *N,N*-dimethylacrylamide and *N,N*-dimethylaminoethyl methacrylate on chloromethylstyrene to produce hyperbranched architectures^{18, 21, 32}. In addition, iniferters have been used to significantly control the molecular weight and polydispersity of grafted linear polymer chains attached to the surface of the particle (i.e., “hairy” particles)¹⁷. Tsuji and coworkers have created hairy particles by grafting Poly(*N*-isopropylacrylamide) on polystyrene core particles via “living” polymerization³³.

In addition, these reactions have been used to graft cognitive polymer networks to surfaces^{34,35}. Titirici and coworkers have taken an L-phenylalanine anilide imprinted poly(methacrylic acid-co-ethylene glycol dimethacrylate) polymer and grafted it on silicon substrate beads³⁴. Wei and Husson have grafted Boc-L-Trp imprinted polymers upon silica gel and have used high pressure liquid chromatography (HPLC) columns packed with them to show improved resolution of enantiomers and increased loading capacity³⁶. Piletsky and coworkers have grafted an epinephrine imprinted 3-aminophenylboronic acid network on polystyrene cuvettes³⁷. Delaney and coworkers have created creatine imprinted *N, N*-methylene diacrylamide networks grafted to the surface of gold electrodes³⁸. It is important to note that these papers are based using “living” polymerization to graft imprinted polymer networks onto a surface not to synthesize the imprinted network.

The research of “living/controlled” polymerizations to form crosslinked polymer networks has been very limited. Ward and coworkers use a model based upon Flory-Stockmayer theory to simulate the effect of “living/controlled” radical techniques upon linear polymer chains and crosslinked polymer networks⁵. In addition, Ward and coworkers use “living/controlled” polymerizations to synthesize poly(ethylene glycol 200 dimethacrylate) networks³⁹. However, none of these papers use “living/controlled” polymerization techniques to synthesize imprinted polymer networks.

4.2 Hypothesis

The hypothesis is that a “living/controlled” polymerization mechanism would create shorter overall kinetic chain length of polymer chains, and shorter overall chain length within polymer networks could potentially translate into changes within the polymer network. In addition, a decrease in the polydispersity of the chains within the polymer network would create a more homogeneous macromolecular architecture. Homogeneity within an imprinted crosslinked polymer network would provide a optimum environment for the site specific binding sites. As a result of increased homogeneity within the imprinted network, template binding characteristic such as affinity, capacity, and selectivity would be enhanced compared to conventional free-radical produced networks.

4.3 Recognitive Polymer Synthesis via “Living/Controlled” Polymerization Techniques

This section describes the materials and methods regarding the synthesis of two poly(MAA-co-EGDMA) recognitive systems created with “living/controlled” polymerization techniques. Reaction analysis and binding parameter determination methods were similar to previously described methods in Chapter 3, section 3.2.2, section 3.2.3, and section 3.2.4.

4.3.1 Materials

The monomers, methacrylic acid (MAA) and ethylene glycol dimethacrylate (EGDMA), had inhibitors removed via inhibitor removal packing sieves or vacuum distillation prior to polymerization. The initiator azo-bis(isobutyronitrile) (AIBN), template molecule (ethyl adenine-9-acetate (EA9A)), ethyl 2-amino-1,6-dihydro-6-oxo-4-pyrimidineacetate (EADOP), and iniferter (tetraethylthiuram disulfide (TED)) were used as received. Monomers, inhibitor removal packing sieves, initiator, iniferter, template, and template analogue were purchased from Aldrich (Milwaukee, WI). HPLC grade solvents, acetonitrile and methanol, were used as received from Fisher Scientific (Pittsburgh, PA). The polymerization solvent was acetonitrile and the polymer wash solvent (to remove template and unreacted monomer) was acetonitrile/methanol at a 4:1 volume ratio.

4.3.2 Methods: Synthesis of “Living/Controlled” Poly(MAA-co-EGDMA) Networks

The synthesis of the poly(MAA-co-EGDMA) recognitive polymer prepared via “living/controlled” polymerization was carried out in a similar manner to the recognitive networks presented in Chapter 3. Synthesis method described here prepare highly crosslinked EA9A imprinted poly(MAA-co-EGDMA) networks that will be characterized within this chapter. A typical polymerization solution was made with 2.61 mL of EGDMA(13.83 mmoles), 0.16 mL of MAA(1.87 mmoles), 3.96 mL of acetonitrile(704.30 mmoles), 236.4 mg of AIBN, 47.4 mg of TED, and 35.4 mg of EA9A.

Solutions were placed in a sonicator after each addition until a homogeneous solution was obtained. After all components had been mixed, the poly(MAA-co-EGDMA) pre-polymerization solution was made. The solution was then ready for polymerization. The polymerization was carried out in a Q-100 differential photo calorimeter (DPC) from TA Instruments (New Castle, Delaware). Using the DPC, reaction analysis was used to determine a double bond conversion of 44 % for the poly(MAA-co-EGDMA) network.

The rationale behind a second system was to compare the imprinted system synthesized from literature data with 35% double bond conversion to an imprinted system via “living/controlled” techniques with a 35% double bond conversion. The network was synthesized via trial and error using 254.52 mg of AIBN and 47.46 mg of TED.

The polymerization reaction was carried out in a differential photo calorimeter, DPC, at a temperature of 0°C. The total reaction time of the “living/controlled” polymerization was 33 minutes compared to 10 minutes for the conventional reaction (Figure 4.3). The increased reaction time was due to the addition of a reversible termination step within the polymerization reaction. The wash step was carried out in a Soxhlet extraction apparatus. The binding parameters were determined by equilibrium binding studies using EA9A in acetonitrile. Selectivity studies were performed with the template analogue EADOP. Specific details of the wash step and determination of the binding parameters were presented previously in Chapter 3, section 3.2.3 and 3.2.4.

4.4 Results and Discussion

There are two major results from exploiting “living/controlled” polymerization techniques in the formation and optimization of imprinted or recognitive polymers. We demonstrate an increase in template loading capacity with similar binding affinities and an increase in template binding affinity with similar loading capacities.

4.4.1 Template Loading Capacity Enhancement

The final double bond conversion for a poly(MAA-co-EGDMA) recognitive polymer prepared via “living/controlled” polymerization techniques was 44% (Figure 4.4), and the reaction was approximately three times longer. Longer reaction times are directly influenced by the reversible termination step within the polymerization reaction. The reversible termination step terminates a growing radical until equilibrium dictates the reverse reaction (Figure 4.5).

The binding studies for the poly(MAA-co-EGDMA) recognitive polymer prepared via “living/controlled” polymerization techniques showed an increase in binding for the template EA9A compared to the binding isotherms for the poly(MAA-co-EGDMA) recognitive polymer synthesized from literature and the poly(MAA-co-EGDMA) control (Figure 4.6). The template binding affinity and loading capacity (calculated via Freundlich isotherm analysis) for the poly(MAA-co-EGDMA) recognitive polymer prepared via “living/controlled” polymerization techniques were $2.61 \pm 0.12 \text{ mM}^{-1}$ and $1421 \pm 64 \text{ } \mu\text{mole/g}$, respectively. The template loading capacity for the

recognitive polymer prepared via “living/controlled” polymerization techniques when compared to the template loading capacity for the poly(MAA-co-EGDMA) recognitive polymer synthesized from literature ($776 \pm 54 \mu\text{mole/g}$) shows a 63% increase in the template loading capacity. The values for the template binding affinity and loading capacity calculated via Freundlich analysis are presented for the poly(MAA-co-EGDMA) recognitive polymer prepared via “living/controlled” polymerization techniques and the poly(MAA-co-EGDMA) recognitive polymer synthesized from literature in Table 4.1. Both recognitive polymers have roughly equivalent binding affinities. Linearized forms of the binding data for the poly(MAA-co-EGDMA) recognitive polymer prepared via “living/controlled” polymerization techniques can be viewed in Appendix A, section A.5.

The increase in binding is hypothesized to be due to shorter kinetic chain lengths and/or a more narrow dispersity of kinetic chains, which leads to a more homogeneous network and potentially a more uniform crosslink density. A smaller number of chains with a narrow size distribution would decrease the mesh size of the macromolecular structure and lead to a more uniform and higher population of appropriately sized imprinted macromolecular cavities (Figure 4.7). Evidence in the literature of radical chain homopolymerization of multifunctional monomers using size exclusion chromatography and measurements of crosslink density support this conclusion⁴⁰.

Iniferters used in this work decay into two dithiocarbamyl (DTC) radicals, which are more stable compared to carbon radicals. The stability of the DTC radical negates its significance on the initiation and propagation steps during the polymerization reaction, which in this particular case required the addition of carbon radicals, AIBN, to initiate the polymerization reaction. During termination steps of the polymerization reaction, the

Table 4.2 Calculated Binding Parameters for Poly(MAA-co-EGDMA) Recognitive Networks using Freundlich Isotherm Analysis: Increase in Template Loading

Capacity

Polymer	Affinity (mM^{-1})	Capacity ($\mu\text{mole/gram}$)
Poly(MAA-co-EGDMA) recognitive polymer prepared via “living/controlled” polymerization (44% double bond conversion)	2.61 ± 0.12	1421 ± 64
Poly(MAA-co-EGDMA) recognitive polymer synthesized from literature (35% double bond conversion)	3.12 ± 0.21	776 ± 54

stable DTC radicals reversibly terminates with growing polymer radical chains which forms a chain that can re-absorb UV light and decay back into a polymer radical and a DTC radical ²⁸ (Figure 4.4). The limitations and structural heterogeneity of radical polymerizations caused by fast termination reactions can be reduced since iniferters provide a reversible termination reaction that allows for the frustrations in the growing polymer network to be minimized. Frustrations within a crosslinked polymer network are conformations or arrangements of monomer chains formed during the polymerization which are not in the lowest thermodynamic free energy state. These frustrations are formed via mobility constraint of the growing polymer chains from steric hinderances of the surrounding polymer network⁴¹.

4.4.2 Template Binding Affinity Enhancement

To determine if changes in binding capacity were primarily due to double bond conversion differences, another poly(MAA-co-EGDMA) recognitive network was synthesized via “living/controlled” polymerization with a 35% double bond conversion. The determination of the double bond conversion was performed by reaction analysis. It is important to note that in order to obtain a 35% double bond conversion value a trial and error variation of the initiator and iniferter concentrations was conducted.

Results from the binding study shown in Figure 4.8 show the binding isotherms for the poly(MAA-co-EGDMA) recognitive polymer prepared via “living/controlled” polymerization with 35% final double bond conversion compared to the poly(MAA-co-EGDMA) recognitive polymer synthesized from literature (which had a 35% double

bond conversion) and poly(MAA-co-EGDMA) control. Freundlich isotherm analysis was used to calculate the template binding and loading capacity for the network.

As shown previously in Chapter 3, section 3.2.4, Freundlich analysis takes the values from the linear regression of the Freundlich isotherm and calculates the average affinity and capacity for the recognitive polymers. This analysis was used on all recognitive systems studied within this dissertation. The method of analysis was taken from Rampey and coworkers in their analysis of molecularly imprinted polymers⁴². Equation 4.1 is the Freundlich Isotherm where Q is

$$Q = k_f C_e^n \quad 4.1$$

the amount bound by the recognitive polymer, the equilibrium concentration is C_e , the Freundlich affinity is k_f , and the exponent value is n .

The following equations and their explanations are the basis for the results presented within this dissertation. Equation 4.2 and 4.3 give the maximum affinity (K_{max}) and minimum affinity (K_{min}). K_{max} and K_{min} represent the limits at which the affinity spectrum can be from and are determined from the maximum ($C_{e\ max}$) and minimum equilibrium concentrations ($C_{e\ min}$).

$$K_{min} = \frac{1}{C_{e\ max}} \quad 4.2$$

$$K_{max} = \frac{1}{C_{e\ min}} \quad 4.3$$

The number of sites (N_{K1-K2}) was taken between $K1$ and $K2$. $K1$ and $K2$ are affinity values between K_{min} and K_{max} . Equation 4.4 is the equation used for the number of sites.

$$N_{K1-K2} = k_f (1 - n^2)(K_1^{-n} - K_2^{-n}) \quad 4.4$$

The average affinity ($\bar{K}_{K_1-K_2}$) is calculated by equation 4.5.

$$\bar{K}_{K_1-K_2} = \left(\frac{n}{n-1} \right) \left(\frac{K_1^{1-n} - K_2^{1-n}}{K_1^{-n} - K_2^{-n}} \right) \quad 4.5$$

It is important to note that for all the poly(MAA-co-EGDMA) recognitive polymers the values for K_1 and K_2 were all equivalent which allowed for a comparison between systems.

The results for the template binding affinity and loading capacity were $5.94 \pm 0.40 \text{ mM}^{-1}$ and $846 \pm 57 \text{ } \mu\text{mole/g}$. These results when compared with the poly(MAA-co-EGDMA) recognitive polymer synthesized from literature with a template binding affinity of $3.12 \pm 0.21 \text{ mM}^{-1}$ shows a 85% increase in the template binding affinity. The loading capacities for both networks were statistically similar. The template binding affinity and loading capacity values calculated via the Freundlich analysis for the poly(MAA-co-EGDMA) recognitive polymer synthesized from literature and the poly(MAA-co-EGDMA) recognitive polymer prepared via “living/controlled” polymerization techniques with 35% double bond conversion are shown in Table 4.2. Linearized forms of the binding data for the poly(MAA-co-EGDMA) recognitive polymer prepared via “living/controlled” polymerization techniques with 35% double bond conversion can be viewed in Appendix A, section A.5.

The poly(MAA-co-EGDMA) recognitive polymer prepared via “living/controlled” polymerization techniques with 35% double bond conversion shows a higher affinity for the template EA9A. Intrinsically, this must be due to a higher population of high affinity sites. We hypothesize the increase in the population of higher

Table 4.2 Calculated Binding Parameters for Poly(MAA-co-EGDMA) Recognitive Networks using Freundlich Isotherm Analysis: Increase in Template Binding

Affinity

Polymer	Affinity (mM^{-1})	Capacity ($\mu\text{mole/gram}$)
Poly(MAA-co-EGDMA) recognitive polymer synthesized from literature (35% double bond conversion)	3.12 ± 0.21	776 ± 54
Poly(MAA-co-EGDMA) recognitive polymer prepared via "living/controlled" polymerization (35% double bond conversion)	5.94 ± 0.41	846 ± 57

affinity sites is due to better network control and orientations of functional monomer within the network via polymerization with iniferter which are due to shorter kinetic chain lengths and/or a more narrow dispersity of kinetic chains, leading to a more homogeneous network. Homogeneity within the macromolecular network in conjunction with smaller kinetic chain lengths can potentially yield smaller mesh size distributions within the network forming a more appropriate sized polymer support network for the formation specific high affinity recognition sites. Binding isotherms of all EA9A imprinted poly(MAA-co-EGDMA) polymer networks described and compared within this chapter are presented in Figure 4.9. Similarly, values of template binding affinity and loading capacity calculated via Freundlich analysis for all EA9A imprinted poly(MAA-co-EGDMA) polymer networks are presented in Table 4.3.

4.4.3 Selectivity

Selectivity studies were also performed upon the poly(MAA-co-EGDMA) recognitive polymer prepared via “living/controlled” polymerization techniques. The selectivity study was done in the exact same manner as presented in Chapter 3, section 3.2.3 using the template substitute, EADOP. The binding capacity for EA9A and EADOP for the poly(MAA-co-EGDMA) recognitive polymer with 48% double bond conversion and the poly(MAA-co-EGDMA) recognitive polymer prepared via “living/controlled” polymerization techniques is presented in Figure 4.10. It is important to note that these two recognitive polymers have very similar double bond conversions.

Table 4.3 Calculated Binding Parameters for Poly(MAA-co-EGDMA) Recognitive Networks using Freundlich Isotherm Analysis.

Polymer	Affinity (mM^{-1})	Capacity ($\mu\text{mole/gram}$)
Poly(MAA-co-EGDMA) recognitive polymer synthesized from literature (35% double bond conversion)	3.12 ± 0.21	776 ± 54
Poly(MAA-co-EGDMA) recognitive polymer prepared via "living/controlled" polymerization (35% double bond conversion)	5.94 ± 0.41	846 ± 57
Poly(MAA-co-EGDMA) recognitive polymer (48% double bond conversion)	2.63 ± 0.17	860 ± 60
Poly(MAA-co-EGDMA) recognitive polymer prepared via "living/controlled" polymerization (44% double bond conversion)	2.61 ± 0.12	1421 ± 64

The values of selectivity based upon capacities were 2.4 ± 1.0 and 1.9 ± 0.5 for poly(MAA-co-EGDMA) recognitive polymer with 48% double bond conversion and poly(MAA-co-EGDMA) recognitive polymer prepared via “living/controlled” polymerization techniques, respectively. It is important to note that poly(MAA-co-EGDMA) recognitive polymer prepared via “living/controlled” polymerization techniques had a 63% increase in the number of binding sites while retaining a selective nature for the template. It is hypothesized that “living/controlled” polymerization decreases the kinetic chain length and creates a more homogeneous macromolecular structure which provides an optimum network for the stabilization for the three dimensional spatial arrangement of functional groups which would enhance the template binding parameters. In addition, the minimization of the frustrations through reversible termination reactions reduce the steric hinderences within the growing polymer network and allow the monomers to conform to thermodynamically lower energy states which would translate into a more thermodynamically conducive environment which potentially increase and/or enhance the number of effective specific binding sites within the network.

Selectivity studies based upon affinities was preformed on the poly(MAA-co-EGDMA) recognitive polymer prepared via “living/controlled” polymerization techniques. Specifics on the study can be found in Chapter 3, section 3.3.2. The selectivity number calculated was (1.47 ± 0.07) for the poly(MAA-co-EGDMA) recognitive polymer prepared via “living/controlled” polymerization techniques. These results also indicate that there is an increased number of binding sites by 63% while retaining selectivity for the target molecule, EA9A. Values of the selectivity based upon

Table 4.4 Calculated Selectivity Numbers based upon Affinities and Capacity for Poly(MAA-co-EGDMA) Recognitive Networks.

Polymer	Selectivity (K_{EA9A}/K_{EADOP})	Selectivity (Bound EA9A/Bound EADOP) (2mM^{-1} Concentration)
Poly(MAA-co-EGDMA) recognitive polymer synthesized from literature (35% double bond conversion)	1.63 ± 0.11	N/A
Poly(MAA-co-EGDMA) recognitive polymer (48% double bond conversion)	1.81 ± 0.12	2.4 ± 1.0
Poly(MAA-co-EGDMA) recognitive polymer prepared via “living/controlled” polymerization (44% double bond conversion)	1.47 ± 0.07	1.9 ± 0.5

affinity values for the poly(MAA-co-EGDMA) recognitive polymer synthesized from literature, the poly(MAA-co-EGDMA) recognitive polymer with 48% double bond conversion, and the poly(MAA-co-EGDMA) recognitive polymer prepared via “living/controlled” polymerization techniques are presented in Table 4.4. It is important to note that selectivity studies were not done for the poly(MAA-co-EGDMA) recognitive polymer prepared via “living/controlled” polymerization with 35% double bond conversion.

In addition to these studies a detailed washing analysis on the quantities of template EA9A theoretically in the polymer network, bound by the polymer network (assessed by binding isotherms), and the amount washed out using Soxhlet extraction. These studies are presented and discussed in Appendix B.

4.5 Conclusion

We are the first group within the field to employ “living/controlled” polymerization to synthesize imprinted polymer networks. This work indicates that “living/controlled” polymerization techniques can increase the template binding capacity over that of conventional free-radical polymerizations (demonstrated here by a 63% increase). At matching conversions, “living/controlled” polymerization techniques can increase the template binding affinity (demonstrated here by a 85% increase). In addition, EA9A imprinted poly(MAA-co-EGDMA) polymers show selectivity of 1.47 ± 0.07 with the 63% increase in template loading capacity. The increase in binding parameters is hypothesized from shorter overall kinetic chain lengths, a more homogeneous

macromolecular architecture within the polymeric network, and minimization of limitations and structural heterogeneity of radical polymerizations caused by fast termination reactions through reversible termination reactions that allow the minimization of frustrations in the growing polymer. Additional work with “living/controlled” polymerization strategies in conjunction with reaction analysis of molecular imprinted polymers will inevitably lead to improved binding characteristics via a rationally optimized macromolecular structure. Since imprinted network applications depend implicitly on the extent of control of the structural and binding characteristics, this work and future work in this area are expected to yield promising new materials for sensors, point-of-care diagnostics, and drug delivery carriers.

4.6 List of References

1. Otsu, T.; Yoshida, M., Role of Initiator-Transfer Agent-Terminator (Iniferter) in Radical Polymerizations: Polymer Design by Organic Disulfides as Iniferters. *Die Makromolekulare Chemie, Rapid Communications* **1982**, 3, (2), 127-132.
2. Matyjaszewski, K., A Commentary on "Role of Initiator-Transfer Agent-Terminator (Iniferter) in Radical Polymerizations: Polymer Design by Organic Disulfides as Iniferters" by T. Otsu, M. Yoshida (Macromol. Rapid Commun.1982,3, 127-132). *Macromolecular Rapid Communications* **2005**, 26, (3), 135-142.
3. Haddleton, D. M.; Kukulj, D.; Duncalf, D. J.; Heming, A. M.; Shooter, A. J., Low-Temperature Living "Radical" Polymerization (Atom Transfer Polymerization) of

Methyl Methacrylate Mediated by Copper(I) N-Alkyl-2-Pyridylmethanimine Complexes. *Macromolecules* **1998**, 31, (16), 5201-5205.

4. Endo, K.; Murata, K.; Otsu, T., Living Radical Polymerization of Styrene with Tetramethylene Disulfide. *Macromolecules* **1992**, 25, (20), 5554-5556.

5. Ward, J. H.; Peppas, N. A., Kinetic Gelation Modeling of Controlled Radical Polymerizations. *Macromolecules* **2000**, 33, (14), 5137-5142.

6. Matyjaszewski, K.; Mu Jo, S.; Paik, H. j.; Gaynor, S. G., Synthesis of Well-Defined Polyacrylonitrile by Atom Transfer Radical Polymerization. *Macromolecules* **1997**, 30, (20), 6398-6400.

7. High, K.; Meng, Y.; Washabaugh, M. W.; Zhao, Q., Determination of Picomolar Equilibrium Dissociation Constants in Solution by Enzyme-linked Immunosorbent Assay with Fluorescence Detection. *Analytical Biochemistry* **2005**, 347, (1), 159-161.

8. Qin, D. Q.; Qin, S. H.; Qiu, K. Y., A Reverse ATRP Process with a Hexasubstituted Ethane Thermal Iniferter Diethyl 2,3-Dicyano-2,3-di(p-tolyl)succinate as the Initiator. *Macromolecules* **2000**, 33, (19), 6987-6992.

9. Qin, L.; He, X.-W.; Li, W.-Y.; Zhang, Y.-K., Molecularly Imprinted Polymer Prepared with Bonded [Beta]-cyclodextrin and Acrylamide on Functionalized Silica Gel for Selective Recognition of Tryptophan in Aqueous Media. *Journal of Chromatography A* **2008**, 1187, (2), 94-102.

10. Baek, S. H.; Kim, B. S.; Kim, B. K., Hydrogels Based on Polyurethane-polyacrylic Acid Multiblock Copolymers via Macroiniferter Technique. *Progress in Organic Coatings* **2004**, 49, (4), 353-357.

11. Chen, H.; Peng, C.; Ye, Z.; Liu, H.; Hu, Y.; Jiang, J., Recognition of Multiblock Copolymers on Nanopatterned Surfaces: Insight from Molecular Simulations. *Langmuir* **2007**, *23*, (5), 2430-2436.
12. Cheng, Z.; Zhu, X.; Fu, G. D.; Kang, E. T.; Neoh, K. G., Dual-Brush-Type Amphiphilic Triblock Copolymer with Intact Epoxide Functional Groups from Consecutive RAFT Polymerizations and ATRP. *Macromolecules* **2005**, *38*, (16), 7187-7192.
13. Gabashvili, A.; Medina, D. D.; Gedanken, A.; Mastai, Y., Templating Mesoporous Silica with Chiral Block Copolymers and Its Application for Enantioselective Separation. *J. Phys. Chem. B* **2007**, *111*, (38), 11105-11110.
14. Kwon, I. K.; Matsuda, T., Photo-iniferter-based Thermoresponsive Block Copolymers Composed of Poly(ethylene glycol) and Poly(N-isopropylacrylamide) and Chondrocyte Immobilization. *Biomaterials* **2006**, *27*, (7), 986-995.
15. Qin, Y.; Sukul, V.; Pagakos, D.; Cui, C.; Jakle, F., Preparation of Organoboron Block Copolymers via ATRP of Silicon and Boron-Functionalized Monomers. *Macromolecules* **2005**, *38*, (22), 8987-8990.
16. de Boer, B.; Simon, H. K.; Werts, M. P. L.; van der Vegte, E. W.; Hadziioannou, G., "Living" Free Radical Photopolymerization Initiated from Surface-Grafted Iniferter Monolayers. *Macromolecules* **2000**, *33*, (2), 349-356.
17. Francis, R.; Ajayaghosh, A., Minimization of Homopolymer Formation and Control of Dispersity in Free Radical Induced Graft Polymerization Using Xanthate Derived Macro-photoinitiators. *Macromolecules* **2000**, *33*, (13), 4699-4704.

18. Lee, H. J.; Nakayama, Y.; Matsuda, T., Spatio-Resolved, Macromolecular Architectural Surface: Highly Branched Graft Polymer via Photochemically Driven Quasiliving Polymerization Technique. *Macromolecules* **1999**, 32, (21), 6989-6995.
19. Liu, P.; Liu, Y.; Su, Z., Modification of Poly(hydroethyl acrylate)-Grafted Cross-linked Poly(vinyl chloride) Particles via Surface-Initiated Atom-Transfer Radical Polymerization (SI-ATRP). Competitive Adsorption of Some Heavy Metal Ions on Modified Polymers. *Ind. Eng. Chem. Res.* **2006**, 45, (7), 2255-2260.
20. Matsuda, T.; Ohya, S., Photoiniferter-Based Thermoresponsive Graft Architecture with Albumin Covalently Fixed at Growing Graft Chain End. *Langmuir* **2005**, 21, (21), 9660-9665.
21. Nakayama, Y.; Sudo, M.; Uchida, K.; Matsuda, T., Spatio-Resolved Hyperbranched Graft Polymerized Surfaces by Iniferter-Based Photograft Copolymerization. *Langmuir* **2002**, 18, (7), 2601-2606.
22. Hutchison, J. B.; Lindquist, A. S.; Anseth, K. S., Experimental Characterization of Structural Features during Radical Chain Homopolymerization of Multifunctional Monomers Prior to Macroscopic Gelation. *Macromolecules* **2004**, 37, (10), 3823-3831.
23. Byrne, M. E.; Collins, A.; Vaughan, A. D.; Venkatesh, S. Therapeutic Contact Lenses with Anti-Fungal Delivery. US Patent 2007.
24. Ding, S.; Xing, Y.; Radosz, M.; Shen, Y., Magnetic Nanoparticle Supported Catalyst for Atom Transfer Radical Polymerization. *Macromolecules* **2006**, 39, (19), 6399-6405.

25. Yang, J.; Ding, S.; Radosz, M.; Shen, Y., Reversible Catalyst Supporting via Hydrogen-Bonding-Mediated Self-Assembly for Atom Transfer Radical Polymerization of MMA. *Macromolecules* **2004**, *37*, (5), 1728-1734.
26. Chen, X. P.; Qiu, K. Y., Synthesis of Well-Defined Poly(methyl methacrylate) by Radical Polymerization with a New Initiation System TPED/FeCl₃/PPh₃. *Macromolecules* **1999**, *32*, (26), 8711-8715.
27. Kannurpatti, A. R.; Anderson, K. J.; Anseth, J. W.; Bowman, C. N., Use of "Living" Radical Polymerizations to Study the Structural Evolution and Properties of Highly Crosslinked Polymer Networks. *Journal of Polymer Science Part B: Polymer Physics* **1997**, *35*, (14), 2297-2307.
28. Kannurpatti, A. R.; Lu, S.; Bunker, G. M.; Bowman, C. N., Kinetic and Mechanistic Studies of Iniferter Photopolymerizations. *Macromolecules* **1996**, *29*, (23), 7310-7315.
29. Ajayaghosh, A.; Francis, R., Narrow Polydispersed Reactive Polymers by a Photoinitiated Free Radical Polymerization Approach. Controlled Polymerization of Methyl Methacrylate. *Macromolecules* **1998**, *31*, (4), 1436-1438.
30. Sumerlin, B. S.; Tsarevsky, N. V.; Louche, G.; Lee, R. Y.; Matyjaszewski, K., Highly Efficient "Click" Functionalization of Poly(3-azidopropyl methacrylate) Prepared by ATRP. *Macromolecules* **2005**, *38*, (18), 7540-7545.
31. Sipos, L.; Som, A.; Faust, R.; Richard, R.; Schwarz, M.; Ranade, S.; Boden, M.; Chan, K., Controlled Delivery of Paclitaxel from Stent Coatings Using Poly(hydroxystyrene-*b*-isobutylene-*b*-hydroxystyrene) and Its Acetylated Derivative. *Biomacromolecules* **2005**, *6*, (5), 2570-2582.

32. Nakayama, Y.; Matsuda, T., Surface Macromolecular Microarchitecture Design: Biocompatible Surfaces via Photo-Block-Graft-Copolymerization Using N,N-Diethyldithiocarbamate. *Langmuir* **1999**, 15, (17), 5560-5566.
33. Tsuji, S.; Kawaguchi, H., Effect of Graft Chain Length and Structure Design on Temperature-Sensitive Hairy Particles. *Macromolecules* **2006**, 39, (13), 4338-4344.
34. Titirici, M. M.; Sellergren, B., Thin Molecularly Imprinted Polymer Films via Reversible Addition-Fragmentation Chain Transfer Polymerization. *Chemistry of Materials* **2006**, 18, (7), 1773-1779.
35. Sulitzky, C.; Ruckert, B.; Hall, A. J.; Lanza, F.; Unger, K.; Sellergren, B., Grafting of Molecularly Imprinted Polymer Films on Silica Supports Containing Surface-Bound Free Radical Initiators. *Macromolecules* **2002**, 35, (1), 79-91.
36. Wei, X.; Husson, S. M., Surface-Grafted, Molecularly Imprinted Polymers Grown from Silica Gel for Chromatographic Separations. *Ind. Eng. Chem. Res.* **2007**, 46, (7), 2117-2124.
37. Piletsky, S. A.; Piletska, E. V.; Chen, B.; Karim, K.; Weston, D.; Barrett, G.; Lowe, P.; Turner, A. P. F., Chemical Grafting of Molecularly Imprinted Homopolymers to the Surface of Microplates. Application of Artificial Adrenergic Receptor in Enzyme-Linked Assay for B-Agonists Determination. *Anal. Chem.* **2000**, 72, (18), 4381-4385.
38. Delaney, T. L.; Zimin, D.; Rahm, M.; Weiss, D.; Wolfbeis, O. S.; Mirsky, V. M., Capacitive Detection in Ultrathin Chemosensors Prepared by Molecularly Imprinted Grafting Photopolymerization. *Anal. Chem.* **2007**, 79, (8), 3220-3225.
39. Ward, J. H.; Shahar, A.; Peppas, N. A., Kinetics of 'Living' Radical Polymerizations of Multifunctional Monomers. *Polymer* **2002**, 43, (6), 1745-1752.

40. Odian, G., *Principles of Polymerization*. 2nd edition ed.; John Wiley & Sons: New York, 1981.
41. Pande, V. S.; Grosberg, A. Y.; Tanaka, T., Phase Diagram of Heteropolymers with an Imprinted Conformation. *Macromolecules* **1995**, 28, (7), 2218-2227.
42. Rampey, A. M.; Umpleby, R. J.; Rushton, G. T.; Iseman, J. C.; Shah, R. N.; Shimizu, K. D., Characterization of the Imprint Effect and the Influence of Imprinting Conditions on Affinity, Capacity, and Heterogeneity in Molecularly Imprinted Polymers Using the Freundlich Isotherm-Affinity Distribution Analysis. *Anal. Chem.* **2004**, 76, (4), 1123-1133.

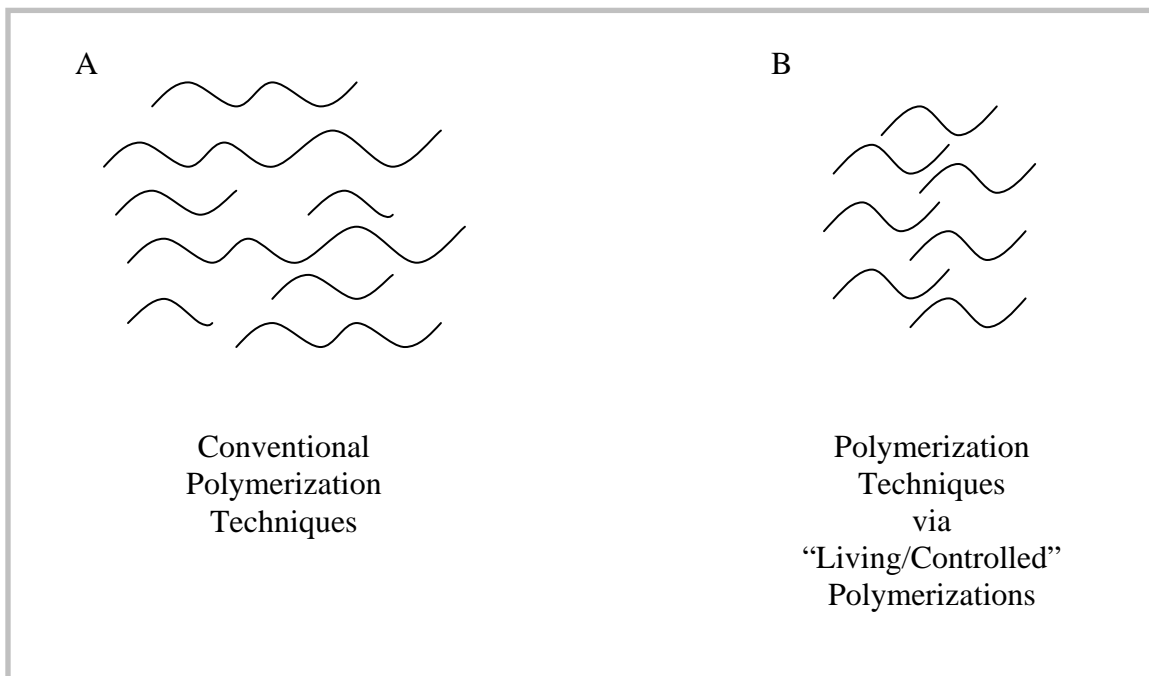


Figure 4.1 Schematic of the “Living/Controlled” Polymerization of Linear Chains.

Conventional free-radical polymerization methods typically yield high chain polydispersities which are distributions of polymer chains of varying lengths (**A**). “Living/controlled” polymerization techniques have been shown to produce linear polymer chains with shorter kinetic chain lengths along with low polydispersities (**B**).

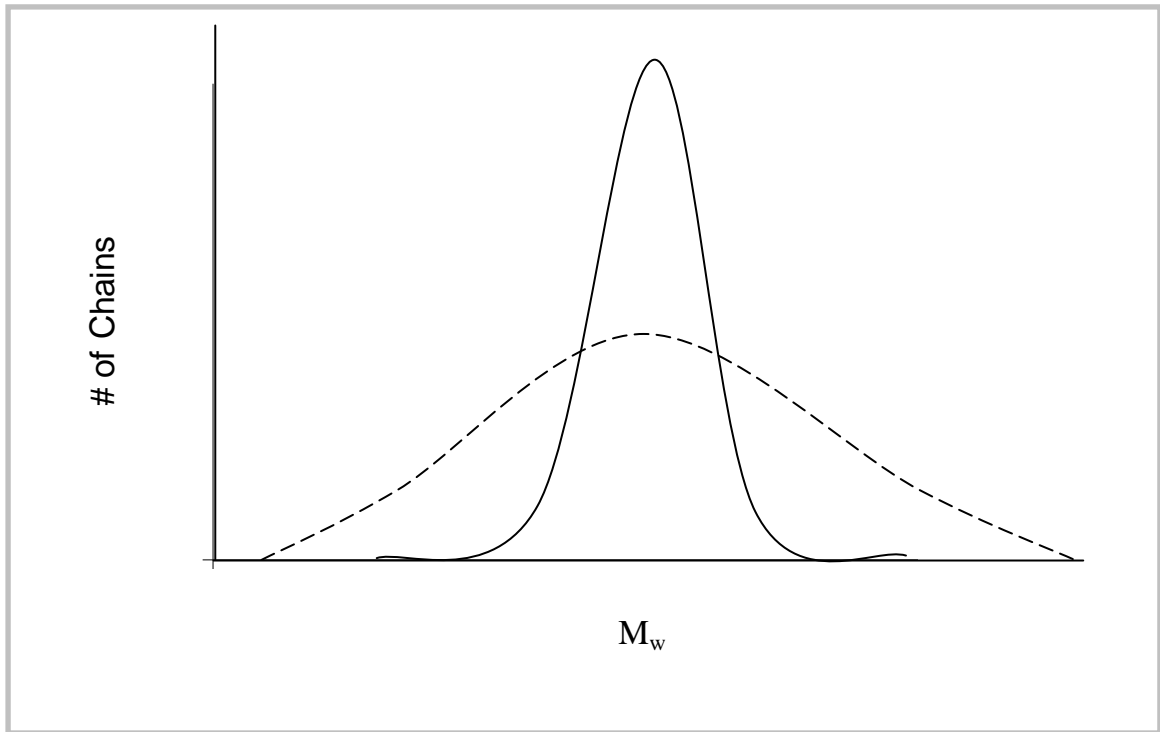


Figure 4.2 Schematic of the Distribution of Linear Polymer Chains. Polydispersity is the ratio of the weight average molecular weight divided by the number average molecular weight (M_w/M_n). The solid line presents linear polymer chain distribution with a low polydispersity. The dashed line presents a linear polymer chain distribution exemplifying a high polydispersity within the linear polymer chains.

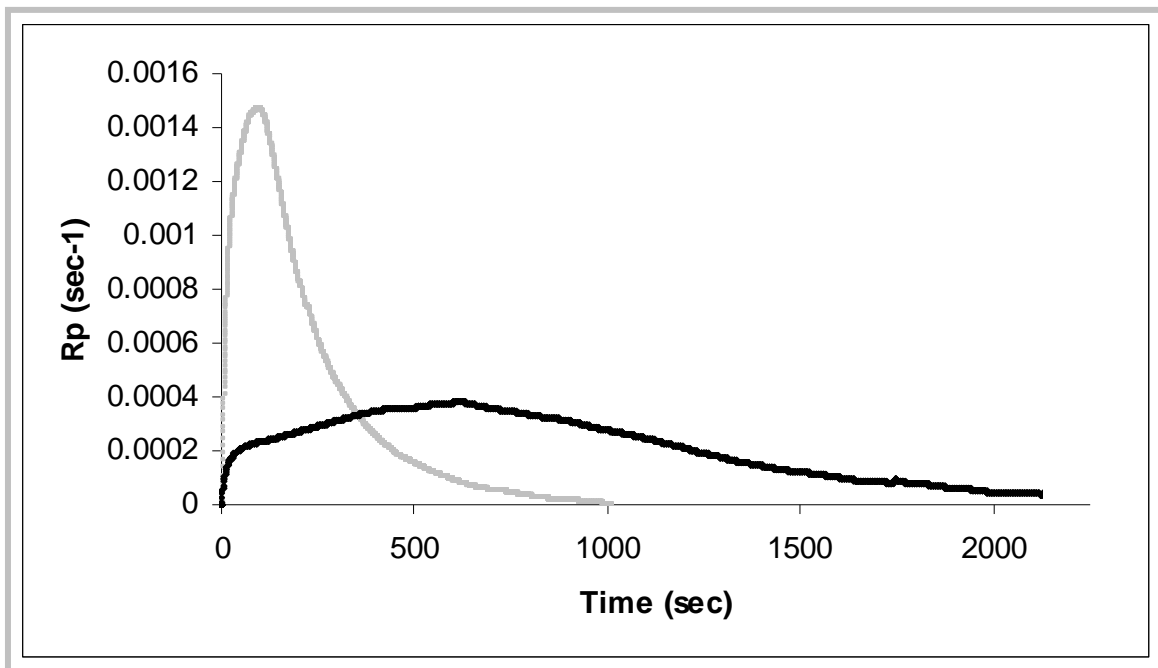


Figure 4.3 Polymerization Time for “Living/Controlled” versus Standard UV Free-radical Polymerization of Poly(MAA-co-EGDMA) Imprinted Networks. The polymerization incorporating “living/controlled” polymerization techniques (—) has a 2200 second polymerization time while the conventional UV-free radical polymerization (—) has a 1000 second polymerization time. Longer polymerization reaction times are typical of “living/controlled” polymerization.

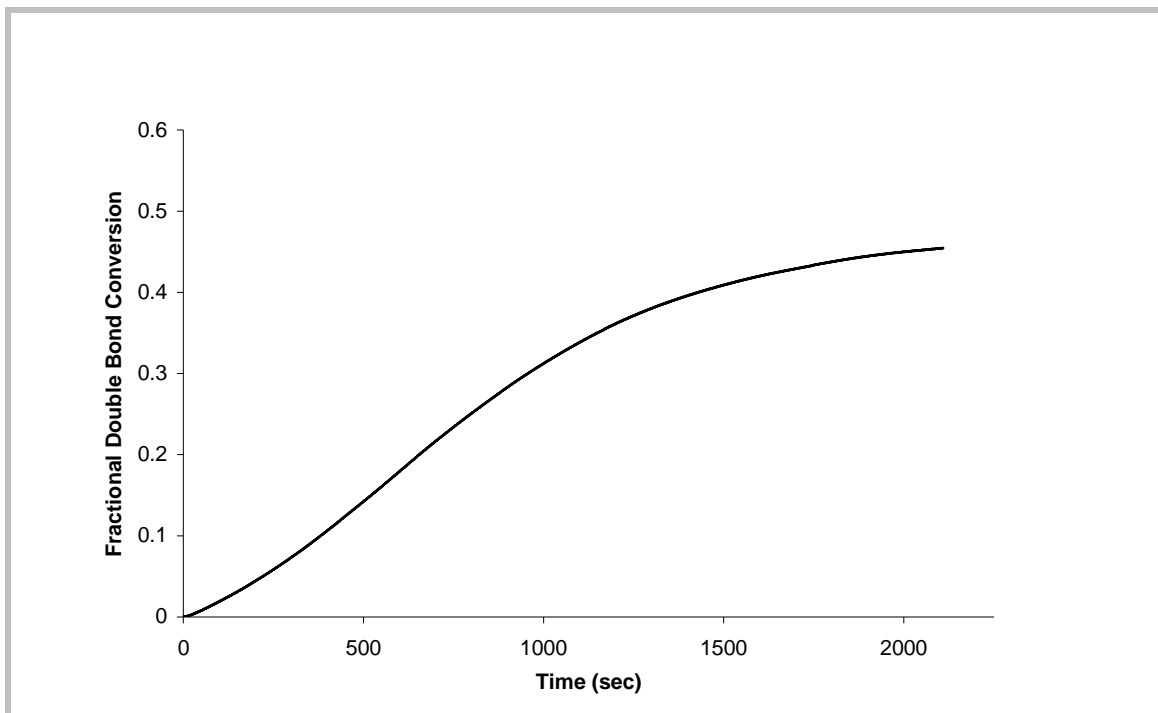


Figure 4.4. Dynamic Double Bond Conversion of a Poly(MAA-co-EGDMA) Polymer Network via “Living/controlled” Polymerization. Double bond conversion verses time for a polymer synthesized with “living/controlled” polymerization with 88% feed crosslinker and monomer-template ratio of 11.79. The final double bond conversion reached is 44%.

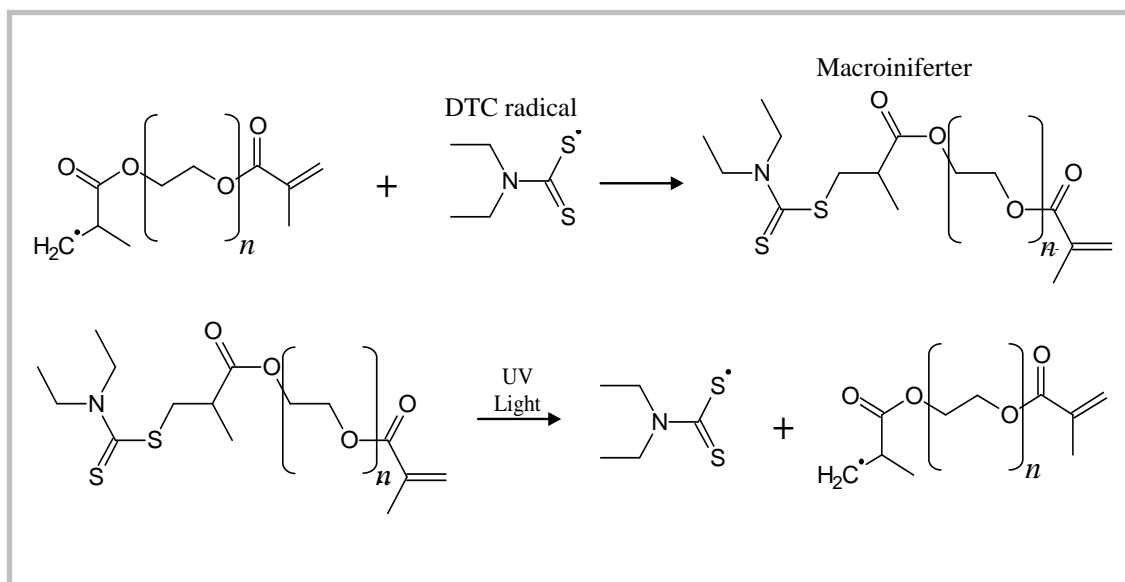


Figure 4.5. Reversible Termination. The schematic shows the reversible termination reaction that occurs with the DTC radical and a growing polymer radical to form a macroiniferter. This macroiniferter can be irradiated with UV light to decay into a DTC radical and polymer radical to continue the reaction process. Note: n = number of repeating ethylene glycol units.

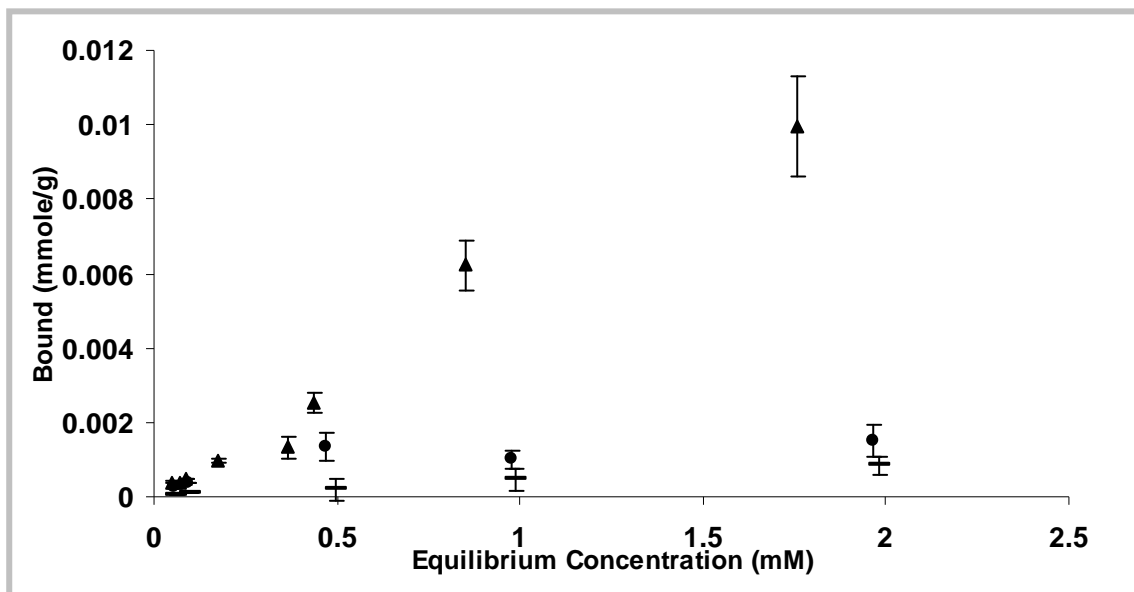


Figure 4.6 Equilibrium Binding Isotherm for a Poly(MAA-co-EGDMA) Recognitive Polymer Synthesized via “Living/controlled” Polymerization Techniques. Poly(MAA-co-EGDMA) recognitive polymer prepared via “living/controlled” polymerization techniques with 44% double bond conversion (▲) has a 63% increase in the number of binding sites over that of the poly(MAA-co-EGDMA) recognitive polymer synthesized from literature (●) (35% double bond conversion). Both recognitive networks showed higher binding than the poly(MAA-co-EGDMA) control (■). Note: Error bars represent the standard error (n = 4).

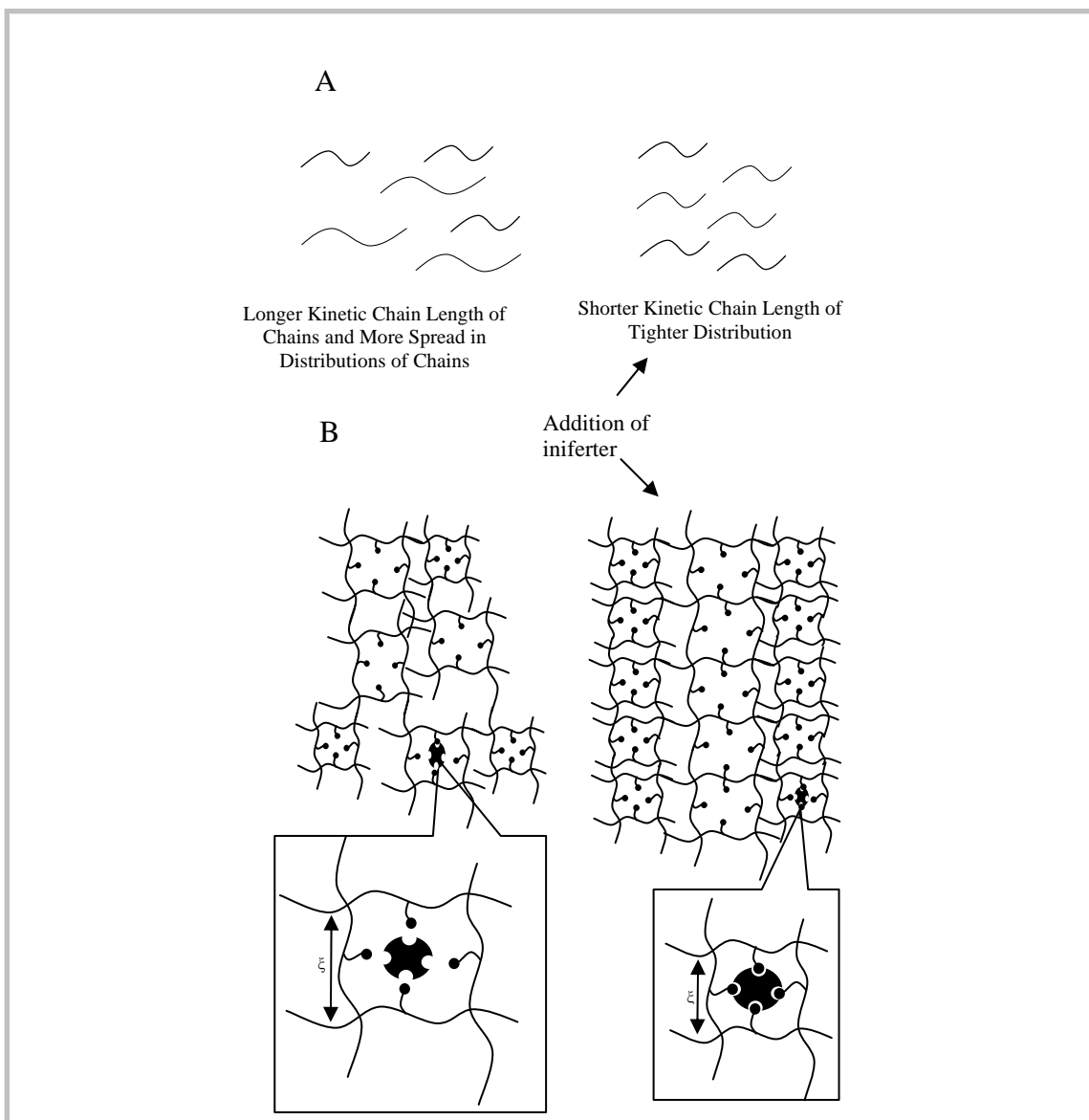


Figure 4.7 Controlled/Living Polymerization and the Effect on Imprinted Network Structure. A. In mono-vinyl polymerization, the use of iniferter yields a lower polydispersity of kinetic chains and decreased average chain length. B. Within crosslinked networks, addition of iniferter leads to a more uniform and higher population of appropriately sized imprinted macromolecular cavities for the template. An optimal mesh size, ξ , gives the binding site a better functional configuration which leads to enhanced binding properties.

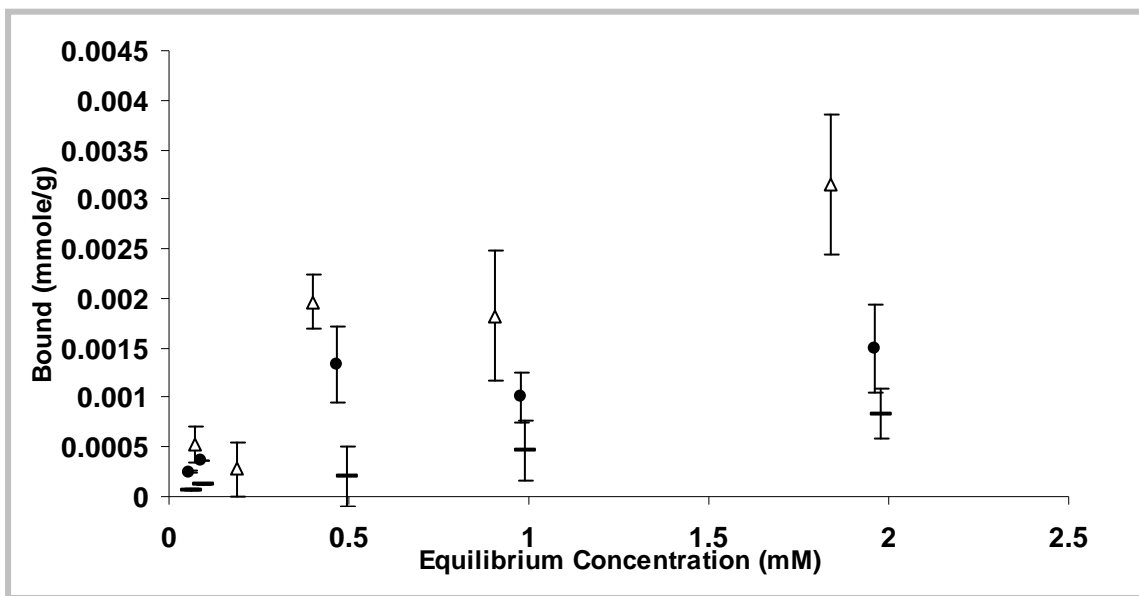


Figure 4.8 Equilibrium Binding Isotherm for Poly(MAA-co-EGDMA) Recognitive Polymer Synthesized via “Living/controlled” Polymerization Techniques: Matching Double Bond Conversions. Poly(MAA-co-EGDMA) recognitive polymer prepared via “living/controlled” polymerization techniques with 35% double bond conversion (Δ) shows a slight increase in loading capacity over that of the poly(MAA-co-EGDMA) recognitive polymer synthesized from literature (\bullet) (35% double bond conversion). However, Freundlich isotherm analysis yields an increase in template binding affinity (5.94 ± 0.40 compared to 3.12 ± 0.21) mM^{-1} . Both recognitive networks showed higher binding than the poly(MAA-co-EGDMA) control (\blacksquare). Note: Error bars represent the standard error ($n = 4$).

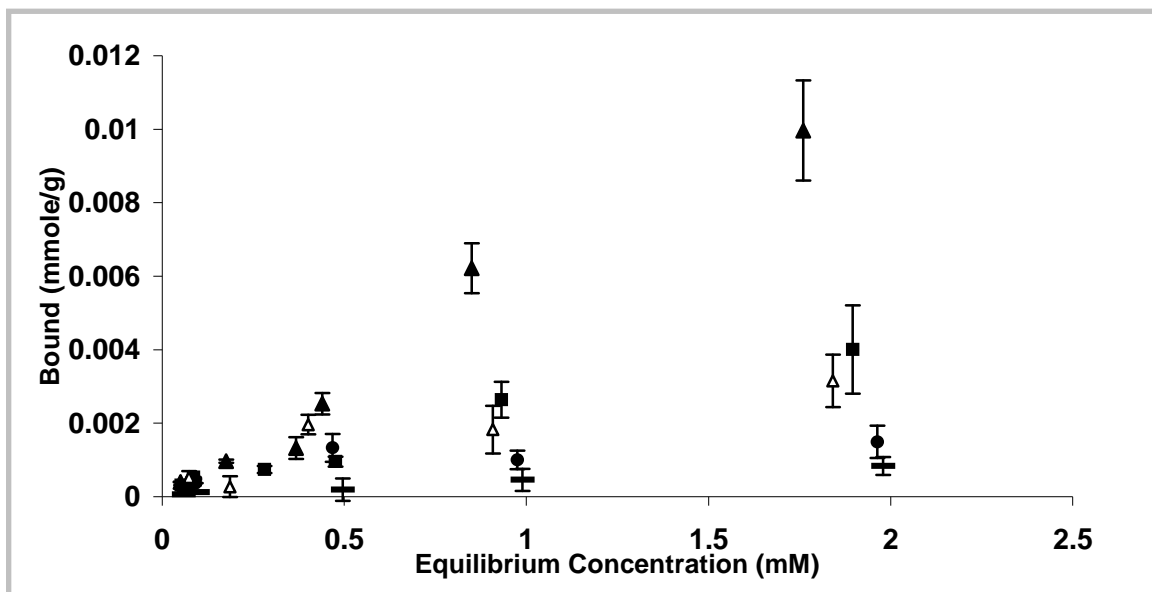


Figure 4.9 Binding Isotherm Comparison of All EA9A Imprinted Poly(MAA-co-EGDMA) Networks Conventional Free-Radical versus “Living/controlled” Polymerization Techniques. This figure presents all the isotherms for EA9A imprinted poly(MAA-co-EGDMA) networks, the poly(MAA-co-EGDMA) recognitive polymer prepared via “living/controlled” polymerization techniques with 44% double bond conversion (▲), the poly(MAA-co-EGDMA) recognitive polymer prepared via “living/controlled” polymerization techniques with 35% double bond conversion (Δ), the poly(MAA-co-EGDMA) recognitive polymer with 48% double bond conversion (■), the poly(MAA-co-EGDMA) recognitive polymer synthesized from literature (●), and the poly(MAA-co-EGDMA) control (—). Error bars represent the standard error (n = 4).

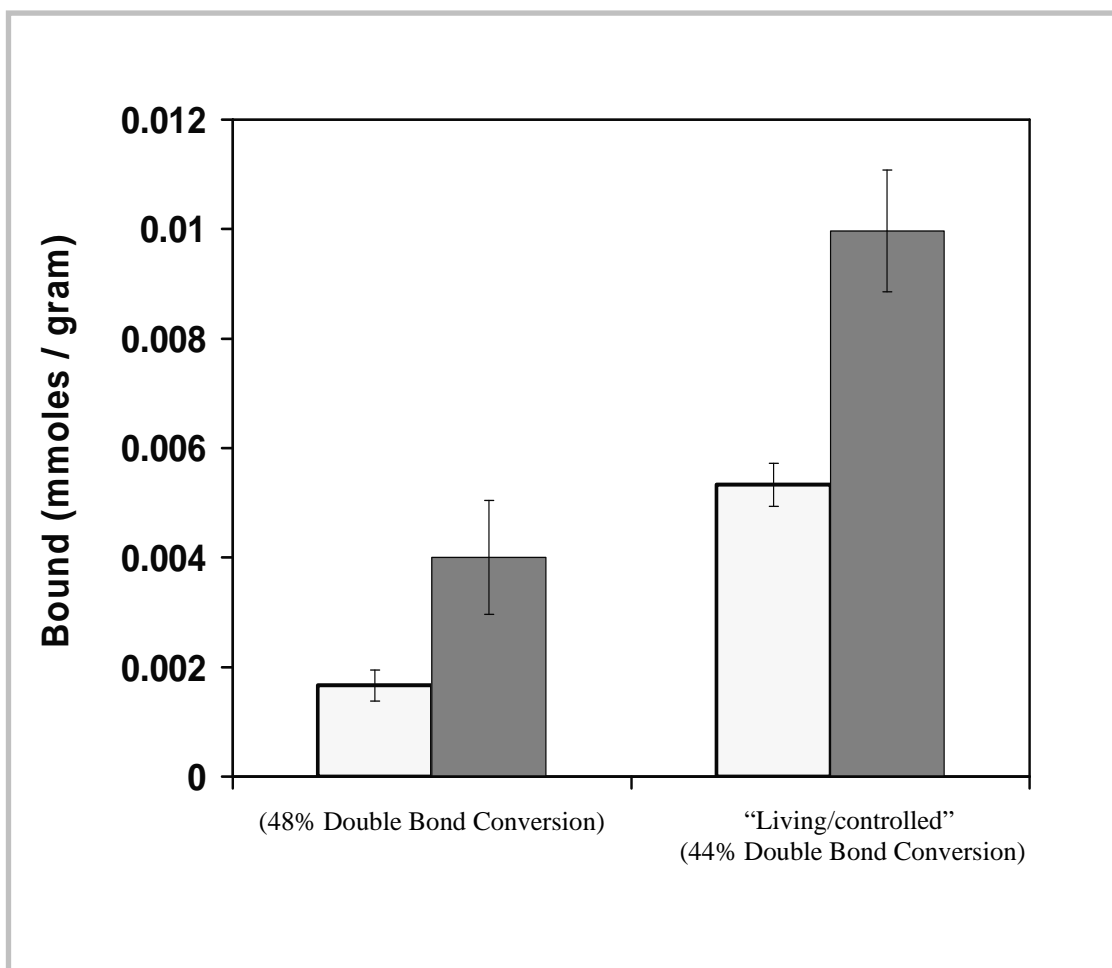


Figure 4.10 Selectivity Comparison for Poly(MAA-co-EGDMA) Recognitive Networks for Ethyladenine (EA9A): Selectivity Study. Both networks were more selective for EA9A (■) than that of the analog molecule EADOP (■) at template and analog concentrations of 2.0 mM. Error bars represent standard deviation (n = 3).

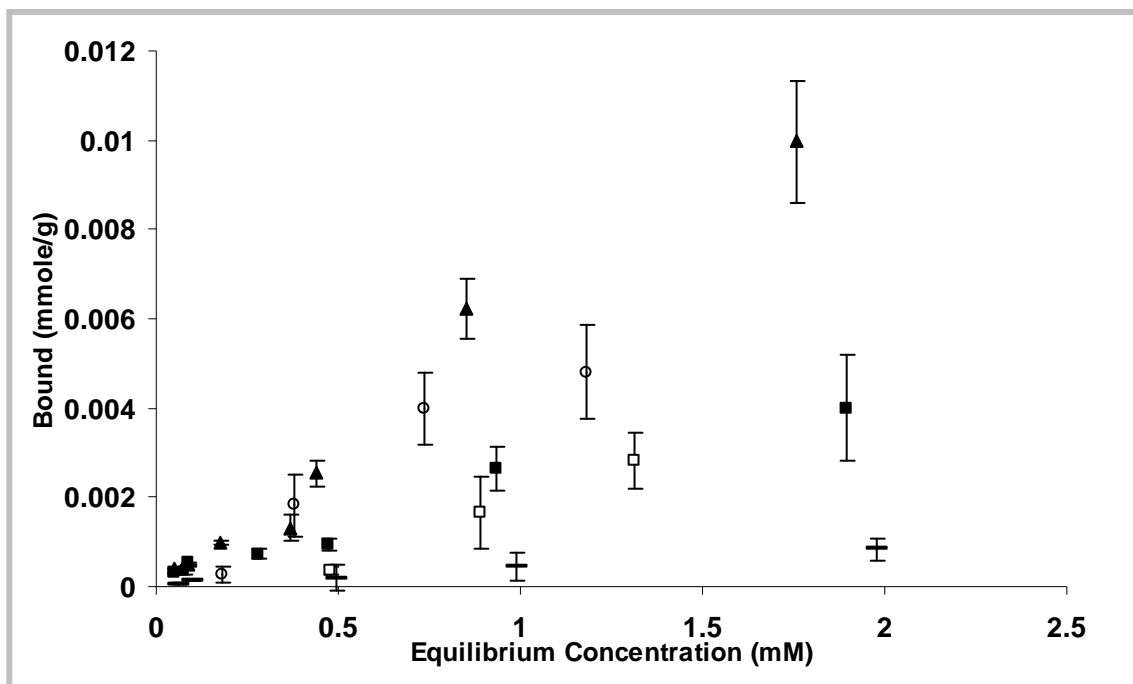


Figure 4.11 Poly(MAA-co-EGDMA) Networks Binding Isotherms for EA9A and EADOP: Selectivity Analysis Poly(MAA-co-EGDMA) recognitive polymer network with 48% double bond conversion (■) and poly(MAA-co-EGDMA) recognitive polymer prepared via “Living/controlled” polymerization techniques (▲) have higher selectivity for the template EA9A than for the template analog EADOP based upon affinities calculated from these isotherms. Binding isotherms for EADOP are shown for poly(MAA-co-EGDMA) recognitive polymer network with 48% double bond conversion (□) and poly(MAA-co-EGDMA) recognitive polymer prepared via “Living/controlled” polymerization techniques (○). Error bars represent standard error (n = 4).

**5.0 ENHANCED TEMPLATE LOADING AND CONTROLLED RELEASE
VIA “LIVING/CONTROLLED” POLYMERIZATION
REACTIONS: FOCUSING ON POTENTIAL
DRUG DELIVERY CARRIERS**

In this chapter, we transition from highly crosslinked imprinted networks to weakly crosslinked imprinted gels. In Chapter 4, the use of “living/controlled” polymerization techniques increased the template binding capacity by 63% in a highly crosslinked network. Thin films employing the use of weakly crosslinked imprinted gels have been the subject of significant merit within the field of advanced drug delivery carriers. Furthermore, an increase in the template binding capacity within weakly crosslinked polymer networks would significantly impact the field of imprinted materials for advanced drug delivery.

Our hypothesis from Chapter 4, explaining the 63% increase in the template binding capacity, was due to shorter kinetic chain lengths and/or a more narrow dispersity of kinetic chains, which leads to a more homogeneous network structure (i.e., structure lends itself to larger number of appropriate sized imprinted cavities). Highly crosslinked imprinted polymer networks, such as those presented in Chapter 4, are very brittle (networks must be solvated at all times to keep from cracking) which make the analysis

of the material properties extremely difficult. However, mechanical analysis of flexible, weakly crosslinked gels has been used to calculate the mesh size of imprinted and non-imprinted gels. The binding parameters of imprinted gels synthesized via “living/controlled” polymerization methodologies along with mesh size analysis could potentially illuminate structural characteristics that influence the increase in binding parameters.

The two weakly crosslinked imprinted networks/gels used in this study were an ethyl-adenine-9-acetate (EA9A) imprinted poly(methacrylic acid-co-ethylene glycol dimethacrylate) (poly(MAA-co-EGDMA)) copolymer network and a diclofenac sodium imprinted poly(diethylaminoethyl-methacrylate-co-2-hydroxyethyl-methacrylate-co-polyethyleneglycol 200 dimethacrylate) (poly(DEAEM-co-HEMA-co-PEG200DMA) copolymer network. Both copolymer networks are weakly crosslinked with 5% crosslinker (moles of crosslinking monomer divided by mole of all monomers in solution).

5.1 Introduction to Controlled Drug Delivery

Controlled drug delivery by definition is a method or technique that delivers a therapeutic amount of drug in an extended duration to the body. Drugs and drug delivery carriers can be delivered via an enteral route or parenteral route. Drug delivered through an enteral route enters the body through the gastrointestinal (GI) tract by absorption and then enters the blood circulation. Specifically, the enteral route refers to drug delivery via the GI tract which means drug can be absorbed via the tongue (i.e., sublingual), the

mouth (i.e., buccal cavity), the stomach (i.e., gastrically), the intestine (i.e., small and large intestines), and the rectum. The parenteral route refers to methods of drug delivery such as intravenous, intramuscular, subcutaneous, intradermal, percutaneous, inhalation, intraarterial, intrathecal, intraperitoneal, and vaginal¹. The most common forms of drug delivery are oral, ingestion, pulmonary, and transdermal². Each drug delivery method has advantages and disadvantages when delivering therapeutic amounts of drug to the body.

In many cases, drug delivery from thin films and coatings is based upon the Fickian model of release kinetics. Gels exhibit high relaxation rates and rate limiting diffusion processes which typically result in the release rate being proportional to the concentration gradient³. The advantage of tuning co-polymer network functionality is the ability to manipulate the macromolecular structure on the micro-scale thus controlling the drug release rate³⁻⁵. The control of diffusional characteristics within these gels is a distinct advantage for drug delivery applications.

Macromolecular memory within co-polymer gels is a relatively new method for additional control of the therapeutic diffusion gel characteristics and is especially useful with thin films and coatings. Imprinting techniques introducing “macromolecular memory” within gels increase the tailorability of the macromolecular structure by producing gel networks with intrinsic template binding parameters of affinity and capacity for the template molecule. Binding and memory of template therapeutics within hydrogel networks have shown extended therapeutic release potential within thin films for use within ocular delivery^{3, 4, 6}.

Over 90% of the current methods of ocular drug delivery are in the form of topical eye drops that treat ocular disease. The drug solution within topical eye drops is

very concentrated because of low bioavailability with only 1-7% of the applied drug being absorbed^{6,7}. The use of topical eye drop solutions deliver effective amounts of drug to the eye; however, within a 15 minute time span after initial application, all the drug from the instilled eye-drop volume has been flushed from the eye by tear turnover. Drug delivery via thin films using enhanced template affinity and loading will allow for an advanced drug delivery device, such as a contact lens, for controlled therapeutic delivery to the eye.

5.2 Hypothesis

The hypothesis is that with the use of a “living/controlled” polymerization mechanism within weakly crosslinked materials, substantial increases in the template loading/capacity for both an EA9A imprinted poly(MAA-co-EGDMA) network and an diclofenac sodium imprinted poly(DEAEM-co-HEMA-co-PEG200DMA) network will be observed. Dynamic mechanical analysis of weakly crosslinked imprinted gels will illuminate inherent changes in network structure (i.e., a more homogeneous imprinted network) resulting from “living/controlled” polymerization. Dynamic template release analysis of these imprinted gel networks formed via “living” reaction schemes with increased loading and altered structural characteristics will show enhanced tailorability of the template release profiles of these imprinted gel networks.

5.3 Materials and Methods

Described in this section are the materials and methods used in the synthesis of two loosely crosslinked networks: poly(MAA-co-EGDMA) imprinted gels and poly(DEAEM-co-HEMA-co-PEG200DMA) imprinted gels. All gels were synthesized containing 5% crosslinker in the feed composition.

5.3.1 Materials

The monomers, methacrylic acid (MAA) and ethylene glycol dimethacrylate (EGDMA), had inhibitors removed via inhibitor removal packing sieves or vacuum distillation prior to polymerization. Monomers used as received were 2-hydroxyethyl methacrylate (HEMA), diethylaminoethyl methacrylate (DEAEM). The initiator azobis(isobutyronitrile) (AIBN), template molecules (ethyl adenine-9-acetate (EA9A) and diclofenac sodium), and iniferter (tetraethylthiuram disulfide (TED)) were used as received. Monomers, inhibitor removal packing sieves, initiator, iniferter, and template were purchased from Aldrich (Milwaukee, WI). Poly(ethylene glycol 200 dimethacrylate (PEG200DMA) was purchased from Polysciences, Inc (Warrington, PA). HPLC grade solvents, acetonitrile and methanol, were used as received from Fisher Scientific (Pittsburgh, PA). The polymer wash solvent (to remove template and unreacted monomer) was acetonitrile/methanol at a 4:1 volume ratio for the EA9A cognitive network or deionized water for the diclofenac sodium cognitive network.

5.3.2 Methods: Synthesis of Poly(MAA-co-EGDMA) Recognitive Gels

A typical polymerization solution resulting in an EA9A imprinted poly(MAA-co-EGDMA) gel, was made with 0.187 mL of EGDMA(0.993 mmole), 0.16 mL of MAA(18.86 mmoles), 18.55 mg of AIBN, and 84.06 mg of EA9A. Solutions were placed in a sonicator for several minutes until all solids were dissolved. Poly(MAA-co-EGDMA) control gel solution was made exactly in the same manner as the recognitive gel except no EA9A template was added. Poly(MAA-co-EGDMA) recognitive gel prepared via “living/controlled” polymerization techniques was made by addition of 3.89 mg of iniferter, TED. The molar ratio of the moles of initiator divided by the moles of iniferter was 8.61. For both recognitive gels, the amount of monomer and template added to mixtures was 0.16 mL of MAA, 0.187 mL of EGDMA, and 84.06 mg of EA9A. For polymerization, the temperature of polymerization was $14^{\circ}\text{C} \pm 1^{\circ}\text{C}$ throughout the exothermic reaction and a light intensity of $52.5 \text{ mW}/\text{cm}^2$. Lower temperatures resulted in freezing of the pre-polymerization mixture. All polymers were polymerized within the DPC resulting in discs having 3 mm diameter and 1 mm in thickness.

Poly(MAA-co-EGDMA) gel disks for template diffusion analysis studies were made with a specially designed glass mold to achieve a disk size of 28 mm diameter and 1 mm thickness. These disks were polymerized at a temperature of 14°C and light intensity of $52.5 \text{ mW}/\text{cm}^2$. The disks were washed in a modified Soxhlet extraction device to ensure the disks were immersed in solvent at all times.

5.3.3 Methods: Synthesis of Poly(DEAEM-co-HEMA-co-PEG200DMA) Recognitive Gels

A typical polymerization solution for the diclofenac sodium imprinted poly(DEAEM-co-HEMA-co-PEG200DMA) gel was made with 0.336 mL of DEAEM (1.673 mmole), 3.659 mL of HEMA (30.118 mmole), 0.538 mL of PEG200DMA (1.673 mmole), 20 mg of AIBN (0.121 mmole), and 150 mg of diclofenac sodium (0.352 mmole). The components were mixed and sonicated until solids were dissolved in solution. The poly(DEAEM-co-HEMA-co-PEG200DMA) recognitive gels were prepared with the template molecule, and the control gels were prepared without the template. Poly(DEAEM-co-HEMA-co-PEG200DMA) control gel was the exact same mixture of monomers and initiator excluding the template molecule. Poly(DEAEM-co-HEMA-co-PEG200DMA) recognitive gel prepared via “living/controlled” polymerization technique was synthesized with 4.20 mg of TED (0.014 mmole) and 40 mg of AIBN (0.242 mmole). The solutions were pipetted between two 6” x 6” glass plates separated by 0.25 mm Teflon spacers using long-stemmed pipettes. The glass plates were coated with trichloromethylsilane to prevent strong adherence of the polymer matrix to the glass. The solutions and equipment were then transferred to a MBraun Labmaster 130 1500/1000 Glovebox (Stratham, NH), which provided an inert (nitrogen) atmosphere for free-radical UV photopolymerization. The solutions were left uncapped and open to the nitrogen until the O₂ levels inside reached negligible levels (<1 PPM). The polymerization reaction was carried out for 8 minutes for the poly(DEAEM-co-HEMA-co-PEG200DMA) control and recognitive gels while for the “living/controlled”

polymerization prepared polymers the reaction time was 24 minutes. The intensity of light from a UV Flood Curing System (Torrington, CT) was 40 mW/cm² at a voltage of 325 V, and the temperature within the glovebox was 25°C.

The glass plates were soaked in deionized (DI) water and the polymers were peeled off the plates and cut into circular discs using a size 10 cork borer (13.5 mm). The gels were washed in a well-mixed 2 L container of DI water for 7 days with a constant 5 mL per minute flowrate of de-ionized water through the container. Absence of detectable drug released from the polymer was verified by spectroscopic monitoring. The discs were allowed to dry under laboratory conditions at a temperature of 20°C for 24 hours and then transferred to a vacuum oven (27 in Hg, 33-34°C) for 24 hours until the disc weight change was less than 0.1 wt%.

5.3.4 Methods: Binding Studies for Poly(MAA-co-EGDMA) Gels

Binding analysis was conducted using poly(MAA-co-EGDMA) recognitive gel disks within acetonitrile. After a 24 hour period, the absorbance of the solution was measured with a Synergy UV-Vis spectrophotometer. Separate kinetic studies were performed to assure equilibrium conditions were reached. A mass balance was used to determine the bound amount of drug within the polymer gel. This binding analysis was performed using similar methods as described previously in Chapter 3, section 3.2.3.

5.3.5 Methods: Binding Studies for Poly(DEAEM-co-HEMA-co-PEG200DMA) Gels

A stock solution of 1 mg/mL of diclofenac sodium was prepared and diluted to five concentrations (0.05 mg/mL, 0.10 mg/mL, 0.15 mg/mL, 0.20 mg/mL, and 0.25 mg/mL) in 50 mL conical vials. Initial absorbances of each concentration were measured in the UV-vis spectrophotometer. After the initial absorbance, a washed poly(DEAEM-co-HEMA-co-PEG200DMA) polymer disk was inserted in each vial and allowed to equilibrate over a 7 day period. After equilibrium was reached, the solutions were vortexed for 10 seconds, and the absorbances of the equilibrium concentrations were measured via the Synergy UV/Vis spectrophotometer (BioTek Instruments, Winooski, VT). The wavelength of absorbance for diclofenac sodium was 276 nm. It is important to note that all gels were analyzed in triplicate. It is important to note all binding values are based upon the dry weight of the gel.

5.3.6 Methods: Template Diffusion Analysis of Poly(MAA-co-EGDMA) Gels

Dried, washed discs were placed in a 2.0 mM solution of EA9A in acetonitrile and allowed to reach equilibrium. Release studies were performed using 50 mL polypropylene conical vials with 25 mL of acetonitrile. Mixing was achieved by placing vials on an Ocelot oscillator (Boekel Scientific, Feasterville, PA). To ensure an infinite sink for the release studies, the fluid was changed every 8 hours for the first 36 hours and thereafter every 24 hours. At every fluid change, a 200 μ L aliquot of the solution was

taken and the EA9A concentration was measured via UV spectrophotometry at a wavelength of 265 nm.

The diffusion coefficient of template was calculated from Fick's law, which describes one-dimensional planar solute release from gels⁸. For geometries with aspect ratios (exposed surface length/thickness) greater than 10, edge effects can be ignored and the problem approached as a one-dimensional process⁸. Solution of Fick's law for short times of diffusion is given by equation, 5.1,

$$\frac{M_t}{M_\infty} = 4 \left[\frac{Dt}{\pi L^2} \right]^{\frac{1}{2}} \quad 5.1$$

where M_t is the mass of EA9A released at time t , M_∞ is the mass of EA9A released at time equal to infinity, D is the diffusion coefficient independent of position and concentration, and L is the thickness of the disk. For each polymer network, the fractional release of EA9A (M_t/M_∞) versus $(t^{0.5}/L)$ was plotted and the diffusion coefficient was calculated from the slope.

5.3.7 Methods: One Dimensional Transport Analysis from Poly(DEAEM-co-HEMA-co-PEG200DMA) Gels

The diffusion studies for the hydrogels employed a Side-Bi-Side Cell Diffusion Apparatus, (PermeGear, Hellertown, PA). After the washing procedure, the thickness of the swollen gels was measured with an electronic micrometer. The gels were then placed between the diffusion cells. An aliquot of 3.4 mL of 1 mM diclofenac sodium aqueous solution was placed on one side of the hydrogel while another 3.4 mL aliquot of DI water

was placed in the other side of the cell. At various times, 0.2 mL aliquots were taken from both the donor and receptor cell and were measured via a Synergy UV-Vis spectrophotometer (BioTek Instruments, Winooski, Vermont) to determine the concentration within each side of the cell. Data was collected and linear regression of the data was analyzed by plotting $(\ln(1-2C_t/C_d))$ against $(-2At/V)$ then calculating the slope to determine the permeability (5.2),

$$\ln\left[1 - \frac{2C_t}{C_d}\right] = -\frac{2A}{V}Pt \quad 5.2$$

where C_t is the concentration in the receptor cell, C_d is the concentration of the donor cell, A is the area of diffusion, V is the volume of each half cell, t is time, and P is the permeability. The diffusion coefficient was calculated from the following two equations,

$$D = \frac{P\delta}{K_d} \quad 5.3$$

$$K_d = \frac{C_m}{C_s} = \frac{V_s(C_i - C_o)}{V_m C_o} \quad 5.4$$

5.3 and 5.4, where D is the diffusion coefficient, P is the permeability, δ is the hydrogel thickness, K_d is the partition coefficient, C_m is the concentration of the solute in the hydrogel at equilibrium, C_s is the concentration of the solute in solution at equilibrium, C_i is the initial concentration of the solute in solution, and C_o is the concentration of the solute in solution after equilibrium. The volumes of the solution and the hydrogel are V_s and V_m , respectively.

5.3.8 Methods: Determination of Polymer Gel Specific Volumes/Swelling Studies

After polymerization, three gels of each polymer system were taken for dry, swollen, and relaxed specific volume determination experiments. These were calculated for the poly(MAA-co-EGDMA) recognitive gel, the poly(MAA-co-EGDMA) recognitive gel prepared via “living/controlled” polymerization techniques, the poly(DEAEM-co-HEMA-co-PEG200DMA) recognitive gel, and the poly(DEAEM-co-HEMA-co-PEG200DMA) recognitive gel prepared via “living/controlled” polymerization techniques. For the dry specific volume determination, gels were placed in the vacuum oven at a temperature and pressure of 30°C 28 inches of Hg vacuum until the weight change was less than 0.1 wt%. Once dry, the gels were then taken out and the dry mass was measured on a Sartorius scale. Afterward, a density determination kit was installed on the Sartorius scale. The mass of the gel was then measured in heptane, a non-solvent (density of 0.684 g/mL at a temperature of 25°C). Once measurements were taken, Archimedes bouyancy principle was used to calculate the density of the dry polymer as shown in equation 5.5,

$$\rho_x = \frac{W_a \cdot \rho_h}{W_a - W_h} \quad 5.5$$

where ρ_x is the density of the sample, W_a is the mass of the sample in air, ρ_h is the density of heptane, and W_h is the weight of the sample in heptane. The specific volume of the polymer was calculated as the reciprocal of density. The experiment was repeated for both the relaxed and swollen gel. The relaxed gel specific volume was calculated directly after the polymerization reaction without any additional solvent being introduced into the

gel. The swollen gel specific volume was calculated after the gel reached swelling equilibrium with the solvent for each system. The equilibrium volume swelling ratio Q was calculated with the swollen volume V_s and the volume of the dry polymer, V_{dry} , (5.6).

$$Q = \frac{V_s}{V_{dry}} \quad 5.6$$

Dynamic swelling studies of the poly(DEAEM-co-HEMA-co-PEG200DMA) gels were performed by measuring the initial gel dry weight to determine the dry mass of polymer. The gel was then placed in a 0.5 mg/mL diclofenac sodium solution (i.e., gel was loading in addition to swelling). The gel was taken out of solution and patted dry with Kimwipes®, and the gel weight measured. After the weight was measured, the gel was placed back in solution to continue swelling. The measurement was repeated once every 5 minutes for the first hour, once every 10 minutes for the second hour, and then every 30 minutes until the gel reached a constant mass which indicated equilibrium.

5.3.9 Methods: Calculation of Mesh Size

Static experiments were performed on EA9A imprinted poly(MAA-co-EGDMA) and diclofenac sodium imprinted poly(DEAEM-co-HEMA-co-PEG200DMA) gels in the equilibrium swollen state (with solvents being acetonitrile and DI water, respectively). Samples of each gel (1 mm x 5 mm x 15 mm strips) were removed from the solvent and analyzed with a RSA III Dynamic Mechanical Analyzer (DMA), (TA Instruments, New Castle, DE) to obtain stress versus strain. Each experiment was conducted in controlled

force mode with a force ramp from 0.001 to 0.3 N. The raw data obtained for each gel is included in Appendix A, section A.4.

Polymer gel mesh size was calculated via data collected from the static experiments via a DMA and by using the theory of rubber elasticity. The following equation⁹⁻¹¹ describes the tension of a swollen, un-stretched polymer sample, τ .

$$\tau = \left(\frac{RTv_e}{Vv_{2,s}^{2/3}} \right) \left(\alpha - \frac{1}{\alpha^2} \right) \quad 5.7$$

R is the universal gas constant, T is the temperature, v_e is the effective number of moles of chains in a real network, V is the volume of the swollen polymer, $v_{2,s}$ is the swollen polymer fraction calculated by polymer dry volume V_{dry} divided by the polymer swollen volume V_s , and α is the deformation of a network structure by elongation which is equivalent to the stretched length over initial length ($\alpha = L/L_0$).

The following equation^{9, 12} takes into account the polymer swollen until equilibrium with the solvent, but not prepared in solvent.

$$\tau = RT \left(\frac{1}{\bar{v}M_c} \right) \left(1 - \frac{2\bar{M}_c}{M_n} \right) \left(\alpha - \frac{1}{\alpha^2} \right) v_{2,s}^{1/3} \quad 5.8$$

where \bar{v} is the specific volume of the polymer in the relaxed state, M_n is the number average molecular weight, and \bar{M}_c is the average molecular weight between crosslinks. Taking equation 5.8 and the fact that the average molecular weight between crosslinks is much smaller than the number average molecular weight (i.e., $\bar{M}_c \ll M_n$) will yield equation 5.9.

$$\tau = RT \left(\frac{1}{\bar{v} \bar{M}_c} \right) \left(\alpha - \frac{1}{\alpha^2} \right) v_{2,s}^{1/3} \quad 5.9$$

The stress and strain data obtained by the static experiments from DMA was plotted with the α term on the y axis and tension τ on the x axis to obtain the slope which gave the average molecular weight between crosslinks \bar{M}_c . To determine the actual mesh size, ξ of the polymer network, the relationship of ξ to \bar{M}_c is needed from Peppas and Barr-Howell^{5,13}.

$$\xi = Q^{1/3} \left(2C_n \left(\frac{\bar{M}_c}{M_r} \right) \right)^{1/2} l \quad 5.10$$

where Q is the equilibrium volume swelling ratio, C_n is the characteristic ratio for the polymer (obtained from the molar average of the C_n from the homopolymers), and M_r is the effective molecular weight of the repeating unit (determined by a weighted average of the copolymer composition). It is important to note the equilibrium volume swelling ratio, Q, is the swollen volume of the gel divided by the dry volume of the gel or the reciprocal of the swollen polymer volume fraction. The C_n values used in this analysis were for polymethacrylic acid ($C_n = 14$), for polyethylene glycol dimethacrylate ($C_n = 3.8$), and for the poly(DEAEM-co-HEMA-co-PEG200DMA) a typical average value of the characteristic ratio ($C_n = 11$) was used^{10,14-16}. The carbon-carbon bond length of the polymer backbone, which is equal to 1.54 Å is represented by length, l .

5.3.10 Methods: Dynamic Template Release Profiles

The gels, after reaching equilibrium with the diclofenac sodium binding solution, were placed in a Sotax Dissolution Apparatus, (Horsham, PA) in 1000 mL of artificial lacrimal solution. The artificial lacrimal solution consisted of solution 6.78 g/L NaCl, 2.18 g/L NaHCO₃, 1.38 g/L KCl, and 0.084 g/L CaCl₂·2H₂O, and the pH of the solution was 8.0¹⁷. The lacrimal solution was stirred at a constant rate of 75 rpm by the paddles within the dissolution apparatus and kept at a constant temperature of 37°C. The solution within the dissolution apparatus was measured via a Biotek Synergy UV/Vis at 276 nm until the change in concentration within the solution did not change more than 1%. The dissolution experiments were performed on two types of poly(DEAEM-co-HEMA-co-PEG200DMA) recognitive gels and the control gel.

The fractional template release profiles were determined by taking the amount of diclofenac sodium released at the specified times during the dissolution experiment, M_t divided by the maximum amount of diclofenac sodium released during the dissolution experiment, M_∞ . The fractional template release profile, M_t/M_∞ was determined for each gel and plotted versus time.

5.3.11 Analysis of Kinetic Parameters

A dark reaction was used to determine the kinetic profile of the poly(MAA-co-EGDMA) control gel, the poly(MAA-co-EGDMA) recognitive gel, and the poly(MAA-co-EGDMA) recognitive gel prepared via “living/controlled” polymerization techniques.

A dark reaction was performed by analysis of the rate of reaction and conversion after the UV light was shut off for a period of time. The reaction analysis was analyzed via the program SAE which is presented in Appendix C. The method was to purge the system with nitrogen, take the system to the reaction temperature, turn on the UV light for a specified amount of time, turn the light off for 5 minutes, and then turn the UV light on to complete the reaction. Each data point on the resulting graphs was obtained by one complete polymerization reaction. For the poly(MAA-co-EGDMA) control gel and recognitive gel, the UV light turn on/off period was 20 seconds. For example, run one would have the UV light on for 20 seconds then the UV light remained off for 5 minutes then UV turned back on to complete the reaction. Run two had the UV light on for 40 seconds, run three had the UV light on for 60 seconds, and so on until the total reaction was analyzed. Similar studies were done by Anseth and coworkers^{18,19}. The equations used to find the termination and propagation constants, k_t and k_p , are 5.11 and 5.12, and the derivation of these equations can be seen in Odian or Flory^{9,20}. The equation 5.11 is a rearrangement of the equation in Chapter 3, equation 3.14,

$$\frac{k_p}{k_t^{1/2}} = \frac{R_p}{[M](fI_0\varepsilon[I])^{1/2}} \quad 5.11$$

where $[M]$ is the monomer concentration, the initiator efficiency is f , I_0 is the light intensity, ε is the extinction coefficient, and $[I]$ is the initiator concentration. The unsteady state equation used to decouple the propagation constant and the termination constant is shown in 5.12,

$$k_t^{\frac{1}{2}} = \frac{\frac{k_p}{k_t^{\frac{1}{2}}}}{2(t_1 - t_0)} \left[\frac{[M]_{t=t_1}}{Rp_{t=t_1}} - \frac{[M]_{t=t_0}}{Rp_{t=t_0}} \right] \quad 5.12$$

where t_1 and t_0 are the time final and time initial for the time increment, $[M]_{t=t_1}$ and $[M]_{t=t_0}$ are the monomer concentration at time final and time initial, respectively, and $Rp_{t=t_1}$ and $Rp_{t=t_0}$ are the rate of polymerization at final time and initial time, respectively.

Thirteen dark reactions for the kinetic analysis for poly(MAA-co-EGDMA) control gel are shown in Figure 5.1. Similar dark reactions were performed to obtain the kinetic data for poly(MAA-co-EGDMA) reconfigurable gel and poly(MAA-co-EGDMA) reconfigurable gel prepared via “living/controlled” polymerization techniques. It is important to note that time intervals for the “living/controlled” polymerization kinetic analysis were 30 seconds due to a longer reaction time. Once the data was obtained from the dark reaction experiments and ensuing reaction analysis of the data was analyzed via the program SAE, the program KINO (Appendix D) was used to evaluate the kinetic parameters.

5.4 Results and Discussion

Template binding results for the poly(MAA-co-EGDMA) control gel, the poly(MAA-co-EGDMA) reconfigurable gel, and the poly(MAA-co-EGDMA) reconfigurable gel prepared via “living/controlled” polymerization techniques are presented in Figure 5.2. As demonstrated by the equilibrium binding isotherm, the poly(MAA-co-EGDMA) reconfigurable gel had a 42% increase in template binding capacity over that of the control

network. The template loading capacity for the poly(MAA-co-EGDMA) control gel and recognitive gel was $(1.40 \pm 0.30$ and $2.00 \pm 0.20) \times 10^{-2}$ mmole/g, respectively. The increase in capacity of the poly(MAA-co-EGDMA) recognitive gel results from the macromolecular memory produced by the imprinting process. The concept of macromolecular recognition manifests itself from two major synergistic effects, (i) shape specific cavities that match the template molecule, which provide stabilization of the chemistry in a crosslinked matrix, and (ii) chemical groups oriented to form multiple complexation points with the template. Macromolecular memory and the imprinting effect demonstrated in weakly crosslinked gels is significant since most imprinted systems to date are highly crosslinked polymers. The imprinting effect is the result of “training” macromolecular memory with the intrinsic template binding parameters of affinity and loading capacity.

The poly(MAA-co-EGDMA) recognitive gel prepared via “living/controlled” polymerization techniques had a 90% increase in template binding capacity over that of the poly(MAA-co-EGDMA) recognitive gel and a 171% increase in template binding capacity over the control (Figure 5.2) (both the recognitive gel and control were prepared using conventional free-radical polymerization). The template loading capacity for the poly(MAA-co-EGDMA) recognitive gel prepared via “living/controlled” polymerization techniques was $3.80 \pm 0.40 \times 10^{-2}$ mmole/g. The increase in template binding capacity for the gel formed via “living” polymerization indicates enhanced macromolecular memory for the template above standard free-radical polymerization methods. Template binding affinities calculated for the poly(MAA-co-EGDMA) control, recognitive, and recognitive gel prepared via “living/controlled” polymerization techniques by the

Freundlich analysis are $(1.93 \pm 0.10, 2.45 \pm 0.13, \text{ and } 2.21 \pm 0.11) \text{ mM}^{-1}$, respectively. It is important to note that the template binding affinity of the recognitive gel and the recognitive gel prepared via “living/controlled” polymerization techniques had a similar average affinity; however, both recognitive gels had a higher average affinity than the control network. The increased template binding affinity is a direct result of imprinting within the poly(MAA-co-EGDMA) polymer network. All the binding parameters for the weakly crosslinked poly(MAA-co-EGDMA) networks are presented in Table 5.1.

Diclofenac sodium binding results for the poly(DEAEM-co-HEMA-co-PEG200DMA) control gel, the poly(DEAEM-co-HEMA-co-PEG200DMA) recognitive gel, and the poly(DEAEM-co-HEMA-co-PEG200DMA) recognitive gel prepared via “living/controlled” polymerization techniques are presented in Figure 5.3. The poly(DEAEM-co-HEMA-co-PEG200DMA) recognitive gel had a 94% increase in template loading over that of the control network. The diclofenac sodium loading capacities for the poly(DEAEM-co-HEMA-co-PEG200DMA) control and recognitive gel are $(0.96 \pm 0.12 \text{ and } 1.87 \pm 0.20) \times 10^2 \text{ mmole/g}$, respectively. As discussed for the EA9A imprinted weakly crosslinked gels, an increase in template loading capacity indicates macromolecular memory within the recognitive gel.

The poly(DEAEM-co-HEMA-co-PEG200DMA) recognitive gel prepared via “living/controlled” polymerization techniques had a 89% increase in template loading capacity over that of the recognitive gel and a 168% increase over that of the control gel. The template loading capacity for the poly(DEAEM-co-HEMA-co-PEG200DMA) recognitive gel prepared via “living/controlled” polymerization techniques was $(3.54 \pm$

Table 5.1. Poly(MAA-co-EGDMA) Recognitive Gel Binding Characteristics:

Binding affinity and loading capacity for the 5% crosslinked recognitive gels.

Gel Type	Ka(mM ⁻¹)	Capacity(mmole/g)
Poly(MAA-co-EGDMA) recognitive gel	2.45 ± 0.13	2.0 ± 0.2 x 10 ⁻²
Poly(MAA-co-EGDMA) recognitive gel prepared via "living/controlled" polymerization techniques	2.21 ± 0.11	3.8 ± 0.4 x 10 ⁻²

0.16) $\times 10^{-2}$ mmole/g (Figure 5.3). Template binding affinities calculated by the Freundlich isotherm show statistically similar values for the poly(DEAEM-co-HEMA-co-PEG200DMA) recognitive gels. Both recognitive gels have significantly higher template binding affinities (15.05 ± 0.82 and 14.57 ± 0.73 for the recognitive gel and recognitive gel prepared via “living/controlled” polymerization techniques, respectively) than the control gel which had a template binding affinity of $9.91 \pm 0.49 \text{ mM}^{-1}$. As presented previously for the EA9A imprinted gels, the higher affinities for the diclofenac sodium imprinted gels compared to the control gel affinity show the imprinting effect of macromolecular memory. All binding parameters for the diclofenac imprinted poly(DEAEM-co-HEMA-co-PEG200DMA) recognitive gels are presented in Table 5.2.

In comparison, the EA9A imprinted poly(MAA-co-EGDMA) gels and the diclofenac sodium imprinted poly(DEAEM-co-HEMA-co-PEG200DMA) gels have very similar overall trends. Typical imprinting techniques show an increase in template loading capacity which can be attributed to macromolecular memory. “Living/controlled” polymerization techniques enhance the template loading capacity of both networks by approximately 90% which indicate that “living” polymerization techniques augment the macromolecular memory compared to the typical free-radical polymerization techniques.

While these networks have similar trends, the affinities for the poly(MAA-co-EGDMA) recognitive gels have smaller affinities compared to the poly(DEAEM-co-HEMA-co-PEG200DMA) recognitive gels. Poly(DEAEM-co-HEMA-co-PEG200DMA) imprinted gels have a 4.5 times longer crosslinking monomer than the poly(MAA-co-EGDMA) gels. Increased crosslinking monomer length has shown to decrease the

binding affinity and capacity due to flexibility of the gel network. However, the non-covalent bonding which take place between the functional groups on the template and the “trained” macromolecular memory site for the EA9A imprinted network and the diclofenac sodium imprinted network are different. The EA9A imprinted gel uses hydrogen bonding with strengths of 0.2-3 kCal/mole²¹ to create macromolecular memory, and in comparison, diclofenac sodium imprinted gels use ionic bonding, which are the strongest non-covalent bonds (ionic bonds are 20-30 times stronger than hydrogen bonds²²), to create macromolecular memory. Stronger non-covalent bonds used to create macromolecular memory would translate into higher affinities for the template molecule as shown in the case of EA9A imprinted gels compared to diclofenac sodium imprinted gels.

The rebinding solvent used for EA9A imprinted gels and diclofenac sodium imprinted gels are acetonitrile and DI water, respectively. A polar solvent has a permanent dipole moment and can form hydrogen bonding between molecules. A polar aprotic solvent has a permanent dipole moment and does not form hydrogen bonding between molecules. DI water is a polar protic solvent with a dielectric constant of 80.4 at a temperature of 25°C, and acetonitrile is a polar aprotic solvent with a dielectric constant of 37.5 at a temperature of 25°C. Acetonitrile does not competitively bind to the template with the EA9A imprinted polymer network because there is no hydrogen bonding interaction with the template molecule. The diclofenac sodium imprinted polymer network does have competitive binding due to DI water hydrogen bonding with the template molecule. In addition, the diclofenac sodium imprinted polymer has ionic bonding which increases the binding affinity in DI water. However the addition of ionic

Table 5.2 Poly(DEAEM-co-HEMA-co-PEG200DMA) Recognitive Gel Binding

Characteristics: Binding affinity and loading capacity for the 5% recognitive gels.

Gel Type	$K_a(\text{mM}^{-1})$	Capacity(mmole/g)
Poly(DEAEM-co-HEMA-co-PEG200DMA) recognitive gel	15.05 ± 0.82	$(1.87 \pm 0.30) \times 10^{-2}$
Poly(DEAEM-co-HEMA-co-PEG200DMA) recognitive gel prepared via "living/controlled" polymerization techniques	14.57 ± 0.73	$(3.54 \pm 0.25) \times 10^{-2}$

bonding interactions between the recognitive polymer network and template molecule within a polar protic or a polar aprotic solvent would enhance the resulting template binding affinity of the network. The overall binding trends of the recognitive polymer gels prepared via “living/controlled” polymerization, recognitive gels, and control are similar between the two systems and are similar despite the differences within the solvents.

Comparing values of loading capacity from the equilibrium binding isotherms of EA9A imprinted gels and diclofenac sodium imprinted gels, diclofenac sodium imprinted gels bind a higher capacity of diclofenac sodium at lower concentrations. Higher binding at lower concentrations translate into higher binding affinities which again is representative of the higher affinity and correlates well with the data calculated via the Freundlich isotherm with diclofenac sodium imprinted gels. Initial points on the binding curve at lower concentrations have a high degree of influence upon the strength of the template binding affinity.

To ensure the enhanced loading from the poly(MAA-co-EGDMA) gel and poly(DEAEM-co-HEMA-co-PEG200DMA) gel prepared via “living/controlled” polymerization techniques was not a result from changes in double bond conversion, reaction analysis was performed on both gels to determine double bond conversion. The double bond conversion calculated via reaction analysis for the poly(MAA-co-EGDMA) recognitive gel and recognitive gel prepared via “living/controlled” polymerization techniques was $(56 \pm 3.2$ and $59 \pm 3.5)\%$, respectively. Similarly, reaction analysis was performed on the poly(DEAEM-co-HEMA-co-PEG200DMA) recognitive gel and recognitive gel prepared via “living/controlled” polymerization techniques to determine

the double bond conversion. The results show that both the poly(DEAEM-co-HEMA-co-PEG200DMA) recognitive gels had similar double bond conversions of (80 ± 5.1 and 83 ± 4.7)%.

Double bond conversion results conclusively rule out increases in template binding capacity due to increased double bond conversion. An increase in reacted double bonds would alter the structure by incorporation of more polymer chains into the network. These systems have 5% crosslinking for the both EA9A imprinted gels and the diclofenac sodium imprinted gels. Higher double bond conversions for these networks would decrease the kinetic chain length potentially increasing the crosslinking density thus decreasing the mesh size which would alter the polymer structure. The goal of this study is to determine what changes “living/controlled” polymerization mechanisms have on the structure and by keeping the double bond conversion constant. Then theoretically, the structural changes will be affected only by the “living/controlled” polymerization mechanism.

To determine whether the increase in template loading via “living” polymerization techniques was due to a incorporation of more functional monomer within the network, a poly(DEAEM-co-HEMA-co-PEG200DMA) control gel prepared via “living/controlled” polymerization techniques was synthesized and diclofenac sodium binding studies were performed on the resulting co-polymer network. It is important to note the control gel was synthesized in the exact same manner as the recognitive gel excluding the template molecule. A control gel formed via “living/controlled” polymerization techniques having a higher binding capacity than the control gel made with standard free-radical polymerization would indicate an increase in non-specific

binding in the template loading capacity. The result could be explained by a greater percentage of functional monomer incorporated in the network (i.e., “living/controlled” polymerization techniques affect the reactivity ratios). However, the experimental results show that the equilibrium template binding isotherm for the poly(DEAEM-co-HEMA-co-PEG200DMA) control gel prepared via “living/controlled” polymerization techniques was a statistical match to the equilibrium template binding isotherm for the poly(DEAEM-co-HEMA-co-PEG200DMA) control gel. The similar binding parameters indicate that “living/controlled” polymerization does not potentially affect the amount of functional monomer incorporated within the gel (i.e., reactivity ratios). This statement is based upon similar non-specific binding shown by both the poly(DEAEM-co-HEMA-co-PEG200DMA) controls gel made with conventional free-radical polymerization and the poly(DEAEM-co-HEMA-co-PEG200DMA) control gel prepared via “living/controlled” polymerization techniques.

Two types of diffusion studies were used to determine the template diffusion coefficients of the EA9A imprinted poly(MAA-co-EGDMA) gels and the diclofenac sodium imprinted poly(DEAEM-co-HEMA-co-PEG200DMA) gels. Fractional template release analysis and one-dimensional transport analysis were the two methods used to calculate diffusion coefficients. Fractional template release analysis was used to calculate the diffusion coefficients for the EA9A imprinted poly(MAA-co-EGDMA) gels. One-dimensional diffusion was not used to determine the diffusion coefficients for the EA9A imprinted polymers due to the poly(MAA-co-EGDMA) gels cracking and causing leaks within the side by side diffusion cells. The cracking was caused by the fast evaporation of acetonitrile from the poly(MAA-co-EGDMA) gels which would cause

stress within the network due to contraction of polymer chains within the network. The diffusion coefficients for the diclofenac sodium imprinted poly(DEAEM-co-HEMA-co-PEG200DMA) gels were calculated by both the one dimensional transport analysis and fractional template release analysis.

The EA9A diffusion coefficients for the poly(MAA-co-EGDMA) recognitive gel and recognitive gel prepared via “living/controlled” polymerization in acetonitrile were $(7.15 \pm 0.13$ and $7.26 \pm 0.15) \times 10^{-9}$ cm²/s, respectively. The EA9A diffusion coefficients poly(MAA-co-EGDMA) recognitive gels were statistically the same indicating the polymer network structure for the recognitive gel and recognitive gel prepared via “living” polymerization techniques are similar. The data from the EA9A diffusion analysis studies (release curves) for the EA9A imprinted gels are presented in Appendix A, section A.4

The diclofenac sodium diffusion coefficients in water for the poly(DEAEM-co-HEMA-co-PEG200DMA) recognitive gel and the poly(DEAEM-co-HEMA-co-PEG200DMA) recognitive gel prepared via “living/controlled” polymerization techniques were $(1.69 \pm 0.10$ and $1.66 \pm 0.06) \times 10^{-9}$ cm²/s. The diffusion coefficients for the poly(DEAEM-co-HEMA-co-PEG200DMA) recognitive gel and recognitive gel prepared via “living/controlled” polymerization techniques indicate that the network structure for the recognitive gels are similar. The data obtained during the experiment and the data needed for the calculation of template diffusion coefficients can be viewed in Appendix A, section A.4.

Template diffusion through an imprinted polymer network can be influenced by three main variables, average mesh size, template size, and template – polymer chain

interactions (i.e., the imprinting effect). Manipulation of one or more of these variables can alter the diffusion coefficient. An increase in polymer mesh size holding template size and template-polymer chain interactions constant would correspond to an increase in template diffusion. An increase in template size holding mesh size and template – polymer chain interactions constant would correspond to a decrease in the template diffusion coefficient. An increase in template – polymer chain interactions holding template size and mesh size constant would correspond to a decrease in the template diffusion coefficient. Before comparing the diffusion coefficients of the EA9A imprinted gels to the diclofenac sodium gels, mesh size analysis for the gels is needed to complete the discussion.

To further investigate the poly(MAA-co-EGDMA) network structure, the mesh sizes were calculated for both EA9A imprinted gels. The mesh sizes were $(4.13 \pm 0.20) \text{ \AA}$ and $(4.13 \pm 0.30) \text{ \AA}$ for the poly(MAA-co-EGDMA) recognitive gel prepared via “living/controlled” polymerization techniques and poly(MAA-co-EGDMA) recognitive gel, respectively. The small mesh size resulting from the calculations indicate both poly(MAA-co-EGDMA) recognitive gels are in a collapsed state. Although these poly(MAA-co-EGDMA) networks have a small mesh size, mesh sizes for similar poly(MAA-co-PEGDMA) gel networks have been presented within literature having mesh sizes ranging from 3.4-23.8 \AA ^{23, 24}. The mesh sizes calculated for the poly(MAA-co-EGDMA) gels are within the literature ranges for a similar poly(MAA-co-PEGDMA) gel. Crosslinked polymer networks in a collapsed state would have a high Flory interaction parameter ($\chi_1 > 0$) with the solvent which decreases the equilibrium swelling

ratio thus decreasing the mesh size¹². The Flory interaction parameter is a unitless representation of the enthalpy of mixing (ΔH_m) which relates to the thermodynamic relationships between the crosslinked polymer chains in contact with a solvent. Swelling behavior within crosslinked polymer networks are very similar to linear polymer chains being solvated by a solvent to form a polymer solution. Swelling behavior is dictated by the change in Gibbs free energy change ΔG , which is a combination of Gibbs free energy of mixing G_m , and Gibbs elastic free energy G_{el} (details of the thermodynamics of swelling with Gibbs free energy can be found in Chapter 2, section 2.2.2). The poly(MAA-co-EGDMA) recognitive gels in acetonitrile have a collapsed network which will be indicated by the Flory polymer solvent interaction parameter, χ .

Similar mesh sizes for the poly(MAA-co-EGDMA) recognitive gels and recognitive gel prepared via “living/controlled” polymerization techniques confirm the network structure being the same which was indicated by the similar diffusion coefficients. The structural results of the poly(MAA-co-EGDMA) recognitive gels do not indicate significant changes within the network structure. However, the results also show more effective binding sites with a 90% increase in the binding capacity for the poly(MAA-co-EGDMA) recognitive gel prepared via “living/controlled” polymerization techniques. “Living/controlled” polymerization techniques have shown to produce shorter kinetic chain lengths and low polydispersities in linear polymer networks²⁵⁻²⁷. Hypothetically, more effective binding sites relate to the homogeneity within the gel based upon how the specific orientations of functional groups interact with the template. Homogeneity within the macromolecular structure could potentially have similar calculated average mesh sizes within the network; however, those same gels with a

similar average mesh sizes could have significantly different mesh size distribution profiles within the calculated average mesh size population.

Further investigations into the network structure of the diclofenac imprinted poly(DEAEM-co-HEMA-co-PEG200DMA) gels determined mesh sizes of (30.3 ± 1.7) and (19.7 ± 2.1) Å for the poly(DEAEM-co-HEMA-co-PEG200DMA) recognitive gel and poly(DEAEM-co-HEMA-co-PEG200DMA) recognitive gel prepared via “living/controlled” polymerization techniques, respectively. These mesh size values compare with literature values of 21-31 Å for a similar hydrogel network produced with 90% HEMA and 5% PEG200DMA³. The poly(DEAEM-co-HEMA-co-PEG200DMA) recognitive gel prepared via “living/controlled” polymerization techniques demonstrates a smaller mesh size (19.7 ± 2.1) Å compared to (30.3 ± 1.7) Å at equivalent conversions. “Living/controlled” polymerizations create smaller mesh sizes, which hypothetically originates from smaller kinetic chain lengths within the copolymer network which contributes to the overall homogeneity of the network structure.

In comparison, the diffusion coefficients for the poly(MAA-co-EGDMA) recognitive gel and the poly(DEAEM-co-HEMA-co-PEG200DMA) recognitive gel show diffusion coefficients of $(7.15 \pm 0.13) \times 10^{-9}$ and $(1.69 \pm 0.10) \times 10^{-9}$ cm²/s for EA9A and diclofenac sodium, respectively. The diffusion coefficients were calculated via fractional template release analysis and one-dimensional template diffusion analysis, respectively.

Differences in the diffusion coefficients between the networks can be explained by size of the template molecule and length of crosslinking monomer within the network. The EA9A has a molecular weight of 221.22 g/mole and the diclofenac sodium has a

molecular weight of 318.14 g/mole. The adenine base of the molecule EA9A has a hydrodynamic radius calculated via Gaussian 94 of 5 \AA^{28} , and diclofenac sodium has a hydrodynamic radius of 16 \AA^{29} . A network produced with PEG200DMA crosslinking monomer would translate into a larger mesh sizes within the polymer network since it is a longer crosslinking monomer ($n = 4.5$ for PEG200DMA and $n = 1$ for EGDMA). Mesh size analysis confirms the mesh size differences of the EA9A imprinted gel and the diclofenac sodium imprinted gel; the mesh size results were $(4.13 \pm 0.3) \text{ \AA}$ and $(30.7 \pm 1.7) \text{ \AA}$, respectively. Comparing just the template molecule size and corresponding network mesh size, the EA9A imprinted gels have a smaller template molecule with a smaller average mesh size, and the diclofenac sodium imprinted gels have a larger template molecule and a larger average mesh size. Peppas and coworkers show poly(methacrylic acid-co-polyethylene glycol) non-imprinted polymers (50% crosslinker) with various mesh sizes from $(216 - 163) \text{ \AA}$ correspond to small diffusion coefficient changes $(1.3 - 1.6) \times 10^{-8} \text{ cm}^2/\text{s}$ with a Calcitonin (a 32 amino acid polypeptide hormone)³⁰.

The diffusion coefficient for the poly(MAA-co-EGDMA) recognitive gel is higher than the diffusion coefficient for the poly(DEAEM-co-HEMA-co-PEG200DMA) recognitive gel ($7.15 \pm 0.13 \times 10^{-9} \text{ cm}^2/\text{s}$ compared to $1.69 \pm 0.10 \times 10^{-9} \text{ cm}^2/\text{s}$, respectively). The diffusion coefficients for imprinted polymers are heavily influenced by the template binding affinities. The template binding affinities calculated by the Freundlich isotherm analysis for the poly(MAA-co-EGDMA) recognitive gel and for the poly(DEAEM-co-HEMA-co-PEG200DMA) were $2.45 \pm 0.13 \text{ mM}^{-1}$ and 15.05 ± 0.82

mM⁻¹, respectively. While mesh size and template molecular size are important to the diffusional transport, there was a significant increase comparatively in template binding affinity which results in a significant increase in the template – polymer chain interaction. The increase in binding affinity would influence the diffusion coefficient through stronger intrinsic macromolecular recognition sites. The diclofenac sodium would diffuse through the gel binding and rebinding to macromolecular memory sites with strong ionic non-covalent bonding on its way through the network while EA9A would have to diffuse through the network binding and rebinding to macromolecular memory sites with relatively weak hydrogen bonding. The strength of the diclofenac sodium binding site based upon affinity is approximately 6x as strong as the EA9A binding site which would significantly influence the template – polymer chain. A similar argument can be presented for the recognitive gels prepared via “living/controlled” polymerizations. Table 5.3 lists all the factors that influence template diffusion.

Dynamic swelling studies were performed on the diclofenac sodium imprinted poly(DEAEM-co-HEMA-co-PEG200DMA) gels (Figure 5.4). The poly(DEAEM-co-HEMA-co-PEG200DMA) control gel and recognitive gel had very similar trends as shown Figure 5.4. The similar dynamic equilibrium swelling curve for the control and recognitive gel indicate the mesh sizes of these two copolymer networks are very similar. Swelling is ultimately dictated by the thermodynamic equilibrium as presented previously in this chapter and in Chapter 2, section 2.2.2. If the Gibbs free energy of mixing is negative, the gel is solvated by the solvent. Smaller mesh sizes correspond to smaller amounts of solvent in the gel; thus polymers with smaller mesh sizes have smaller equilibrium swelling ratios if the solvent and polymer composition are held constant.

Table 5.3 Characteristics that Influence Template Diffusion within Imprinted Gels

Gel Type	Ka (mM ⁻¹)	Template Molecular Weight	Template Hydrodynamic Radius Å	Mesh Size Å	Diffusion Coefficient (cm ² /s) x 10 ⁻⁹
Poly(DEAEM-co-HEMA-co-PEG200DMA) recognitive gel	15.05 ± 0.82	318.14	16	30.3 ± 1.7	1.69 ± 0.10
Poly(MAA-co-EGDMA) recognitive gel	2.45 ± 0.13	221.22	5	4.13 ± 0.20	7.15 ± 0.13

The smaller swelling ratio also indicates a smaller molecular weight between crosslinks (more crosslinking points decrease swelling). The dynamic equilibrium swelling curve for the poly(DEAEM-co-HEMA-co-PEG200DMA) recognitive gel prepared via “living/controlled” polymerization techniques is lower than both the poly(DEAEM-co-HEMA-co-PEG200DMA) control and recognitive gels indicating that the gel structure swells to a smaller extent. Thus, the polymer volume fraction in the swollen state is higher. The smaller mesh size is confirmed by the mesh size analysis for the poly(DEAEM-co-HEMA-co-PEG200DMA) gels.

Release profiles versus time for the diclofenac sodium imprinted poly(DEAEM-co-HEMA-co-PEG200DMA) gels are shown in Figure 5.5. The poly(DEAEM-co-HEMA-co-PEG200DMA) recognitive gel releases 179% more template compared to the control network over a period of 7 days. The poly(DEAEM-co-HEMA-co-PEG200DMA) control gel released 0.48 ± 0.01 mg of diclofenac sodium over a 7 day time period while the poly(DEAEM-co-HEMA-co-PEG200DMA) recognitive gel released 1.34 ± 0.04 mg of diclofenac sodium. Larger quantities of template released from the poly(DEAEM-co-HEMA-co-PEG200DMA) recognitive gel indicates the “trained” macromolecular memory increases the template loading capacity and confirms the increases in template binding shown in the previous binding analysis for the recognitive gel.

The fractional template release profile for the poly(DEAEM-co-HEMA-co-PEG200DMA) recognitive gel showed that 70% of the template was released over a time period of 700 minutes (Figure 5.6). The recognitive gel showed a two-fold extension in the release time over that of the control gel. The control gel released 70% of the template

over a time period of 300 minutes. The diffusion coefficients calculated from the fractional template release profiles for the poly(DEAEM-co-HEMA-co-PEG200DMA) recognitive gel and the poly(DEAEM-co-HEMA-co-PEG200DMA) recognitive gel prepared via “living/controlled” polymerization techniques were $3.20 \pm 0.48 \times 10^{-9} \text{ cm}^2/\text{s}$ and $1.49 \pm 0.33 \times 10^{-9} \text{ cm}^2/\text{s}$, respectively. These values correspond to the values calculated for the diclofenac sodium imprinted gels via one-dimensional transport analysis.

To determine how well the release curves matched the Fickian release profile coefficient ($n = 0.5$), the log of the fractional release was plotted on the y axis and the log of the time was plotted on the x axis. The results of the analysis show that the poly(DEAEM-co-HEMA-co-PEG200DMA) control gel conforms very well to the Fickian release profile ($n = 0.48$). The poly(DEAEM-co-HEMA-co-PEG200DMA) recognitive gel and recognitive gel prepared via “living/controlled” polymerization technique release profiles are less Fickian and moving toward zero-order release profiles with profile coefficients of $n = 0.68$ and $n = 0.70$, respectively. “Living/controlled” polymerization techniques along with molecular imprinting shifted the release profiles toward a zero-order release profile. Zero-order release has a linear release profile which is constant and not dependant upon time or concentration. The slower release profile for imprinted gels has been shown within our research group to be due to the intrinsic template binding characteristics of the polymer network³. The “trained” macromolecular memory within hydrogels display controlled release profiles that can be explained by the “tumbling hypothesis” presented in a recent research article³. The hypothesis states that as the molecule diffuses through the network it binds and unbinds to multiple binding

sites. Because of the flexibility of the gel network, the template molecule, diclofenac sodium, can unbind from one complexation point and move to another complexation point on its way through the network.

The poly(DEAEM-co-HEMA-co-PEG200DMA) recognitive gel prepared via “living/controlled” polymerization techniques released 34% more drug over a 7 day period in a more controlled manner than the poly(DEAEM-co-HEMA-co-PEG200DMA) recognitive gel (Figure 5.5). The recognitive gel prepared via “living/controlled” polymerization techniques released 1.87 ± 0.06 mg over a 7 day time period. The increase in amount of template released from the recognitive gel prepared via “living/controlled” polymerization techniques can be attributed to the 89% increase in template loading capacity over that of the recognitive gel as shown in the previous template binding analysis for the poly(DEAEM-co-HEMA-co-PEG200DMA) recognitive gel prepared via “living/controlled” polymerization techniques.

The fractional template release profile for the diclofenac sodium imprinted poly(DEAEM-co-HEMA-co-PEG200DMA) gel formed via “living/controlled” polymerization techniques showed that 70% of the template is released over a time period of 1400 minutes (Figure 5.6). This means imprinting via “living” polymerization techniques extend or delay the template release profile by two fold over that of imprinting via free-radical polymerization techniques and four fold over that of the control network.

The “tumbling hypothesis” states that the template tumbles from binding site to binding site on the way out of the gel. Template binding analysis showed an 89% increase of the loading capacity for the poly(DEAEM-co-HEMA-co-PEG200DMA) recognitive gel prepared via “living/controlled” polymerization over that of the

poly(DEAEM-co-HEMA-co-PEG200DMA) cognitive gel. This would mean there are almost twice as many sites within the same volume of polymer network (i.e., polymer dimensions were the same for all polymers analyzed in this chapter). Twice as many sites would mean a template molecule would bind and unbind to binding sites twice as many times thus increasing/extending the dynamic release profile. The smaller mesh size of the poly(DEAEM-co-HEMA-co-PEG200DMA) gel prepared via “living/controlled” polymerization techniques in conjunction with a the two fold increase in sites with imprinted the “trained” macromolecular memory is the reason for the extended release profile.

In addition to the binding, diffusion, and structural analysis of these gels, the kinetic parameters of these poly(MAA-co-EGDMA) gels were analyzed to determine what changes the “living” polymerization technique had upon the kinetic constants of propagation and termination. The propagation constant k_p , termination constant k_t , and k_t/k_p versus double bond conversion are shown in Figure 5.7, Figure 5.8, and Figure 5.9, respectively.

The propagation constant versus conversion (Figure 5.7) for the poly(MAA-co-EGDMA) cognitive and control gel follow typical experimental values found in the literature^{18, 19, 31}. The propagation constant remains relatively constant where the chemical reaction is controlling the propagation mechanism for the gels (less than 0.23 fractional double bond conversion). At higher conversions, the propagation constant for the cognitive and control gel start to decrease indicating that the propagation is being controlled by the diffusion controlled mechanism. The diffusion controlled propagation

mechanism is where the controlling factor is the radical diffusing through the network to react with double bonds thus propagating chains³².

For the “living/controlled” recognitive gel, propagation remains relatively constant until the fractional double bond conversion reaches between 0.3 and 0.4. This indicates that the addition of iniferter increases the amount of network formed during the chemical reaction controlled propagation mechanism. After a fractional double bond conversion of 0.4, the propagation constant decreases indicating the diffusion controlled propagation mechanism.

The termination constants for the poly(MAA-co-EGDMA) control, recognitive gels, and gels prepared via “living/controlled” techniques have similar trends (Figure 5.8). The termination constant, k_t , versus conversion has a relatively constant range with a decrease of termination constant at higher conversions. Typically, the termination constant has three regions. The regions are represented by a decrease in termination constant, a plateau in termination constant, and a decrease in termination constant. These regions represent termination through segmental diffusion, limitation of segmental diffusion and the increasing dominance of reaction diffusion, and diffusion controlled termination dependant upon propagating events, respectively. The segmental diffusion for the poly(MAA-co-EGDMA) networks is not evident in the data. Crosslinking reactions have a much earlier onset of gelation as early as 5% conversion¹⁹. The reactions presented in Figure 5.8 have the first data point at or above 5% conversion. Evident with the poly(MAA-co-EGDMA) gels is the plateau region from a fractional double bond conversion of (0.05 – 0.42). Segmental diffusion is limited and the reaction diffusion becomes increasingly dominant during this section of the polymerization. After

a fractional double bond conversion of 0.42, the termination constant decreases which is consistent with literature. The decrease in the termination constant at higher double bond conversions is due to a decrease in propagation events and monomer controlled diffusion. The ratio of k_t/k_p is shown in Figure 5.9.

The results from the kinetic analysis for the poly(MAA-co-EGDMA) imprinted gels indicate that “living/controlled” polymerization specifically increases the chemical controlled propagation mechanism. The increase in the chemical controlled propagation mechanism in combination with increasing the binding capacity for these gels indicate that effective binding sites are formed during chemical controlled segment of the polymerization.

Macromolecular memory is formed during the polymerization reaction and manifests itself from two major synergistic effects, (i) shape specific cavities that match the template molecule, which provide stabilization of the chemistry in a crosslinked matrix, and (ii) chemical groups oriented to form multiple complexation points with the template. “Living/controlled” polymerizations have reversible termination which increases the chemical controlled propagation mechanism during which the growing polymer chains are not hindered by diffusion limitations which lead to frustrations formed via mobility constraint from steric hindrances of the surrounding polymer network. By increasing the duration of the chemical controlled propagation mechanism through “living” polymerization techniques, the growing polymer chains (i.e., including growing polymer chains forming macromolecular memory) would have more time during the reaction to move to the lowest energy conformation.

5.5 Conclusions

The work presented in this chapter confirms the hypothesis that the use of “living/controlled” polymerization techniques substantially increased template loading/capacity. Both EA9A imprinted poly(MAA-co-EGDMA) gels and diclofenac sodium imprinted poly(DEAEM-co-HEMA-co-PEG200DMA) gels prepared via “living/controlled” polymerizations show a 90% and 89% increase in template loading capacity over conventional free-radical imprinting techniques, respectively, while both systems retain statistically similar binding affinities. Increases in template binding trends were similar for both poly(MAA-co-EGDMA) and poly(DEAEM-co-HEMA-co-PEG200DMA) imprinted gels and imprinted gels prepared via “living/controlled” polymerization techniques despite solvent differences (i.e., acetonitrile and DI water are polar aprotic and polar protic solvents, respectively). Mesh size analysis of diclofenac sodium imprinted poly(DEAEM-co-HEMA-co-PEG200DMA) gels reveal a mesh size decrease at equivalent double bond conversion from $(30.3 \pm 1.7) \text{ \AA}$ to $(19.7 \pm 2.1) \text{ \AA}$ which strongly indicate that “living/controlled” polymerization techniques shorten the kinetic chain length which leads to a more homogeneous polymer network. Shorter overall kinetic chain length would increase the uniformity and integrity of the binding sites formed within the polymer network thus increase the template binding/loading capacity.

The use of “living/controlled” polymerization techniques with an increase in “trained” macromolecular memory sites result in a larger quantity of template released in solution for a given gel. “Living/controlled” polymerization of a diclofenac sodium

imprinted poly(DEAEM-co-HEMA-co-PEG200DMA) gel yields a more homogeneous network with twice as many macromolecular memory binding pockets that significantly extend the fractional template release profile by a factor of two. A detailed kinetic analysis reveals that “living/controlled” reaction mechanisms increase the chemically controlled propagation mechanism within the polymerization reaction. This in conjunction with the increase in binding indicates that binding sites are formed during the chemical controlled segment of the polymerization. “Living/controlled” polymerization techniques as shown within this chapter have significant enhancement potential for the tailorability of weakly crosslinked imprinted polymer networks for advanced drug delivery carriers.

5.6 List of References

1. Fournier, R. L., *Basic Transport Phenomena in Biomedical Engineering*. Taylor and Francis: Lillington, 1999.
2. Hilt, J. Z.; Peppas, N. A., Microfabricated Drug Delivery Devices. *International Journal of Pharmaceutics* **2005**, 306, (1-2), 15-23.
3. Venkatesh, S.; Saha, J.; Pass, S.; Byrne, M. E., Transport and Structural Analysis of Molecular Imprinted Hydrogels for Controlled Drug Delivery. *European Journal of Pharmaceutics and Biopharmaceutics* **2008**, In Press, doi: 10.1016/j.ejpb.2008.01.036.
4. Venkatesh, S.; Sizemore, S. P.; Byrne, M. E., Biomimetic Hydrogels for Enhanced Loading and Extended Release of Ocular Therapeutics. *Biomaterials* **2007**, 28, (4), 717-724.

5. Peppas, N. A.; Bar-Howell, B. D., *In Hydrogels in Medicine and Pharmacy*. CRC Press, Inc.: Boca Raton, 1987; Vol. 1.
6. Ali, M.; Horikawa, S.; Venkatesh, S.; Saha, J.; Hong, J. W.; Byrne, M. E., Zero-order Therapeutic Release from Imprinted Hydrogel Contact Lenses within in vitro Physiological Ocular Tear Flow. *Journal of Controlled Release* **2007**, 124, (3), 154-162.
7. T. J. Zimmerman; Kooner, K. S.; Sharir, M.; Fechtner, R. D., *Textbook of Ocular Pharmacology*. Lippincott-Raven: Philadelphia, 1997; p 119-138.
8. Crank, J., *The Mathematics of Diffusion*. Oxford University Press: New York, 1975.
9. Flory, P. J., *Principles of Polymer Chemistry*. 1st ed.; Cornell University Press: Ithica, 1953; p 663.
10. Hariharan, D.; Peppas, N. A., Characterization, Dynamic Swelling Behaviour and Solute Transport in Cationic Networks with Applications to the Development of Swelling-Controlled Release Systems. *Polymer* **1996**, 37, (1), 149-161.
11. Peppas, N. A.; Merrill, E. W., Crosslinked Poly(vinyl alcohol) Hydrogels as Swollen Elastic Networks. *Journal of Applied Polymer Science* **1977**, 21, (7), 1763-1770.
12. Sperling, L. H., *Introduction to Physical Polymer Science*. 4th ed.; John Wiley & Sons, Inc: Hoboken, 2005.
13. Brazel, C. S.; Peppas, N. A., Synthesis and Characterization of Thermo- and Chemomechanically Responsive Poly(N-isopropylacrylamide-co-methacrylic acid) Hydrogels. *Macromolecules* **1995**, 28, (24), 8016-8020.

14. Kavimandan, N. J.; Losi, E.; Peppas, N. A., Novel Delivery System Based on Complexation Hydrogels as Delivery Vehicles for Insulin-transferrin Conjugates. *Biomaterials* **2006**, *27*, (20), 3846-3854.
15. Berger, J.; Reist, M.; Mayer, J. M.; Felt, O.; Peppas, N. A.; Gurny, R., Structure and Interactions in Covalently and Ionically Crosslinked Chitosan Hydrogels for Biomedical Applications. *European Journal of Pharmaceutics and Biopharmaceutics* **2004**, *57*, (1), 19-34.
16. Lowman, A. M.; Dziubla, T. D.; Bures, P.; Peppas, N. A.; Sefton, M. V., Structural and Dynamic Response of Neutral and Intelligent Networks in Biomedical Environmnets. In *Advances in Chemical Engineering*, Academic Press: 2004; Vol. Volume 29, pp 75-130.
17. Hägerström, H.; Paulsson, M.; Edsman, K., Evaluation of Mucoadhesion for Two Polyelectrolyte Gels in Simulated Physiological Conditions using a Rheological Method. *European Journal of Pharmaceutical Sciences* **2000**, *9*, (3), 301-309.
18. Anseth, K. S.; Kline, L. M.; Walker, T. A.; Anderson, K. J.; Bowman, C. N., Reaction Kinetics and Volume Relaxation during Polymerizations of Multiethylene Glycol Dimethacrylates. *Macromolecules* **1995**, *28*, (7), 2491-2499.
19. Anseth, K. S.; Wang, C. M.; Bowman, C. N., Reaction Behaviour and Kinetic Constants for Photopolymerizations of Multi(meth)acrylate Monomers. *Polymer* **1994**, *35*, (15), 3243-3250.
20. Odian, G., *Principles of Polymerization*. 2cd edition ed.; John Wiley & Sons: New York, 1981.

21. Srinivasan, R.; Feenstra, J. S.; Park, S. T.; Xu, S.; Zewail, A. H., Direct Determination of Hydrogen-Bonded Structures in Resonant and Tautomeric Reactions Using Ultrafast Electron Diffraction. *Journal of the American Chemical Society* **2004**, 126, (8), 2266-2267.
22. Smith, D. A.; Wallwork, M. L.; Zhang, J.; Kirkham, J.; Robinson, C.; Marsh, A.; Wong, M., The Effect of Electrolyte Concentration on the Chemical Force Titration Behavior of ω -Functionalized SAMs: Evidence for the Formation of Strong Ionic Hydrogen Bonds. *Journal of Physical Chemistry B* **2000**, 104, (37), 8862-8870.
23. Bell, C. L.; Peppas, N. A., Water, Solute and Protein Diffusion in Physiologically Responsive Hydrogels of Poly(methacrylic acid-g-ethylene glycol). *Biomaterials* **1996**, 17, (12), 1203-1218.
24. Spizzirri, U. G.; Peppas, N. A., Structural Analysis and Diffusional Behavior of Molecularly Imprinted Polymer Networks for Cholesterol Recognition. *Chem. Mater.* **2005**, 17, (26), 6719-6727.
25. Qin, D. Q.; Qin, S. H.; Qiu, K. Y., A Reverse ATRP Process with a Hexasubstituted Ethane Thermal Iniferter Diethyl 2,3-Dicyano-2,3-di(p-tolyl)succinate as the Initiator. *Macromolecules* **2000**, 33, (19), 6987-6992.
26. Chen, X. P.; Qiu, K. Y., Synthesis of Well-Defined Poly(methyl methacrylate) by Radical Polymerization with a New Initiation System TPED/FeCl₃/PPh₃. *Macromolecules* **1999**, 32, (26), 8711-8715.
27. Matyjaszewski, K.; Mu Jo, S.; Paik, H. j.; Gaynor, S. G., Synthesis of Well-Defined Polyacrylonitrile by Atom Transfer Radical Polymerization. *Macromolecules* **1997**, 30, (20), 6398-6400.

28. Vega, J.; Michaelian, K.; Garzón, I. L.; Beltrán, M. R.; Hernández, L., Isomers of Adenine. *Journal of Molecular Structure: THEOCHEM* **1999**, 493, (1-3), 275-285.
29. Maitani, Y.; Kugo, M.; Nakagaki, M.; Nagai, T., Ionic Size and Behavior of Diclofenac Salts in Water and Ethanol/Water Mixtures by Conductivity at 25°C. *Journal of Pharmaceutical Sciences* **1993**, 82, (12), 1245-1249.
30. Torres-Lugo, M.; Peppas, N. A., Molecular Design and in Vitro Studies of Novel pH-Sensitive Hydrogels for the Oral Delivery of Calcitonin. *Macromolecules* **1999**, 32, (20), 6646-6651.
31. Khudyakov, I. V.; Legg, J. C.; Purvis, M. B.; Overton, B. J., Kinetics of Photopolymerization of Acrylates with Functionality of 1-6. *Ind. Eng. Chem. Res.* **1999**, 38, (9), 3353-3359.
32. Sigwalt, P.; Moreau, M., Carbocationic polymerization: Mechanisms and kinetics of propagation reactions. *Progress in Polymer Science* **2006**, 31, (1), 44-120.

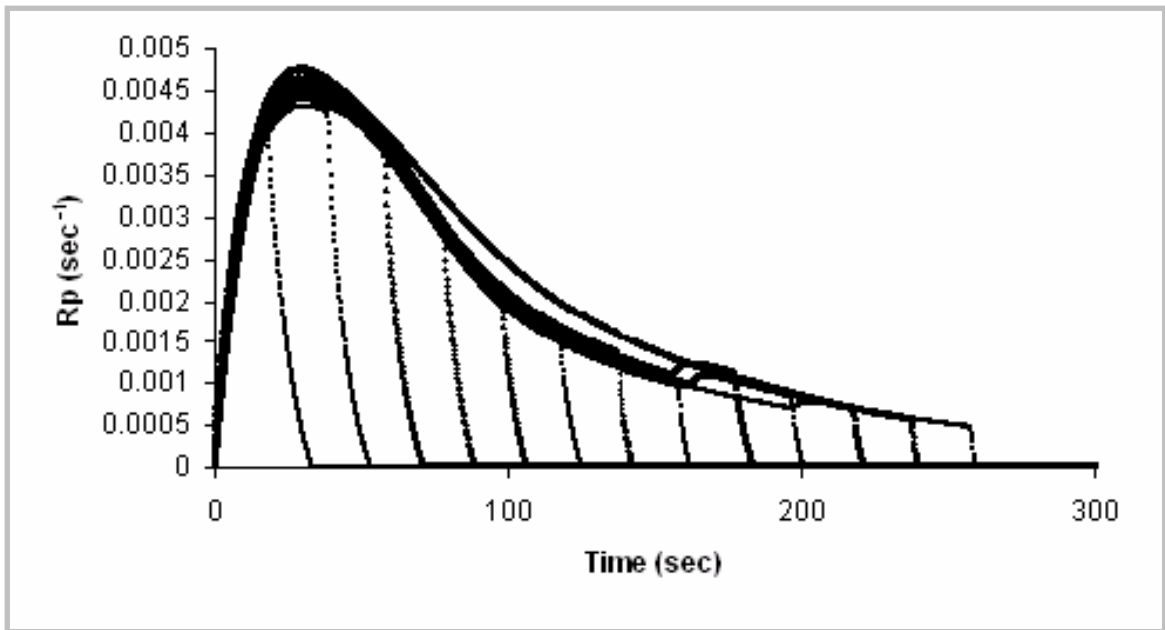


Figure 5.1 Poly(MAA-co-EGDMA) Dark Reaction Kinetic Analysis. Thirteen dark reactions shown in the figure demonstrate the dark reaction analysis for the determination of propagation and termination kinetic constants. This graph represents the rate of polymerization of poly(MAA-co-EGDMA) control gel versus time.

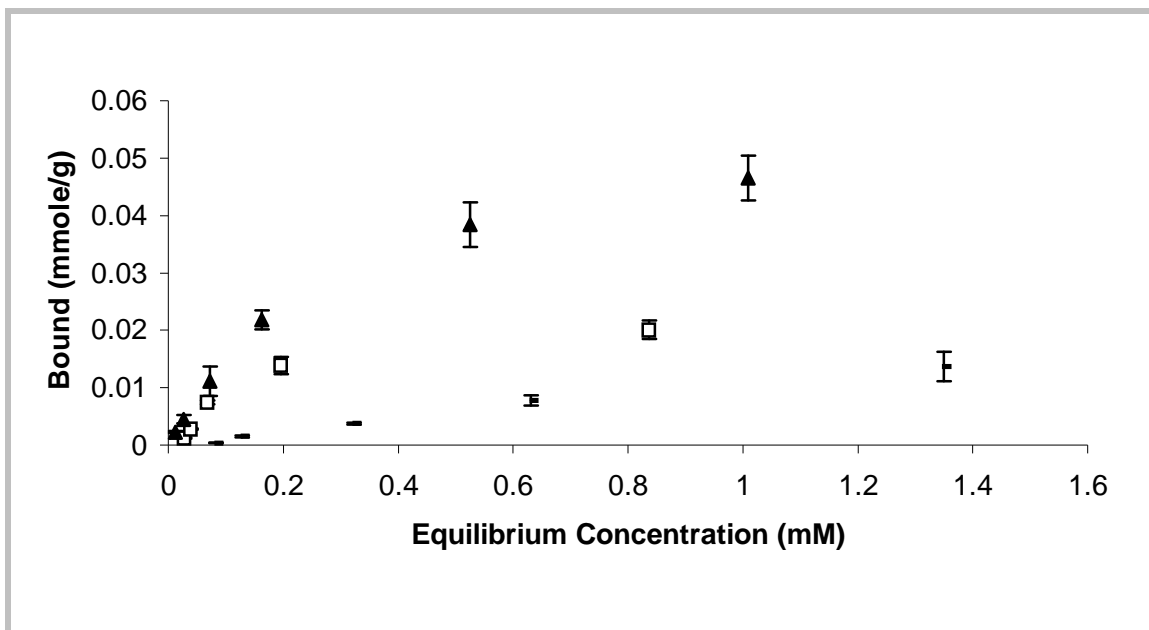


Figure 5.2 Poly(MAA-co-EGDMA) Recognitive Gel Binding Isotherms. Data points (●) represent the poly(MAA-co-EGDMA) control gel, (□) represent the poly(MAA-co-EGDMA) recognitive gel, and (▲) represent the poly(MAA-co-EGDMA) recognitive gel via “living/controlled” polymerization techniques. The poly(MAA-co-EGDMA) recognitive gel prepared via “living/controlled” polymerization techniques has a loading capacity 90% higher than the poly(MAA-co-EGDMA) recognitive gel capacity and 171% higher than the control. Error bars represent the standard error with n=4.

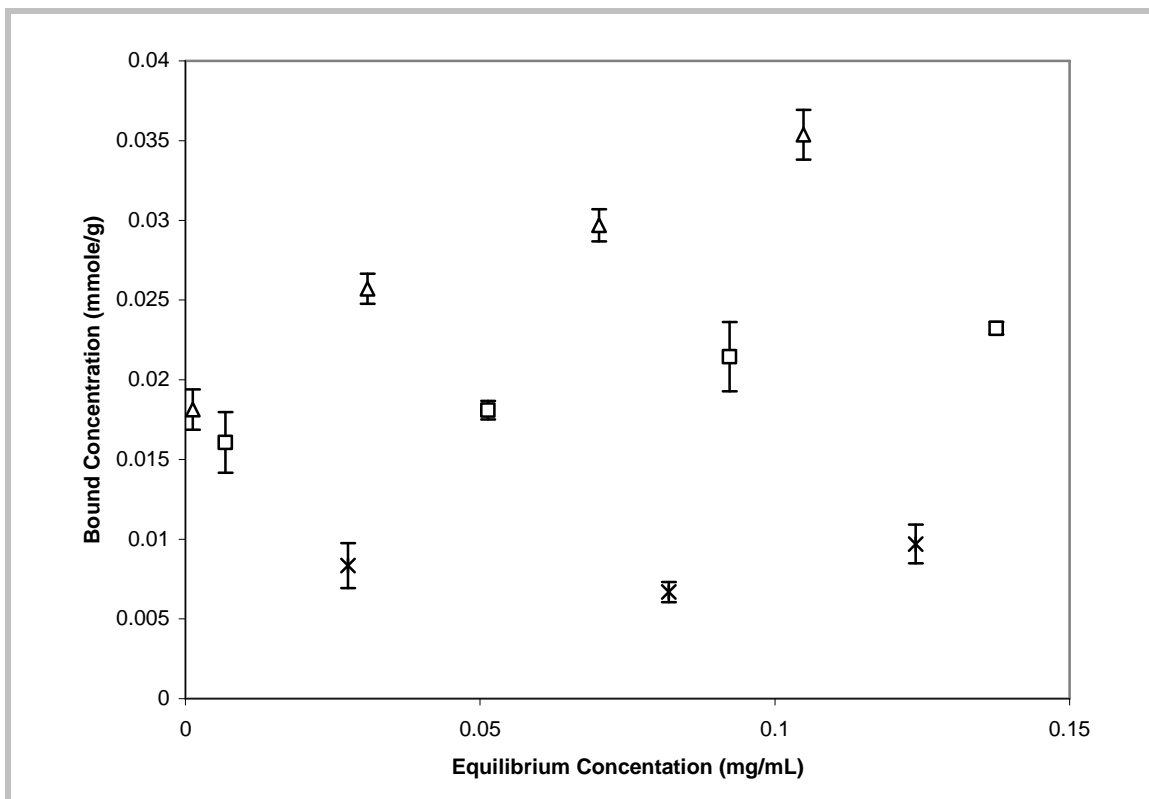


Figure 5.3 Poly(DEAEM-co-HEMA-co-PEG200DMA) Recognitive Gel Binding Isotherms. Imprinted hydrogel binding is demonstrated for the template, diclofenac sodium. Poly(DEAEM-co-HEMA-co-PEG200DMA) recognitive gel via “living/controlled” polymerization techniques (Δ) shows a 89% increase in loading capacity over that of poly(DEAEM-co-HEMA-co-PEG200DMA) recognitive gel (\square) and a 168% increase in loading over that of the control. Both recognitive gels bound more diclofenac sodium compared to the control gel (x). Error bars represent the standard error with $n=3$.

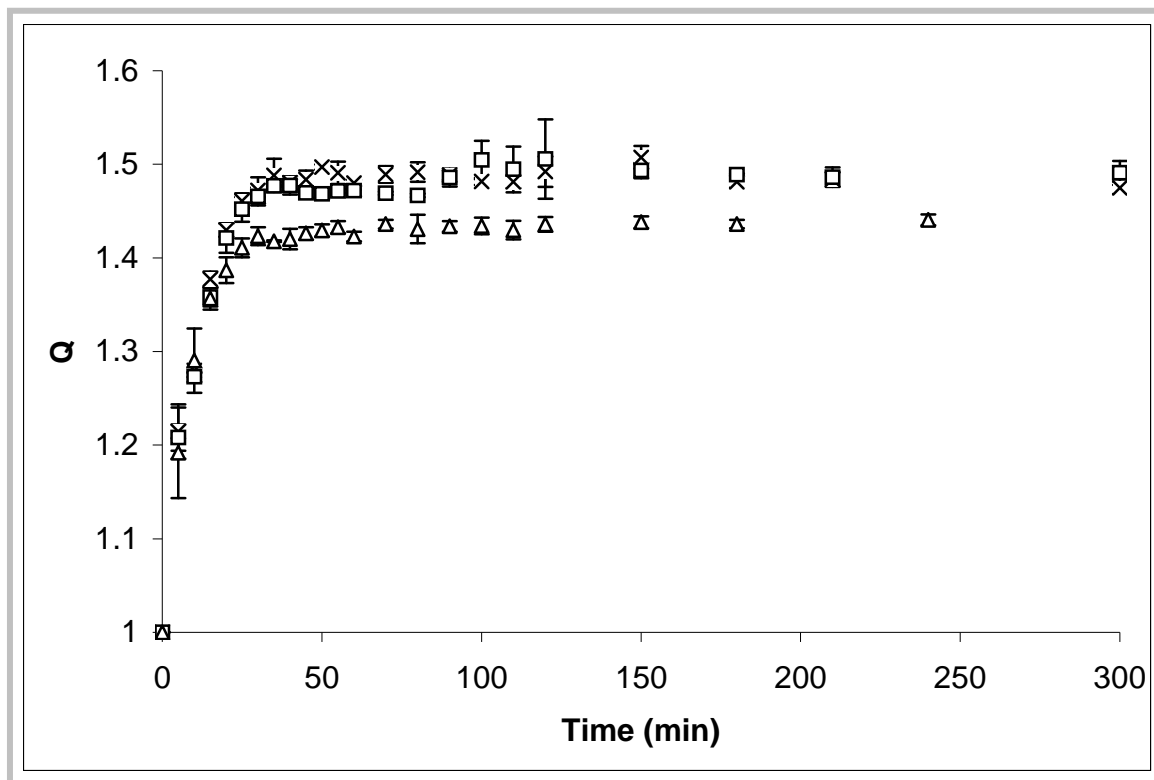


Figure 5.4 Equilibrium Swelling Studies for Poly(DEAEM-co-HEMA-co-PEG200DMA) Recognitive Gels. The recognitive gel (□) and the control gel (x) had similar swelling characteristics in the aqueous solution of diclofenac sodium (concentration was 2 mg/mL). The recognitive gel prepared via “living/controlled” polymerization (Δ) had lower swelling values in the aqueous solution of diclofenac sodium which indicates a smaller mesh size within the macromolecular structure. Mesh size studies confirmed the mesh size was smaller for the recognitive gel prepared via “living/controlled” polymerization. The error bars represent the standard error with n=3.

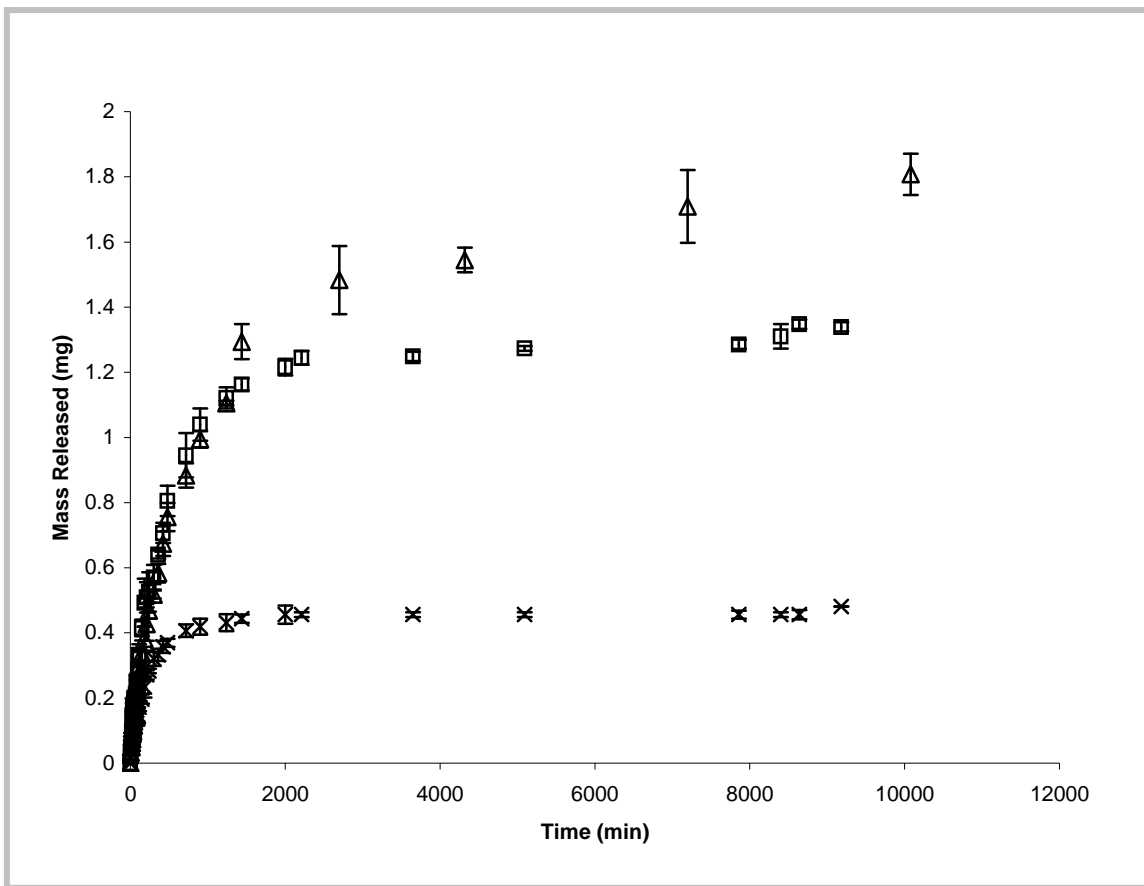


Figure 5.5 Dynamic Release Studies for Poly(DEAEM-co-HEMA-co-PEG200DMA) Recognitive Gels. The recognitive gel prepared via “living/controlled” polymerization (Δ) released a higher amount of diclofenac sodium when compared with the recognitive gel (\square) and the control gel (x). It is important to note that the recognitive gel via “living/controlled” did not reach equilibrium with the solution until after 6 days. The error bars represent the standard error with $n=3$.

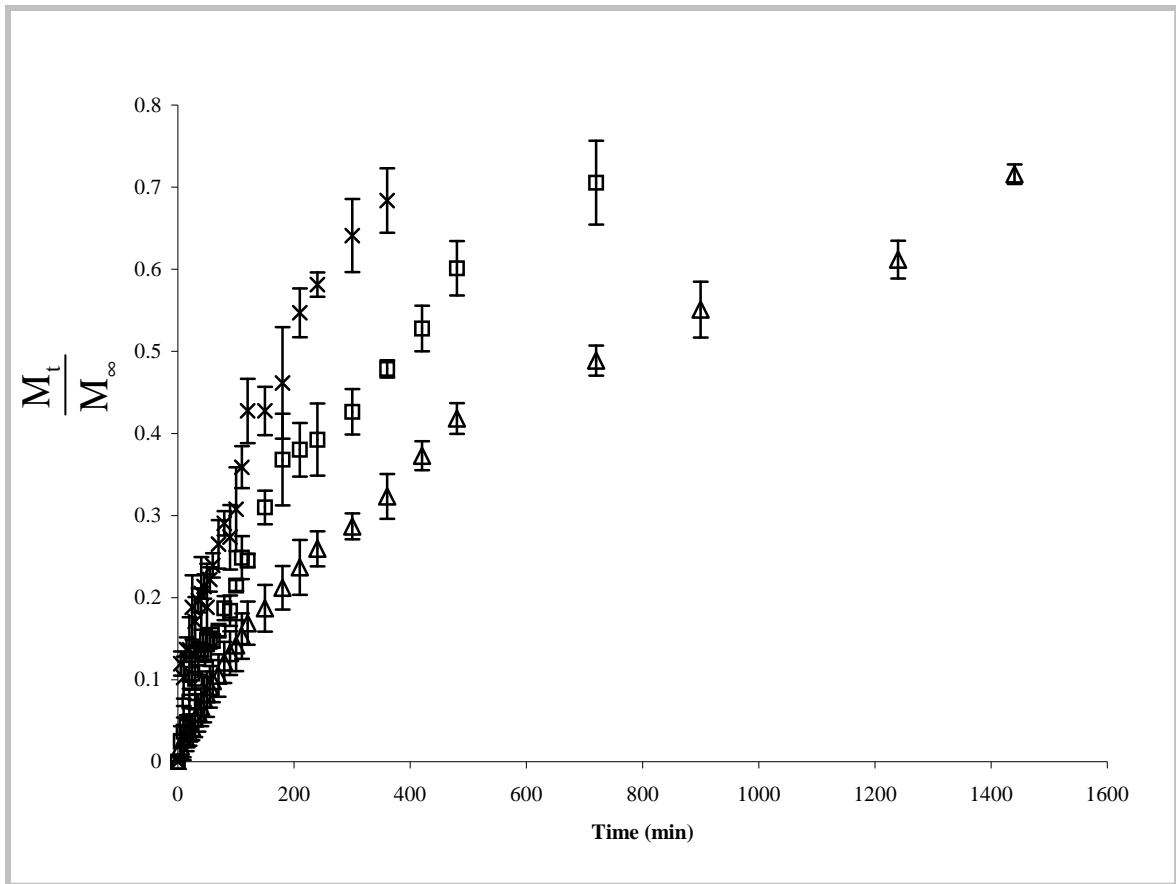


Figure 5.6 Fractional Release of Template for Poly(DEAEM-co-HEMA-co-PEG200DMA) Recognitive Gels. The recognitive gel prepared via “living/controlled” polymerization (Δ) had a longer release time when compared with the recognitive gel (\square) and the control gel (x). It is important to note that this graph shows the release profile only until 70% of the diclofenac sodium is released. The error bars represent the standard error with $n=3$.

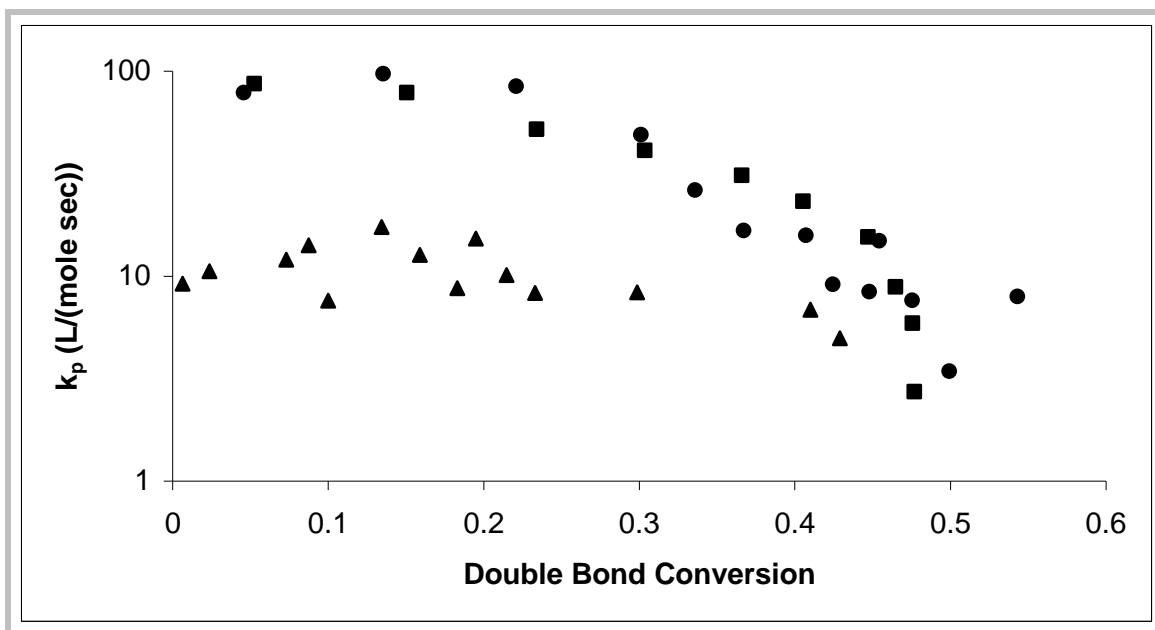


Figure 5.7 Propagation Constant from Poly(MAA-co-EGDMA) Kinetic Analysis.

The propagation constant for the Poly(MAA-co-EGDMA) recognitive gel (■) and control gel (●) had statistically similar trends with double bond conversion. Chemically controlled propagation mechanism occurs until about 0.23 fractional double bond conversion. Higher conversions have a decrease in propagation indicating diffusion controlled propagation. The “living/controlled” recognitive gel (▲) shows a more constant rate of propagation until a fractional double bond conversion of 0.40 indicating a longer chemical controlled propagation mechanism.

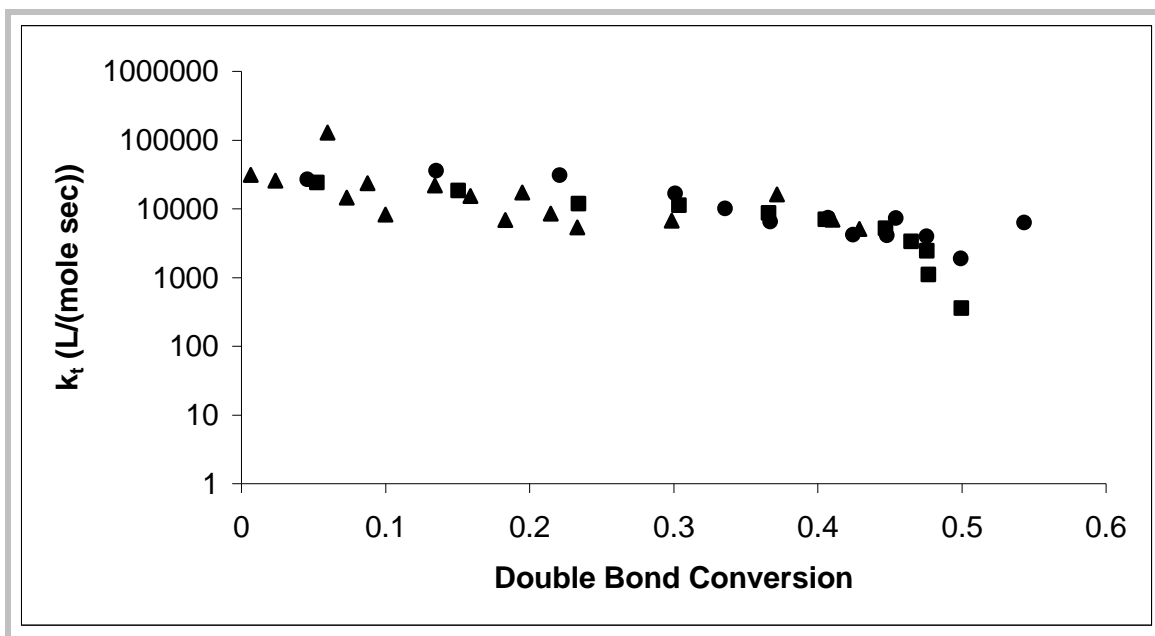


Figure 5.8 Termination Constant from Poly(MAA-co-EGDMA) Kinetic Analysis.

The termination constant for the Poly(MAA-co-EGDMA) cognitive gel (■), control gel (●), and “living/controlled” cognitive gel (▲) shows statistically similar trends.

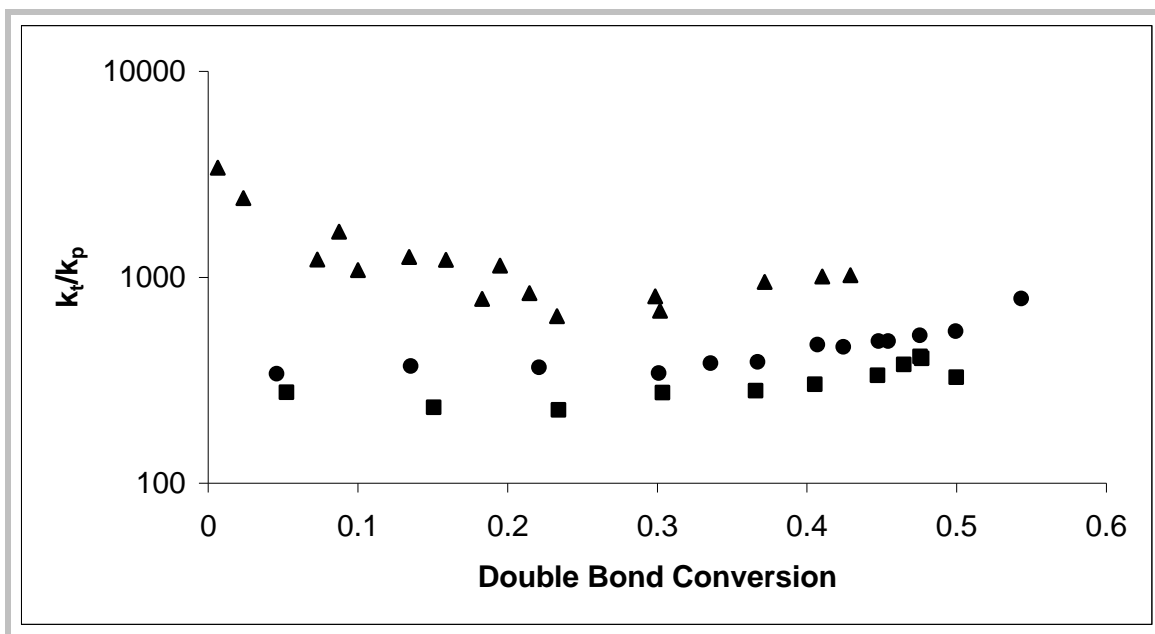


Figure 5.9 Ratio of k_t/k_p from Poly(MAA-co-EGDMA) Kinetic Analysis. The ratios are shown for poly(MAA-co-EGDMA) recognitive gel (■), control gel (●), and “living/controlled” recognitive gel (▲). It is important to note that both the propagation and termination constant trends matched literature for copolymer networks.

6.0 CONCLUSIONS

Reaction analysis of templated polymer systems has the potential to yield a greater understanding of the imprinting mechanism and associated binding parameters as related to the structural architecture of the polymeric network. Low double bond conversions (35 ± 2.3 %) are determined via reaction analysis for highly crosslinked poly(MAA-co-EGDMA) imprinted networks. Low double bond conversions are significant because most researchers within the literature use feed compositions to represent the final polymer product. It is important to note that 80% of the imprinting field uses a poly(MAA-co-EGDMA) copolymer network as the backbone for their imprinted polymers.

“Living/controlled” polymerization techniques have the potential to yield higher affinities and higher capacities within imprinted networks while retaining selectivity for the target molecule for highly crosslinked networks. We show for a typical highly crosslinked cognitive polymer system a 63% increase in the loading capacity with retention of selectivity for the template molecule ethyl-adenine-9-acetate (EA9A) using “living/controlled” polymerization techniques. In addition, the use of “living” polymerization techniques at equivalent conversions increases the template binding affinity by 85% over conventional UV free-radical polymerizations.

“Living/controlled” polymerization techniques can also increase the binding capacity within a recognitive polymer network that has a low amount of crosslinking and a high degree of flexibility within the polymer network. An EA9A recognitive poly(MAA-co-EGDMA) gel and diclofenac sodium imprinted poly(DEAEM-co-HEMA-co-PEG200DMA) gel show an increase in capacity of 90% and 89%, respectively, compared to conventional reactions. It is important to note the diclofenac sodium imprinted poly(DEAEM-co-HEMA-co-PEG200DMA) gel synthesized with conventional free-radical techniques and synthesized via “living/controlled” polymerization techniques have statistically similar binding affinities. Similar results were found for poly(MAA-co-EGDMA) recognitive gel. Mesh size analysis of diclofenac sodium imprinted poly(DEAEM-co-HEMA-co-PEG200DMA) gels reveal a mesh size decrease (30.3 +/- 1.7 to 19.7 +/- 2.1) Å at equivalent double bond conversion with the use of “living” polymerization strategy. The decrease in mesh size strongly indicates that “living/controlled” polymerization techniques shorten the kinetic chain length which leads to a more homogeneous polymer network when compared to conventional free-radical polymerizations.

The use of “living/controlled” polymerization techniques with an increase in “trained” macromolecular memory sites result in a larger quantity of template released in solution for a given gel as well as more control over the release profile. A diclofenac sodium imprinted poly(DEAEM-co-HEMA-co-PEG200DMA) gel with a smaller mesh size in conjunction with twice as many macromolecular memory binding pockets significantly extend the fractional template release profile by two-fold. A detailed kinetic analysis reveals that “living/controlled” reaction mechanisms increase the chemically

controlled propagation mechanism during the polymerization reaction which would decrease the growing chain frustrations within the network potentially providing a optimum environment for the formation of “tailored” macromolecular memory binding sites. “Living/controlled” polymerization techniques as shown within this dissertation have significant enhancement potential for the tailorability of both highly crosslinked and weakly crosslinked imprinted polymer networks for sensors, point of care devices, and advanced drug delivery carriers.

APPENDIX A

Appendix A is a supplemental data set that is needed for verification of data presented within the main chapters of this dissertation. Section A.1 has the determination of adequate purge times for nitrogen to remove the oxygen (a radical scavenger) within the polymerization reaction. Section A.2 has the linear fits of the binding data to each of the three binding isotherms mentioned in Chapter 3 (Scatchard, Langmuir, and Freundlich isotherms). Section A.3 has the raw stress versus strain curves for the static experiment via the RSA III Dynamic Mechanical Analyzer (DMA) used for the calculation of the mesh size for the poly(MAA-co-EGDMA) and poly(DEAEM-co-HEMA-co-PEG200DMA) responsive gels. Data for the calculation of diffusion coefficients in Chapter 5 are presented in Section A.4.

A.1 Nitrogen Purge Times

Oxygen is a radical scavenger which inhibits the polymerization reaction. Removal of the oxygen from the polymerization reaction was performed by allowing the pre-polymerization solution to purge with nitrogen. To determine if 20 minutes (5 minutes with quartz cover plate off before beginning the sample run and 15 minutes with

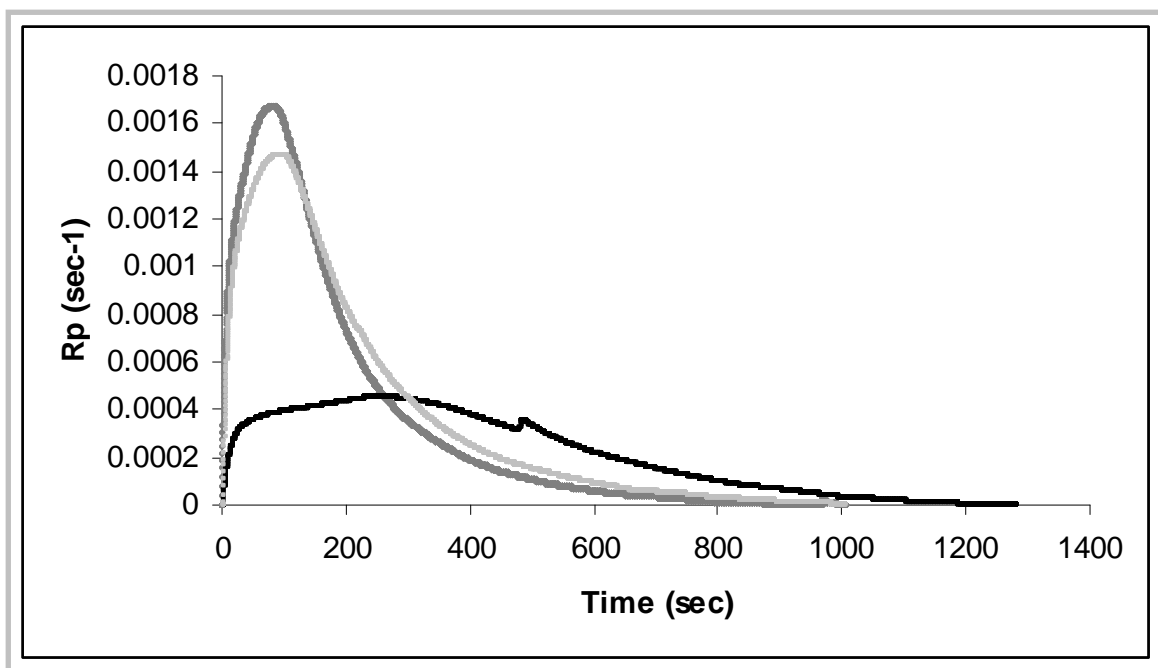


Figure A.1 Purge Time Experiments for Poly(MAA-co-EGDMA) Recognitive Gels.

For the poly(MAA-co-EGDMA) recognitive polymer gel polymerized with no nitrogen purge (—), nitrogen purge time of 2 hours (—), and nitrogen purge time (20 min) used in all experiments (---). The purpose was to determine if the 20 minute purge time was adequate. The results show that the 20 minute purge time was an adequate purge time.

quartz cover plate on during the sample run) was an adequate purge time for the polymerization reaction, two purging experiments were analyzed. The first experiment was a polymerization of the pre-polymerization solution with oxygen present, without purging with nitrogen. The second experiment was polymerization of the pre-polymerization solution in an oxygen free atmosphere with a 2 hour purge time (1 hour with quartz plate off and 1 hour with quartz plate on) to ensure complete oxygen removal. These two experiments were analyzed and were plotted on the same graph as the 20 minute purge time (Figure A.1). Results show 20 minute purge time was an adequate purge time to remove any oxygen in the cell that would inhibit the reaction.

A.2 Poly(MAA-co-EGDMA) Recognitive Networks Binding Isotherm Fit Analysis.

The Freundlich isotherm was the method of analysis for the binding parameters for the poly(MAA-co-EGDMA recognitive networks. The reason the Freundlich isotherm was used is that the data gave the best fit to the Freundlich isotherm, and it does not assume a monolayer of template-site interaction. The data was fitted to Scatchard plot, Langmuir isotherm, and Freundlich isotherm and these are given in Figure A.2, Figure A.3, and Figure A.4, respectively. The linear forms of the equations can be derived from the equations given in chapter 3. The binding data is fitted to the linear forms of the Scatchard (equation 3.1), Langmuir isotherm (equation 3.2), and the Freundlich isotherm (equation 3.3), and subsequent linear regression is used to find the parameters necessary to calculate the binding affinity and capacity.

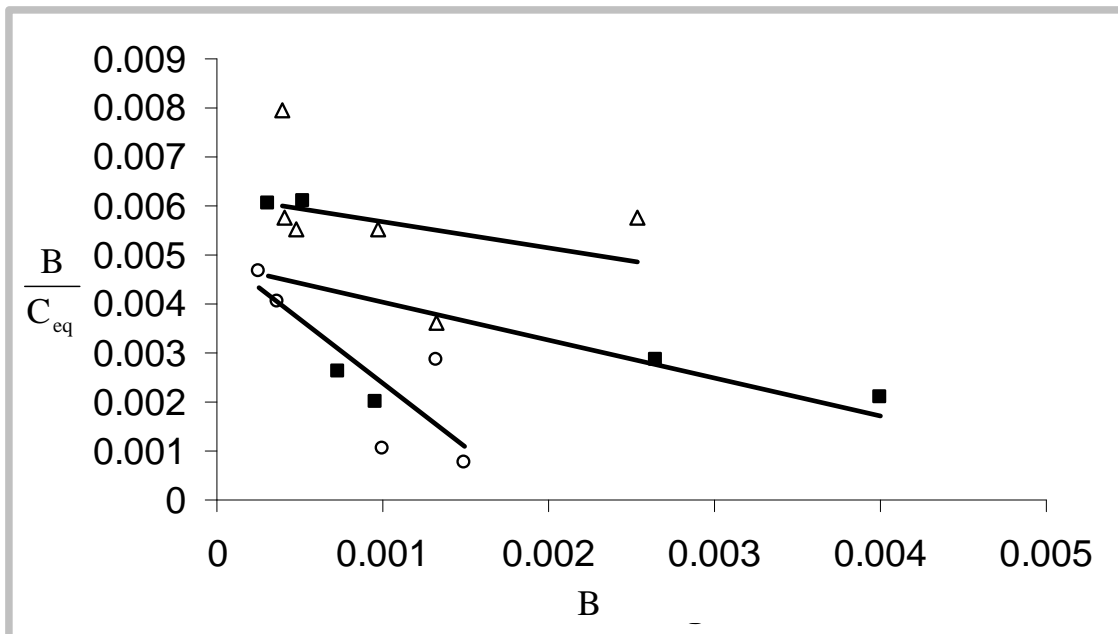


Figure A.2 Scatchard Plot of Poly(MAA-co-EGDMA) Recognitive Polymers. The linear regression of the following curves gave a R squared value of 0.69, 0.35, and 0.12 for the poly(MAA-co-EGDMA) recognitive polymer from literature(35% double bond conversion)(○), poly(MAA-co-EGDMA) recognitive polymer with 48% double bond conversions(■), and poly(MAA-co-EGDMA) recognitive polymer via “living/controlled” polymerization techniques(44% double bond conversion)(Δ), respectively. The x-axis is the bound amount (B), and the y-axis is the bound amount divided by the equilibrium concentration (B/C_{eq}).

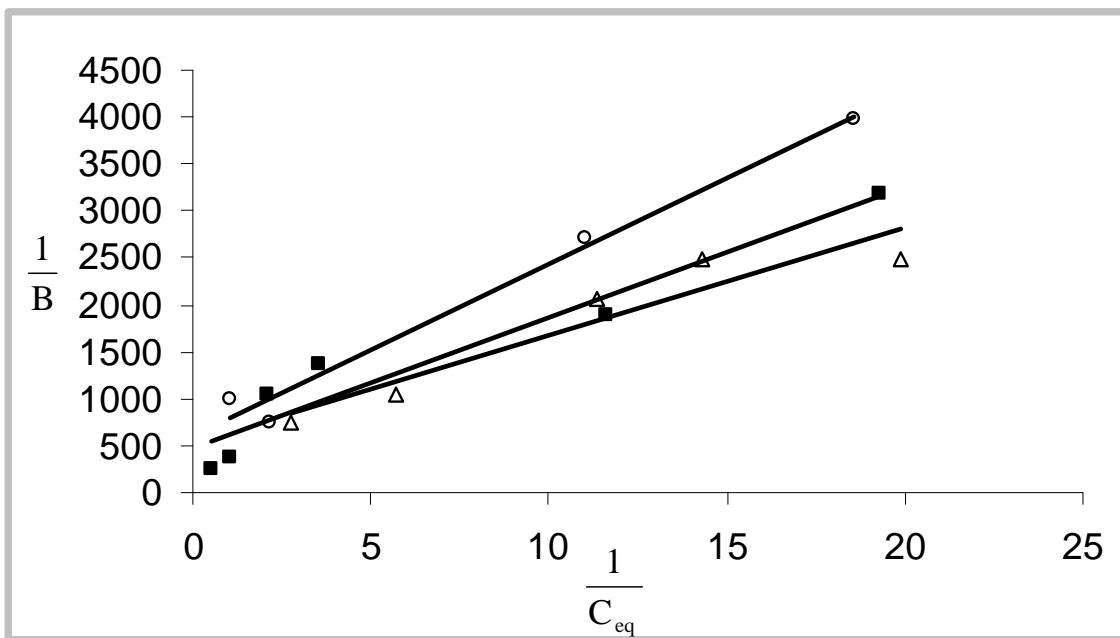


Figure A.3 Langmuir Isotherm Linear Regression of Poly(MAA-co-EGDMA) Recognitive Polymers. The linear regression of the following curves gave a R squared value of 0.98, 0.93, and 0.90 for the poly(MAA-co-EGDMA) recognitive polymer from literature(35% double bond conversion)(○), poly(MAA-co-EGDMA) recognitive polymer with 48% double bond conversion (■), and poly(MAA-co-EGDMA) recognitive polymer via “living/controlled” polymerization techniques(44% double bond conversion) (Δ), respectively. The x-axis is 1 divided by the equilibrium concentration ($1/C_{eq}$), and the y-axis is 1 divided by the bound amount ($1/B$).

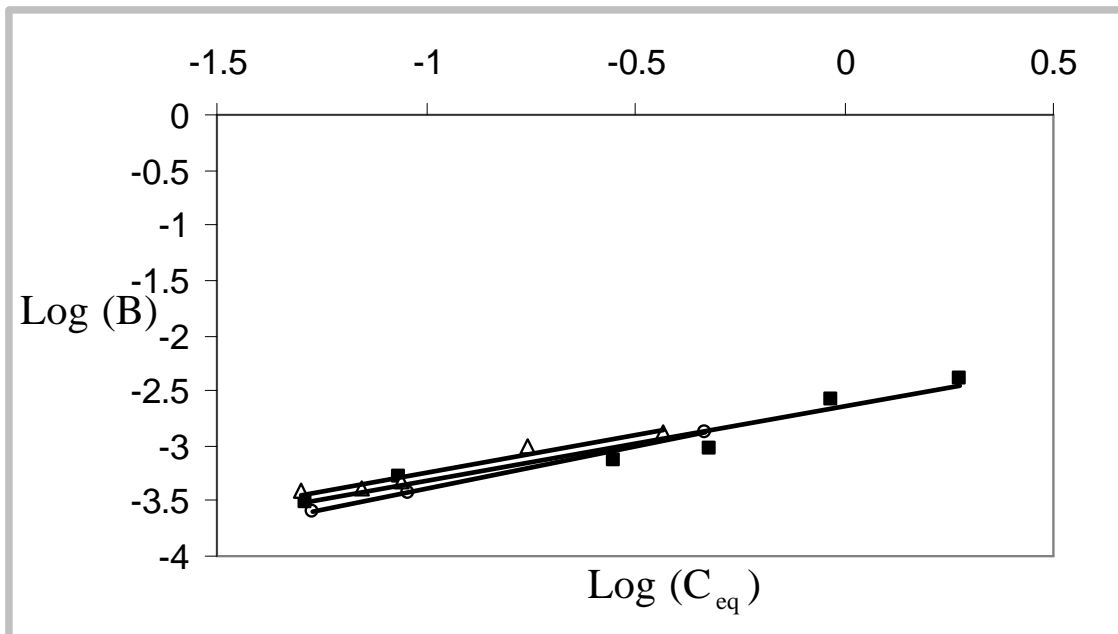


Figure A.4 Freundlich Isotherm Linear Regression of Poly(MAA-co-EGDMA) Recognitive Polymers(LOG-LOG). The linear regression of the following curves gave a R squared value of 1.00, 0.94, and 0.96 for the poly(MAA-co-EGDMA) recognitive polymer from literature(35% double bond conversion)(○), poly(MAA-co-EGDMA) recognitive polymer with 48% double bond conversions(■), and poly(MAA-co-EGDMA) recognitive polymer via “living/controlled” polymerization techniques(44% double bond conversion)(Δ), respectively. The x-axis for the plot is the log of the equilibrium concentration (C_{eq}), and the y-axis is the log of the bound amount (B).

The basis for the best fit to the data is the average R squared (R^2) value (square of the correlation coefficient). The curve fits shown are for poly(MAA-co-EGDMA) recognitive polymer from literature(35% double bond conversion), poly(MAA-co-EGDMA) recognitive polymer with 48% double bond conversions, and poly(MAA-co-EGDMA) recognitive polymer via “living/controlled” polymerization techniques(44% double bond conversion).

It is important to note that both the Freundlich isotherm and the Langmuir isotherm gave similar values for the binding affinity for the poly(MAA-co-EGDMA) recognitive polymer from literature.

A.3 Raw Data from Static Experiment for Calculation of Mesh Size for Poly(MAA-co-EGDMA) and Poly(DEAEM-co-HEMA-co-PEG200DMA) Recognitive Gels

The data presented in this section is the raw data taken from the static experiment from the RSA III DMA. The data obtained and used for calculation of mesh size is the linear stress versus strain data presented in these graphs. Each graph has three sample runs for each type of polymer network. It is important to note all analysis of gels was preformed with $\alpha < 2$. The mesh size analysis is presented in Chapter 5.

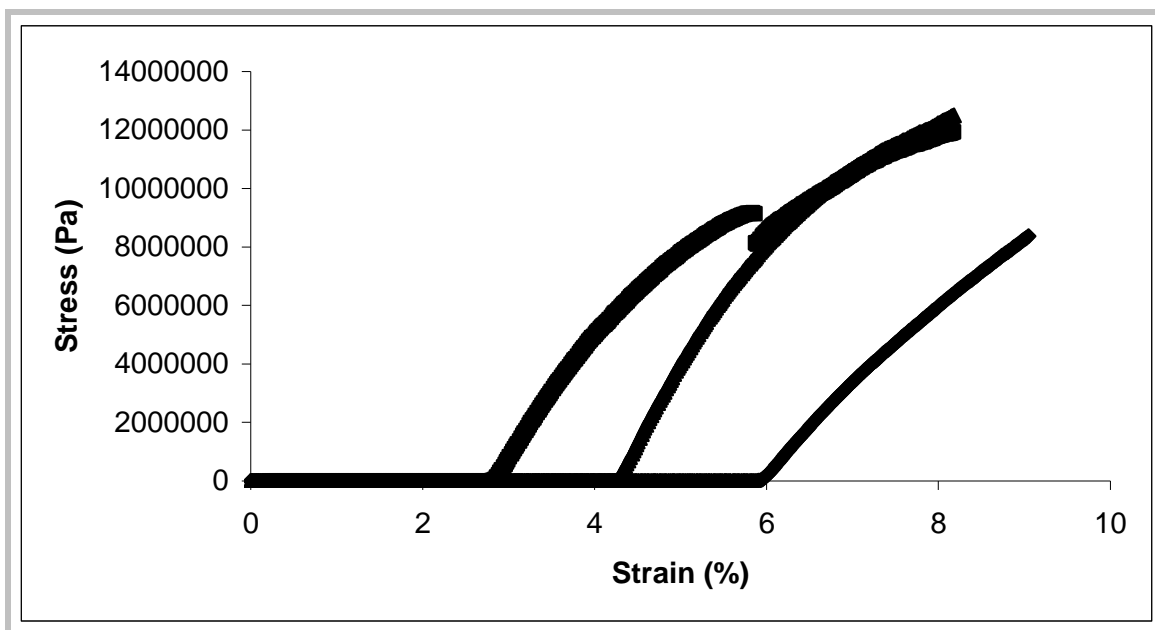


Figure A.5. Raw Stress versus Strain Data for Three Poly(MAA-co-EGDMA) Recognitive Gels. The raw data for stress versus strain is used to calculate the mesh size. It is important to note the strain in % is equal to $\Delta L/L_o \cdot 100\%$, where ΔL is $(L - L_o)$, L is the extended length, and L_o is the original un-stretched length. Also, $\alpha < 2$ for all experimental analysis of mesh size.

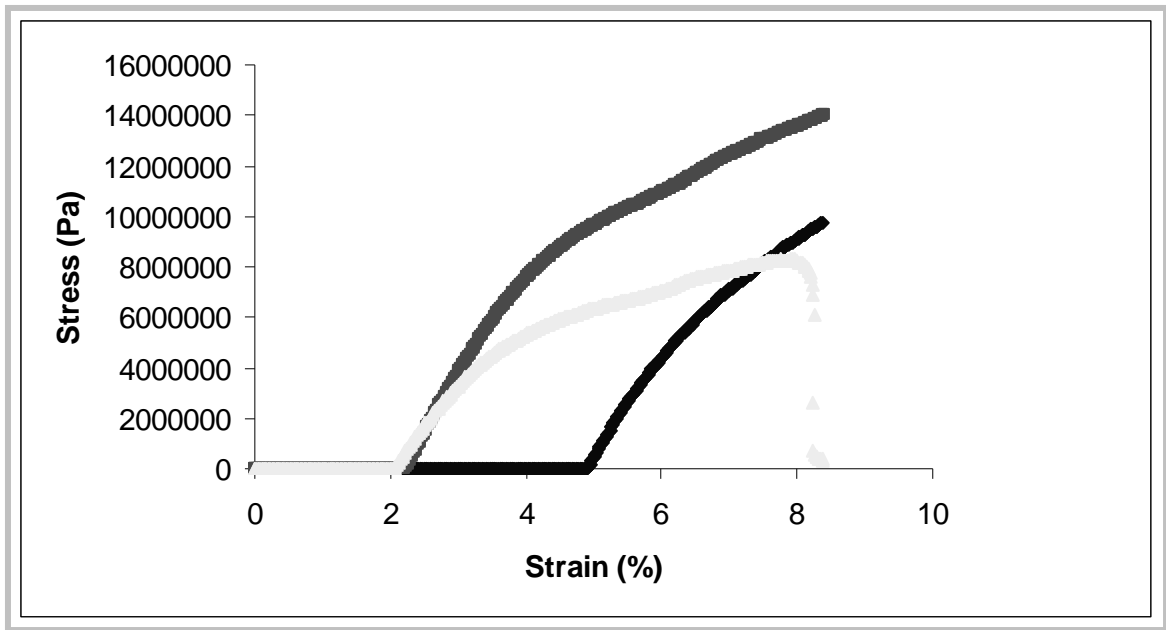


Figure A.6. Raw Stress versus Strain Data for Three Poly(MAA-co-EGDMA) Recognitive Gels via “Living/controlled” Polymerization. The raw data for stress versus strain is used to calculate the mesh size. It is important to note the strain in % is equal to $\Delta L/L_o \cdot 100\%$, where ΔL is $(L - L_o)$, L is the extended length, and L_o is the original un-stretched length. Also, $\alpha < 2$ for all experimental analysis of mesh size.

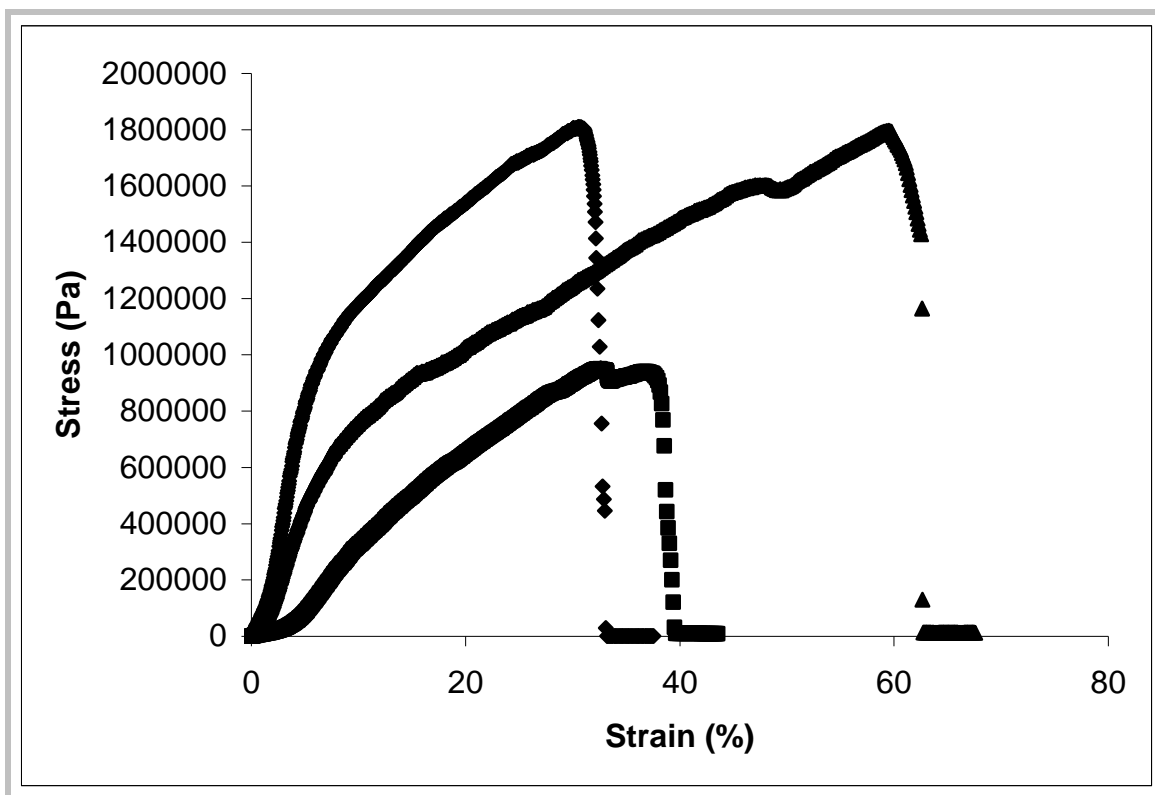


Figure A.7. Raw Stress versus Strain Data for Three Poly(DEAEM-co-HEMA-co-PEG200DMA) Recognitive Gels. The raw data for stress versus strain is used to calculate the mesh size. It is important to note the strain in % is equal to $\Delta L/L_o \cdot 100\%$, where ΔL is $(L - L_o)$, L is the extended length, and L_o is the original un-stretched length. Also, $\alpha < 2$ for all experimental analysis of mesh size.

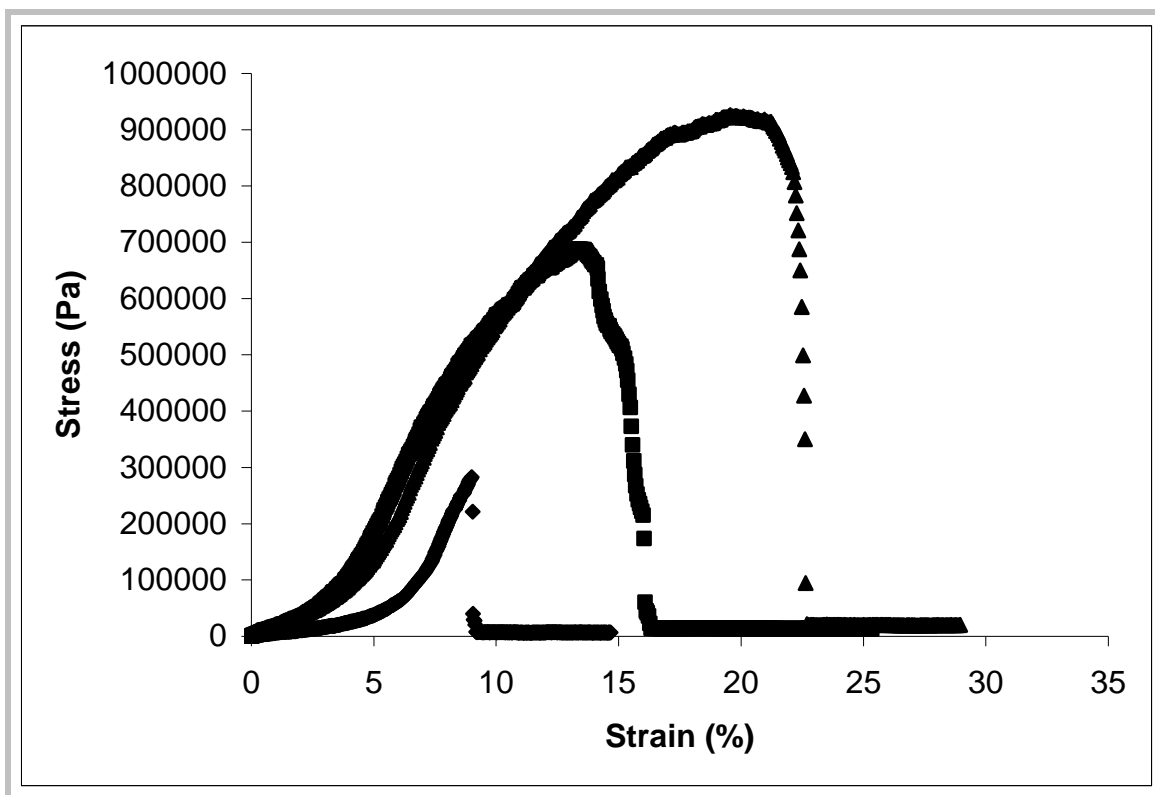


Figure A.8. Raw Stress versus Strain Data for Three Poly(DEAEM-co-HEMA-co-PEG200DMA) Recognitive Gels via “Living/controlled” Polymerization. The raw data for stress versus strain is used to calculate the mesh size. It is important to note the strain in % is equal to $\Delta L/L_0 \cdot 100\%$, where ΔL is $(L - L_0)$, L is the extended length, and L_0 is the original un-stretched length. Also, $\alpha < 2$ for all experimental analysis of mesh size.

A.4 Data used for the Calculation of Diffusion Coefficients.

Data for the calculation of the diffusion coefficients for the EA9A imprinted poly(MAA-co-EGDMA) gels and gels prepared via “living/controlled” polymerization techniques are presented in Figure A.9. Data for the calculation of the diffusion coefficients for the diclofenac sodium imprinted poly(DEAEM-co-HEMA-co-PEG200DMA) gels and gels prepared via “living/controlled” polymerization techniques are presented in Figure A.10.

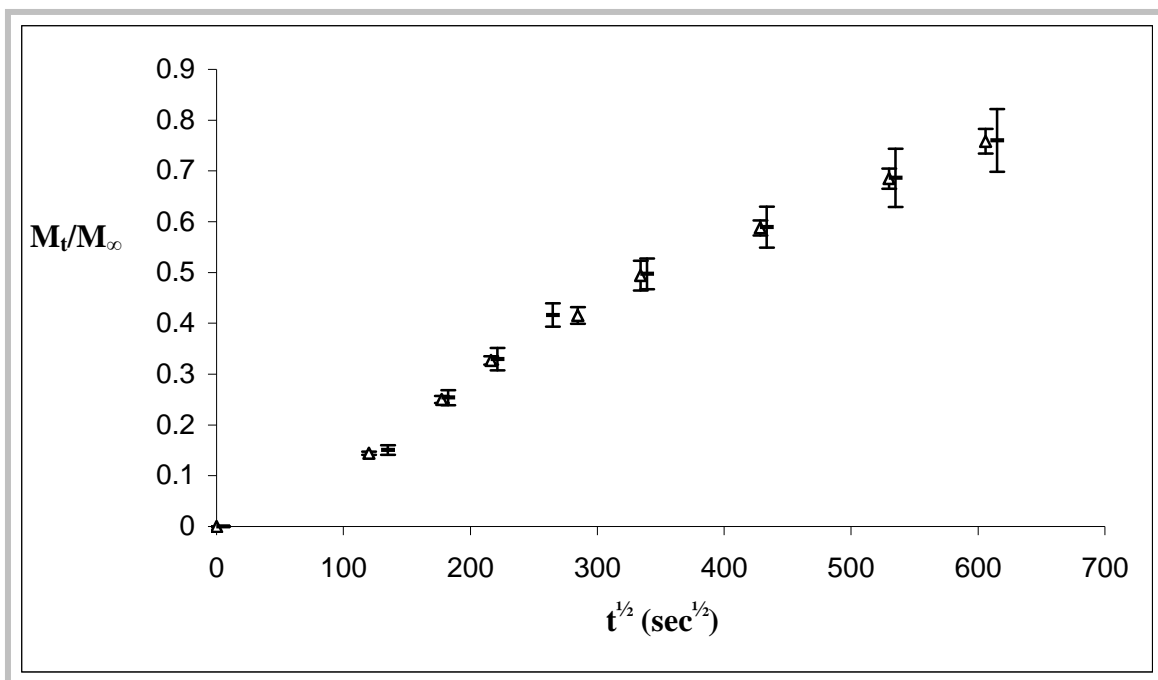


Figure A.9. Fractional Release for the Calculation of Diffusion Coefficients for EA9A Imprinted Poly(MAA-co-EGDMA) Gels. M_t/M_∞ was plotted to only 70% to calculate the diffusion coefficients. Poly(MAA-co-EGDMA) cognitive gel (Δ) and poly(MAA-co-EGDMA) cognitive gel prepared via “living/controlled” polymerization techniques (\blacksquare) curves are presented. The slope was obtained from linear regression and the diffusion coefficients were calculated. Details of this analysis are presented in Chapter 5, section 5.3.6.

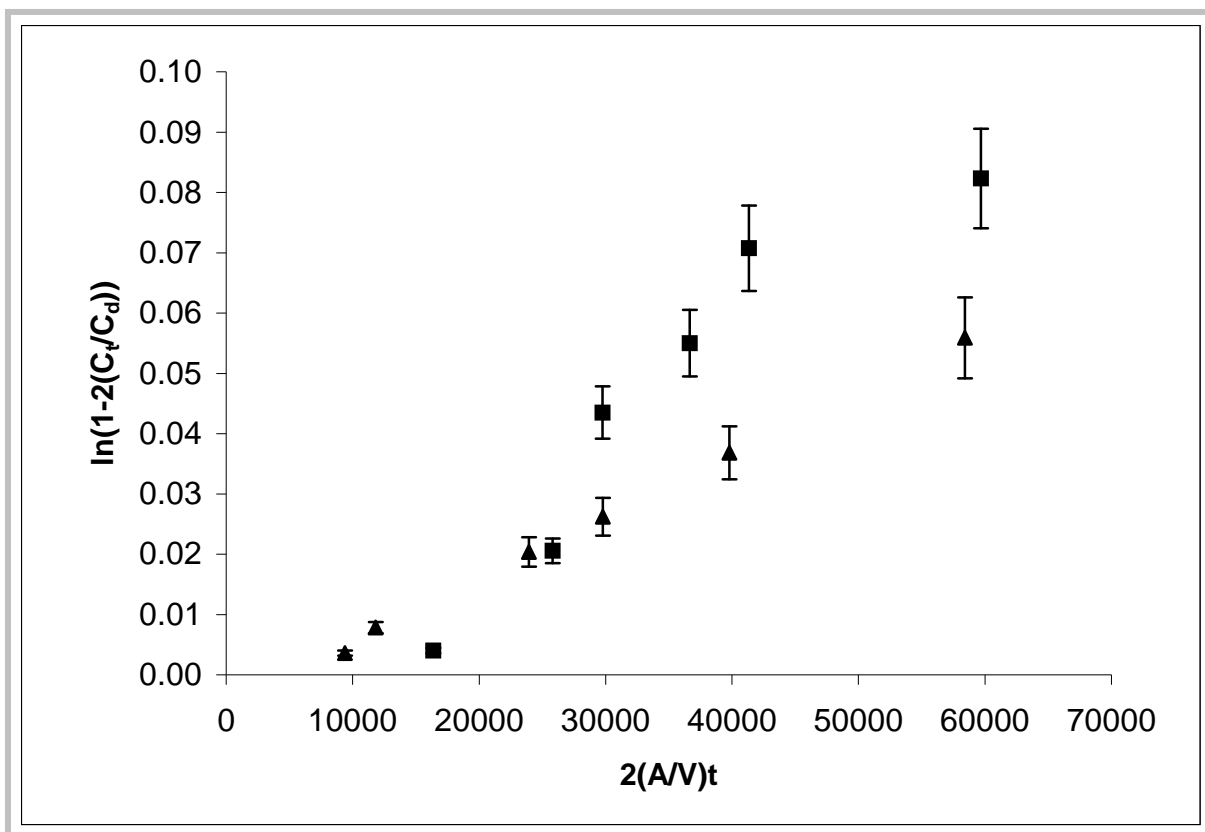


Figure A.10 One Dimensional Transport Data for Diclofenac Sodium Imprinted Poly(DEAEM-co-HEMA-co-PEG200DMA) Gels. Linear regression of the graph will yield the permeability P for the poly(DEAEM-co-HEMA-co-PEG200DMA) recognitive gel (▲) and the poly(DEAEM-co-HEMA-co-PEG200DMA) recognitive gel prepared via “living/controlled” polymerization techniques (■). The specifics of the calculation of values for the x axis and y axis see Chapter 5, section 5.3.7, the concentration in the receptor cell is C_t , the concentration of the donor cell is C_d , the area of diffusion is A , the volume of each half cell is V , and time is t . Important to note values are calculated post-lag time.

A.5 Linearization of Selected Data for Freundlich Isotherm Analysis.

In this section linear regressions of the poly(MAA-co-EGDMA) recognitive polymer synthesized via “living/controlled” polymerization techniques with 35% double bond conversion binding data, and the selectivity studies for the poly(MAA-co-EGDMA) recognitive polymer synthesized from literature, poly(MAA-co-EGDMA) recognitive polymer with 48% double bond conversion, and poly(MAA-co-EGDMA) recognitive polymer synthesized via “living/controlled” polymerization techniques with 44% double bond conversion. These data sets are presented in (Log-Log) format.

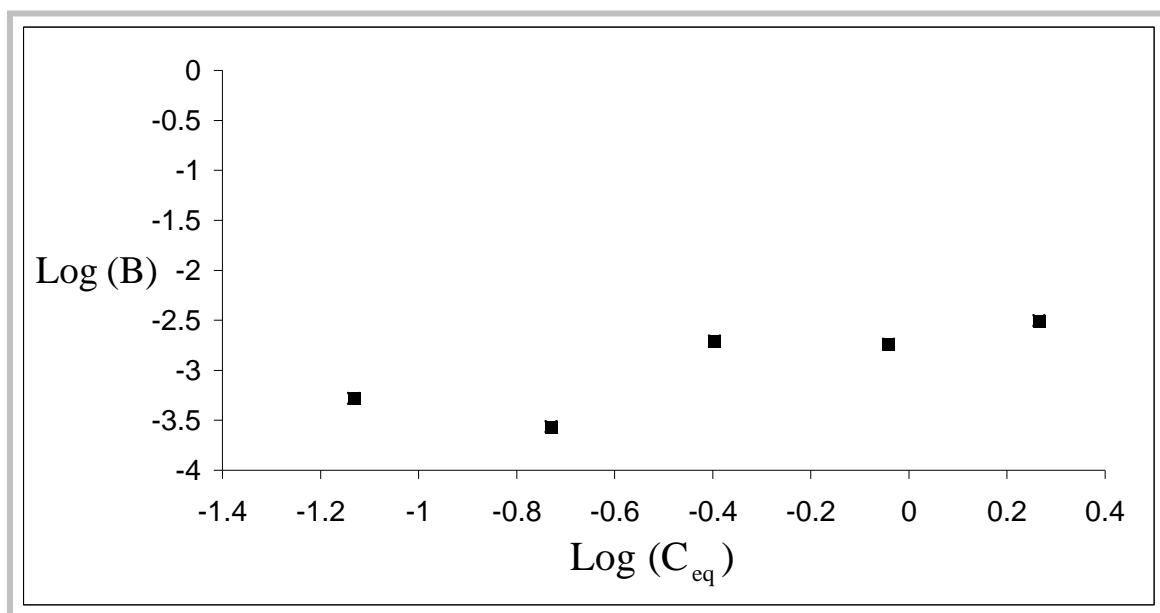


Figure A.11 Freundlich Isotherm Linear Regression of Poly(MAA-co-EGDMA) Recognitive Polymers Synthesized via “Living” Polymerization (35% Double Bond Conversion) (LOG-LOG). The linear regression of the following curves gave a R squared value of 0.70 for the poly(MAA-co-EGDMA) recognitive polymer synthesized via “living/controlled” polymerization techniques (35% double bond conversion)(■). The x-axis for the plot is the log of the equilibrium concentration (C_{eq}), and the y-axis is the log of the bound amount (B). The Langmuir isotherm gave an affinity of 5.52 ± 0.55 mM^{-1} .

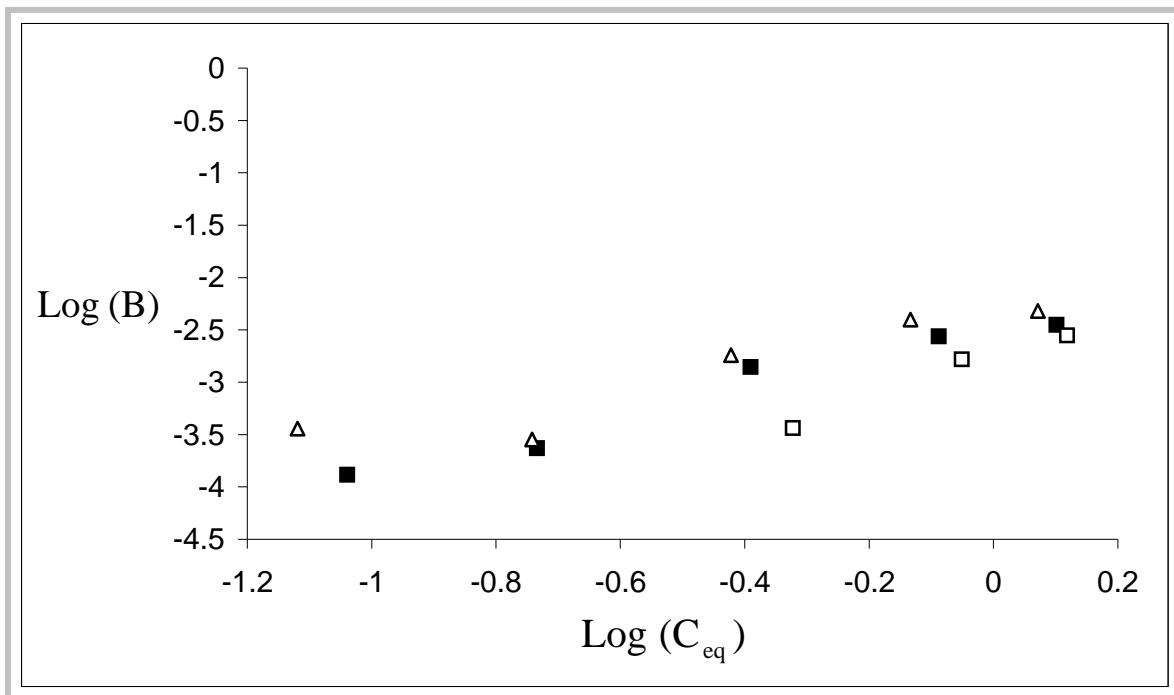


Figure A.12 Freundlich Isotherm Linear Regression of Poly(MAA-co-EGDMA) Recognitive Polymers for Selectivity Analysis (LOG-LOG). The linear regression of poly(MAA-co-EGDMA) recognitive polymers are presented, poly(MAA-co-EGDMA) recognitive polymer from literature(35% double bond conversion)(■), poly(MAA-co-EGDMA) recognitive polymer with 48% double bond conversions(□), and poly(MAA-co-EGDMA) recognitive polymer via “living/controlled” polymerization techniques(44% double bond conversion)(Δ), respectively. The x-axis for the plot is the log of the equilibrium concentration (C_{eq}), and the y-axis is the log of the bound amount (B).

APPENDIX B

In Appendix B, the washing analysis is presented for the highly crosslinked poly(MAA-co-EGDMA) recognitive polymers described in Chapters 3 and 4. Three types of recognitive polymers were washed in three micro-Soxhlet extraction devices that were custom made at the Auburn University Glass Shop. The micro-Soxhlet extraction device was specifically made for a 10 mm x 50 mm Whatman Extraction Thimble filter. The wash solvent used was a 1 to 4 ratio of methanol to acetonitrile. The washing procedure was performed on a hot plate in a sand bath to keep the temperature of each Soxhlet extraction device the same.

B.1 Method of Micro-Soxhlet Extraction for Poly(MAA-co-EGDMA) Recognitive Polymer Disks.

A sample of approximately 100 mg for each recognitive network, literature recognitive polymer, recognitive polymer with 48% double bond conversion, and recognitive polymer via “living/controlled” polymerization techniques were placed in separate micro-Soxhlet extraction devices to wash each one separately. The effluent within flask at the bottom of each Soxhlet extraction device was measured via a Synergy UV-vis spectrophotometer to measure the concentration of EA9A. The volume of the

effluent was then measured in a graduated cylinder. The concentration and the volume data was used to calculate the mass of EA9A washed out of the polymer.

B.2 Results of Micro-Soxhlet Extraction for Poly(MAA-co-EGDMA) Recognitive Polymer Disks.

The results of the extraction experiment yield that the poly(MAA-co-EGDMA) recognitive polymer from literature released 0.135 ± 0.014 mg of the EA9A within the polymer wash. The poly(MAA-co-EGDMA) recognitive polymer with 48% double bond conversion released 0.084 ± 0.017 mg of the EA9A within the polymer wash, and poly(MAA-co-EGDMA) recognitive polymer via “living/controlled” polymerization techniques released 0.087 ± 0.013 mg of the EA9A in the polymer wash (Figure B.1). In literature, the polymers are ground to a powder with 50 μm particle size¹. Smaller particle sizes would allow for removal of trapped EA9A and faster template transport thus giving higher wash out efficiencies. Literature states that 90% of the EA9A is washed out in a 24 hour time period¹. A schematic of how the diffusion of drug diffuses out from a highly crosslinked network (Figure B.2). By grinding the polymer into smaller particles, more template would be able to diffuse out from the polymer network thus leaving less template trapped within the polymer network.

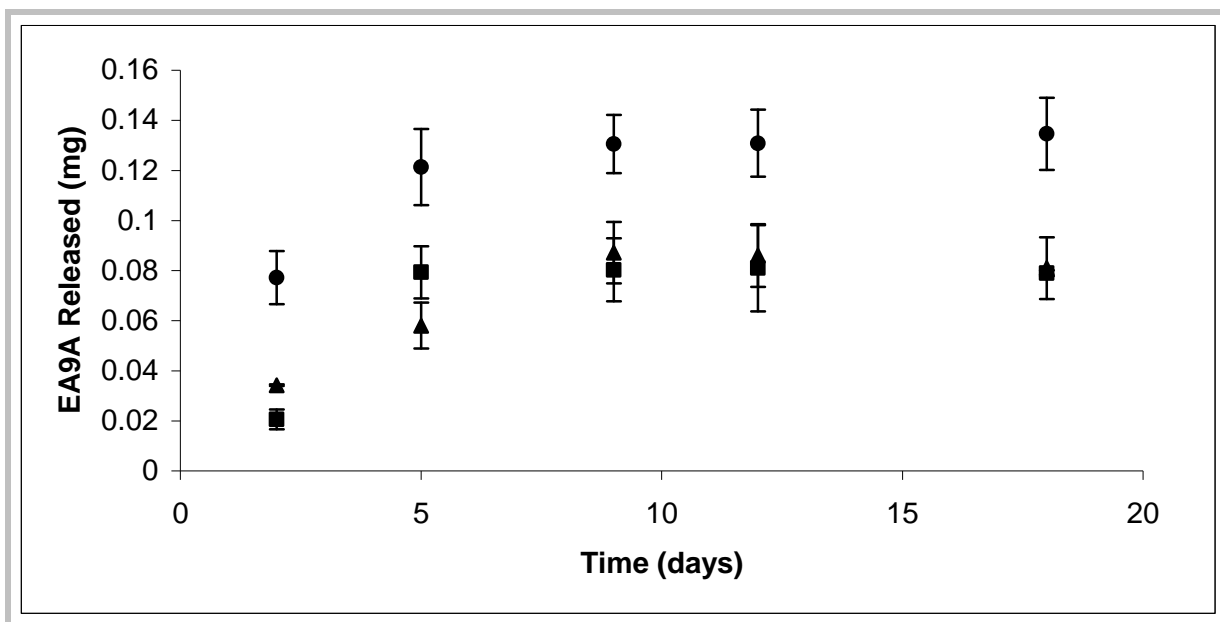


Figure B.1 Wash Analysis for Highly Crosslinked Poly(MAA-co-EGDMA) Recognitive Networks. The release of the EA9A over the given time period indicates that poly(MAA-co-EGDMA) recognitive polymer from literature (●) released more EA9A than the poly(MAA-co-EGDMA) recognitive polymer with 48% double bond conversion (■) and the poly(MAA-co-EGDMA) recognitive polymer via “living/controlled” polymerization techniques (▲). Error bars represent the standard error. (n=3) It is important to note that later experiments show that the Whatman extraction filter did absorb a significant amount of EA9A which would cause the numbers presented in the graph to be significantly lower than the actual amount of EA9A washed out of the imprinted polymer.

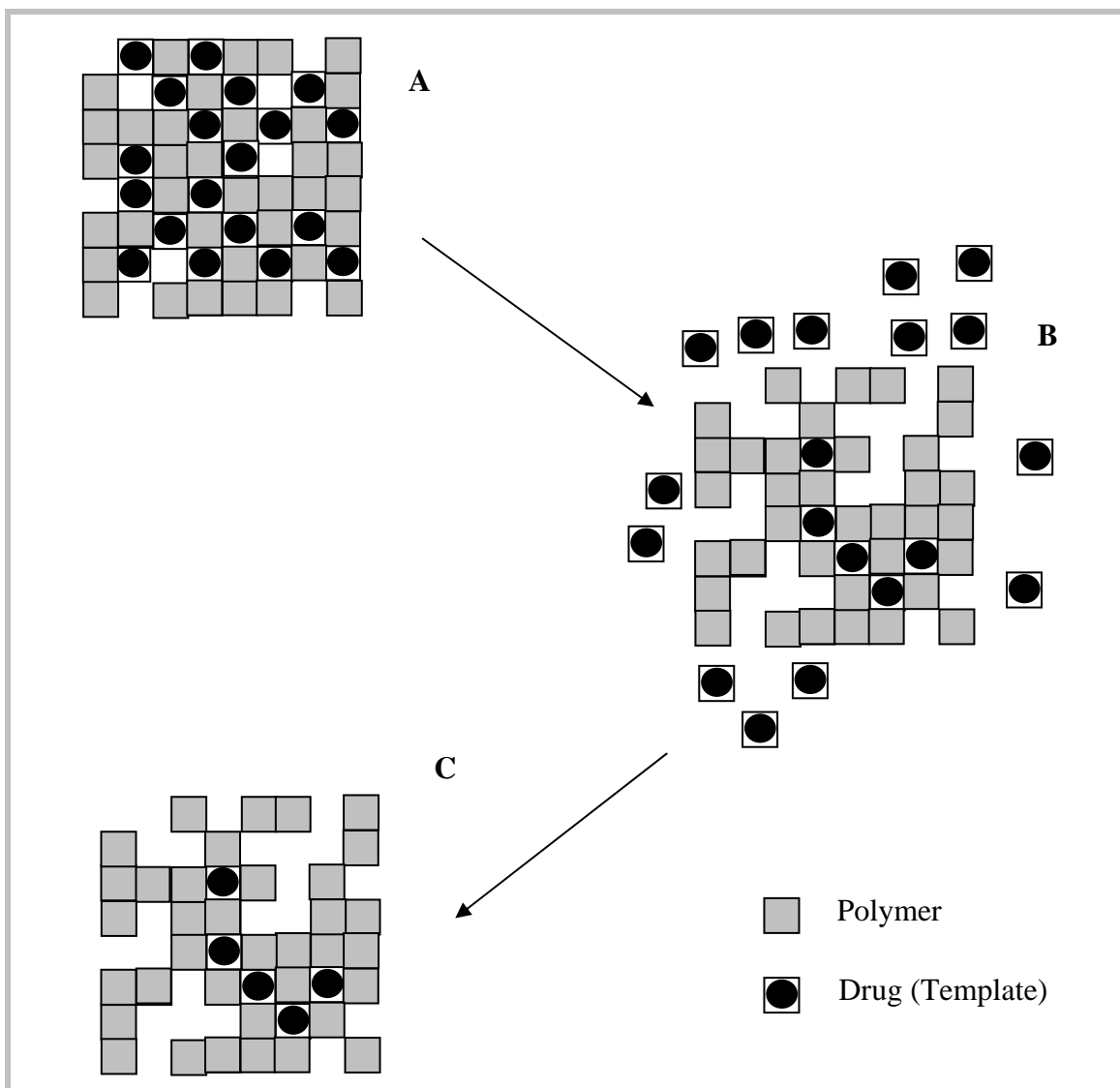


Figure B.2 Schematic of Diffusion Through a Crosslinked Polymer Network. The diffusion of the template takes place through the polymer network. The polymer with template laced throughout the network (**A**). The template diffuses out through the open portions of the polymer network (**B**). The network with template locked within the polymer network due to the template not having sufficient space to diffuse out of the polymer (**C**). Smaller particle size would contribute to lower amounts of trapped template within the polymer network.

B.3 Calculation of Masses of EA9A Bound, Removed, and Initially for EA9A Imprinted Poly(MAA-co-EGDMA) Polymer Networks.

This section is dedicated to the evaluation whether the amounts of EA9A initially within the polymer (during synthesis), loading capacity of the polymer, and template washed out of the polymer within the poly(MAA-co-EGDMA) recognitive networks are scientifically feasible. The calculation the actual amount of EA9A within the poly(MAA-co-EGDMA) recognitive network synthesized from literature, the poly(MAA-co-EGDMA) recognitive network with 48% increased conversion, and poly(MAA-co-EGDMA) recognitive network via “living/controlled” polymerization techniques. The wt% calculated from the initial solutions (based on all solvent evaporated from the polymer network) for the poly(MAA-co-EGDMA) recognitive network synthesized from literature, the poly(MAA-co-EGDMA) recognitive network with 48% increased conversion, and poly(MAA-co-EGDMA) recognitive network via “living/controlled” polymerization techniques are 0.01193, 0.0114, and 0.01097, respectively. The molecular weight of EA9A is 221.22 mg/mmol. For poly(MAA-co-EGDMA) recognitive polymer synthesized from literature the calculation is shown in B.1. It is important to note all values will be listed a value of mg of template divided by g of dry polymer.

$$0.01193 \left(\frac{\text{mg EA9A}}{\text{mg polymer}} \right) \left(\frac{1000 \text{mg polymer}}{\text{g polymer}} \right) = 11.93 \frac{\text{mg EA9A}}{\text{g dry polymer}} \quad \text{B.1}$$

The corresponding values for the initial EA9A within the network for the poly(MAA-co-EGDMA) recognitive network with 48% increased conversion, and poly(MAA-co-

EGDMA) recognitive network via “living/controlled” polymerization techniques are 11.4 and 10.97 mg EA9A/g dry polymer, respectively.

The loading capacity for the EA9A imprinted poly(MAA-co-EGDMA) gels are calculated via the binding isotherms obtained from the binding analysis of the recognitive gels presented in Chapter 3 and Chapter 4. The values for the loading capacity are $(0.0015 \pm 0.0004, 0.004 \pm 0.0012, \text{ and } 0.00996 \pm 0.0013)$ mmole EA9A/g of dry polymer. Equation B.2 calculates the mg of EA9A bound by the poly(MAA-co-EGDMA) recognitive gel synthesized from literature, and B.3 calculates the error.

$$0.0015 \frac{\text{mmole EA9A}}{\text{g dry polymer}} \left(\frac{221.22 \text{mg EA9A}}{\text{mmole EA9A}} \right) = 0.33 \frac{\text{mg EA9A}}{\text{g dry polymer}} \quad \text{B.2}$$

$$\frac{0.00044 \frac{\text{mmole EA9A}}{\text{g dry polymer}}}{0.0015 \frac{\text{mmole EA9A}}{\text{g dry polymer}}} \left(0.33 \frac{\text{mg EA9A}}{\text{g dry polymer}} \right) = 0.0968 \frac{\text{mg EA9A}}{\text{g dry polymer}} \quad \text{B.3}$$

The results show for the loading capacity in mg EA9A per g of dry polymer to be $(0.33 \pm 0.097, 0.88 \pm 0.26, \text{ and } 2.20 \pm 0.28)$ mg EA9A/g of dry polymer for the poly(MAA-co-EGDMA) recognitive network synthesized from literature, the poly(MAA-co-EGDMA) recognitive network with 48% increased conversion, and poly(MAA-co-EGDMA) recognitive network via “living/controlled” polymerization techniques.

The washing procedure presented in Appendix B, section B.2 calculated the amount of EA9A washed from the imprinted polymer networks. The weight of polymer used was (78.37, 92.20, and 83.90) mg of dry polymer for the poly(MAA-co-EGDMA) recognitive network synthesized from literature, the poly(MAA-co-EGDMA) recognitive

network with 48% increased conversion, and poly(MAA-co-EGDMA) recognitive network via “living/controlled” polymerization techniques, respectively.

The weights washed out of the polymer were (0.135 ± 0.014 , 0.081 ± 0.017 , and 0.087 ± 0.013) mg for the poly(MAA-co-EGDMA) recognitive network synthesized from literature, the poly(MAA-co-EGDMA) recognitive network with 48% increased conversion, and poly(MAA-co-EGDMA) recognitive network via “living/controlled” polymerization techniques, respectively. It is important to note four main assumptions were made in this wash out analysis (i) none of the EA9A decomposes during the washing procedure, (ii) none of the EA9A adsorbed to the sides of the round bottom flask during measurement of the wash, (iii) the extraction filter does not significantly absorb EA9A, and (iv) all EA9A washed from the polymer is contained within the acetonitrile:methanol wash effluent in the flask. Wash out values are calculated via equation B.4, and equation B.5 is used to calculate the error.

$$0.135 \text{ mg of EA9A} \left(\frac{1}{78.37 \text{ mg dry polymer}} \right) \left(\frac{1000 \text{ mg}}{\text{g}} \right) = 1.75 \frac{\text{mg EA9A}}{\text{g dry polymer}} \quad \text{B.4}$$

$$\frac{0.014 \text{ mg}}{0.135 \text{ mg}} \left(1.748 \frac{\text{mg EA9A}}{\text{g dry polymer}} \right) = 0.18 \frac{\text{mg EA9A}}{\text{g dry polymer}} \quad \text{B.5}$$

The amounts of template washed out of the EA9A imprinted poly(MAA-co-EGDMA) networks are (1.75 ± 0.18 , 0.88 ± 0.18 , and 1.04 ± 0.16) mg EA9A/ g dry polymer for the poly(MAA-co-EGDMA) recognitive network synthesized from literature, the poly(MAA-co-EGDMA) recognitive network with 48% increased conversion, and poly(MAA-co-EGDMA) recognitive network via “living/controlled” polymerization

techniques, respectively. It is important to note that later experiments show that the Whatman extraction filter did absorb a significant amount of EA9A which would cause the numbers presented in the graph to be significantly lower than the actual amount of EA9A washed out of the imprinted polymer.

B.4 Discussion of Results

The washing analysis reveals that the poly(MAA-co-EGDMA) copolymer network is synthesized with more than enough template to compensate for the amount of EA9A bound within the network. The poly(MAA-co-EGDMA) recognitive network synthesized from literature and the poly(MAA-co-EGDMA) recognitive network with 48% increased conversion had enough drug washed out of the polymer to compensate for the EA9A loading capacity. However, the poly(MAA-co-EGDMA) recognitive network via “living/controlled” polymerization techniques did not have enough EA9A washed out of the network to compensate for the associated binding parameters.

The template EA9A washed out of the polymer is presented in Figure B.1. Examination of the curve indicate that the poly(MAA-co-EGDMA) recognitive polymer with 48% double bond conversion and poly(MAA-co-EGDMA) recognitive polymer prepared via “living/controlled” polymerization techniques have lower amounts of drug washed out of the polymer network. The poly(MAA-co-EGDMA) recognitive polymer with 48% double bond conversion has an increased initiator which as shown in Chapter 3 translates into smaller kinetic chain length. Hypothetically, a more homogeneous network with shorter kinetic chain length (Chapter 4) suggests smaller mesh sizes which

in effect lock more template within the polymer network. The reasons for the low amounts of EA9A washing out for the “living” polymerization could be due to decomposition of EA9A in the effluent from the wash over a 2.5 week period at a temperature of 80°C and/or adsorption on the side of the glass round bottom flask. Later experiments determined that the Whatman extraction filter did absorb a significant amount of EA9A which would cause the amounts removed from the imprinted polymer be significantly lower than the actual amount of EA9A removed. All the amounts of EA9A from the synthesis, loading, and wash are presented in Table B.1.

B.5 References

1. Spivak, D.; Gilmore, M. A.; Shea, K. J., Evaluation of Binding and Origins of Specificity of 9-Ethyladenine Imprinted Polymers. *J. Am. Chem. Soc.* **1997**, 119, (19), 4388-4393.

Table B.1 Amounts of EA9A Contained in the Synthesis, Loading, and Wash Effluent for Poly(MAA-co-EGDMA) Recognitive Networks.

Polymer	Synthesis mg EA9A/g dry polymer	Loading mg EA9A/g dry polymer	Wash mg EA9A/g dry polymer*
Poly(MAA-co-EGDMA) recognitive polymer literature match (35% double bond conversion)	11.93	0.33 ± 0.097	1.75 ± 0.18
Poly(MAA-co-EGDMA) recognitive polymer (48% double bond conversion)	11.40	0.88 ± 0.26	0.88 ± 0.18
Poly(MAA-co-EGDMA) recognitive polymer via “living/controlled” polymerization techniques	10.97	2.20 ± 0.28	1.04 ± 0.16

* Later experiments determined that the Whatman extraction filter did absorb a significant amount of EA9A which would cause the amounts removed from the imprinted polymer be lower than the actual amount of EA9A removed.

APPENDIX C

In appendix C, the Visual Basic code developed for the calculation of double bond conversion is presented. The Visual Basic code was used to analyze all recognitive polymers presented within this dissertation. The program name is “SAE”. The program was designed and developed for the express purpose of analysis of the data obtained from the DPC.

C.1 Program Setup

Procedure for the analysis is in chronological order. Open an Excel workbook containing the Visual Basic program presented in this appendix, press “CTRL-S” to set up the spreadsheet. Second data from the differential photo calorimeter is taken from the Universal Analysis program (TA Instruments, New Castle, DE) and pasted into the first three columns under the cells labeled, Time (sec), Temperature (°C), and Heat Flow (W/g). Third the theoretical heat of reaction must be placed in the cell below the labeled cell heat of reaction, and the average molecular weight of the solution must be placed in the cell below the average molecular weight. It is important to note if any sudden drops in data are observed a correction factor of the exact amount of the drop (10 W/g etc determined from the heat flow just before the drop subtracting the heat flow just after the

drop) must be added to the program under the cell light intensity correction. The analysis of the data is done by pressing “CTRL-A”. The program to set up and analyze for kinetic parameters is “CTRL-E”. Before pressing “CTRL-E”, data must be placed within the cells below Delta Time, which is the time after the peak of the reaction for analysis (it normally takes 25 sec for the rate to come to equilibrium after the light shut off time) and Light Shutoff Time (min) which is the time the light is shut off after the beginning of the data collection, respectively. Graphs of the data can be made by pressing “CTRL-G” after the data is analyzed.

C.2 Program Code for “SAE”

```
Sub Setup()  
,  
' Setup Macro  
' Macro recorded 2/21/2006 by Asa Vaughan  
" Keyboard Shortcut: Ctrl+s  
' Cells.Select  
    With Selection  
        .HorizontalAlignment = xlGeneral  
        .VerticalAlignment = xlBottom  
        .WrapText = True  
        .Orientation = 0
```

```
.AddIndent = False
.IndentLevel = 0
.ShrinkToFit = False
.ReadingOrder = xlContext
.MergeCells = False
```

End With

With Selection.Font

```
.Name = "Arial"
.FontStyle = "Regular"
.Size = 8
.Strikethrough = False
.Superscript = False
.Subscript = False
.OutlineFont = False
.Shadow = False
.Underline = xlUnderlineStyleNone
.ColorIndex = xlAutomatic
```

End With

Selection.Rows.AutoFit

Selection.Columns.AutoFit

```
Cells(1, 1) = "Heat of Reaction J/mole"
```

```
Cells(1, 2) = "MW avg"
```

```
Cells(1, 3) = "Intensity Heat Flow W/g"
```

Cells(1, 4) = "Rp Max (sec-1)"
Cells(1, 5) = "Final Conversion"
Cells(1, 6) = "Temperature (°C)"
Cells(1, 7) = "TimeRpmax"
Cells(1, 8) = "Conversion RpMax"
Cells(1, 9) = "program kmax"
Cells(1, 10) = "Total Polymerization Time (min)"
Cells(1, 11) = "kmax override"
Cells(1, 12) = "Total Time Data Taken (sec)"
Cells(1, 13) = "Time for Kinetic Time Analysis (min) "
Cells(1, 14) = "Light Intesity Correction"
Cells(3, 1) = "Time (sec)"
Cells(3, 2) = "Temperature (°C)"
Cells(3, 3) = "Heat Flow (W/g)"
Cells(3, 4) = "Actual Heat Flow (W/g)"
Cells(3, 5) = "Rp (sec-1)"
Cells(3, 6) = "Time"
Cells(3, 7) = "Conversion"
Cells(3, 9) = "rpsum"
Cells(3, 12) = "rp initial"
Cells(3, 13) = "rp final"
Cells(11, 10) = "Kinetic Rp Max (sec-1)"
Cells(11, 11) = "Kinetic Final Converion"

```
Cells(11, 12) = "Temperature (°C)"
Cells(11, 13) = "Kinetic Time Rpmax"
Cells(11, 14) = "Kinetic Conversion RpMax"
End Sub

Sub Analyze()
' Analyze Macro
' Macro recorded 2/21/2006 by Asa Vaughan
'
' Keyboard Shortcut: Ctrl+a

Dim x As Double
Dim y As Double
Dim z As Double
Dim i As Double
Dim j As Double
Dim k As Double
Dim time As Double
Dim temp As Double
Dim heatflow As Double
Dim avgmw As Double
Dim heatofreaction As Double
Dim lightintensity As Double
Dim rp As Double
Dim rpnew As Double
```

Dim correctedheatflow As Double
Dim hf As Double
Dim hfnew As Double
Dim rpold As Double
Dim kmax As Double
Dim rpinitial As Double
Dim rpfinal As Double
Dim rpsum As Double
Dim conversion As Double
Dim finalconversion As Double
Dim rpmax As Double
Dim rpmaxold As Double
Dim rpmaxnew As Double
Dim polyrxtime As Double
Dim kmaxoverride As Double
Dim timerpmax As Double
Dim initialdatapoint As Double
Dim finaldatapoint As Double
Dim numberofpoints As Double
Dim conversionrpmax As Double
Dim lightintensitycorrection As Double
Dim ii As Double
lightintensitycorrection = Cells(2, 14)

```
ii = 4

Do While Cells(ii, 1) > 0

initialdatapoint = Cells(4, 1)

finaldatapoint = Cells(ii, 1)

ii = ii + 1

Loop

numberofpoints = ii - 4

heatofreaction = Cells(2, 1)

avgmw = Cells(2, 2)

kmax = numberofpoints

lightintensity = Cells(kmax, 3)

Cells(2, 3) = lightintensity

Cells(2, 9) = kmax

i = 4

j = 1

k = 0

time = 0

rp = 0

rpnew = 0

hf = 0

hfnew = 0

rpinitial = 0
```

```

rpfinal = 0
rpsum = 0
rpmax = 0
rpold = 0
rpmaxold = 0
rpmaxnew = 0
timerpmax = 0
temp = Cells(3000, 2)
Cells(2, 6) = temp
converionrpmax = 0
Do While k < kmax

hfnew = Cells(i, 3) - (lightintensity + lightintensitycorrection)
If hfnew < 0 Then Cells(i, 4) = hf
If hfnew > 0 Then hf = hfnew
Cells(i, 4) = hf
rpold = rp
rpnew = Cells(i, 4) * avgmw / heatofreaction
If rpnew < 0 Then rp = rp
If rpnew > 0 Then rp = rpnew
Cells(i, 5) = rp
Cells(i, 6) = time
If rp = rpold Then time = time

```

If $rp > rpold$ Then $time = time + 0.2$

If $rp < rpold$ Then $time = time + 0.2$

If $time = 0.2$ Then $rpinitial = rp$

$Cells(4, 12) = rpinitial$

$rpfinal = rp$

$Cells(4, 13) = rpfinal$

$rpsum = rpsum + rp$

$Cells(i, 9) = rpsum$

$i = i + 1$

$k = k + 1$

Loop

$k = 0$

$i = 4$

Do While ($k < kmax$)

If $Cells(i, 6) = 0$ Then $conversion = 0$

If $Cells(i, 6) > 0$ Then $conversion = (time * (rpinitial + rpfinal + 2 * Cells(i, 9))) / (time * 2 * 5)$

$Cells(i, 7) = conversion$

$finalconversion = conversion$

$Cells(2, 5) = finalconversion$

$k = k + 1$

$i = i + 1$

Loop

```

k = 0
i = 4
Do While (k < kmax)
  rpmaxnew = Cells(i, 5)
  If rpmaxnew > rpmax Then rpmax = rpmaxnew
  If rpmaxnew < rpmax Then rpmax = rpmax
  If rpmaxnew = rpmax Then rpmax = rpmax
  Cells(2, 4) = rpmax
  i = i + 1
  k = k + 1
Loop
i = 4
k = 0
Do While k < kmax
  rpmaxnew = Cells(i, 5)
  If rpmaxnew = rpmax Then timerpmax = Cells(i, 6)
  Cells(2, 7) = timerpmax
  If rpmaxnew = rpmax Then conversionrpmax = Cells(i, 7)
  Cells(2, 8) = conversionrpmax
  i = i + 1
  k = k + 1
Loop
'kinetic section'

```

```

Dim kmaxoverride As Double

Dim kineticconversion As Double

kmaxoverride = Cells(2, 13) * 60 * 5

Cells(2, 11) = kmaxoverride

i = 4

k = 0

rpmaxnew = 0

rpmax = 0

kineticconversion = 0

Cells(12, 12) = temp

Do While (k < kmaxoverride)

rpmaxnew = Cells(i, 5)

If rpmaxnew > rpmax Then rpmax = rpmaxnew

If rpmaxnew < rpmax Then rpmax = rpmax

If rpmaxnew = rpmax Then rpmax = rpmax

Cells(12, 10) = rpmax

i = i + 1

k = k + 1

Loop

i = 4

k = 0

Do While k < kmaxoverride

rpmaxnew = Cells(i, 5)

```

```

If rpmaxnew = rpmax Then timerpmax = Cells(i, 6)

Cells(12, 13) = timerpmax

If rpmaxnew = rpmax Then conversionrpmax = Cells(i, 7)

Cells(12, 14) = conversionrpmax

kineticconversion = Cells(i, 7)

Cells(12, 11) = kineticconversion

i = i + 1

k = k + 1

Loop

Rows("14:14").RowHeight = 60

Range("J14").Select

ActiveCell.FormulaR1C1 = "Rp at Light"

With ActiveCell.Characters(Start:=1, Length:=11).Font

    .Name = "Arial"

    .FontStyle = "Regular"

    .Size = 8

    .Strikethrough = False

    .Superscript = False

    .Subscript = False

    .OutlineFont = False

    .Shadow = False

    .Underline = xlUnderlineStyleNone

    .ColorIndex = xlAutomatic

```

End With

Range("J14").Select

ActiveCell.FormulaR1C1 = "Rp at Light Shutdown"

With ActiveCell.Characters(Start:=1, Length:=20).Font

.Name = "Arial"

.FontStyle = "Regular"

.Size = 8

.Strikethrough = False

.Superscript = False

.Subscript = False

.OutlineFont = False

.Shadow = False

.Underline = xlUnderlineStyleNone

.ColorIndex = xlAutomatic

End With

Range("K14").Select

ActiveCell.FormulaR1C1 = "Rp at Light Shutdown plus deltatime"

With ActiveCell.Characters(Start:=1, Length:=32).Font

.Name = "Arial"

.FontStyle = "Regular"

.Size = 8

.Strikethrough = False

.Superscript = False

```

.Subscript = False

.OutlineFont = False

.Shadow = False

.Underline = xlUnderlineStyleNone

.ColorIndex = xlAutomatic

End With

Range("L14").Select

ActiveCell.FormulaR1C1 = "Conversion at light shutdown"

With ActiveCell.Characters(Start:=1, Length:=28).Font

.Name = "Arial"

.FontStyle = "Regular"

.Size = 8

.Strikethrough = False

.Superscript = False

.Subscript = False

.OutlineFont = False

.Shadow = False

.Underline = xlUnderlineStyleNone

.ColorIndex = xlAutomatic

End With

Range("M14").Select

ActiveCell.FormulaR1C1 = "Conversion at Light shutdown plus deltatime"

With ActiveCell.Characters(Start:=1, Length:=40).Font

```

```
.Name = "Arial"  
.FontStyle = "Regular"  
.Size = 8  
.Strikethrough = False  
.Superscript = False  
.Subscript = False  
.OutlineFont = False  
.Shadow = False  
.Underline = xlUnderlineStyleNone  
.ColorIndex = xlAutomatic
```

End With

```
Range("N14").Select
```

```
ActiveCell.FormulaR1C1 = "Delta time sec"
```

```
With ActiveCell.Characters(Start:=1, Length:=10).Font
```

```
.Name = "Arial"  
.FontStyle = "Regular"  
.Size = 8  
.Strikethrough = False  
.Superscript = False  
.Subscript = False  
.OutlineFont = False  
.Shadow = False  
.Underline = xlUnderlineStyleNone
```

```

        .ColorIndex = xlAutomatic

End With

Range("o14").Select

ActiveCell.FormulaR1C1 = "Light Shutoff time min"

With ActiveCell.Characters(Start:=1, Length:=10).Font

    .Name = "Arial"

    .FontStyle = "Regular"

    .Size = 8

    .Strikethrough = False

    .Superscript = False

    .Subscript = False

    .OutlineFont = False

    .Shadow = False

    .Underline = xlUnderlineStyleNone

    .ColorIndex = xlAutomatic

End With

Range("J15").Select

Range("P1").Select

ActiveCell.FormulaR1C1 = "Rp SS Analysis"

With ActiveCell.Characters(Start:=1, Length:=14).Font

    .Name = "Arial"

    .FontStyle = "Regular"

    .Size = 8

```

```

.Strikethrough = False

.Superscript = False

.Subscript = False

.OutlineFont = False

.Shadow = False

.Underline = xlUnderlineStyleNone

.ColorIndex = xlAutomatic

End With

Range("Q1").Select

ActiveCell.FormulaR1C1 = "Time Start min"

With ActiveCell.Characters(Start:=1, Length:=10).Font

.Name = "Arial"

.FontStyle = "Regular"

.Size = 8

.Strikethrough = False

.Superscript = False

.Subscript = False

.OutlineFont = False

.Shadow = False

.Underline = xlUnderlineStyleNone

.ColorIndex = xlAutomatic

End With

Range("R1").Select

```

```
ActiveCell.FormulaR1C1 = "Deltatime min"
```

```
With ActiveCell.Characters(Start:=1, Length:=9).Font
```

```
.Name = "Arial"
```

```
.FontStyle = "Regular"
```

```
.Size = 8
```

```
.Strikethrough = False
```

```
.Superscript = False
```

```
.Subscript = False
```

```
.OutlineFont = False
```

```
.Shadow = False
```

```
.Underline = xlUnderlineStyleNone
```

```
.ColorIndex = xlAutomatic
```

```
End With
```

```
Range("s1").Select
```

```
ActiveCell.FormulaR1C1 = "Endtime min"
```

```
With ActiveCell.Characters(Start:=1, Length:=9).Font
```

```
.Name = "Arial"
```

```
.FontStyle = "Regular"
```

```
.Size = 8
```

```
.Strikethrough = False
```

```
.Superscript = False
```

```
.Subscript = False
```

```
.OutlineFont = False
```

```

.Shadow = False

.Underline = xlUnderlineStyleNone

.ColorIndex = xlAutomatic

End With

Range("Q3").Select

End Sub

Sub drkrxnanalyze()

' drkrxnanalyze Macro

' Macro recorded 6/20/2006 by Asa Dee Vaughan'

' Keyboard Shortcut: Ctrl+e

'

Dim lightofftime As Double

Dim rplightofftime As Double

Dim rplightouttime As Double

Dim convlightofftime As Double

Dim convlightouttime As Double

Dim drkrxndeltatime As Double

Dim a As Double

Dim b As Double

Dim c As Double

Dim i As Double

Dim heatofreaction As Double

```

```

Dim avgmw As Double

heatofreaction = Cells(2, 1)

avgmw = Cells(2, 2)

lightofftime = Cells(15, 15)

drkrxdeltatime = Cells(15, 14)

lightofftime = (lightofftime * 60)

a = 0

i = 4

Do While a < (lightofftime - drkrxdeltatime)

a = Cells(i, 1)

rplightofftime = Cells(i, 5)

convlightofftime = Cells(i, 7)

i = i + 1

Loop

Cells(15, 10) = rplightofftime

Cells(15, 12) = convlightofftime

b = 0

i = 4

Do While b < (lightofftime)

b = Cells(i, 1)

rplightouttime = Cells(i, 3) * avgmw / heatofreaction

convlightouttime = Cells(i, 7)

i = i + 1

```

```

Loop

Cells(15, 11) = rplightouttime

Cells(15, 13) = convlightouttime

End Sub

Sub Graph()
' Graph Macro
' Macro recorded 2/21/2006 by Asa Vaughan'
' Keyboard Shortcut: Ctrl+g
'

Range("P7").Select

Charts.Add

ActiveChart.ChartType = xlXYScatter

ActiveChart.SetSourceData Source:=Sheets("Sheet1").Range("P7")

ActiveChart.SeriesCollection.NewSeries

ActiveChart.SeriesCollection(1).XValues = "=Sheet1!R4C6:R18984C6"

ActiveChart.SeriesCollection(1).Values = "=Sheet1!R4C4:R18984C4"

ActiveChart.SeriesCollection(1).Name = """"Heat Flow""""

ActiveChart.Location Where:=xlLocationAsNewSheet, Name:="Heat Flow vs Time"

With ActiveChart

.HasTitle = True

.ChartTitle.Characters.Text = "Heat Flow"

```

```

.Axes(xlCategory, xlPrimary).HasTitle = True

.Axes(xlCategory, xlPrimary).AxisTitle.Characters.Text = "Time (sec)"

.Axes(xlValue, xlPrimary).HasTitle = True

.Axes(xlValue, xlPrimary).AxisTitle.Characters.Text = "Heat Flow (W/g)"

End With

ActiveChart.PlotArea.Select

Selection.Interior.ColorIndex = xlNone

ActiveChart.Axes(xlValue).MajorGridlines.Select

Selection.Delete

Sheets("Sheet1").Select

Charts.Add

ActiveChart.ChartType = xlXYScatter

ActiveChart.SetSourceData Source:=Sheets("Sheet1").Range("P7")

ActiveChart.SeriesCollection.NewSeries

ActiveChart.SeriesCollection(1).XValues = "=Sheet1!R4C6:R18984C6"

ActiveChart.SeriesCollection(1).Values = "=Sheet1!R4C5:R18984C5"

ActiveChart.SeriesCollection(1).Name = """"Rp""""

ActiveChart.Location Where:=xlLocationAsNewSheet, Name:="Rp vs Time"

With ActiveChart

.HasTitle = True

.ChartTitle.Characters.Text = "Rp"

.Axes(xlCategory, xlPrimary).HasTitle = True

.Axes(xlCategory, xlPrimary).AxisTitle.Characters.Text = "Time (sec)"

```

```

.Axes(xlValue, xlPrimary).HasTitle = True

.Axes(xlValue, xlPrimary).AxisTitle.Characters.Text = "Rp (sec -1)"

End With

ActiveChart.PlotArea.Select

Selection.Interior.ColorIndex = xlNone

ActiveChart.Axes(xlValue).MajorGridlines.Select

Selection.Delete

Sheets("Sheet1").Select

Charts.Add

ActiveChart.ChartType = xlXYScatter

ActiveChart.SetSourceData Source:=Sheets("Sheet1").Range("P7")

ActiveChart.SeriesCollection.NewSeries

ActiveChart.SeriesCollection(1).XValues = "=Sheet1!R4C6:R18984C6"

ActiveChart.SeriesCollection(1).Values = "=Sheet1!R4C7:R18984C7"

ActiveChart.SeriesCollection(1).Name = """"Conversion""""

ActiveChart.Location Where:=xlLocationAsNewSheet, Name:= _

    "Conversion vs Time"

With ActiveChart

    .HasTitle = True

    .ChartTitle.Characters.Text = "Conversion"

    .Axes(xlCategory, xlPrimary).HasTitle = True

    .Axes(xlCategory, xlPrimary).AxisTitle.Characters.Text = "Time"

    .Axes(xlValue, xlPrimary).HasTitle = True

```

```

.Axes(xlValue, xlPrimary).AxisTitle.Characters.Text = _
    "Fractional Double Bond Conversion"

End With

ActiveChart.PlotArea.Select

Selection.Interior.ColorIndex = xlNone

ActiveChart.Axes(xlValue).MajorGridlines.Select

Selection.Delete

ActiveChart.Axes(xlValue).Select

With ActiveChart.Axes(xlValue)

    .MinimumScaleIsAuto = True

    .MaximumScale = 1

    .MinorUnitIsAuto = True

    .MajorUnitIsAuto = True

    .Crosses = xlAutomatic

    .ReversePlotOrder = False

    .ScaleType = xlLinear

    .DisplayUnit = xlNone

End With

Sheets("Sheet1").Select

Charts.Add

ActiveChart.ChartType = xlXYScatter

ActiveChart.SetSourceData Source:=Sheets("Sheet1").Range("P7")

ActiveChart.SeriesCollection.NewSeries

```

```
ActiveChart.SeriesCollection(1).XValues = "=Sheet1!R4C6:R18984C6"  
ActiveChart.SeriesCollection(1).Values = "=Sheet1!R4C2:R18984C2"  
ActiveChart.SeriesCollection(1).Name = ""Temperature""  
ActiveChart.Location Where:=xlLocationAsNewSheet, Name:="Temp vs Time"
```

```
With ActiveChart
```

```
    .HasTitle = True  
    .ChartTitle.Characters.Text = "Temperature"  
    .Axes(xlCategory, xlPrimary).HasTitle = True  
    .Axes(xlCategory, xlPrimary).AxisTitle.Characters.Text = "Time (sec)"  
    .Axes(xlValue, xlPrimary).HasTitle = True  
    .Axes(xlValue, xlPrimary).AxisTitle.Characters.Text = "Temperature °C"
```

```
End With
```

```
ActiveChart.PlotArea.Select
```

```
Selection.Interior.ColorIndex = xlNone
```

```
ActiveChart.Axes(xlValue).MajorGridlines.Select
```

```
Selection.Delete
```

```
Sheets("Conversion vs Time").Select
```

```
ActiveChart.Axes(xlCategory).AxisTitle.Select
```

```
Selection.Characters.Text = "Time (sec)"
```

```
Selection.AutoScaleFont = False
```

```
With Selection.Characters(Start:=1, Length:=10).Font
```

```
    .Name = "Arial"
```

```
    .FontStyle = "Bold"
```

```

.Size = 10

.Strikethrough = False

.Superscript = False

.Subscript = False

.OutlineFont = False

.Shadow = False

.Underline = xlUnderlineStyleNone

.ColorIndex = xlAutomatic

End With

Sheets("Sheet1").Select

Charts.Add

ActiveChart.ChartType = xlXYScatter

ActiveChart.SetSourceData Source:=Sheets("Sheet1").Range("P7")

ActiveChart.SeriesCollection.NewSeries

ActiveChart.SeriesCollection(1).XValues = "=Sheet1!R4C7:R18984C7"

ActiveChart.SeriesCollection(1).Values = "=Sheet1!R4C5:R18984C5"

ActiveChart.SeriesCollection(1).Name = """"Rp""""

ActiveChart.Location Where:=xlLocationAsNewSheet, Name:="Rp vs Conversion"

With ActiveChart

.HasTitle = True

.ChartTitle.Characters.Text = "Rp"

.Axes(xlCategory, xlPrimary).HasTitle = True

.Axes(xlCategory, xlPrimary).AxisTitle.Characters.Text = _

```

```

    "Fractional Double Bond Conversion"

    .Axes(xlValue, xlPrimary).HasTitle = True

    .Axes(xlValue, xlPrimary).AxisTitle.Characters.Text = "Rp (sec -1)"

End With

ActiveChart.PlotArea.Select

Selection.Left = 33

Selection.Top = 40

Selection.Interior.ColorIndex = xlNone

ActiveChart.Axes(xlValue).MajorGridlines.Select

Selection.Delete

ActiveWindow.ScrollWorkbookTabs Sheets:=1

Sheets("Sheet1").Select

End Sub

```

APPENDIX D

The kinetic parameters for the recognitive system were analyzed in order to find the termination constant (k_t) and propagation constant (k_p). The program name is “KINO”. All kinetic constants were analyzed by this program. The program was developed and designed to collect and analyze the data from the dark reaction analysis presented in Chapter 5. The first step was to take the data from the DPC and analyze the data with the program “SAE” presented in Appendix C. After the data has been analyzed with the program “SAE”, the kinetic parameters for the data set can be calculated via the program “KINO”.

D.1 Program Setup and Use

The first step is to take each excel file for the dark reaction and rename them as 1, 2, 3, 4, etc. Chronological order is important in the renaming of the Excel files. The second step is to open up a workbook containing the Visual Basic program “KINO”. The third step is to open up the program file and edit the location of the data. Default location is found within the code within the subroutine kineticgetdata line 19. Insert the location of the data in the C:\DocumentsandSettings\vaughad\MyDocuments\MAATEMPLATE

KINETIC\" by replacing the file name. Forth step is to open up a new workbook. Press “CTRL+K” which sets up the Excel spreadsheet. Step five is to insert the values under the labeled cells for monomer concentration steady state (Monomer Concentration SS), feed crosslinking, light intensity value in Einsteins (Io), initiator concentration, and the initiator extinction coefficient. Once these values are inputted the operator may press “CTRL+I” this opens up all the workbooks in the data form until done. An error message may pop up at this point. To correct this error the operator must go back to line 18 of the subroutine kineticgetdata and change the value of 14 to the required number of files to be analyzed. Step six is to press “CTRL-N” which analyzes the data and gives values in the labeled columns for the kinetic constants of propagation and termination. Step seven is to press “CTRL-O” to create the graphs of the data. This completes the analysis program.

D.2 Program Code for “KINO”

```
Sub kineticsetup()  
,  
,  
' kineticsetup Macro  
' Macro recorded 6/20/2006 by Asa Dee Vaughan  
,  
,  
' Keyboard Shortcut: Ctrl+k  
,  
,  
  
    Rows("1:1").RowHeight = 51.75  
  
    Rows("1:1").Select
```

With Selection

.HorizontalAlignment = xlGeneral

.VerticalAlignment = xlBottom

.WrapText = True

.Orientation = 0

.AddIndent = False

.IndentLevel = 0

.ShrinkToFit = False

.ReadingOrder = xlContext

.MergeCells = False

End With

Range("A1").Select

ActiveCell.FormulaR1C1 = "Rp at Light shut down"

With ActiveCell.Characters(Start:=1, Length:=21).Font

.Name = "Arial"

.FontStyle = "Regular"

.Size = 10

.Strikethrough = False

.Superscript = False

.Subscript = False

.OutlineFont = False

.Shadow = False

.Underline = xlUnderlineStyleNone

```

        .ColorIndex = xlAutomatic

End With

Range("B1").Select

ActiveCell.FormulaR1C1 = "Rp at Light out plus deltatime"

With ActiveCell.Characters(Start:=1, Length:=30).Font

    .Name = "Arial"

    .FontStyle = "Regular"

    .Size = 10

    .Strikethrough = False

    .Superscript = False

    .Subscript = False

    .OutlineFont = False

    .Shadow = False

    .Underline = xlUnderlineStyleNone

    .ColorIndex = xlAutomatic

End With

Range("C1").Select

ActiveCell.FormulaR1C1 = "Conversion at light shut down"

With ActiveCell.Characters(Start:=1, Length:=29).Font

    .Name = "Arial"

    .FontStyle = "Regular"

    .Size = 10

    .Strikethrough = False

```

```
.Superscript = False
.Subscript = False
.OutlineFont = False
.Shadow = False
.Underline = xlUnderlineStyleNone
.ColorIndex = xlAutomatic

End With

Range("D1").Select

ActiveCell.FormulaR1C1 = "Conversion at light out plus deltatime"

With ActiveCell.Characters(Start:=1, Length:=38).Font

.Name = "Arial"

.FontStyle = "Regular"

.Size = 10

.Strikethrough = False

.Superscript = False

.Subscript = False

.OutlineFont = False

.Shadow = False

.Underline = xlUnderlineStyleNone

.ColorIndex = xlAutomatic

End With

Range("E1").Select

Columns("D:D").ColumnWidth = 10
```

```

Columns("C:C").ColumnWidth = 10.57

ActiveCell.FormulaR1C1 = "Delta time"

With ActiveCell.Characters(Start:=1, Length:=10).Font

    .Name = "Arial"

    .FontStyle = "Regular"

    .Size = 10

    .Strikethrough = False

    .Superscript = False

    .Subscript = False

    .OutlineFont = False

    .Shadow = False

    .Underline = xlUnderlineStyleNone

    .ColorIndex = xlAutomatic

End With

Range("E1").Select

ActiveCell.FormulaR1C1 = "Delta time sec"

With ActiveCell.Characters(Start:=1, Length:=14).Font

    .Name = "Arial"

    .FontStyle = "Regular"

    .Size = 10

    .Strikethrough = False

    .Superscript = False

    .Subscript = False

```

```

.OutlineFont = False

.Shadow = False

.Underline = xlUnderlineStyleNone

.ColorIndex = xlAutomatic

End With

Range("F1").Select

ActiveCell.FormulaR1C1 = "Time light Shut off"

With ActiveCell.Characters(Start:=1, Length:=19).Font

.Name = "Arial"

.FontStyle = "Regular"

.Size = 10

.Strikethrough = False

.Superscript = False

.Subscript = False

.OutlineFont = False

.Shadow = False

.Underline = xlUnderlineStyleNone

.ColorIndex = xlAutomatic

End With

Range("H1").Select

ActiveCell.FormulaR1C1 = "Monomer Conc SS"

With ActiveCell.Characters(Start:=1, Length:=15).Font

.Name = "Arial"

```

```
.FontStyle = "Regular"
.Size = 10
.Strikethrough = False
.Superscript = False
.Subscript = False
.OutlineFont = False
.Shadow = False
.Underline = xlUnderlineStyleNone
.ColorIndex = xlAutomatic

End With

Range("J1").Select

ActiveCell.FormulaR1C1 = "Feed Crosslinking"

With ActiveCell.Characters(Start:=1, Length:=16).Font

.Name = "Arial"

.FontStyle = "Regular"

.Size = 10

.Strikethrough = False

.Superscript = False

.Subscript = False

.OutlineFont = False

.Shadow = False

.Underline = xlUnderlineStyleNone

.ColorIndex = xlAutomatic
```

End With

Range("K1").Select

ActiveCell.FormulaR1C1 = "kp/kt^.5 ss"

With ActiveCell.Characters(Start:=1, Length:=11).Font

.Name = "Arial"

.FontStyle = "Regular"

.Size = 10

.Strikethrough = False

.Superscript = False

.Subscript = False

.OutlineFont = False

.Shadow = False

.Underline = xlUnderlineStyleNone

.ColorIndex = xlAutomatic

End With

Range("L1").Select

ActiveCell.FormulaR1C1 = "Io"

With ActiveCell.Characters(Start:=1, Length:=2).Font

.Name = "Arial"

.FontStyle = "Regular"

.Size = 10

.Strikethrough = False

.Superscript = False

```

.Subscript = False

.OutlineFont = False

.Shadow = False

.Underline = xlUnderlineStyleNone

.ColorIndex = xlAutomatic

End With

Range("M1").Select

ActiveCell.FormulaR1C1 = "Initiator Concentration"

With ActiveCell.Characters(Start:=1, Length:=23).Font

.Name = "Arial"

.FontStyle = "Regular"

.Size = 10

.Strikethrough = False

.Superscript = False

.Subscript = False

.OutlineFont = False

.Shadow = False

.Underline = xlUnderlineStyleNone

.ColorIndex = xlAutomatic

End With

Range("N1").Select

ActiveCell.FormulaR1C1 = "Initiator extinction coefficient"

With ActiveCell.Characters(Start:=1, Length:=32).Font

```

```
.Name = "Arial"  
.FontStyle = "Regular"  
.Size = 10  
.Strikethrough = False  
.Superscript = False  
.Subscript = False  
.OutlineFont = False  
.Shadow = False  
.Underline = xlUnderlineStyleNone  
.ColorIndex = xlAutomatic
```

End With

```
Range("H2").Select
```

```
Range("O1").Select
```

```
ActiveCell.FormulaR1C1 = "Rp SS"
```

```
With ActiveCell.Characters(Start:=1, Length:=5).Font
```

```
.Name = "Arial"  
.FontStyle = "Regular"  
.Size = 10  
.Strikethrough = False  
.Superscript = False  
.Subscript = False  
.OutlineFont = False  
.Shadow = False
```

```

.Underline = xlUnderlineStyleNone

.ColorIndex = xlAutomatic

End With

Range("P1").Select

ActiveCell.FormulaR1C1 = "Conv ss"

With ActiveCell.Characters(Start:=1, Length:=7).Font

.Name = "Arial"

.FontStyle = "Regular"

.Size = 10

.Strikethrough = False

.Superscript = False

.Subscript = False

.OutlineFont = False

.Shadow = False

.Underline = xlUnderlineStyleNone

.ColorIndex = xlAutomatic

End With

Range("Q1").Select

ActiveCell.FormulaR1C1 = "Time"

With ActiveCell.Characters(Start:=1, Length:=4).Font

.Name = "Arial"

.FontStyle = "Regular"

.Size = 10

```

```

.Strikethrough = False

.Superscript = False

.Subscript = False

.OutlineFont = False

.Shadow = False

.Underline = xlUnderlineStyleNone

.ColorIndex = xlAutomatic

End With

Range("Q2").Select

Range("G1").Select

ActiveCell.FormulaR1C1 = "kt^.5 uss"

With ActiveCell.Characters(Start:=1, Length:=9).Font

    .Name = "Arial"

    .FontStyle = "Regular"

    .Size = 10

    .Strikethrough = False

    .Superscript = False

    .Subscript = False

    .OutlineFont = False

    .Shadow = False

    .Underline = xlUnderlineStyleNone

    .ColorIndex = xlAutomatic

End With

```

```

    Range("G2").Select
End Sub

Sub kineticgetdata()
'
' kineticgetdata Macro
' Macro recorded 6/20/2006 by Asa Dee Vaughan
'
' Keyboard Shortcut: Ctrl+i
'

Dim filename As String
Dim filenumber As Double
filenumber = 1
Dim i As Double
i = 4
Dim col As String
Dim row As String
Dim numcol As Integer
Dim numrow As Integer
Dim where As String
Do While filenumber <> 14
filename = "C:\Documents and Settings\vaughad\My
Documents\MAATEMPLATEKINETIC\" & filenumber & ".xls"

    Workbooks.Open filename:=filename

```

```
Range("J15:O15").Select
Selection.Copy
ActiveWindow.Close
col = Chr(Asc("A"))
numrow = i
where = col & numrow
Range(where).Select
ActiveSheet.Paste
With Selection.Font
    .Name = "Arial"
    .Size = 8
    .Strikethrough = False
    .Superscript = False
    .Subscript = False
    .OutlineFont = False
    .Shadow = False
    .Underline = xlUnderlineStyleNone
    .ColorIndex = xlAutomatic
End With
Range("A3").Select
i = i + 1
filenumber = filenumber + 1
Loop
```

```

End Sub

Sub ssandussanalysis()
'
' ssandussanalysis Macro
' Macro recorded 6/20/2006 by Asa Dee Vaughan
'
' Keyboard Shortcut: Ctrl+n
'

Dim rpss As Double
Dim convss As Double
Dim monconc As Double
Dim iniconc As Double
Dim iniext As Double
Dim io As Double
Dim kpktss As Double
Dim i As Double
Dim j As Double
Dim k As Double
Dim timeuss As Double
Dim prob As Double
prob = 1 / (Cells(2, 8) + 1)
iniext = Cells(2, 14)

```

```

iniconc = Cells(2, 13)
monconc = Cells(2, 8)
io = Cells(2, 12)
i = 4
j = 0
timeussa = 1
timeuss = 1
Do While timeuss > 0
    rpss = Cells(i, 1)
    convss = Cells(i, 3)
    monconc = monconc * (1 - (prob * convss))
    iniconc = iniconc * (1 - (prob * convss))
    kpktss = rpss / (monconc * Abs((io * iniext * iniconc) ^ 0.5))
    Cells(i, 11) = kpktss
    timeuss = Cells(i, 6)
    i = i + 1
Loop
Dim rpto As Double
Dim rpti As Double
Dim mto As Double
Dim mti As Double
Dim convo As Double
Dim convi As Double

```

Dim kpktsss As Double

Dim deltat As Double

Dim a As Double

Dim b As Double

Dim c As Double

Dim ktuss As Double

Dim kp As Double

a = 4

b = 0

timeuss = 1

Cells(3, 7) = "kt^.5"

Cells(3, 8) = "kp"

Cells(3, 12) = "kt/kp"

Cells(3, 13) = "kt"

Do While timeuss > 0

 rpto = Cells(a, 1)

 rpti = Cells(a, 2)

 convo = Cells(a, 3)

 convi = Cells(a, 4)

 mto = monconc * (1 - (prob * convo))

 mti = monconc * (1 - (prob * convi))

 kpktsss = Cells(a, 11)

```

deltat = Cells(a, 5)

If rpto = 0 Then ktuss = 0

If rpto > 0 Then ktuss = (kpktsss / (2 * deltat)) * ((mti / rpti) - (mto / rpto))

Cells(a, 7) = ktuss

kp = ktuss * kpktsss

Cells(a, 8) = kp

If kp = 0 Then kp = 1

Cells(a, 12) = (ktuss * ktuss) / kp

Cells(a, 13) = (ktuss * ktuss)

timeuss = Cells(a, 6)

a = a + 1

Loop

End Sub

Sub Macro3()
'
' Macro3 Macro
' Macro recorded 12/11/2006 by Asa Dee Vaughan
'
' Keyboard Shortcut: Ctrl+o
'

Charts.Add

ActiveChart.ChartType = xlXYScatter

ActiveChart.SetSourceData Source:=Sheets("Sheet1").Range("A1:Q16"), PlotBy _

```

:=xlRows

ActiveChart.SeriesCollection(1).Delete

ActiveChart.SeriesCollection.NewSeries

ActiveChart.SeriesCollection(1).XValues = "=Sheet1!R4C3:R16C3"

ActiveChart.SeriesCollection(1).Values = "=Sheet1!R4C13:R16C13"

ActiveChart.SeriesCollection(1).Name = ""kt vs conversion""

ActiveChart.Location where:=xlLocationAsObject, Name:="Sheet1"

With ActiveChart

.HasTitle = True

```

.ChartTitle.Characters.Text = "kt vs conversion"

.Axes(xlCategory, xlPrimary).HasTitle = True

.Axes(xlCategory, xlPrimary).AxisTitle.Characters.Text = _
"Fractional Conversion"

.Axes(xlValue, xlPrimary).HasTitle = True

.Axes(xlValue, xlPrimary).AxisTitle.Characters.Text = "kt (L/(mole-sec))"

End With

ActiveChart.PlotArea.Select

Selection.Interior.ColorIndex = xlNone

ActiveChart.Axes(xlValue).MajorGridlines.Select

Selection.Delete

ActiveWindow.Visible = False

Range("J18").Select

Charts.Add

ActiveChart.ChartType = xlXYScatter

ActiveChart.SetSourceData Source:=Sheets("Sheet1").Range("J18")

ActiveChart.SeriesCollection.NewSeries

ActiveChart.SeriesCollection(1).XValues = "=Sheet1!R4C3:R16C3"

ActiveChart.SeriesCollection(1).Values = "=Sheet1!R4C8:R16C8"

ActiveChart.SeriesCollection(1).Name = """"kp vs conversion""""

ActiveChart.Location where:=xlLocationAsObject, Name:="Sheet1"

With ActiveChart

.HasTitle = True

```

```

.ChartTitle.Characters.Text = "kp vs conversion"

.Axes(xlCategory, xlPrimary).HasTitle = True

.Axes(xlCategory, xlPrimary).AxisTitle.Characters.Text = _
"Fractional Conversion"

.Axes(xlValue, xlPrimary).HasTitle = True

.Axes(xlValue, xlPrimary).AxisTitle.Characters.Text = "kp (L/(mole-sec))"

End With

ActiveChart.PlotArea.Select

Selection.Interior.ColorIndex = xlNone

ActiveChart.Axes(xlValue).MajorGridlines.Select

Selection.Delete

ActiveWindow.Visible = False

Range("M20").Select

Charts.Add

ActiveChart.ChartType = xlXYScatter

ActiveChart.SetSourceData Source:=Sheets("Sheet1").Range("M20"), PlotBy:= _
    xlColumns

ActiveChart.SeriesCollection.NewSeries

ActiveChart.SeriesCollection(1).XValues = "=Sheet1!R4C3:R16C3"

ActiveChart.SeriesCollection(1).Values = "=Sheet1!R4C12:R16C12"

ActiveChart.SeriesCollection(1).Name = """"ktp vs conversion""""

ActiveChart.Location where:=xlLocationAsObject, Name:="Sheet1"

With ActiveChart

```

```
.HasTitle = True

.ChartTitle.Characters.Text = "kt to kp vs conversion"

.Axes(xlCategory, xlPrimary).HasTitle = True

.Axes(xlCategory, xlPrimary).AxisTitle.Characters.Text = _
"Fractional Conversion"

.Axes(xlValue, xlPrimary).HasTitle = True

.Axes(xlValue, xlPrimary).AxisTitle.Characters.Text = "kt over kp"
```

End With

```
ActiveChart.PlotArea.Select
```

```
Selection.Interior.ColorIndex = xlNone
```

```
ActiveChart.Axes(xlValue).MajorGridlines.Select
```

```
Selection.Delete
```

```
ActiveChart.ChartTitle.Select
```

```
Selection.Characters.Text = "kt to kp vs conversion"
```

```
Selection.AutoScaleFont = False
```

```
With Selection.Characters(Start:=1, Length:=22).Font
```

```
.Name = "Arial"
```

```
.FontStyle = "Regular"
```

```
.Size = 12
```

```
.Strikethrough = False
```

```
.Superscript = False
```

```
.Subscript = False
```

```
.OutlineFont = False
```

```
.Shadow = False  
.Underline = xlUnderlineStyleNone  
.ColorIndex = xlAutomatic  
End With  
ActiveChart.ChartArea.Select  
End Sub
```

APPENDIX E

Appendix E gives an overview of the error analysis used in the dissertation.

E.1 Error Analysis

Average values of multiple experiments were reported with their corresponding standard deviations. When multiplying or dividing quantities, the fractional standard deviations were squared, added, and then the square root of the sum was used to calculate the fractional total deviation. For example, consider $A \pm dA$ and $B \pm dB$, where dA and dB are the corresponding standard deviations. To calculate the multiplication of A and B (i.e., $X = A \times B$ with total error $\pm dX$) equation E.1 was used.

$$\frac{dx}{x} = \sqrt{\left(\frac{dA}{A}\right)^2 + \left(\frac{dB}{B}\right)^2 + \dots} \quad \text{E.1}$$

For addition or subtraction of average values with standard deviations, sum of squares analysis was also used (equation E.2).

$$dx = \sqrt{(dA)^2 + (dB)^2 + \dots} \quad \text{E.2}$$

Sample average values were calculated where appropriate with 95% confidence limits for the mean. For example consider, equation E.3.

$$\bar{Y} \pm \frac{t_{(\alpha/2, n-1)} s}{\sqrt{N}} \quad \text{E.3}$$

where \bar{Y} is the sample mean, $t_{(\alpha/2, n-1)}$ is the upper critical value of the t -distribution with $n-1$ degrees of freedom, s is the standard deviation, and N is the number of observations.